Iowa Research Online
The University of Iowa's Institutional Repository

University of Iowa
Iowa Research Online

Theses and Dissertations

Fall 2011

Chemical investigations of fungicolous and endophytic fungi

Kristina Danielle Rogers
University of Iowa

Copyright 2011 Kristina D. Rogers

This dissertation is available at Iowa Research Online: http://ir.uiowa.edu/etd/2762

Recommended Citation
Rogers, Kristina Danielle. "Chemical investigations of fungicolous and endophytic fungi." PhD (Doctor of Philosophy) thesis, University of Iowa, 2011.
http://ir.uiowa.edu/etd/2762.

Follow this and additional works at: http://ir.uiowa.edu/etd


Part of the Chemistry Commons

CHEMICAL INVESTIGATIONS OF FUNGICOLOUS AND ENDOPHYTIC FUNGI

by

Kristina Danielle Rogers

An Abstract

Of a thesis submitted in partial fulfillment
of the requirements for the Doctor of
Philosophy degree in Chemistry
in the Graduate College of
The University of Iowa

December 2011

Thesis Supervisor: Professor James B. Gloer

ABSTRACT

Fungi are rich sources of structurally diverse secondary metabolites, some of which possess biological activities of importance to medicine and agriculture. Research in our group focuses on application of ecological considerations to the selection of underexplored fungi for chemical analysis in search of new natural products with potentially important bioactivities. The work described in this thesis involved studies of members of two different fungal ecological groups, fungicolous and endophytic fungi.

Fungicolous fungi colonize other fungi and are viewed as potential sources of antifungal agents due to the negative effects often exerted on the host organisms. Our prior studies of such fungi have proven them to be productive sources of new bioactive natural products. Fractionation of extracts produced from eleven fungicolous fungal isolates resulted in the isolation and identification of 24 different, structurally-diverse natural products, many of which were bioactive. Most of these were previously known, but six were new compounds, with one being a distinctive new peptaibol-type metabolite.

Endophytic fungi colonize the inner tissues of host plants, often asymptomatically, and occur widely in most plant species. Some endophytes may benefit the host, possibly through production of protective secondary metabolites, but in most cases, their roles are not well understood. *Stenocarpella maydis* is a widely occurring fungal endophyte and pathogen of corn and is associated with diplodiosis (a neuromycotoxicosis) of cattle. Investigations of extracts of *S. maydis* and *S. macrospora* cultures led to the identification of seven compounds, including diplodiatoxin, diplosporin, chaetoglobosins K, L, M, and O, and (all-*E*) trideca-4,6,10,12-tetraene-2,8-diol, none of which were previously known from U.S. *Stenocarpella* isolates. Diplodiatoxin was detected as a major component of *S. maydis*-rotted maize grain, stalks, and stalk residues, and chaetoglobosin M was detected in extracts of naturally-diseased *S. maydis*-rotted maize seeds collected in the field. Chaetoglobosin K displayed potent

antifungal and antiinsectan activity, while diplodiatoxin displayed phytotoxicity. Because of their well-known cytotoxic effects, we proposed that mixtures of chaetoglobosins are responsible, at least in part, for inducing diplodiosis in livestock.

Our prior investigations of another common corn endophyte, *Acremonium zeae*, led to isolation of the pyrrocidines, which display potent antifungal and antibacterial activities against a range of corn pathogens. Further studies of these extracts led to the isolation and identification of three resorcylic acid lactone (RAL)-type compounds, one of which was new. These RAL's, did not exhibit antifungal activity, but demonstrated mild phytotoxicity to maize leaves in assays. They are also members of a compound class we have encountered among other endophytes that inhibit the heat shock protein Hsp90, and have been proposed to play a role in the colonization process. These chemical investigations provide further knowledge that may be useful in determining the roles that endophytes, in particular *S. maydis* and *A. zeae*, play in maize.

The metabolites encountered during these investigations represented different biosynthetic pathways, and included polyketides, terpenoids, and compounds of mixed biogenetic origin. Structures were characterized by analysis of 1D and 2D NMR data, mass spectrometry, chemical degradation or derivatization reactions, and/or X-ray diffraction analysis. Absolute configuration assignments were determined using Mosher's method, Marfey's method, or chiral amino acid analysis methods.

Abstract Approved: _____
Thesis Supervisor

_____
Title and Department

_____
Date

CHEMICAL INVESTIGATIONS OF FUNGICOLOUS AND ENDOPHYTIC FUNGI

by

Kristina Danielle Rogers

A thesis submitted in partial fulfillment
of the requirements for the Doctor of
Philosophy degree in Chemistry
in the Graduate College of
The University of Iowa

December 2011

Thesis Supervisor: Professor James B. Gloer

Graduate College
The University of Iowa
Iowa City, Iowa

CERTIFICATE OF APPROVAL

_____

PH.D. THESIS

_____

This is to certify that the Ph.D. thesis of

Kristina Danielle Rogers

has been approved by the Examining Committee
for the thesis requirement for the Doctor of Philosophy
degree in Chemistry at the December 2011 graduation.

Thesis Committee: _____
James B. Gloer, Thesis Supervisor

_____
Edward G. Gillan

_____
Daniel M. Quinn

_____
Donald T. Wicklow

_____
David F. Wiemer

To my parents Dennis and Ki Sun,
and to my husband Mark,
whose love, patience, encouragement,
and never-ending support
made this opportunity possible.

A person who never made a mistake never tried anything new.

Albert Einstein

ACKNOWLEDGMENTS

I would like express my deepest gratitude to my thesis supervisor, Dr. James Gloer, for his understanding, dedication, never-ending patience, and expertise, which truly made this thesis possible. Words alone cannot begin to express my appreciation for his meaningful guidance, motivation, and encouragement throughout my graduate career at the University of Iowa. To me he is not only an exceptional professor, but also an outstanding mentor, friend, and fellow tennis enthusiast.

I would like to thank Dr. Donald T. Wicklow at the USDA Agricultural Research Service in Peoria, IL for providing fungicolous and endophytic fungal extracts and performing antifungal bioassays. I am also grateful for his guidance during my two years as his mentee, for encouraging me to continue my career in research at the University of Iowa with Dr. Gloer, and for serving on my committee.

I am grateful to my committee members, Drs. Edward Gillan, Daniel Quinn, and David Wiemer for their guidance, thoughtful comments, and support during my graduate career. I would also like to thank Dr. Patrick F. Dowd at the USDA for conducting the antiinsectan bioassays, as well as Mr. Steve Poling for his guidance regarding our studies of *Acremonium zeae*. Assistance from Dr. Santhana Velupillai of the University of Iowa NMR Central Research Facility and Dr. Lynn Teesch and Mr. Vic Parcell of the University of Iowa High Resolution Mass Spectrometry Facility was very much appreciated. I would like to thank Dr. Dale C. Swenson of the University of Iowa Department of Chemistry X-Ray Crystallography Facility for conducting X-ray diffraction analyses. Thank you to the Wiemer group members for helping me with the setup of a variety of chemical derivatizations. I would also like to thank the Gloer group members who have helped me throughout the course of my career. I am lucky to have had the opportunity to get to know numerous individuals through the Chemistry Department and the Graduate Student Senate, many of whom have become life-long

friends and colleagues. Financial support from the National Science Foundation, National Institutes of Health, and the U.S. Department of Education (GAANN Fellowship to KDR) is greatly appreciated.

I would like to thank my husband and best friend, Mark, for his love, patience, and support. I treasure the memories and experiences we have already shared, and I look forward to seeing what the future has in store for us.

I am forever indebted to my parents Dennis and Ki Sun for everything they have done for me. They have always stressed that I can do anything if I put my mind to it. They have taught me that the value of my education is priceless and will influence the rest of my life. They have sacrificed so much for me and I am grateful to have both of them in my life. Mom and Dad - Thank you for everything you have always done for me. I love you very much.

TABLE OF CONTENTS

LIST OF TABLES

Table

LIST OF FIGURES

Figure

LIST OF ABBREVIATIONS

$[\alpha]_D^{25}$	specific rotation at 25 ºC
Å	Angstrom
Ac	acetyl
Aib	aminoisobutyric acid
Ala	alanine
APCI	atmospheric pressure chemical ionization
Ar	aryl group
ARS	Agricultural Research Service
ATCC	American Type Culture Collection
ATP	adenosine triphosphate
ax	axial
BDS	base-deactivated silica
br	broad
ºC	degree Celsius
C_{18}	octadecylsilyl
calcd	calculated
CC	column chromatography
CCDC	Cambridge Crystallographic Data Centre
CD	circular dichroism
C_6H_6	benzene
$CHCl_3$	chloroform
CH_2Cl_2	dichloromethane
cm	centimeter(s)
cm^{-1}	wavenumber
COSY	correlation spectroscopy

cz	clear zone
δ	chemical shift
d	doublet
1D	one-dimensional
2D	two-dimensional
DEPT	distortionless enhancement by polarization transfer
DMAP	4-N,N-dimethylaminopyridine
DMSO	dimethylsulfoxide
DPI	days post inoculation
DS	dummy scans
DW	dwell time
ε	extinction coefficient
EF	elongation factor
EIMS	electron impact mass spectrometry
ENDO	endophyte culture collection
eq	equatorial
ESIMS	electrospray ionization mass spectrometry
EtOAc	ethyl acetate
eV	electron volt
EXPO	experiment number
FABMS	fast atom bombardment mass spectrometry
FID	free induction decay
Fr	fraction
FR	fermented rice
FTIR	Fourier transform infrared spectroscopy
g	gram(s)
GC	gas chromatography

GS	green stalks
He	helium
Hex	hexanes
hr	hour(s)
HMBC	heteronuclear multiple bond correlation
HMQC	heteronuclear multiple quantum correlation
HPLC	high performance liquid chromatography
HREIMS	high resolution electron impact mass spectroscopy
HRESIMS	high resolution electrospray ionization mass spectrometry
HRESITOFMS	high resolution electrospray ionization time-of-flight mass spectrometry
HRESITOFMSMS	high resolution electrospray ionization time-of-flight tandem mass spectrometry
Hyp	hydroxyproline
Hz	hertz
IE	inoculated ears
Ile	isoleucine
INEPT	insensitive nuclei enhanced by polarization transfer
IR	infrared
Iva	isovaline
J	coupling constant
L	liter(s)
LC	liquid chromatography
Leu	leucine
µ	micro
m	multiplet
M	mortality
M^+	molecular ion

MeCN	acetonitrile
MeOH	methanol
mg	milligram(s)
MHz	megahertz
min	minute(s)
mL	milliliter(s)
mm	millimeter(s)
MS	mass spectrometry
MTPA	α-methoxy-α-trifluoromethylphenylacetic acid
MYC	mycotoxin
mz	mottled zone
m/z	mass-to-charge ratio
NER	natural ear rot
NOE	nuclear Overhauser effect
NOESY	nuclear Overhauser effect spectroscopy
NRRL	Northern Regional Research Laboratory
NCAUR	National Center for Agricultural Utilization Research
NMR	nuclear magnetic resonance
obsd	observed
PDA	potato dextrose agar
PDB	potato dextrose broth
ppm	parts per million
Pro	proline
q	quartet
Rel. int.	relative intensity
R_f	retention factor
rg	reduced growth

ROESY	rotating frame Overhauser effect spectroscopy
RP	reversed phase
rpm	rotations per minute
RT	room temperature
s	singlet
SF	spectral frequency
SI	size
SW	spectral width
t	triplet
TD	number of data points to acquire
TFA	trifluoroacetyl
TFAA	trifluoroacetic anhydride
TLC	thin-layer chromatography
TMS-CHN_2	trimethylsilyldiazomethane
TOCSY	total correlation spectroscopy
TOF	time of flight
t_R	retention time
USDA	United States Department of Agriculture
UV	ultraviolet
ν	frequency
Val	valine
Vis	visible
VLC	vacuum liquid chromatography
VT	variable temperature
WR	write
ZG	zero and go

CHAPTER 1

INTRODUCTION

The fungal kingdom contains an estimated 1.5 million species, with only an estimated 74,000 to 120,000 formally described by taxonomists.[1] Fungi are ubiquitous eukaryotic organisms that can be found on virtually any organic substrate and are often characterized by the presence of filamentous hyphae, which are long, branching structures that extend as they grow. Unlike plants, which have cellulose-containing cell walls, fungi are composed of a cell wall that contains chitin, a polymer of *N*-acetylglucosamine that provides structural support that is also found in the exoskeleton of insects and arthropods. Fungi do not use photosynthesis as a source of energy, but instead they utilize the organic material found in their habitats.

The primary classes of fungi include mushrooms, yeasts, and molds. Mushrooms include basidiomycetes and ascomycetes that possess a fruiting-body, or reproductive organ responsible for the production of spores, which are distributed in the environment by insects and animals or carried through the air by wind. The edible varieties of mushrooms are used in a wide variety of culinary applications, and some mushrooms have been in use for thousands of years in traditional Chinese medicine. Examples of medicinal mushrooms include oyster, reishi, shiitake, and himematsutake mushrooms, which produce secondary metabolites with activity against tumor cells, viruses, bacteria, and fungi, as well as a number of other reported medicinal functions.[4-8]

Yeasts are unicellular organisms often isolated from sugar-rich materials and are recognized and exploited by the food industry for conversion of carbohydrates to carbon dioxide for baking applications and the production of alcohol in beer and wine. Deactivated yeasts are used for nutritional benefits, such as a source of proteins and B-complex vitamins, whereas some activated yeasts have been used as probiotic

supplements to help maintain gastrointestinal health. Yeasts are not generally known for secondary metabolite production.

Molds are multicellular organisms commonly associated with the spoilage of foods and degradation of organic matter in the environment, and can be found in homes and buildings. If present in high concentrations, spores can be inhaled and may lead to allergic reactions, fungal infections, or other respiratory illnesses. Some molds have proven to be valuable sources of pharmacologically important secondary metabolites, such as the beta-lactam antibiotics including thiazolidine ring-containing penicillins (**1.1**) from *Penicillium chrysogenum*, and dihydrothiazine ring-containing cephalosporins (**1.2**) from *Cephalosporium acremonium*. The cholesterol-lowering drug lovastatin (**1.3**) from *Aspergillus terreus* was the first statin on the market. This was later replaced by other analogues, including compounds modeled after it such as the synthetic statin Lipitor (**1.4**), the world's largest-selling branded pharmaceutical manufactured by Pfizer with $12.4 billion in sales during 2008.[9] The drug cyclosporin A (**1.5**) was isolated from *Tolypocladium inflatum* and is used to suppress the immune system to minimize the risk of organ rejection.[10]

Although there are three main classes of fungi, the work in our group focuses primarily on the molds that will be referred to hereafter as "fungi." Fungi serve as valuable sources of chemically diverse secondary metabolites that may be potentially useful for medicinal or agricultural purposes. Secondary metabolites, or natural products, are isolated from plants, animals, and microorganisms and are not absolutely necessary for the normal growth, development, or reproduction of the organism. Their functions are seldom clear. They may be used as defense mechanisms or for communication purposes. For example, some fungi produce toxic secondary metabolites, or mycotoxins, that could serve as defensive mechanisms against attack by other microorganisms and/or insects. Fungal metabolites are renewable resources that commonly exhibit a wide range of biological activity in assays. Such activities could be useful in medicine or agriculture.

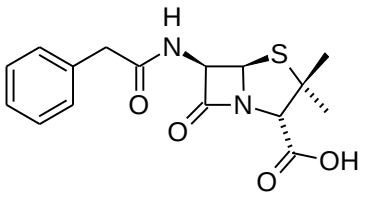

1.1

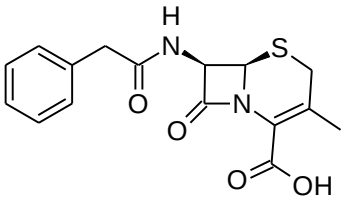

1.2

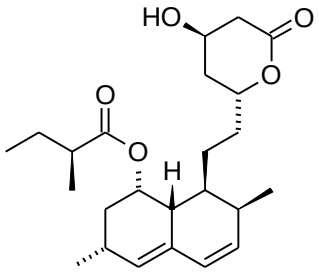

1.3

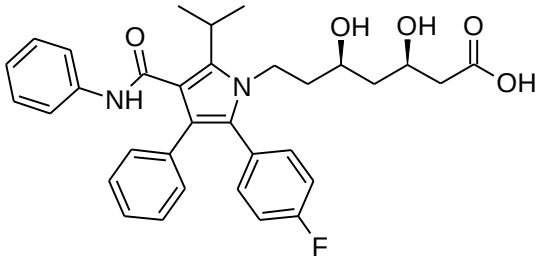

1.4

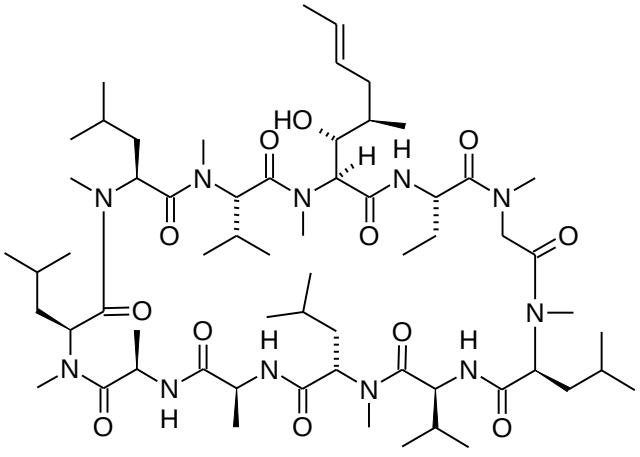

1.5

Thus, discovery of new bioactive fungal metabolites is an important objective. The process of seeking new fungal natural products involves several steps, including (1) selection of the fungal source; (2) plating of source material to obtain fungal colonies present; (3) isolation of individual fungal colonies; (4) preliminary taxonomic assessment (to minimize studies of fungal types that have been extensively explored in the past); (5) preparation of liquid- and/or solid-substrate fermentations; (6) extraction of fermented material; (7) testing of the crude extract for biological activity; (8) dereplication to spot bioactive fungal metabolites that are already well known; (9) purification of active components; (10) structure determination of the active components as well as other metabolites present in the extract; and (11) testing of the pure compounds in biological assays. Our prior studies have resulted in the discovery of a number of new bioactive natural products from a variety of fungal ecological niche groups.[11-13] New metabolites recently encountered in our work include compounds with polyketide (**1.6**),[14] terpenoid (**1.7**),[15] amino acid (**1.8**),[16] and nucleoside (**1.9**)[12] biogenetic origins, as well as compounds of mixed biogenesis (**1.10**).[17] Some of these new compounds show antifungal and antibacterial effects. However, in most cases, these have only been tested in our assays and may exhibit biological activity in other assays as well.

Many different types of assays could be used as effective guides in the search for new, bioactive secondary metabolites. Our work focuses on antifungal metabolites because of their role as potential biocontrol agents against a variety of plant pathogens. Specifically, our antifungal assays target two common fungal pathogens of corn, *Aspergillus flavus* and *Fusarium verticillioides*. These fungi cause ear and stalk rot of maize, which in turn results in hundreds of millions of dollars of losses in the corn industry each year. These fungi also produce mycotoxins, including aflatoxins and fumonisins that may contaminate grain stored for human consumption and/or livestock feed. Not only are these fungal pathogens of corn, but they are also opportunistic human pathogens, which further warrants a search for new natural products with antifungal

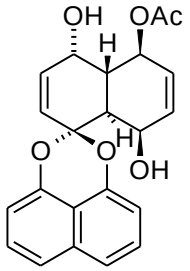

1.6

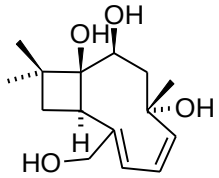

1.7

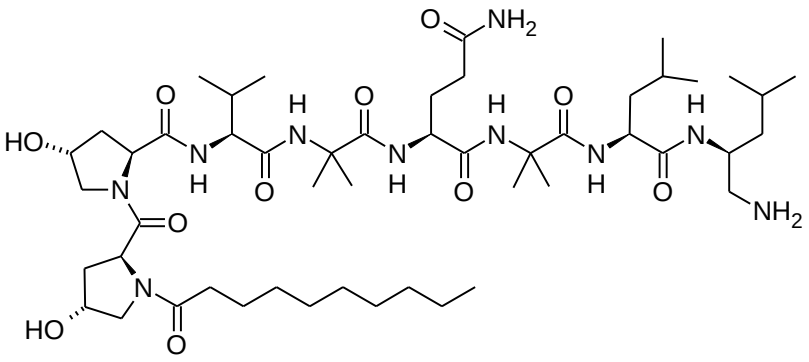

1.8

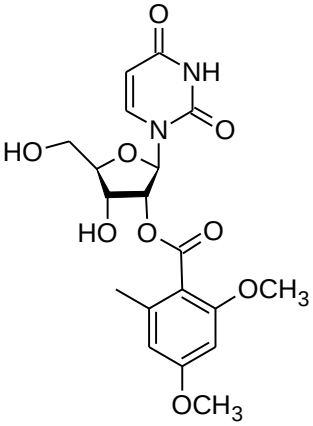

1.9

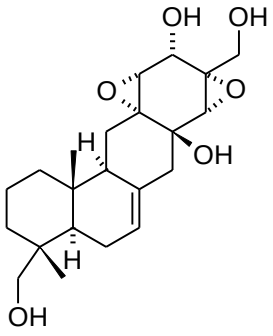

1.10

effects against them. *Aspergillus* spp. are particularly problematic as sources of human infections, so agents effective against *Aspergillus* could have medicinal utility.

Fungi are widespread in nature and colonize a variety of ecological niches. Inhabitants of a niche are often adapted to particular environmental conditions related to temperature, moisture content, acidity, pressure, light exposure, etc., and such conditions may promote the most efficient growth and reproduction for the species. The content of Chapters 3-5 focuses on the isolation of new secondary metabolites from a fungal niche group that includes fungicolous and/or mycoparasitic fungi. Mycoparasitic fungi, commonly referred to as mycoparasites, colonize, and parasitize other fungi and generally cause damage to the host organism. The antagonistic effects observed are often attributed to production of antibiotics, toxins, and/or enzymes that are destructive to the host.[18] For example, some *Trichoderma* spp. parasitize other fungi and have been studied as potential biocontrol agents effective against a number of agriculturally problematic phytopathogenic fungi.[19] The antifungal effects of these *Trichoderma* spp. have been attributed to the presence of endo- and exochitinases that cause cell wall degredation, as well as peptaibol antibiotics.[20] It has been reported that these antibiotic metabolites act synergistically with chitinases to degrade the host cell wall.[21] Some *Gliocladium* spp., which will be discussed in Chapter 5, are known mycoparasites, and are also morphologically similar to *Trichoderma* spp.

A mycoparasitic relationship involves a complex process including the following steps: (1) chemotrophic growth of hyphae of the mycoparasite toward the host organism; (2) recognition of the host by the mycoparasite; (3) attachment of the mycoparasite, often by coiling around the host or attaching to the host using hook-like anchors; (4) excretion of cell-wall degrading enzymes; and (5) localized lysis and invasion of the host organism.[20] Detailed studies are required to prove a true mycoparasitic relationship.[22] Thus, our group also focuses on the investigation of so-called "fungicolous" fungi. Fungicolous fungi colonize others, but have not necessarily been proven to be truly

parasitic to the host. The term "fungicolous fungi" is a broader classification that also includes mycoparasitic fungi. Because of the antifungal effects commonly exerted by both mycoparasitic and fungicolous fungi, both types have been targeted by our research group as promising sources of antifungal and other bioactive compounds.[17,23,24]

Another important fungal niche group that has been a promising source of bioactive secondary metabolites with a wide range of biological activities consists of endophytic fungi, which are discussed in Chapters 6 and 7. These organisms, commonly referred to as endophytes, colonize the inner tissues of host plants, often without causing any apparent disease.[25] Numerous fungal endophytes have been isolated from surface-sterilized plant segments incubated on culture media seeded with antibiotics, and almost all plants contain an endophytic flora.[26] Although this is a simple and inexpensive method, fungi that are obligate biotrophs, or parasites dependent on the host organism, or those that do not grow well in the culture media employed are typically overlooked. The majority of natural products reported from endophytic fungi display some level of antimicrobial activity.[27]

Because of the widespread occurrence of endophytes in plants, it is believed that some endophytes may be mutualists that can benefit the host plant, e.g., by providing protection from attack by other fungi, bacteria, insects, and/or herbivorous animals. Among the most notable examples providing evidence for such relationships are endophytes of certain grasses. At least four major alkaloid classes have been identified as metabolites of endophytic fungi, and include ergot alkaloids (e.g., ergovaline; **1.11**), aminopyrrolizidines (e.g., loline and *N*-formylloline; **1.12**), indole diterpenes (e.g., lolitrem B; **1.13**), and pyrrolopyrazine (e.g., peramine). Only the ergot, indole diterpene, and pyrrolopyrazine alkaloids have been produced by endophytes in culture.[28]

Grass-endophyte relationship studies are of great importance to the livestock industry. Numerous studies have been pursued to better understand grass-endophyte relationships, with the most studied symbiotic relationships including *Neotyphodium*

lolii-Lolium perenne (perennial ryegrass) and *N. coenophialum-Schedonorus arundinaceus* (tall fescue grass), both of which are widely distributed in the United States.[29] Perennial ryegrass is commonly found in pastures, and is often asymptomatically infected with the fungal endophyte *Neotyphodium lolii*.[30] The effects of this fungal endophyte within its plant host were revealed in the mid-1970's when endophytes of such grasses were reportedly associated with toxic effects to cattle.[31] In an effort to determine if ergot alkaloids are commonly associated with endophyte infection of tall fescue grass, samples were obtained from infected and uninfected pastures in Georgia. Selected sections of the leaf blade were stained with aniline blue and analyzed for the presence of ergot alkaloids on the basis of the formation of a blue complex with *p*-dimethylaminobenzaldehyde.[32] The identities of the ergot alkaloids present in the endophyte-infected grass material were determined by tandem MS experiments.[32] The toxic properties were found to result from the presence of secondary metabolites produced by the endophyte, in particular ergovaline (**1.11**), which was implicated as the principal ergot alkaloid responsible for the observed effects (84-97% of the total ergopeptide alkaloids present in the samples).[32] The concentrations were determined by tandem MS analysis of samples spiked with known concentrations of **1.11**, and ranged from 0.1 to 0.3 μg/g in the blades and from 0.3 to 2.8 μg/g in the sheaths.[32] Biosynthetically, ergot alkaloids are derived from 4-prenyltryptophan.

In the late 1970's, a report appeared that linked the toxicity of tall fescue grass to the endophyte *Epichloe typhina*.[33] *Epichloe* is the teleomorphic form of the asexual *Neotyphodium* genus.[28] Pyrrolizidine alkaloids were identified as the toxic metabolites responsible for reduced weight gain and decreased milk production in cattle, including loline alkaloids such as *N*-formylloline (**1.12**), one of the most abundant lolines in endophyte-infected grasses.[28,34,35] It is generally accepted that the alkaloids are produced by the endophyte and not by the grass since they are produced in vitro by the fungus and are absent from uninfected samples, with the exception of the lolines as described above.

Loline alkaloids are 1-aminopyrrolizidines biosynthesized from L-proline and L-homoserine.

Lolitrems A-D are indole-diterpenes isolated in 1981 from *N. lolii*-infected perennial ryegrass.[36] These compounds, particularly lolitrem B (**1.13**), were found to be responsible for the tremorgenic effects of ryegrass staggers, a neurotoxic disorder of livestock.[37] In each of the cases cited here, endophyte-infected grasses result in hundreds of millions of dollars in losses in the U.S. livestock industry each year.[34]

In grasses, endophytes can benefit their host through changes in plant physiology and growth patterns.[34] It has been reported that there are no differences in the quality of the tall fescue grass with regard to forage quality.[38] Under controlled conditions, the endophyte-infected plants had greater rates of photosynthesis, increased efficiency with

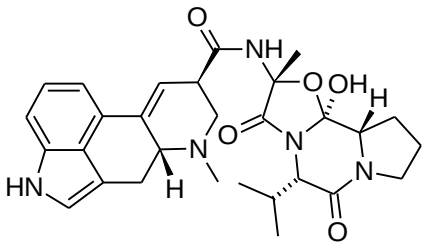

1.11

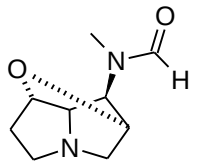

1.12

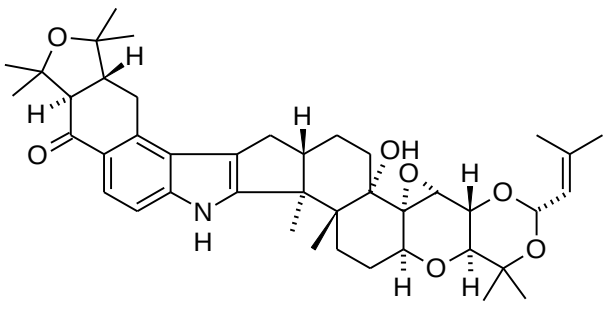

1.13

regard to water uptake, and increases in leaf area and leaf growth-rates when comparing *A. lolii*-infected perennial ryegrass and uninfected plants.[34] Endophyte-infected grasses are also more resistant to attack by insects.[34] As an example, compounds isolated from *A. coenophialum*-infected tall fescue grasses that were deemed responsible for protecting the plant against insect attack by the large Milkweed bug *Oncopeltus fasciatus* included the clavine ergot and pyrrolizidine alkaloids.[32] Peramine, which occurs in both *A. coenophialum*- and *A. lolii*-infected plants, was effective against *O. fasciatus* at 10 μg/mL.[34] In addition to growth and antiinsectan effects, it has been suggested that endophyte-infected grasses also have a greater potential for disease resistance.[39]

The corn endophyte *Acremonium zeae* is one of the most common fungi isolated from corn and is antagonistic to the common corn pathogens *Aspergillus flavus* and *Fusarium verticillioides.* Chemical studies conducted in our research group led to the identification of pyrrocidines A (**1.14**) and B (**1.15**), unusual metabolites that were first reported as metabolites of *Cylindrocarpon* sp. LL-Cyan426 by researchers at Wyeth-Ayerst. The pyrrocidines were found to be responsible for the antifungal activity observed for *A. zeae* extracts.[40] Although our group assigned the structures independently before the Wyeth-Ayerst report appeared, their description of the metabolites made them known compounds. Even so, these were the first natural products reported from *A. zeae*.[41] The pyrrocidines exhibited potent antifungal activity in our assays against *A. flavus* and *F. verticillioides* (Table 1), as well as other major pathogens of corn (Table 2).[42] In some assays, the pyrrocidines were more effective against these corn pathogens than the commercial antifungal agent nystatin. In addition to these potent antifungal effects, the pyrrodicines also showed potent antibacterial activity in assays against gram-positive bacteria (Table 3),[40] including bacterial endophytes and pathogens of maize (Table 4).[42]

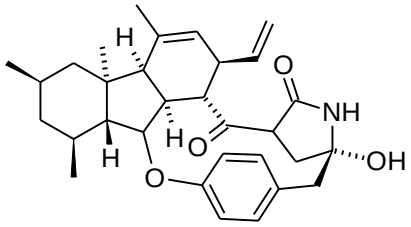

1.14

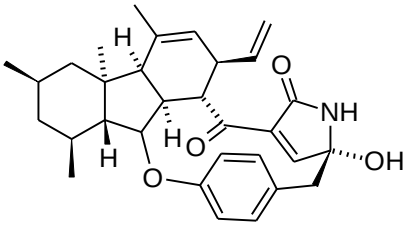

1.15

Because of the potent antibacterial and antifungal effects observed for these metabolites against agriculturally relevant disease-causing organisms, *A. zeae* has been described as a protective endophyte of maize.[41] However, evaluation of *A. zeae* isolates deposited with the Agricultural Research Service Northern Regional Research Laboratory (NRRL) and Centraalbureau voor Schimmelcultures (CBS) culture collections showed that they varied greatly with regard to the production of pyrrocidines. A population survey of *A. zeae* isolates, representing populations from maize seeds from nine states, was undertaken in order to determine their ability to produce pyrrocidines. During the course of this work, three other metabolites unrelated to the pyrrocidines were found to have widespread occurrence and were often produced in amounts comparable to the pyrrocidines. These studies are discussed in detail in Chapter 6.

Table 1. Antifungal Activities of Pyrrocidines A (**1.14**) and B (**1.15**)[a,b] Against *A. flavus* and *F. verticillioides*[42]

	Pyrrocidine A		Pyrrocidine B		Nystatin	
Isolate	MIC	GI_{50}	MIC	GI_{50}	MIC	GI_{50}
A. flavus	≤5	>1	>50	>50	≤10	>3
F. verticillioides	≤10	>2	>50	>25	≤25	>5

[a]Concentrations tested were 1, 2, 3, 5, 10, 25, and 50 μg/mL.

[b]MIC = minimum inhibitory concentration and GI_{50} = growth inhibition >50% relative to the control.

Table 2. Antifungal Activities of Pyrrocidines A (**1.14**) and B (**1.15**)[a,b] Against Stalk- and Ear-Rotting Corn Pathogens[42]

	Pyrrocidine A		Pyrrocidine B		Nystatin	
Isolate	MIC	GI_{50}	MIC	GI_{50}	MIC	GI_{50}
Fusarium graminearum	≤1	<1	>50	>25	≤10	>1
Nigrospora oryzae	≤1	<1	≤5	>1	≤1	>1
Rhizoctonia zeae	≤2	<1	>50	>10	≤10	>3
Stenocarpella (Diplodia) maydis	≤1	<1	≤25	>10	≤1	>1

[a]Concentrations tested were 1, 2, 3, 5, 10, 25, and 50 μg/mL.

[b]MIC = minimum inhibitory concentration and GI_{50} = growth inhibition >50% relative to the control.

Table 3. Antibacterial Activity of Pyrrocidines A (**1.14**) and B (**1.15**) Against Gram-Positive Bacteria[40]

	MIC (μg/mL)	
Test Organism	Pyrrocidine A	Pyrrocidine B
Staphylococcus aureus[a]	0.25–2	4–8
Staphylococcus haemolyticus	0.25	8
Enterococcus faecalis	0.5	4–8
Enterococcus faecium[a]	0.5–1	4–8

[a]Includes drug-resistant strains; MIC values determined using broth dilution method in Mueller-Hunton II, incubated at 35 °C for 18 h.

Table 4. Antibacterial Activity of Pyrrocidines A (**1.14**) and B (**1.15**)[a,b] Against Bacterial Endophytes and Pathogens of Maize[42]

	Pyrrocidine A		Pyrrocidine B	
Isolate	MIC (μg/mL)	GI_{50}	MIC (μg/mL)	GI_{50}
Bacillus mojavensis	≤1	>1	≤5	>3
Clavibacter michiganense subsp. *Nebraskenese*	≤1	>0.25	≤10	>1
Pseudomonas fluorescens	≤1	>1	≤10	>1

[a]Concentrations tested were 0.25, 1, 2, 3, 5, 10, 25, and 50 μg/mL.

[b]MIC = minimum inhibitory concentration and GI_{50} = growth inhibition >50% relative to the control.

Other fungal pathogens of corn that were investigated during this work include members of the genus *Stenocarpella*, which have also been found to be antagonistic to the common corn pathogens *A. flavus* and *F. verticillioides* and the fall armyworm *S. frugiperda.* The genus *Stenocarpella* contains two species that cause a dry-rot of maize ears; *Stenocarpella macrospora* (Earle) B. Sutton (Basionym: *Diplodia macrospora*), and

Stenocarpella maydis (Berk.) B. Sutton (Basionym: *Diplodia maydis*).[43] Maize diseases caused by these *Stenocarpella* spp. are worldwide in their distribution and are recognized as the most important ear rot pathogens in nearly all countries where maize is produced.[44] While *S. maydis* is reported from humid zones wherever corn is grown, *S. macrospora* is most prevalent in humid subtropical and tropical zones where plants exhibiting dry-ear rot and stalk rot may also display symptoms of leaf striping.[45] Severe crop infestation can result in significant yield losses from the presence of light-weight, rotted ears with discolored, shriveled, and non-viable seeds (Figure 1). *Stenocarpella maydis* ear rot is of further importance because of its association with field outbreaks of diplodiosis, a common nervous disorder (neuromycotoxicosis) of cattle and sheep grazing on infected maize crop residues in southern Africa and, more recently, in Argentina.[46,47]

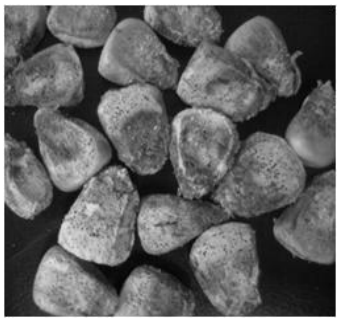

Figure 1. Corn Kernels Infected with *S. maydis*

Diplodiatoxin (**1.16**) has been isolated and characterized from *S. maydis*-fermented maize seed culture material in bioassay-guided chemical studies of the $CHCl_3$-MeOH extract, but accounted for only 10 % of the total activity of the maize culture material based on its toxicity to poultry.[48,49] No further chemistry had been described for *S. maydis*, a prevalent fungal colonist of maize seeds from Zambia. *S. macrospora*-fermented sterile maize seed culture material, added to either commercial chicken or rat feed, was acutely toxic to ducklings and rats.[50] Culture material from a toxigenic strain

of *S.macrospora* (MRC 143) was extracted with $CHCl_3$-MeOH and fractionation monitored by bioassay in day-old ducklings led to the isolation of diplosporin (**1.17**).[51] Diplodiol (=diplosporin) and chaetoglobosin K (**1.18**) were reported as metabolites of *S. macrospora* (ATCC 36896) isolated from maize produced in Costa Rica.[52,53] Both compounds were found to be toxic to day-old-chicks and may have contributed to reported losses in poultry in Mexico that were fed maize seeds rotted by *Stenocarpella* spp.[52]

Stenocarpella metabolites have not been investigated for their relevance to the fungal disease cycle, including the biochemistry and physiology of infection, or an understanding of the interactions between *Stenocarpella* and other fungal colonists of maize or maize insects. Surprisingly, there have been no reports on the detection or

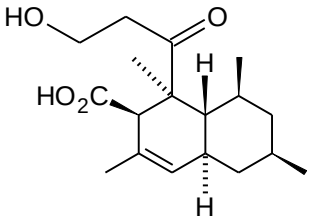

1.16

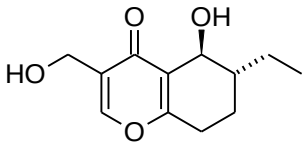

1.17

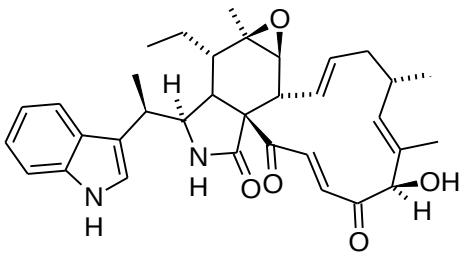

1.18

isolation of diplodiatoxin, diplosporin, or chaetoglobosin K from *Stenocarpella*-rotted maize stalks, ears, or seeds. An ability to exclude other fungi from *Stenocarpella*-parasitized and senescent/necrotic maize tissues would contribute to pathogen establishment, survival, and repeated production of conidia as infective inoculum from the *Stenocarpella* pycnidia that form on maize crop residues (Figure 2).[54,55]

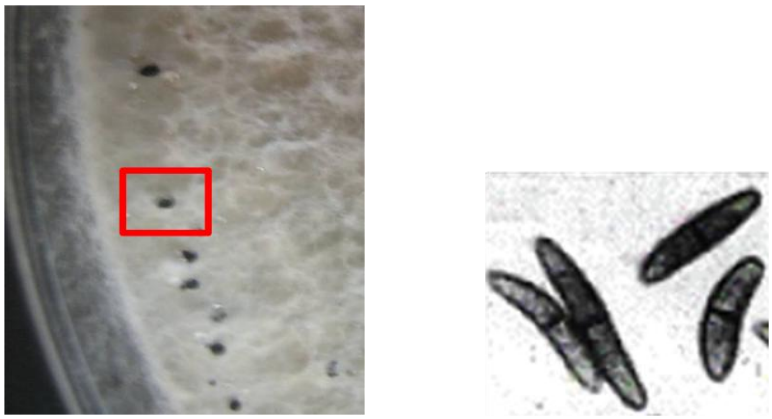

Figure 2. Pycnidia of *S. maydis* ENDO 3037 (left); Spores of *S. maydis* (right)

Stenocarpella maydis conidia germinate and colonize stalk, leaf, and shank tissues by directly penetrating the epidermal cell walls and host cytoplasm through the formation of an appressorium and enzymatic degradation.[56] The fungus may grow undetected in maize stalks and ears until several weeks after silking or until the soft dough stage .[45] Maize stalks become more susceptible to *Stenocarpella* stalk rot during the transition from vegetative to reproductive stages and the onset of pith senescence.[57]

There are no reports of purified diplodiatoxin having been administered to ruminants. The first clinical and biochemical evidence that diplodiatoxin might be associated with symptoms of neuromycotoxicosis was offered by Rahman *et al.*[58] Acute and subacute doses of purified diplodiatoxin, administered to male and female rats, caused symptoms of irritation, dullness, tremors, and convulsions. Furthermore,

significant inhibition of brain acetylcholinesterase activity was observed in both acute and subacute treated animals indicating an effect on nerve synapses. Thirteen of 20 *S. maydis* isolates from maize grown in different regions of South Africa produced diplodiatoxin when cultured in potato dextrose broth with some cultures producing a "high amount" of the compound.[59] Diplodiatoxin was dismissed as the "main toxic principle" or "unknown toxin" produced by *S. maydis* based on experiments in which animals received (fed or dosed) culture material from *S. maydis* sterile whole yellow maize seed fermentations.[46,48,49,60,61]

There is much interest in this common pathogen of corn with regard to whether strains in the U.S. produce any of these compounds (**1.16**-**1.18**), as previously reported in South Africa, or other, as-yet unidentified bioactive metabolites. Preliminary tests for antifungal activity, using a traditional paper disk assay, revealed that organic solvent extracts of fermented rice and fermented maize seed cultures inoculated with *S. maydis* and *S. macrospora* inhibited the growth of *A. flavus* and *F. verticillioides*. These extracts also exhibited potent antiinsectan activity in a dietary assay against the fall armyworm (*S. frugiperda*) and significant phytotoxicity in a maize leaf puncture wound assay. Detailed discussion of the occurrences of known *Stenocarpella* metabolites **1.16** – **1.18** and metabolites identified for the first time from *S. maydis* will be presented in Chapter 7.

CHAPTER 2

SCREENING OF ORGANISMS AND KNOWN COMPOUNDS ENCOUNTERED

Collection of fungicolous and/or mycoparasitic fungal isolates from Hawaii, and endophytic fungal isolates from several different parts of the U.S. was carried out by Dr. Donald T. Wicklow and colleagues at the United States Department of Agriculture (USDA) National Center for Agricultural Utilization Research (NCAUR) in Peoria, Illinois. Fungal isolates were maintained on potato dextrose agar (PDA) slants for 14 days at 25 °C. Hyphal-fragment spore suspensions of these isolates served as inocula for solid-substrate fermentations on rice. Fermentation cultures were extracted with EtOAc and the resulting solutions were collected and evaporated to dryness to afford crude extracts, which were tested for antifungal activity against *Aspergillus flavus* (NRRL 6541) and *Fusarium verticillioides* (NRRL 25457). These test species were selected due to their impact on U.S. crops. The fungi *A. flavus* and *F. verticillioides* cause ear rot of corn kernels, produce aflatoxins and fumonisins, and are also known opportunistic human pathogens. Aspergillosis describes a wide variety of diseases caused by *Aspergillus* spp. that most commonly affect the respiratory system, but can also cause infection in other organs in the body. Certain *Fusarium* spp. can also affect the respiratory system (sinusitis), and cause a wide variety of infections that affect the eye (keratitis), and fingernails and toenails (onychomycosis).[62] Both of these classes of compounds are considered important mycotoxins and cause significant economic losses to producers of corn-based food, grain, livestock, and poultry. The extracts were also tested for antiinsectan activity against *Spodoptera frugiperda* (fall army worm), an economically important crop pest that causes damage to corn leaves and ears. Standard disk assays were performed against the gram-positive bacteria *Bacillus subtilis* (ATCC 6051), *Escherichia coli* (ATCC 25922) and *Staphylococcus aureus* (ATCC 29213), as well as

the yeast *Candida albicans* (ATCC 14053). In addition to these assays, the endophytic fungal extracts were evaluated for phytotoxicity using a leaf puncture wound assay on leaves of the commercial maize hybrids Burrus 794sRR and B73 (Table 6). .

Cultures that exhibited activity were fractionated and biological assays were used as a guide in order to aid in the isolation of the active metabolites. Assay results for crude extracts summarized in Tables 5 and 6 were used in conjunction with ^{1}H NMR spectra of the MeCN-soluble portions of the extracts (see below) to prioritize organisms for investigation. Extracts whose NMR spectra showed only the presence of lipids, simple aromatic compounds, or common, well-known fungal metabolites were de-prioritized. Analysis of selected extracts began with solvent partitioning of the extract between MeCN and hexanes. The hexanes-soluble fraction typically contained mostly simple lipids, but such fractions were stored in the freezer in case the source of the biological activity was not found in the MeCN-soluble fraction. If NMR analysis did not lead to de-prioritization of the extract at this stage, the MeCN-soluble fraction was subjected to gravity or flash column chromatography using silica gel, or high pressure liquid chromatography (HPLC) using reversed- or normal-phased columns. Fractions were analyzed by ^{1}H NMR spectroscopy and subjected to further purification if needed. The structures of secondary metabolites obtained through these separation processes were determined using 1D and 2D NMR and HRMS methods. Pure compounds were tested for biological activity in the assays listed above. Known compounds were identified by comparison of NMR and/or MS data with literature values or with NMR spectra in our in-house library of NMR spectra of secondary metabolites isolated from fungi by members of our research group in the past. Details of chemical investigations of new metabolites encountered in these studies are presented in the following chapters.

Table 5. Antifungal and Antiinsectan Bioassay Results for EtOAc Extracts of Mycoparasitic/Fungicolous Fungal Cultures

Organism	Culture number[a]	*A. flavus*[b]		*F. verticillioides*[b]		*S. frugiperda*[c]
		2 days	4 days	2 days	4 days	(% RGR)
Acremonium luzulae	MYC-1799	cz = 33	cz = 33	cz = 23 mz = 23	cz =23 mz = 23	>75
Unidentified	MYC-1840	rg/mz = 23	NA	rg/mz = 21	rg = 23	50
Colletotrichum gloeosporioides	MYC-1875	cz = 33	cz = 29	NA	NA	NA
Fusarium merismoides var. *violaceum*	MYC-1935	cz = 27 mz = 23	cz = 27 mz = 27	cz = 27 mz = 23	cz = 23 mz = 23	NA
Phialemonium curvatum	MYC-2005	NA	NA	mz/rg = 33	rg = 17	100%M
Unidentified	MYC-2054	mz = 23	mz = 21	mz = 23	mz = 19	NA
Penicillium sp.	MYC-2058	mz = 23	mz = 27	mz/rg = 27	mz = 17	75 (67%M)
Acremonium crotocinigenum	MYC-2072	NA	NA	mz = 43	mz = 27	100M
Unidentified	MYC-2181	cz = 23	not read	cz = 23	cz = 17 rg = 21	NA
Bionectriaceae	MYC-2186	mz = 23	not read	NA	rg = 29	75
Gliocladium sp.	NRRL 22971	NA	NA	NA	NA	NT

[a]MYC = Coding for collection of fungicolous and/or mycoparasitic fungi maintained by our collaborators at the ARS, NCAUR, USDA, Peoria, IL.

[b]These assays were performed at a concentration of 500 μg of extract per disk (disk diameter = 12.5 mm), and the diameters of the resulting inhibition zones are given in mm. CZ = clear zone (no growth throughout zone, agar surface to dish bottom); MZ = mottled zone (mosaic of clear zone areas and appearance of patch colony growth, a result of retarded development of individual tiny colonies spread rapidly to fully cover the agar surface); RG = reduced growth (fungus fully covers the agar surface, but colony development suppressed when contrasted with colony development outside the zone of inhibition); NA = not active; NT = not tested.

[c]These assays were performed at a 2000 ppm dietary level; % RGR = % reduction in growth rate relative to controls (%M = % mortality).

Table 6. Antifungal and Antiinsectan Bioassay Results for EtOAc Extracts of Endophytic Fungal Cultures

	Location	Antifungal[a]		Antiinsectan[b]	Leaf Necrosis[c]	
		A. flavus	*F. verticillioides*	*S. frugiperda*	B73	Burrus 794
Stenocarpella maydis						
NRRL 43670	Illinois	37	43	90	0.26	0.78
NRRL 52415	Illinois	NA	41	26	0.40	0.45
NRRL 53563	Illinois	33	25	50	1.41	2.05
NRRL 53565	Illinois	43	43	90 (50 %M)	1.00	1.61
NRRL 53566	Illinois	43	43	90	0.56	1.11
NRRL 53567	Illinois	43	43	90 (10 %M)	0.53	1.10
NRRL 31249	Indiana	33	33	75	2.10	0.50
NRRL 53560	Indiana	37	41	90	1.60	2.00
NRRL 13608	Kentucky	NA	NA	25	1.50	1.74
NRRL 53564	Kentucky	29	27	50	0.56	0.41
NRRL 53561	Nebraska	43	43	90	0.52	1.90
NRRL 53562	Nebraska	43	43	90 (85 %M)	1.01	1.10
NRRL 13609	Unreported (USA)	NA	NA	NA	1.33	2.21
NRRL 13615	Unreported (USA)	37	41	90	0.66	0.81
Stenocarpella macrospora						
NRRL 13610	Costa Rica	NA	NA	25	0.66	0.50
NRRL 13611	Zambia	43	43	90	1.20	0.46
NRRL 13612	Georgia (USA)	NA	NA	50	0.80	0.28
				Oxalic Acid	2.50	2.30

[a]These assays are presented as a clear zone (CZ) and were performed at a concentration of 500 μg of extract per disk (disk diameter = 12.5 mm). The diameters of the resulting inhibition zones are given in mm.

[b]These assays were performed at a 2000 ppm dietary level; recorded as % RGR = % reduction in growth rate relative to control and %M = % mortality.

[c]Leaf puncture wound assays were recorded as average lesion length (mm) of six wounds at 10 μg/5 μL compared with a MeOH:H_2O (50:50) blank and an oxalic acid (5 μg) positive control.

An isolate of *Acremonium luzulae* (MYC-1799), also known as *Gliomastix luzulae*,[63] was obtained from a red irregular growth on the undersurface of a dead hardwood branch collected in Hawaii. The EtOAc extract exhibited antifungal activity against *A. flavus* and *F. verticillioides*, and antiinsectan activity against the fall armyworm. The ^{1}H NMR spectrum of the MeCN-soluble fraction showed a major constituent displaying seven N-methyl singlets and four amide doublets, suggesting that the major component was a peptide that contained at least 11 amino acid residues. Analysis of the ^{1}H NMR and LRESIMS data, along with a database search led to the identification of this major metabolite as the known compound cyclosporin C (**2.1**).[64] Cyclosporins are well-known as important fungal metabolites. Cyclosporin A is a clinically useful immunosuppressive agent,[10] and has been reported to have antiinsectan activity.[65] Interestingly, it has also been reported that compound **2.1** is the only cyclosporin produced by an isolate of *A. luzulae* obtained from a different source.[66] Although compound **2.1** was identified by initial analysis of the MeCN-soluble fraction, other NMR signals were evident so the extract was subjected to vacuum liquid chromatography (VLC) using silica gel to afford several fractions. Fraction seven eluted with the 100% MeOH wash and consisted of a nearly pure sample of mevalonolactone (**2.2**), a commonly encountered fungal metabolite that exists in equilibrium with mevalonic acid.[67] Compound **2.1** has been reported to be active against a number of phytopathogenic fungi, but not against bacteria or yeasts.[66] Compound **2.2** is also a known antifungal agent.[68] Although these compounds were not tested in our antifungal assays, compound **2.1** and **2.2** are likely to be responsible for the antifungal activity observed for the crude extract.

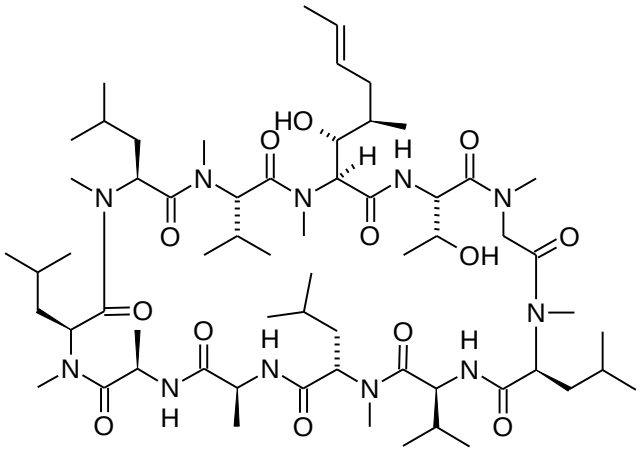

2.1

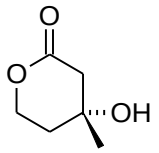

2.2

An unidentified fungal isolate (MYC-1840) isolated from the black stromata of a pyrenomycete found on a dead hardwood branch in Hawaii exhibited antifungal activity against *A. flavus* and *F. verticillioides*, as well as antiinsectan activity against the fall armyworm. The MeCN layer from the partition of the EtOAc extract was fractionated using silica gel VLC. The fifth fraction, eluting with 40:60 EtOAc-hexanes, consisted mainly of the known heptaketide scytalol A (**2.3**), which was identified by analysis of ^{1}H NMR and HMBC data, along with a database search. Compound **2.3** was originally isolated from a *Scytalidium* sp. and selectively inhibited dihydroxynapthalene (DHN) melanin biosynthesis in agar cultures of *Lachnellula* sp. (100 μg/disk).[69] Melanins are pigments that have been associated with the survival of fungal species by protecting the organisms against heat stress, chemical stress, and other pathogenic microorganisms.[70] DHN-melanin pathway inhibition has been linked to virulence in phytopathogenic fungi, such as *Magnaporthe grisea*, the rice blast disease fungus. Inhibition of melanin biosynthesis allows for a decrease in virulence of these organisms, and minimizes the production of plant appressoria, or needlelike "pegs" that are necessary for phytopathogenic fungi to penetrate plant leaves.[71] Unfortunately, due to sample

limitations, compound **2.3** could not be tested in our assays, and the source of the antifungal and antiinsectan activity of the EtOAc extract was not determined.

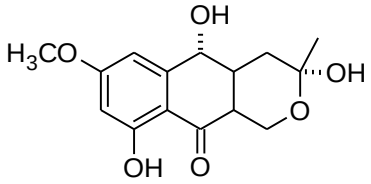

2.3

An isolate of *Colletotrichum gloeosporioides* (MYC-1875) was obtained from a basidioma of *Pycnoporus sanguineus* found on a dead hardwood branch in Hawaii. The EtOAc extract of solid-substrate fermentation cultures of this isolate showed antifungal activity against *A. flavus*. The MeCN-soluble portion of the EtOAc extract was fractionated using silica gel column chromatography, and fractions eluting with 10% MeOH/EtOAc were found to contain the major component acremoauxin B (**2.4**) and the minor component acremoauxin A (**2.5**) by comparison of ESIMS, ^{1}H NMR and ^{13}C NMR spectral data with literature values. Compound **2.4** was previously described by our group as a metabolite of *C. gloeosporioides*,[72] and compound **2.5**, a known plant-growth inhibitor, was previously isolated from *Acremonium roseum*.[73] The two structures are closely related with the only difference being that the sugar unit in **2.4** is a hexitol unit instead of a pentitol. Compound **2.4** was found to be inactive against *A. flavus*.[72] Compound **2.5** was present as a minor constituent in the same fraction as compound **2.4**. Efforts to isolate this analogue were not undertaken, and the source of the antifungal activity observed against *A. flavus* was not determined. *C. gloeosporioides* has been reported to produce colletotric acid, an antimicrobial agent.[74] However, this metabolite was not encountered during our investigation.

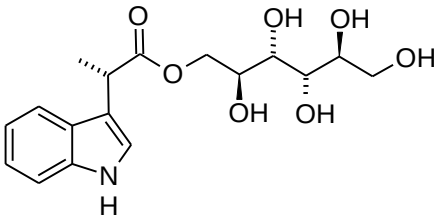

2.4

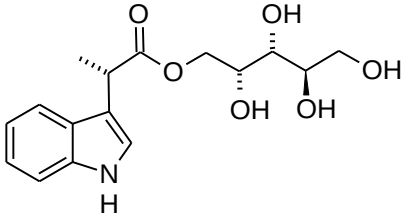

2.5

An isolate of *Fusarium merismoides* var. *violaceum* (MYC-1935) was obtained from the black stromata of a pyrenomycete found on a dead hardwood branch in Hawaii. The EtOAc extract of solid-substrate fermentation cultures of this isolate showed antifungal activity against *A. flavus* and *F. verticillioides*. The MeCN-soluble fraction was subjected to VLC using silica gel. The tenth fraction, eluting with the 100% MeOH wash, was further separated using reversed-phase HPLC. Analysis of ^{1}H NMR and HRESIMS data, along with a database search led to the identification of this metabolite as the known cyclic depsipeptide acuminatum A (**2.6**), also known as antibiotic CDPC 3510A.[75] Compound **2.6** was originally isolated from *Fusarium roseum*, and other *Fusarium* spp. including *F. acuminatum, and F. tricinctum*. This compound has been reported to possess antifungal properties and is likely responsible for the antifungal activity of the EtOAc extract but was not tested in our assays.[76]

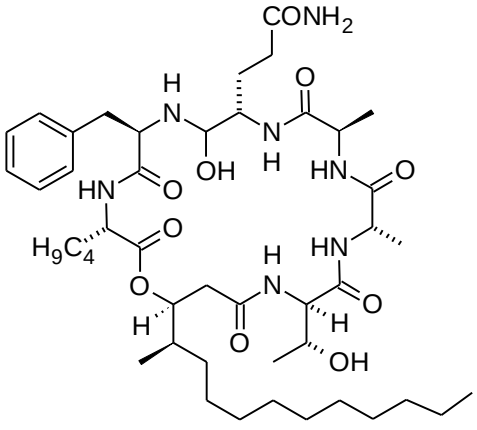

2.6

The EtOAc extract of cultures of an unidentified fungal isolate (MYC-2054) obtained from a basidioma of *Rigidoporus microsporus* found on a dead hardwood branch in Hawaii showed antifungal activity against *A. flavus* and *F. verticillioides.* Analysis of the MeCN-soluble fraction by ^{1}H NMR led to the identification of the major component as the known compound nicotinic acid (**2.7**), also known as niacin or vitamin B_3. In high doses, compound **2.7** exhibits antifungal properties. In a previous report by our group, compound **2.7** caused a 30-mm zone of inhibition in disk assays against *F. verticillioides* at 250 μg/disk, but was not active against *A. flavus*.[77] Because the ^{1}H NMR spectrum of the MeCN-soluble fraction contained mostly nicotinic acid and lipids, this extract was not pursued further.

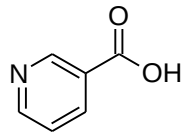

2.7

The EtOAc extract of fermentation cultures of a *Penicillium* sp. (MYC-2058) isolated from a basidioma of *Trametes hirsutum* found on a dead hardwood branch in Hawaii showed antifungal activity against *A. flavus* and *F. verticillioides,* and potent antiinsectan activity against the fall armyworm. The antiinsectan activity could be explained by the presence of large quantities of the known compound sterigmatocystin (**2.8**), which is a well-known polyketide metabolite originally isolated from *Aspergillus versicolor*.[78,79] Compound **2.8** is a biogenetic precursor of aflatoxins, is structurally similar to aflatoxin B1, and has many of the same carcinogenic, mutagenic, and teratogenic properties. The source of the antifungal effects observed was not determined.

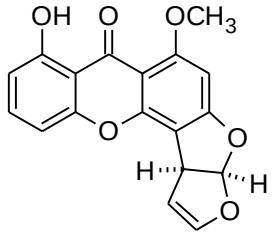

2.8

The EtOAc extract of an isolate of *Acremonium crotocinigenum* (MYC-2072) obtained from a basidioma of *Phellinus gilvus* found on a dead hardwood branch in Hawaii exhibited antifungal activity against *F. verticillioides* and antiinsectan activity against the fall armyworm. The MeCN-soluble fraction was subjected to silica gel column chromatography leading to the identification of four known compounds, two of which have been previously reported by our group.[13] Fraction 6 eluted with 50% EtOAc/hexanes and was identified as a sample of 6,8-dimethoxy-4,5-dimethyl-3-methyleneisochroman-1-one (**2.9**). Fraction 7 eluted with 60% EtOAc/hexanes and was identified as a mixture of compound **2.9** and compound **2.10**. Fraction 9 eluted with 80% EtOAc/hexanes and afforded 5,7-dimethoxy-3,4-dimethyl-3-hydroxyisobenzofuranone (**2.11**). Fraction 10 eluted with 90% EtOAc/hexanes and yielded compound **2.12**. The absolute configuration of compounds **2.9** and **2.10** was proposed by analysis of CD spectra in comparison with model compounds, which led to the assignment of the 4*S* configuration of compound **2.9** and 3*R* configuration of compound **2.10**.[80] Neither the relative nor the absolute configuration of compound **2.12** was determined. Compound **2.9** exhibited antifungal effects against *F. verticillioides*, showing a 33-mm zone of inhibition at 100 μg/disk and is deemed to be responsible for the antifungal effects observed. This compound was inactive when tested against *B. subtilis*, *E. coli*, *S. aureus*, and *C. albicans*.[13] The source of the antiinsectan activity of the crude extract was not determined.

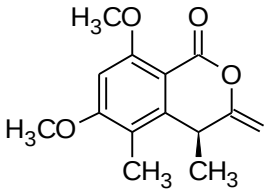

2.9

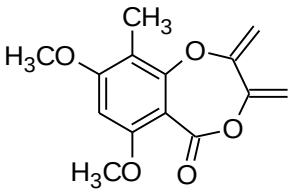

2.10

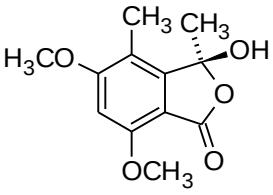

2.11

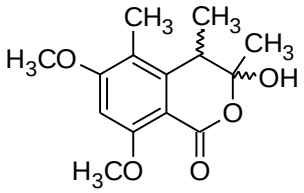

2.12

Extracts of cultures of an additional unidentified fungal isolate (MYC-2181), also obtained from a basidioma of *Phellinus gilvus* found on a dead hardwood branch in Hawaii, showed antifungal activity against *F. verticillioides* and *A. flavus.* In this instance, NMR analysis of the crude extract showed the presence of large quantities of mycophenolic acid (**2.13**), a well-known and widely occurring fungal metabolite known to display antifungal activity. Thus further studies of this extract were not pursued.

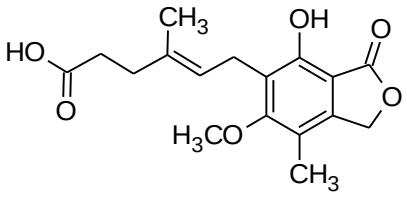

2.13

Although the fungal metabolites described briefly in this chapter are known compounds, the diversity of the metabolites encountered nicely highlights the wide range of structure-types that can be produced by fungi from these habitats. The next five chapters will discuss studies of additional fungicolous, mycoparasitic, and endophytic fungal isolates that led to the isolation, characterization, and biological activities of both new and additional known secondary metabolites of varying structural classes.

CHAPTER 3
CHEMICAL INVESTIGATION OF A FUNGICOLOUS FUNGUS FROM THE FAMILY BIONECTRIACEAE

Mycoparasitic and fungicolous fungi continue to serve as productive sources of new bioactive natural products.[81-83] In the course of our ongoing studies of such fungi, a fungicolous fungal isolate (MYC-2186 = NRRL 54009) was obtained from a basidioma of *Phellinus gilvus* found on a decaying hardwood branch on the island of Hawaii. Basidiomata are club-shaped, fleshy structures responsible for the production of spores of many basidiomycete fungi including mushrooms. This fungicolous isolate was identified as a mitosporic fungus of the family Bionectriaceae with a 98% match to the chemically unexplored species *Stilbocrea macrostoma.* This evaluation was based on partial sequence analysis of the internal transcribed spacer region (ITS) and domains D1 and D2 of the nuclear large subunit (28S) rDNA gene using ITS5 and NL4 as polymerase chain reaction and sequencing primers via a nucleotide-to-nucleotide BLAST query of the GenBank database.[84,85] Although sequence analysis did not enable identification of this isolate to species with 100% certainty, most of the taxa that comprise the Bionectriaceae are relatively unexplored from a chemical standpoint.[86,87] Since DNA sequence analysis did not allow for identification of this species, the fungus is described here only as a member of the family Bionectriaceae.

Solid-substrate fermentation cultures of this isolate were grown by our collaborators at the ARS, NCAUR, USDA in Peoria, Illinois using the fermentation conditions described in Chapter 2. The EtOAc extract of the resulting solid-substrate fermentation cultures exhibited antifungal and antiinsectan activity and was partitioned between hexanes and MeCN. The MeCN-soluble fraction was separated by silica gel column chromatography and reversed-phase HPLC, leading to the isolation of the major component, a new 10-residue linear peptide named bionectrin A (**3.1**), along with the

known compounds guaiane mannoside (**3.2**)[88] and pseurotin A (**3.3**),[89] and three chlamydocin analogues *cyclo*[-Aib-S-Phe-R-Pro-S-Aoh-] **(3.4)**,[90] *cyclo*[-D-Pro-Phe-Iva-(9*R*)-Aoh-] (**3.5**),[91] and *cyclo*[-L-Asu-Aib-L-Phe-D-Pro-] (**3.6**),[92] which contain aminoisobutyric acid (Aib), 2-amino-8-oxo-9-hydroxydecanoic acid (Aoh), aminosuberic acid (Asu), isovaline (Iva), phenylalanine (Phe), and proline (Pro) amino acid units.

The molecular formula of compound **3.6** was determined to be $C_{26}H_{36}N_4O_6$ (11 units of unsaturation) on the basis of HRESIMS data. The ^{1}H NMR spectrum of **3.6** contained resonances in the aromatic and alpha proton regions that were characteristic of a Phe unit. A database search[86] was performed using this information, leading to the identification of this metabolite as the known compound *cyclo*[-L-Asu-Aib-L-Phe-D-Pro-] (**3.6**).[92] The MS and ^{1}H NMR data obtained for this sample matched the literature values.

The ^{1}H NMR spectrum of compound **3.4** resembled that of **3.6**, including the presence of signals for Phe and Pro moieties. The molecular formula of **3.4** was determined to be $C_{29}H_{42}N_4O_6$ (11 units of unsaturation) on the basis of HRESIMS data. A database search[86] was again performed, and again led to the identification of the compound in this case as *cyclo*[-Aib-S-Phe-R-Pro-S-Aoh-] **(3.4)**.[90] The MS and ^{1}H NMR data for the sample from the MYC-2186 extract again matched the literature values.

Compound **3.5** was identified by comparison of its ^{1}H NMR data with those obtained for **3.4**, together with a database search. The ^{1}H NMR spectrum of **3.5** lacked the methyl triplet and methylene resonances observed in the ^{1}H NMR spectrum for **3.4**, and contained an additional methyl singlet near δ_H 1.5. These data suggested that the Iva unit of **3.4** was replaced by an Aib unit in **3.5**. Further database searching[86] using this information enabled identification of **3.5** as *cyclo*[-D-Pro-Phe-Iva-(9*R*)-Aoh-] (**3.5**).[91]The ^{1}H NMR data were consistent with literature values.

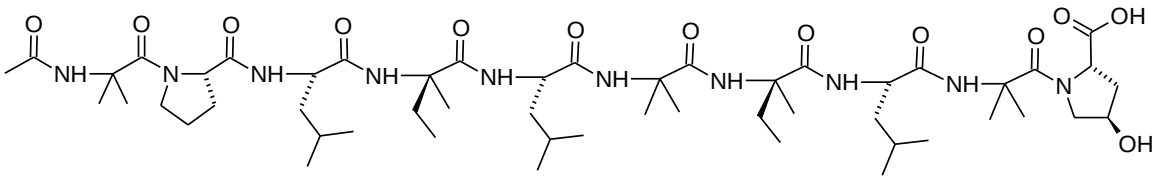

3.1

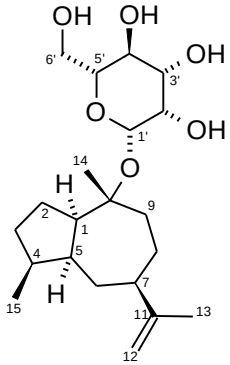

3.2

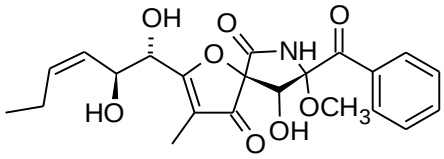

3.3

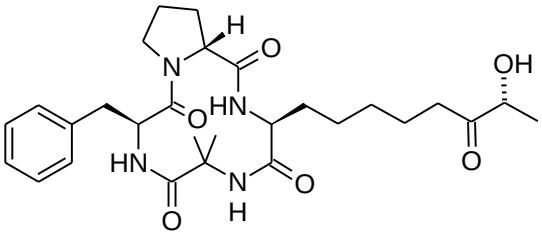

3.4

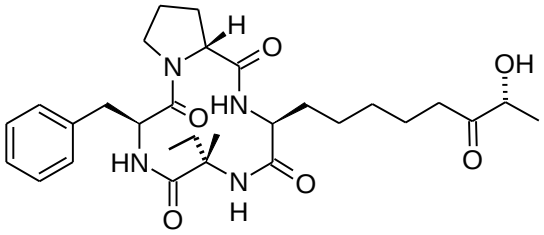

3.5

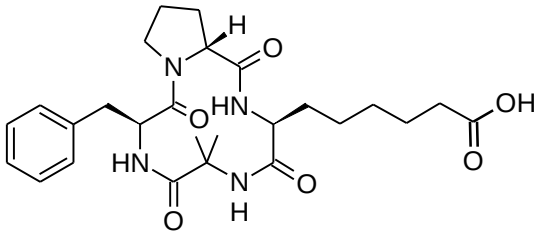

3.6

Compounds **3.5** and **3.6** are known synthetic analogues of the naturally occurring chlamydocins,[91,92] but have not been previously reported as natural products. Chlamydocins are naturally occurring cyclic tetrapeptides that are potent inhibitors of histone deacetylase (HDAC). It has been reported that histone acetylation and deacetylation play a key role in gene transcription regulation and induction of apoptosis in cells, and may be useful targets for the development of cancer treatments.[93] Compound **3.4** has been isolated from the fungus *Verticillum coccosporum.*[90] It is somewhat interesting that cyclic peptides **3.4** and **3.6** contain Aib, since nearly all naturally-occurring Aib-containing peptides described in the literature are linear.

The structure of guaiane mannoside (**3.2**) was independently determined by detailed analysis of 2D NMR data, but the structure appeared in the literature in a report from another laboratory soon thereafter. Details of the isolation and structure determination of compounds **3.1** and **3.2** are presented here.

Structure Elucidation of Bionectrin A (**3.1**)

Bionectrin A (**3.1**) eluted from the silica gel column with the 100% MeOH wash and was obtained as the major component of an inseparable mixture that contained trace homologues and/or conformers. This polar compound had poor solubility properties in medium-polarity solvents, and the use of $CDCl_3$ for ^1H NMR analysis resulted in overlap and broadening of most signals. However, it was evident from the initial ^1H NMR data that **3.1** was peptidal in nature. Efforts to obtain better-resolved or sharpened ^1H NMR signals using other solvents, including acetone-d_6 and pyridine-d_5, as well as thorough variable-temperature NMR experiments were not successful. Use of CD_3OD ultimately provided the best ^1H NMR profile, although a number of the signals remained broad and the resulting exchange of amide protons also reduced the number of useful signals. The apparent presence of minor homologues and/or conformers and overlapping signals in 1D

and 2D NMR spectra rendered the data difficult to interpret. Efforts to separate these conformers and/or homologues were undertaken, and a portion of the fraction was subjected to RP-HPLC. When a single, sharp, well-resolved major peak in the chromatogram was collected and re-injected, the chromatogram showed the same profile as the original fraction. The return of one peak to the same chromatographic profile with multiple peaks confirmed the presence of other inseparable conformers in the mixture.

The molecular formula of **3.1** was determined to be $C_{52}H_{90}O_{13}N_{10}$ (13 units of unsaturation) on the basis of HRESIMS data. ^{13}C and DEPT-135 NMR data were collected and confirmed the presence of 52 carbons, including 11 amide or ester carbonyls, five quaternary sp^3 carbons, 17 methyls, 10 methylenes, and nine methines. The ^1H NMR spectrum contained resonances suggestive of the peptaibol-type family of peptides, which are generally characterized by three primary structural features: an acylated N-terminus, a high content of α,α-dialkylated amino acids, particularly α- Aib, and a C-terminal amino alcohol unit. The ^1H NMR data for **3.1** contained an acetyl group signal at δ_H 2.06 (possibly indicating an acylated N-terminus) and a cluster of methyl singlets at *ca.* δ_H 1.5 that are diagnostic for α,α-dialkylated amino acids such as Aib. Peptaibols are produced by a non-ribosomal biosynthesis process involving very large protein complexes that possess different peptide synthetases that bind, activate, and condense a variety of amino acids to form the peptide.[94,95] The peptaibol backbone is generally helical due to the presence of multiple Aib residues. Peptaibols can be grouped according to the number of amino acid residues, with long-sequence peptaibols containing 18-20 residues, and short-sequence peptaibols containing 11-16 residues.[96] Long-sequence peptaibols typically display antibacterial, antifungal, and/or antiviral activity by virtue of their membrane-pore-forming abilities (see below), whereas short-sequence peptaibols have a narrower range of activities due to the apparent inability to span across the lipid bilayer.[97] It has been proposed that short-sequence peptaibols that do show bioactivity might stack pairwise, with peptaibols containing 11-residues

suggested as the minimum length necessary for the production of structures long enough to span the bilayer.[98]

Peptaibols that exhibit antibacterial and antifungal properties have been suggested as possible pharmaceutical agents for treatment of antibiotic-resistant infections due to their membrane insertion and pore-forming abilities by barrel stave, carpet, or torroidal-pore mechanisms.[97,99,100] The carpet model (Figure 3.1a) explains the activity of antimicrobial peptides such as the 18-residue peptide ovispirin.[101,102] At very high concentrations, peptides aggregate on the membrane surface in a carpet-like manner and disrupt the bilayer by penetrating into the membrane, leading to the formation of micelles. In the barrel-stave model (Figure 3.1b), peptide helices form a bundle and insert into the membrane bilayer with the hydrophobic peptide regions along the core of the lipid bilayer and hydrophilic regions forming the interior of the pore. One barrel-stave example is a pore induced by the best-known peptaibol, alamethicin,[103] a 20-amino acid residue-containing antibiotic produced by the fungus *Trichoderma viride*.[99] Alamethicin forms voltage-dependent channels across lipid bilayer membranes for the permeabilization of mitochondria.[104,105] Mitochondrial membrane permeabilization (MMP) is responsible for cell survival or cell death. Inhibition of MMP would prevent unwanted cell death, whereas induction of MMP in tumor cells constitutes a goal of cancer treatments.[101] The torroidal model (Figure 3.1c) is similar to the barrel-stave model since both incorporate helical peptide bundles inserted into the membrane, but differ because the peptides are always associated with the lipid head groups and not the lipid core region when inserted into the bilayer.[99] The internal diameter of pores formed by peptaibols can be varied by controlling the sequence and number of amino acids in the peptide to allow for efficient transport of ions, H_2O, and larger molecules.[106]

The molecular formula of the peptide encountered here was suggestive of a peptaibol with a size on the low end of the short-sequence peptaibol range. In addition to the cluster of Aib methyl singlets, the ^{1}H NMR spectrum of **3.1** contained typical amino

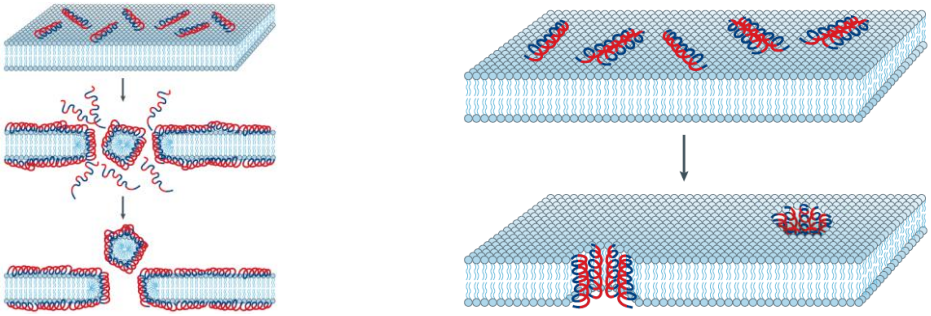

a. Carpet Model

b. Barrel-Stave Model

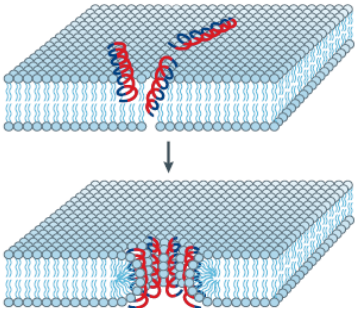

c. Torroidal Model

Figure 3. Models of Antimicrobial-Peptaibol-Induced Cell-Killing Mechanism[99]

acid α-proton signals in the region between δ_H 3.5-4.5, β- and γ-proton signals in the region between δ_H 1.5-2.5, and an upfield methyl cluster near δ_H 1.0. Because of the broad, overlapping signals in the ^{1}H NMR spectrum, the ^{1}H NMR data alone could not be used to assign the identity of all amino acid residues contained in **3.1**. Thus, GC-MS analysis of *N*-trifluoroacetyl-*n*-butyl (*N*-TFA-*n*-butyl) ester derivatives of the constituents obtained upon hydrolysis, a common method for amino acid analysis, was employed to determine the identity of the remaining amino acid residues in the peptide. The protocol for preparation of these derivatives is summarized in Figure 4. In some cases, NMR data

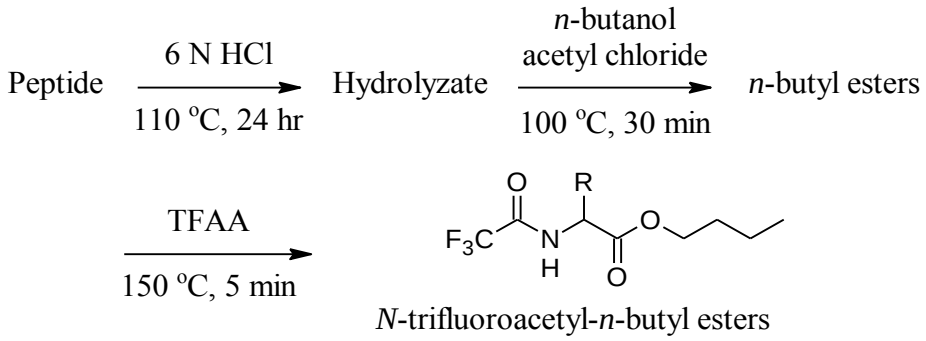

Figure 4. Peptide Hydrolysis and Amino Acid Derivatization Scheme

for **3.1** in combination with these GCMS data were helpful in clearing up minor ambiguities at this stage. For example, both GC-MS and ^{13}C NMR data for Iva and Aib, including the two upfield shifted δ-CH_3 units of Iva, were useful in the assignment of the Iva and Aib units contained in **3.1**. In addition, leucine (Leu) and 4-hydroxyproline (Hyp), could be distinguished from possible isomers by comparison of the α-proton region of the ^{1}H NMR spectrum and ^{13}C NMR data to literature values for such units.[107] The α-proton of each Leu residue appeared as a dd in the ^{1}H NMR spectrum, thus **3.1** was determined to contain Leu rather than isoleucine residues. The hydroxy group of Hyp was determined to be located at the γ-position instead of the β-position because the α-proton appeared as a triplet in the ^{1}H NMR spectrum, requiring a methylene unit at the β-position, and the chemical shifts of the protons of the δ-CH_2 unit (δ_H 3.62 and 3.83) required linkage of the δ-CH_2 unit to the N atom of Hyp.

The amino acid composition of **3.1** was determined by GC-MS analysis of the *N*-TFA-*n*-butyl esters of the amino acids present in the acid hydrolyzate of **3.1** and comparison to similarly derivatized amino acid standards. Analysis of the data confirmed the presence of Aib, Leu, Hyp, and Pro, as expected on the basis of the NMR data, and

allowed for the identification of two Iva units that were also present in **3.1** by comparison to NMR and HRESIMS data.After the amino acid composition had been determined, TOCSY NMR data were collected and analyzed to determine the ^{1}H NMR chemical shift values of the protons contained in each amino acid spin-system (Table 7). After these assignments were made, HMBC data were collected and analyzed in an attempt to determine the sequence of the amino acid residues in **3.1**. These data were analyzed for three-bond correlations between α-proton signals and the corresponding amide carbonyl carbons of their acylating units. Although some intraunit correlations were observed from α-protons to β- and γ-carbons, a number of correlations in the methyl regions as well as the amide carbonyl carbon regions were overlapping. More importantly, no interunit correlations were observed between α-proton signals and the corresponding amide carbonyl carbon of the acylating units, rendering the HMBC data inadequate for sequencing the peptide. Therefore, an alternative method, high resolution electrospray ionization time-of-flight tandem mass spectrometry (HRESITOFMSMS) analysis, was pursued.

The negative-ion high resolution electrospray ionization time-of-flight mass spectrometry (HRESITOFMS) data for **3.1** showed an $(M–H)^-$ ion while the positive-ion data showed an $(M+Na)^+$ ion. The negative ion HRESITOFMSMS data showed a series of ions derived from fragmentation of the $(M-H)^-$ ion at *m/z* 1061.6587. This pattern did not provide clear sequencing information for **3.1** except for the presence of a loss of Hyp-OH (131.0538), suggestive of its incorporation as a terminal unit. No fragmentations considered useful were observed below *m/z* 690.4930. The positive ion HRESITOFMSMS data provided much more useful fragmentation information. Figure 5 shows a key series of HRESITOFMSMS fragmentation results measured for *m/z* 932.6215 $(M-Hyp-OH)^+$, with sequential losses of Aib (85.0512), Leu (113.0854), Iva (99.0675), Aib (85.0518), Leu (113.0859), Iva (99.0696), and Leu (113.0842), which allowed for the assignment of the partial sequence Leu-Iva-Leu-Aib-Iva-Leu-Aib-Hyp.

Table 7. NMR Data for Bionectrin A (**3.1**) in CD_3OD

residue	position	δ_H (mult., J_{HH})[a]	δC[b]	HMBC[a]
Ac	C=O	-	172.9	-
	CH_3	2.06 (s)	22.6	172.9
Aib-1	C=O	-	175.1	-
	α	-	57.5	-
	β_1-CH_3	1.51 (s)	25.7	57.5, 175.1, 22.5
	β_2-CH_3	1.46 (s)	23.8[d]	57.5, 175.1
Pro	C=O	-	176.5	-
	α-CH	4.32 (m)	65.2	27.1, 30.1, 176.5
	β_1-CH_2	2.39 (m)	30.1	50.1, 65.2, 176.5
	β_2-CH_2	1.78 (m)		50.1, 65.2, 176.5
	γ_1-CH_2	2.03 (m)	27.1	50.1, 65.2
	δ_1-CH_2	3.94 (m)	50.1	27.1, 30.1, 65.2
	δ_2-CH_2	3.50 (m)		30.1
Leu-1	C=O	-	174.6	-
	α-CH	3.71 (dd, 9.5, 8.4)	62.9	27.6, 36.4, 174.6
	β_1-CH_2	1.64 (m)	27.6	15.9
	β_2-CH_2	1.25 (m)		10.9, 15.9
	γ-CH	2.10 (m)	36.4	-
	δ_1-CH_3	0.99 (d, 6.8)	15.9	27.6, 36.4
	δ_2-CH_3	0.96 (d, 6.4)	10.9	27.6, 36.4, 62.9
Iva-1	C=O	-	178.2	-
	α	-	60.5	-
	β-CH_3	1.44 (s)	23.7[d]	60.5, 178.2
	β-CH_2	2.33 (m)	26.6	7.6, 60.5
	δ-CH_3	0.84 (d, 7.6)	7.6	26.6, 60.5
Leu-2[f]	C=O	-	175.9	-
	α-CH	4.02 (dd, 10, 5.2)	56.1	26.0, 40.7, 175.9
	β_1-CH_2	1.75 (m)	40.7[e]	56.1
	β_2-CH_2	1.64 (m)		-
	γ-CH	1.78 (m)	26.0	-
	δ_1-CH_3	0.95 (d, 6.4)	23.3	26.0, 40.7
	δ_2-CH_3	0.89 (d, 6.4)	21.8	23.3, 26.0, 40.7
Aib-2[g]	C=O	-	177.6	-
	α	-	57.8	-
	β_1-CH_3	1.55 (s)	26.9	57.8, 177.6
	β_2-CH_3	1.48 (s)	26.6	57.8, 177.6
Iva-2	C=O	-	176.7	-
	α	-	61.5	-
	β-CH_3	1.49 (s)	20.8[c]	33.9, 61.5
	β-CH_2	1.88 (m)	33.9	8.6, 61.5, 176.7
	δ-CH_3	0.93 (d, 7.6)	8.6	33.9, 61.5

Table 7-continued

Leu-3[f]	C=O	-	174.6	-
	α-CH	4.21 (dd, 2.9, 12.3)	54.2	40.9
	β_1-CH_2	1.95 (m)	40.9[e]	-
	β_2-CH_2	1.64 (m)		-
	γ-CH	1.87 (m)	24.1	-
	δ_1-CH_3	0.94 (d, 6.4)	23.7[d]	24.1
	δ_2-CH_3	0.86 (d, 7.6)	20.6[c]	24.1
Aib-3[g]	C=O	-	174.6	-
	α	-	57.9	-
	β_1-CH_3	1.55 (s)	25.6	25.5, 57.9
	β_2-CH_3	1.53 (s)	25.5	25.6, 57.9
Hyp	C=O	-	179.6	-
	α-CH	4.45 (t, 8.2)	63.6	38.0, 179.6
	β_1-CH_2	2.15 (m)	38.0	-
	β_2-CH_2	1.95 (m)		179.6
	γ-CH	4.38 (br s)	71.8	-
	δ_1-CH_2	3.83 (m)	57.5	71.8
	δ_2-CH_2	3.68 (m)		

[a]Recorded at 600 MHz.

[b]Recorded at 100 MHz.

[c-g]Assignments marked with the same letter are interchangeable.

Unfortunately, there were no further fragments observed below *m/z* 225.1239 that would enable the remaining units to be located. Considering the high resolution mass values together with the amino acid composition, we determined that the remaining unassigned units included the acetyl unit, one Aib residue, and one Pro residue. There are two possible sequences for these three units: Ac-Pro-Aib and Ac-Aib-Pro. The major MSMS fragment-ions were further fragmented, and MS^n data were collected (n=3-5), but unfortunately, no useful fragmentations were observed below *m/z* 225. With the two sequences in mind, the HMBC data were analyzed once more to determine if a three-

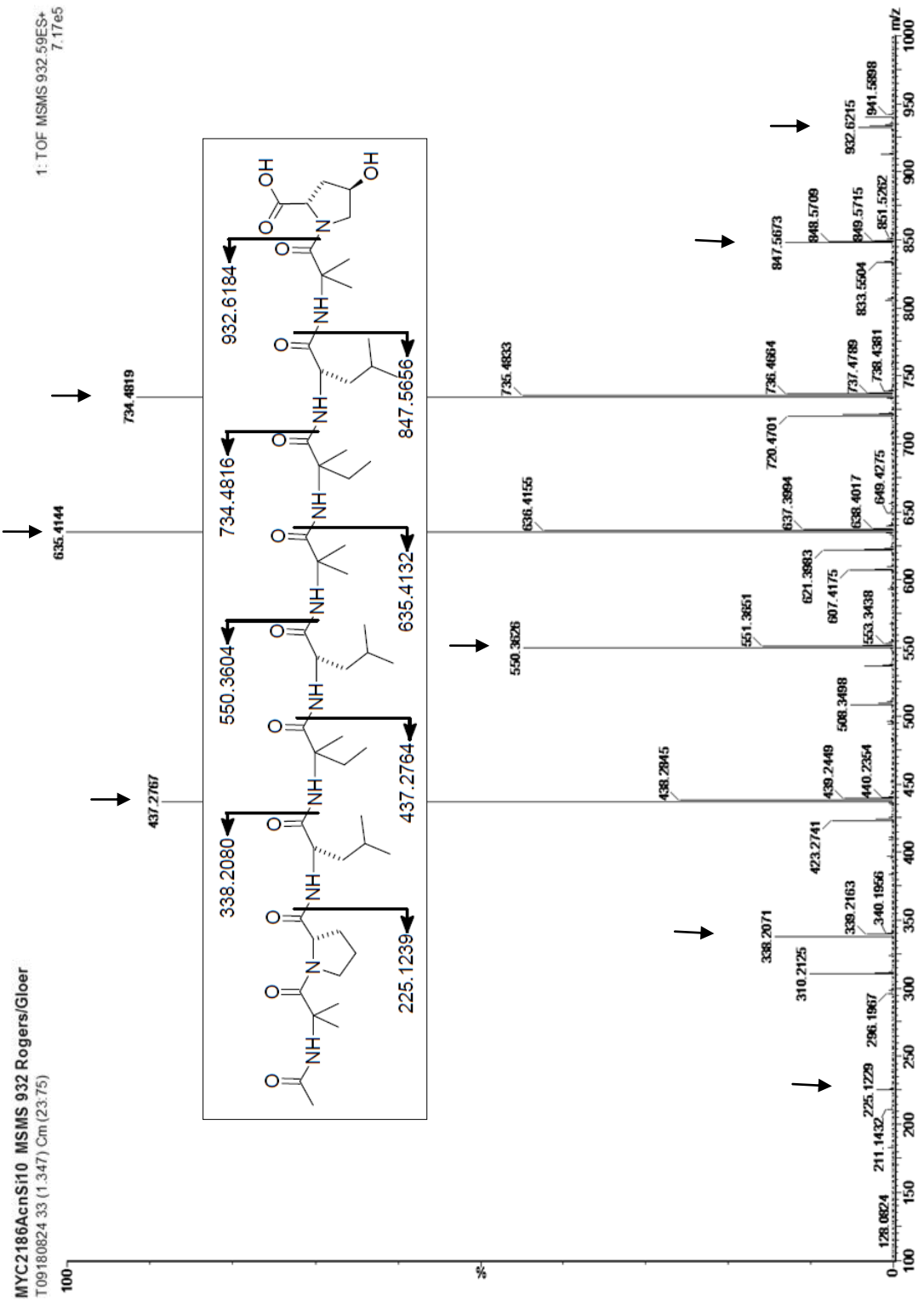

Figure 5. HRESITOFMSMS Fragmentation of *m/z* 932 Ion $(M\text{-}Hyp)^{+}$ of Bionectrin A

bond correlation was observed between the α-CH or δ-CH_2 of Pro to the carbonyl of the acetyl unit. Unfortunately, no correlations to the acetyl carbonyl unit were observed aside from that of the acetyl methyl group. Further 2D NMR data were collected and analyzed, including ROESY and NOESY data, to determine if a through-space ^{1}H-^{1}H correlation could be observed between the Ac unit and the methyl groups of an Aib unit, suggesting the sequence Ac-Aib-Pro, or between the Ac unit and protons of the Pro unit, suggesting the sequence Ac-Pro-Aib, but unfortunately, these data were also inconclusive.

Because MSMS, HMBC, NOESY, and ROESY data were not helpful for completing the sequence and a significant amount of sample was available, ^{1}H-^{15}N NMR HMBC data were collected in an effort to determine the remainder of the sequence. In this case, the data were examined for the presence of correlations between the acetyl CH_3 group at δ_H 2.06 to the ^{15}N signal of either the Pro or Aib units. Upon analysis of the data, clear correlations were observed of one ^{15}N signal (δ_N 138) to the acetyl CH_3 group (δ_H 2.06) as well as to two methyl singlets (δ_H 1.46 and δ_H 1.51) located in the Aib proton region, indicating that the Aib unit was the unit acylated by the acetyl group. These data allowed for the identification of the remaining fragment as Ac-Aib-Pro, and the amino acid sequence of the new peptide **3.1** was therefore assigned as Ac-Aib-Pro-Leu-Iva-Leu-Aib-Iva-Leu-Aib-Hyp.

Since the N-terminus was acylated and each amino acid residue in the sequence had been identified, the next step was to verify that a free carboxylic acid was present at the C-terminus. Compound **3.1** was treated with trimethylsilyldiazomethane (TMS-CHN_2) and ^{1}H NMR data for the product were collected using CD_3OD as the solvent. The data for the product contained a methyl singlet at δ_H 3.70 for the newly formed methoxy group, confirming that **3.1** possesses a free carboxylic acid group. This result indicates that **3.1** lacks the reduced C-terminal amino alcohol that is characteristic of most of the known peptaibols.

At this point, the absolute configuration of the amino acid residues (except for Aib, which lacks a stereocenter), remained to be assigned. *N*-TFA-(±)-2-butyl ester derivatives can be used not only for identification of the amino acid composition, but also the absolute configuration of amino acids using GCMS. *N*-TFA-(±)-2-butyl esters were prepared under the same conditions as described in Figure 4 to form diastereomers, and the resulting mixture was analyzed by GC-MS. The data revealed that all but one pair of the *N*-TFA-(±)-2-butyl esters were well-resolved by GC and the amino acid composition was consistent with the results obtained using *N*-TFA-*n*-butyl derivatives. Only the Iva derivatives failed to resolve. A standard sample of *N*-TFA-(±)-2-butyl Iva esters was prepared, and attempts were made to resolve the diastereomers using a chiral GC column (25-m Chirasil-Val), but unfortunately, the peaks again did not resolve, so another method for analysis of Iva was ultimately necessary (see below).

The amino acid composition of **3.1** was identified using GCMS as described earlier in the chapter, and included Iva, Leu, Pro, Hyp, and Aib. The *N*-TFA-(±)-2-butyl ester derivatives of standards of the amino acids in the acid hydrolyzate of bionectrin A were prepared using all possible stereoisomers and analyzed using GCMS. The identity of each peak was confirmed by comparison of the TIC (total ion current) chromatograms of the *N*-TFA-(±)-2-butyl derivatives to *N*-TFA-(*S*)-(+)-2-butyl ester derivatives prepared using either the D- or L-amino acid standards. As shown in Figure 5, the detector response was different for each *N*-TFA-2-butyl ester, and particularly weak for the Iva derivative, as illustrated by the fact that equivalent concentrations of all of the derivatives were used to generate the chromatogram shown. The *N*-TFA-(*S*)-(+)-2-butyl ester derivatives of the amino acids from the hydrolyzate of peptide **3.1** (Figure 7) were prepared, analyzed, and compared to the standards (Figure 6). Upon analysis, the amino acids in **3.1** were determined to include L-Leu, L-Pro, and *trans*-4-OH-L-Pro. This was confirmed by a 1:1 coinjection of the derivatized bionectrin A (**3.1**) hydrolyzate and the

D- and L-amino acid standards (Figure 8) resulting in the peaks corresponding to the L-isomers in each case.

The absolute configuration of the Iva units remained in question because efforts to resolve the D- and L-Iva N-TFA-(*S*)-(+)-2-butyl esters by GC, including chiral GC, were unsuccessful. A search of the literature led to a report of the successful resolution of derivatized Iva isomers by HPLC using the modified Marfey's reagent 1-fluoro-2,4-dinitrophenyl-5-L-phenylalanine amide (FDPA) instead of the standard 1-fluoro-2,4-dinitrophenyl-5-L-alanine amide (FDAA) derivative.[108] Marfey's reagent adds a highly absorbing chromophore that allows for the conversion of amino acids into strongly UV-active diastereomers, which may be separated by HPLC using nanomole quantities.[108] The modified Marfey's reagent was prepared using the standard Marfey's method,[109] except that L-Phe-NH_2 was used as a reagent instead of L-Ala-NH_2 (Figure 9). The FDPA derivatives of the amino acids in the hydrolyzate of **3.1** were prepared (Figure 10) and subsequent analysis by RP-HPLC allowed the assignment of the D-absolute configuration for the Iva units. This was again confirmed by coinjection of the FDPA derivatives of the amino acids in the hydrolyzate and the corresponding FDPA derivatives of D- and L-Iva amino acid standards showing peak enhancement for the D-isomer. Determination of the absolute configuration of the amino acids in the peptide using GCMS analysis of *N*-TFA-(*S*)-(+)-2-butyl ester derivatives and HPLC analysis of modified Marfey's derivatives led to complete assignment of the new peptide **3.1**. A search of the literature, including the online Peptaibol Database[97] did not reveal a close match for this structure.

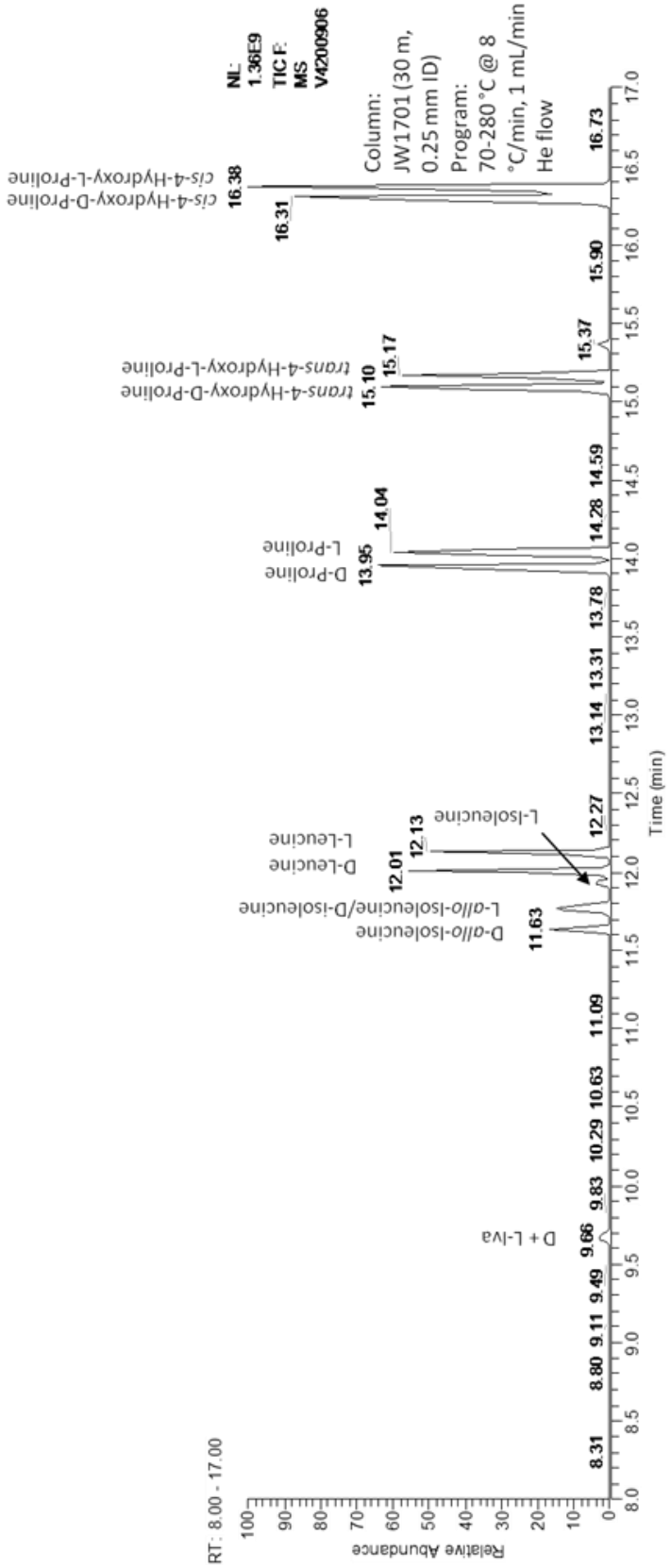

Figure 6. Gas Chromatogram of *N*-TFA-(S)-(+)-2-butyl esters of Amino Acid Standards

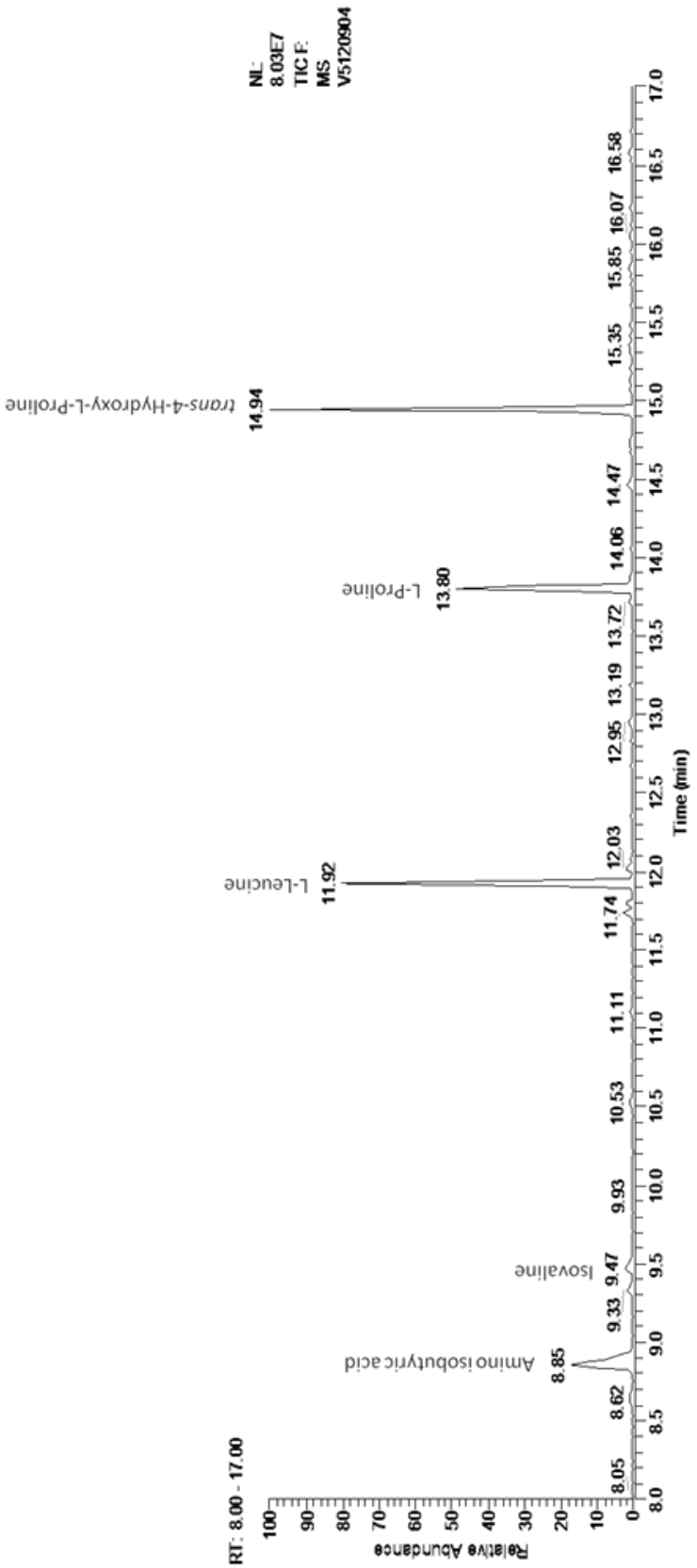

Figure 7. Gas Chromatogram of *N*-TFA-(*S*)-(+)-2-butyl esters of Amino Acids from Hydrolyzate of Peptide **6**

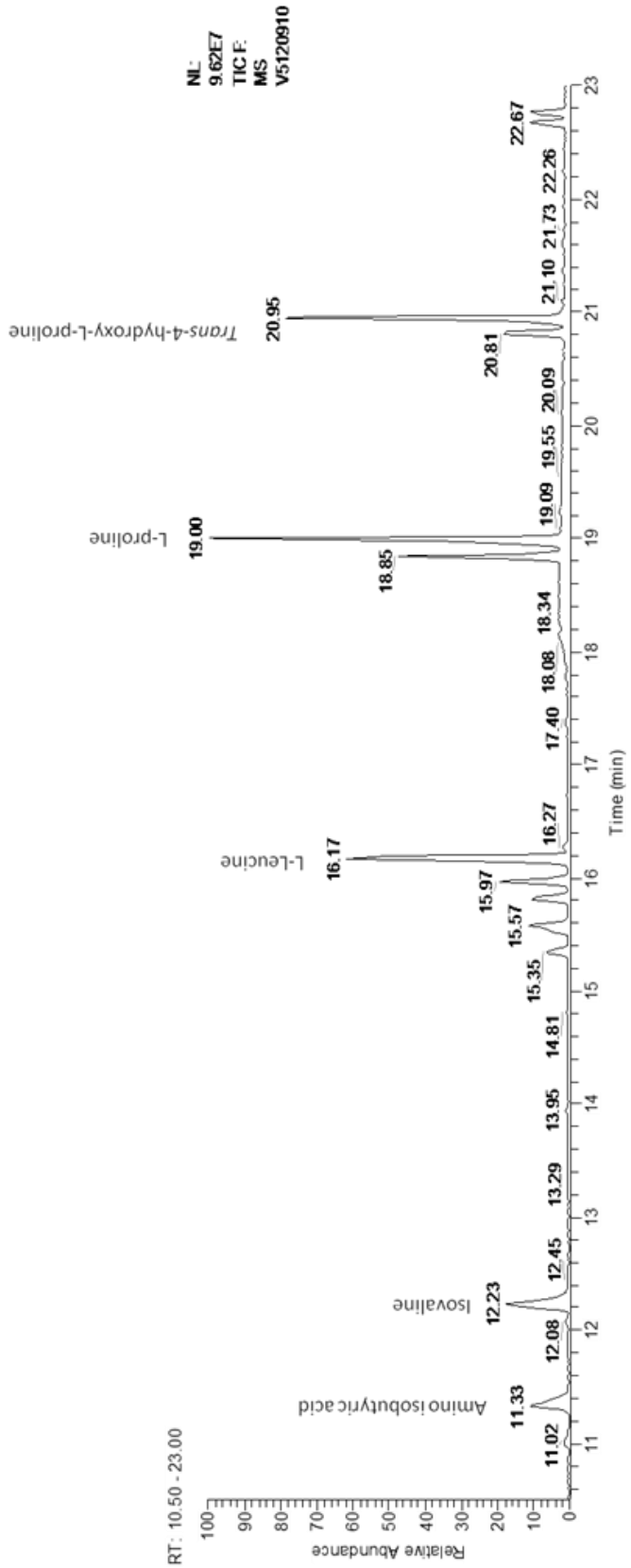

Figure 8. Coinjection of derivatized bionectrin A (**3.1**) hydrolyzate and D- and L-amino acid standards

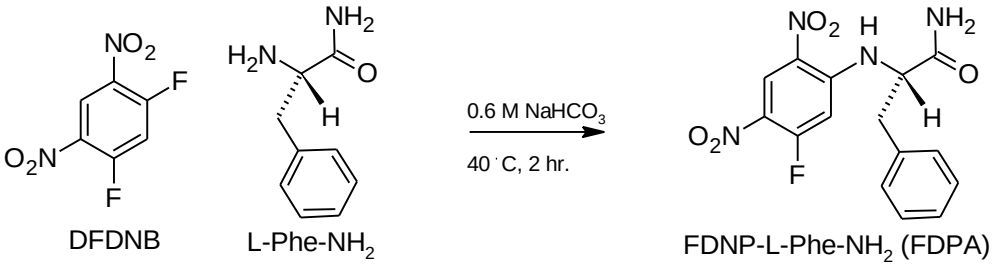

Figure 9. Preparation of the Modified Marfey Reagent FDPA

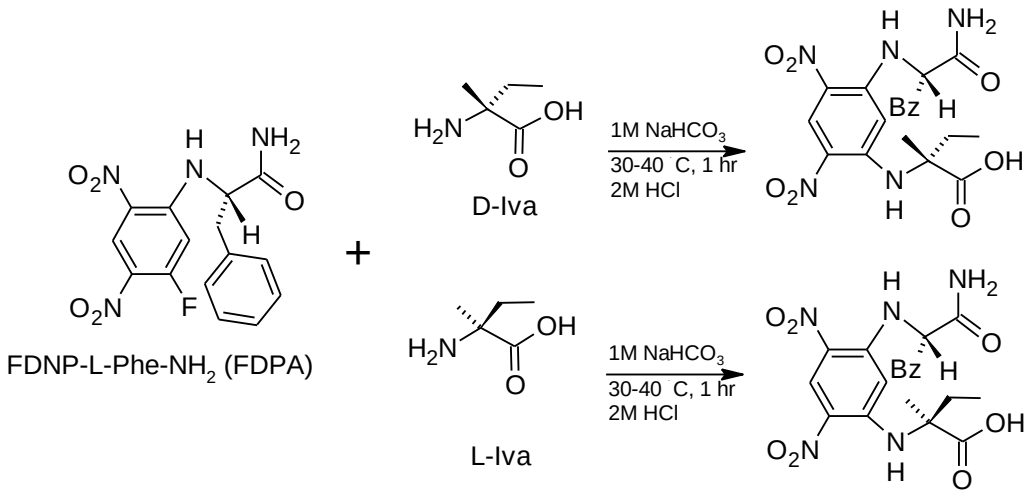

Figure 10. FDPA Derivatization Scheme for D- and L-Isovaline

Compound **3.1** possesses an acylated N-terminus, and 50% of the amino acid composition consists of the α,α-dialkylated amino acids Aib and Iva, which are characteristic features of linear peptaibol antibiotics. However, **3.1** possesses a free carboxylic acid and lacks the reduced C-terminal amino alcohol unit typically found in peptaibols (though the Hyp unit does contain an alcohol group). The EtOAc extract of MYC-2186 exhibited antifungal activity against *A. flavus* and *F. verticillioides*, as well as antiinsectan activity against *S. frugiperda*. However, bionectrin A (**3.1**) was inactive in antibacterial assays against *B. subtilis*, *E. coli*, and *S. aureus* at 200 μg/disk, antifungal assays against *C. albicans*, *F. verticillioides and A. flavus* at 200 μg/disk, and antiinsectan assays against *S. frugiperda* at 1000 ppm. It has been reported that the C-terminal amino alcohol unit of peptaibols, which **3.1** lacks, plays an important role in membrane permeabilization and ion channel formation by the barrel-stave, carpet, and torroidal models of antimicrobial peptide-induced killing, which were described earlier in this Chapter.[97] Also, short-chain peptaibols with 11-amino acid residues are known to have a limited range of biological activities due to the inability to completely span across the bilayer. Compound **3.1** contains only 10 amino acid residues, so this could be a possible explanation for the inactivity of **3.1** in our antimicrobial assays. Since **3.1** contains a free carboxylic acid, it is also possible that bionectrin A might be a truncated version of a higher, biologically active homologue, but no such compounds were encountered during our analysis of this extract.

Structure Elucidation of Guaiane Mannoside (**3.2**)

The molecular formula of compound **3.2** was determined to be $C_{21}H_{36}O_6$ (four units of unsaturation) on the basis of high resolution electrospray ionization mass spectrometry (HRESIMS) data. ^{1}H NMR data were initially collected using $CDCl_3$ as a solvent; however, a number of the observed signals were overlapping and broad. Other solvents were investigated, including acetone-d_6 and CD_3OD, and the latter resulted in the best resolution and line shapes of the signals in the ^{1}H NMR spectrum. Five oxymethine signals were observed in the region between δ_H 3.0-4.0, and an additional signal was observed at δ_H 4.7, suggesting the presence of a glycoside moiety. Subtracting the molecular formula of the glycoside unit from the molecular formula of compound **3.2** ($C_{21}H_{36}O_6 - C_6H_{11}O_6 = C_{15}H_{25}$) resulted in 15-unassigned carbon resonances, suggesting that this compound might be a sesquiterpenoid glycoside. The ^{1}H NMR spectrum included one methyl doublet at δ_H 0.91, one methyl singlet at δ_H 1.21, one olefinic methyl singlet at δ_H 1.68, two terminal olefinic protons at δ_H 4.60 and 4.67, a series of signals from δ_H 3.2-3.9 suggestive of a sugar unit, an apparent anomeric signal at δ_H 4.75, and other complex aliphatic proton multiplets between δ_H 1.20-2.60. ^{13}C NMR and DEPT-135 data included resonances for the terminal olefin (δ_C 157.0 and 108.6), an oxygenated quaternary sp^3 carbon, and six oxygenated sp^3 signals suggestive of a glycoside moiety (Table 8).

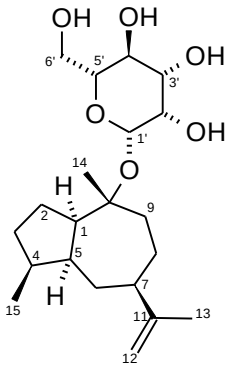

3.2

Table 8. ^{1}H, ^{13}C NMR, and HMBC Data for Guaiane Mannoside (**3.2**) in CD_3OD

position	δ_H (mult., J_{HH})[a]	δ_C[b]	HMBC[a]
1	2.31 (m)	56.0	2
2	1.69 (m)	26.4	1
	1.54 (m)		3
3	1.70 (m)	31.5	
	1.23 (m)		2, 5
4	2.01 (m)	40.0	5
5	2.10 (m)	47.0	
6	1.39 (m)	28.5	1, 4, 5, 7, 11
	1.22 (m)		
7	2.51 (m)	46.2	8, 11
8	1.70 (m)	29.9	
	1.43 (m)		9, 10, 11, 12
9	1.98 (m)	31.5	8, 10
	1.70 (m)		
10		83.0	
11		157.0	
12	4.68 (m)	108.6	7, 11, 13
	4.56 (m)		7, 11, 13
13	1.68 (s)	19.5	7, 11, 12
14	1.21 (s)	28.5	1, 9, 10
15	0.91 (d, 6.9)	16.8	3, 4, 5
1’	4.75 (d, 0.7)	96.0	10, 2’
2’	3.85 (dd, 3.2, 0.7)	73.8	4’
3’	3.47 (dd, 9.5, 3.2)	75.6	2’, 4’
4’	3.57 (t, 9.5)	68.6	3’, 5’
5’	3.20 (ddd, 9.5, 5.5, 2.5)	78.0	3’, 4’, 6’
6’	3.81 (dd, 12, 2.5)	63.0	
	3.68 (dd, 12, 5.5)		4’, 5’

[a]Recorded at 600 MHz.

[b]Recorded at 100 MHz; Assignments are consistent with multiplicities obtained by analysis of DEPT-135 data.

HMQC data allowed for assignment of the protons evident in the ^{1}H NMR spectrum to the corresponding carbon signals in the ^{13}C NMR spectrum. HMBC correlations were observed from H_3-15 to C-3, C-4, and C-5; from H_3-13 to C-7, C-11, and C-12; and from H_3-14 to C-1, C-9, and C-10, thereby establishing the locations and neighborhoods of the three methyl groups. Further key correlations were observed from H_2-6 to C1, C-4, C-5, C-7, C-8, and C-11, linking C-3 to C-5 and the C8-C7-C11 fragment via H_2-6. A correlation from H_2-2 to C-1 was important in identifying the location of H_2-2 due to overlap of other signals with H_2-2 in the ^{1}H NMR spectrum. At this point, all carbons and hydrogens had been assigned, but the connectivity of four methylene units (C-2, C-3, C-8, and C-9) were not yet determined. Two possible structures could be constructed by connecting either C-2 to C-8 and C-3 to C-9, or connecting C-2 to C-3 and C-8 to C-9. Unfortunately, COSY data were not useful in assigning the connectivity of these methylene units due to overlap of the methylene proton signals in the ^{1}H NMR spectrum. Ultimately, meticulous analysis of HMBC data enabled assignment of the structure. Correlations were observed between H_2-9 to C-7 and H_2-8 to C-9, which led to the identification of a guaiane-type ring system in **3.2**.

The sugar unit was clearly a hexose, but to determine the identity, and perhaps provide a sample of the aglycone that would have better NMR properties that might be useful in establishing the relative configuration, acid hydrolysis was attempted to separate the glycoside unit from the guaiane portion of compound **3.2**. Unfortunately, standard acidic hydrolysis conditions resulted in decomposition of the starting material beyond cleavage of the glycoside bond. A search of the literature was performed in an attempt to find milder reaction conditions that have been suitable for successful hydrolysis of similar compounds. This search led to discovery of a very recent (at the time) report that described the isolation and structure elucidation of a guaiane-type sesquiterpenoid with a mannose sugar moiety obtained from an unidentified *Eutypa*-like fungus by a group in Brazil.[88] The ^{13}C and ^{1}H NMR data of the literature compound, including the J_{HH}

coupling constants for the glycoside moiety, matched those of the metabolite under investigation and led to the identification of compound **3.2** as guaiane mannoside. Interestingly, guaiane mannoside is the first guaiane-type sesquiterpenoid to be reported from a fungal source. In the literature report, the relative configuration was determined by analysis of NOESY data, leading to assignment of the relative configuration of compound **3.2** as 1*R**,4*S**,5*S**,7*R**,10*R**. The absolute configuration was proposed by analogy to similar compounds reported in the literature, albeit from plant sources. Guaiane-type sesquiterpenoids typically have the 7*R*-configuration and result from cyclization of *trans,trans*-farnesyl pyrophosphate to first form a strained cyclodecadiene system, which then reacts further through an intramolecular process to form the perhydroazulene system found in the guaiane skeleton.[110] This stereochemical assignment has been supported by data arising from synthetic studies reported for structurally related guaianolides.[88,111]

Compound **3.2** did not show activity in our assays when tested in antibacterial assays against *B. subtilis*, *E. coli*, and *S. aureus,* or antifungal assays against *C. albicans*, *A. flavus*, or *F. verticillioides.* Also, no biological activity has been reported in the literature for this compound. However, related guaiane-type metabolites have been reported to possess antibacterial,[112] antioxidant,[113] antimalarial,[114] and anti-inflammatory[115] effects. Pseurotin A, chlamydocin, and related analogues have been reported to possess antifungal and/or antiinsectan activities, and compounds **3.4**-**3.6** seem likely to be responsible for at least some of the activity observed in our assays.[81,82] On the other hand, a chromatography fraction containing these compounds tested early on in the process did not show significant activity. Due to sample limitations (the compounds were difficult to fully purify), the pure compounds were not tested, so, unfortunately the source of the antifungal and antiinsectan activities originally observed for the extracts could not be identified with certainty. It is, of course, possible that the active constituent

may not have been detected/isolated, or that separation of these compounds may have eliminated synergistic effects that might be shown by certain combinations.

CHAPTER 4
CHEMICAL INVESTIGATION OF AN ISOLATE OF *PHIALEMONIUM CURVATUM*

Pyrenomycetes are fungi that produce flask-shaped fruiting bodies and include plant,[116] fungal,[117] insect,[118] and human pathogens.[119] During our ongoing investigations of fungicolous and mycoparasitic fungi, an isolate was obtained from the black stromata of a pyrenomycete found on a dead hardwood branch in Hawaii and was identified as *Phialemonium curvatum* (MYC-2005).[120] The genus *Phialemonium* is considered to be intermediate between *Acremonium* and *Phialophora*, and includes fungi that possess morphological features characteristic of both of these genera. Three species of this genus have been described: *P. curvatum* (conidia allantoid in shape), *P. obovatum* (conidia obovate or ellipsoidal), and *P. dimorphosporum* (conidia both allantoidal and obovate)[120] *Phialemonium* spp., including *P. curvatum*, are known opportunistic human pathogens. However, this genus appears to be unexplored from a chemical standpoint, and this chapter constitutes the first report of secondary metabolites from *P. curvatum*, as well as the genus *Phialemonium*.

The EtOAc extract of fermentation cultures of this isolate exhibited antifungal activity against *F. verticillioides* and potent antiinsectan activity against *S. frugiperda* in our assays and was selected for chemical investigation. The extract was partitioned between MeCN and hexanes and the MeCN-soluble fraction was subjected to silica gel column chromatography using hexanes/EtOAc/ MeOH to afford a new compound that we named dihydrooxirapentyne (**4.1**). Compound **4.1** was the major component of the extract. The known cyclohexadepsipeptide destruxin A_4 (**4.2**) was also encountered as a major constituent, although in lesser quantities than **4.1**. The ^{1}H NMR spectrum of compound **4.2** was characteristic of the destruxin class of compounds, and the structure was identified by comparison of the ^{1}H NMR data to literature values that had previously

been reported by our group.[16] Destruxins are composed of five amino acid residues and one α-hydroxy acid unit and are well-known for their potent insecticidal and phytotoxic activities.[121] It was ultimately determined that compound **4.2** accounted for the antiinsectan activity observed in our assays. However, this chapter focuses primarily on details of the isolation and structure determination of new compound **4.1**.

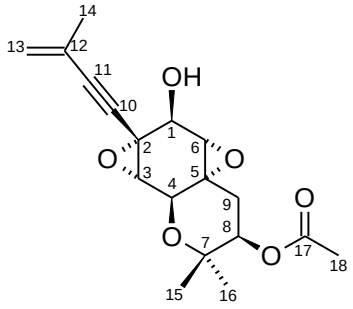

4.1

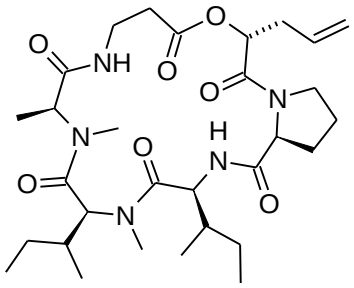

4.2

Structure Elucidation of Dihydrooxirapentyne (**4.1**)

The molecular formula of dihydrooxirapentyne (**4.1**) was determined to be $C_{18}H_{22}O_6$ (eight unsaturations) on the basis of HRESIMS data. The ^{1}H NMR spectrum indicated the presence of a terminal olefin, four oxygenated methines, one vinyl methyl, one acetyl methyl, and two additional methyl groups. The ^{13}C NMR data showed signals for 18 carbons, including an ester or acid, two olefinic carbons, eight oxygenated sp^3 carbons, four methyl carbons, two oxygenated sp^3 or alkyne carbons, and only one other non-oxygenated sp^3 carbon. The ^{1}H NMR, ^{13}C NMR, and HMBC data for **4.1** are summarized in Table 9.

On the basis of these NMR and MS data, a database search led to the tentative identification of **4.1** as a closely related analogue of the known compound oxirapentyne (**4.3**),[122] differing only in the absence of a ^{13}C NMR signal near δ 200 corresponding to the ketone moiety of **4.3**, along with the presence of an exchangeable OH proton signal and an additional oxymethine signal overlapped with that of H-4 at δ 4.45 in the ^{1}H NMR spectrum of **4.1**. Attempts to resolve these latter two signals using different solvents and/or higher field were unsuccessful. It was also noted that all of the signals in the ^{1}H NMR spectrum between δ 2.47 and 4.87 were shifted somewhat upfield relative to those reported in the literature for **4.3**. All of these data would be consistent with replacement of the ketone carbonyl of **4.3** with a secondary alcohol group in **4.1**. The numbering system used for **4.1** is based upon the convention reported in the literature for the known compound oxirapentyne (**4.3**).[122]

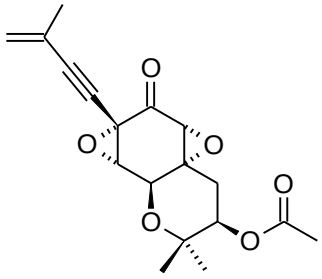

4.3

Detailed analysis of HMQC and HMBC data (Figure 11) was undertaken in an effort to confirm this structure assignment, with key correlations from vinyl methyl H_3-14 to C-11, C-12, and C-13; from epoxide proton H-6 to C-1, C-2, C-4, C-5, and C-9; and from epoxide proton H-3 to C-1, C-2, C-4, C-5, and C-10 enabling assignment of the bis-epoxide-containing, six-membered ring unit, and enyne side chain as shown in Figure 11.

Further correlations were observed from H_2-9 to C-4, C-5, C-6, C-7, and C-8; and from methyl singlet H_3-15 to C-7, C-8, and C-16 extending the structure from C-5 through C-16. A correlation from acetyl methyl singlet H_3-18 to C-17 and a relatively weak long-range coupling from H_3-18 to C-8 allowed for the location of the acetate moiety at C-8. The two epoxide units, cyclohexane ring, one olefin, and one acetyl group accounted for five unsaturations. Recognition of C-10 and C-11 as forming an internal alkyne unit (rather than oxygenated sp^3 carbons) accounted for two additional unsaturations. The final unsaturation was accounted for by a second six-membered (tetrahydropyran) ring linking C-4 and C-7 via an oxygen atom, as would be consistent with their δ values. These data enabled the NMR assignments shown in Table 9, and independently supported the connectivity of the structure of compound **4.1** as illustrated in Figure 11.

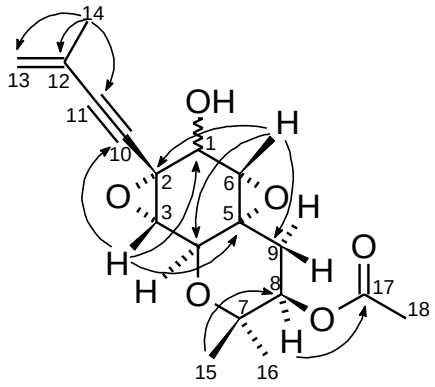

Figure 11. Key HMBC Correlations for Dihydrooxirapentyne (**4.1**)

Most of our further studies of this compound were related to efforts to assign its absolute configuration. Oxidation of **4.1** was carried out under Swern conditions to afford the known compound oxirapentyne (**4.3**), as judged by comparison of the NMR

Table 9. ^{1}H, ^{13}C NMR, and HMBC Data for Dihydrooxirapentyne (**4.1**) in $CDCl_3$

C #	δ_H (mult., J_H)[a]	δ_C[b,c]	HMBC (H→C)[d]
1	4.45 (br s)	63.8	2, 3, 5, 6
2		51.6	
3	3.37 (d, 2.0)	60.1	1, 2, 4, 5, 9, 10
4	4.45 (br s)	63.7	2, 3, 5, 6
5		52.9	
6	2.99 (br s)	60.0	1, 2, 4, 5, 9, 10
7		74.6	
8	4.87 (t, 3.0)	73.6	5, 17
9	1.47 (dd, 15, 3.0) 2.47 (dd, 15, 3.0)	32.5	4, 5, 6, 7, 8 5, 6
10		83.7	
11		86.5	
12		125.3	
13	5.37 (dq, 1.5, 1.5) 5.29 (dq, 1.5. 1.0)	124.4	11, 14 11, 12, 14
14	1.87 (s)	23.0	11, 12, 13
15	1.40 (s)	21.5	7, 8, 16
16	1.24 (s)	25.3	7, 8, 15
17		170.3	
18	2.11 (s)	20.9	8, 17

[a]Recorded at 400 MHz.

[b]Recorded at 100 MHz.

[c]^{13}C NMR multiplicities were established by analysis of DEPT-135 data and are consistent with the assignments.

[d]Recorded at 600 MHz.

data for the product with literature values for **4.3**. The specific rotation of the oxidation product ($[\alpha]_D = -68$) was somewhat different from that reported in the literature for **4.3** ($[\alpha]_D = -112$), whose absolute configuration had been proposed on the basis of CD data.[123] Although the magnitude did not match, the identity of the NMR data for the product with those of the literature compound, together with the matching sign of the specific rotation led to the proposal of the (partial) absolute configuration of **4.1** as 2*R*, 3*S*, 4*S*, 5*S*, 6*S*, 8*R*. The ^{1}H NMR spectrum for the oxidation product indicated that there were minor impurities present in the sample that could be responsible for the difference in the specific rotation magnitudes, especially since the reaction was performed on a small scale. However, no attempts were made to obtain a cleaner sample of the oxidation product because another method to determine the absolute configuration of **4.1**, ultimately leading to a conclusion consistent with these assignments, was available and will be discussed later in this chapter.

At this point, the only remaining stereocenter left unassigned was the secondary alcohol at position 1. The energy-minimized molecular model of **4.1** (Gaussian 09; Figure 12) demonstrates that the presence of the two epoxide units on the six-membered ring forces the ring to adopt a near-planar conformation. In the original report of the known compound **4.3**, the authors proposed the relative stereochemistry on the basis of a long-range $J_{C\text{-}H}$ resolved 2D NMR spectroscopy (LRJR) experiment, where heteronuclear couplings between ^{1}H and ^{13}C were observed.[123] A near-zero coupling constant between H-6 and C-4 (suggesting a near 90° vicinal angle for these protons) suggested a *trans* relationship of these atoms, whereas large long-range coupling constants ($^4J = 1.9$ Hz) from H-6 to C-10 and from H-3 to C-9 ($^4J = 1.8$ Hz) suggested W-type relationships of these atoms.[123] Similarly, the ^{1}H NMR data of **4.1** were analyzed in an effort to determine the relative configuration at C-1 using vicinal and long-range coupling constants (which would automatically provide the absolute configuration since the absolute configuration at all other stereocenters had been determined). Due to overlap of

the H-1 and H-4 signals, and the stereochemical ambiguity of the vicinal J_{HH}-values for such a system even if values could be measured,[107] the coupling constants were not helpful in assigning a *cis*- or *trans*- relationship between H-1 and H-6. NOESY data for **4.1** (Figure 12) supported the assignment of the relative configurations of all stereocenters except C-1, matching those of the known compound **4.3** as already noted above (Figure 11). In the energy-minimized structure for the 1*R*-diastereomer, the distance between H-1 and H_3-18 was expected to be 2.8 Å, as opposed to 4.8 Å in the 1*S*-diastereomer, but no corresponding NOESY correlation was observed. The configuration was therefore tentatively assigned as 1*S*, but this issue required further investigation since only negative evidence was available.

Because absolute configuration had been assigned to all of the other stereocenters as noted above, it was felt that Mosher's method could be applicable. The only two possible stereoisomers are diastereomers, but they differ only in the absolute configuration at C-1. Thus, assignment of this absolute configuration was attempted using Mosher's method.[124] Interestingly, the convention typically used to assign absolute

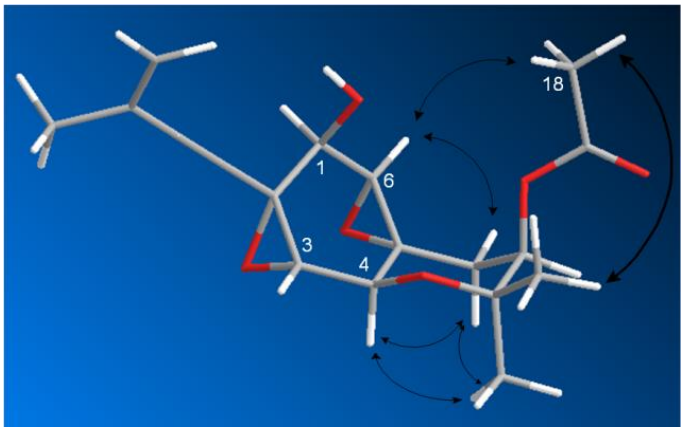

Figure 12. Energy-Minimized Model and Key NOESY Correlations for Dihydrooxirapentyne (**4.1**)

configuration could not be unambiguously applied in this case because all of the protons in the region nearest to the added acyl α-methoxy-α-trifluoromethylphenylacetic acid (MTPA) group in the product showed only positive Δδ values (Figure 13). However, all of the nearby protons that reside on one face of the molecule possessed significantly shifted values, suggesting that the OH in **4.1** is on that same face, thereby enabling a proposed assignment as shown in Figure 13. In addition, the large positive Δδ values observed for H-13a, H-13b, and H_3-14, as well as the near-zero (though still positive) Δδ values observed for H-6, offered indirect support for the configuration shown for **4.1**. More specifically, based on the general principles used in applying Mosher analysis, the much more dramatically positive Δδ values for the enyne substituent would be most consistent with assignment of the 1*S*-configuration (large +Δδ vs. small +Δδ).

While all of the above data collectively and consistently suggested the 1*S* configuration for **4.1**, the perceived stereochemical ambiguity led to efforts to prepare and crystallize the *p*-bromobenzoate derivative of **4.1** in an effort to independently verify the absolute configuration. Ultimately, suitable crystals were obtained from 2:2:1 $CH_3CN/CHCl_3/H_2O$. X-ray diffraction analysis enabled independent confirmation of the absolute configuration as shown, including the *S*-configuration at C-1. An ORTEP plot of the crystal structure is shown in Figure 14. Energy-minimized molecular models of the 1*R*- and 1*S*-dihydrooxirapentyne diastereomers were calculated and optimized via Gaussian09 using the Hartree-Fock 3-21G basis set. The lowest-energy conformer of 1*S*-dihydrooxirapentyne was determined to be 7 kcal/mol more stable than that of 1*R*-dihydrooxirapentyne, and the corresponding molecular model shown in Figure 12 was very similar to the conformation in the solid-state indicated by the X-ray derived ORTEP plot (Figure 14).

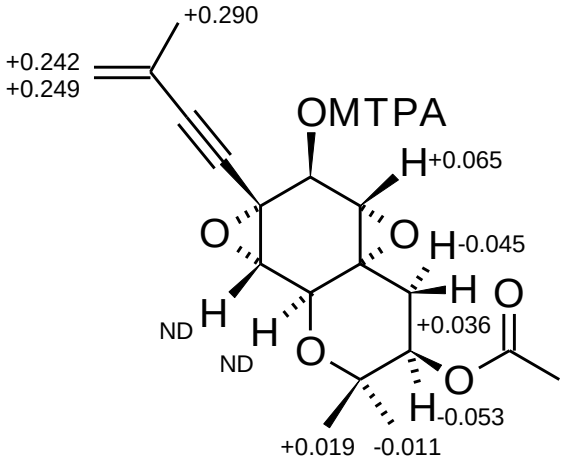

Figure 13. Mosher Ester Analysis of Dihydrooxirapentyne (**4.1**; Δδ values in ppm; ND = not determined due to signal overlap)

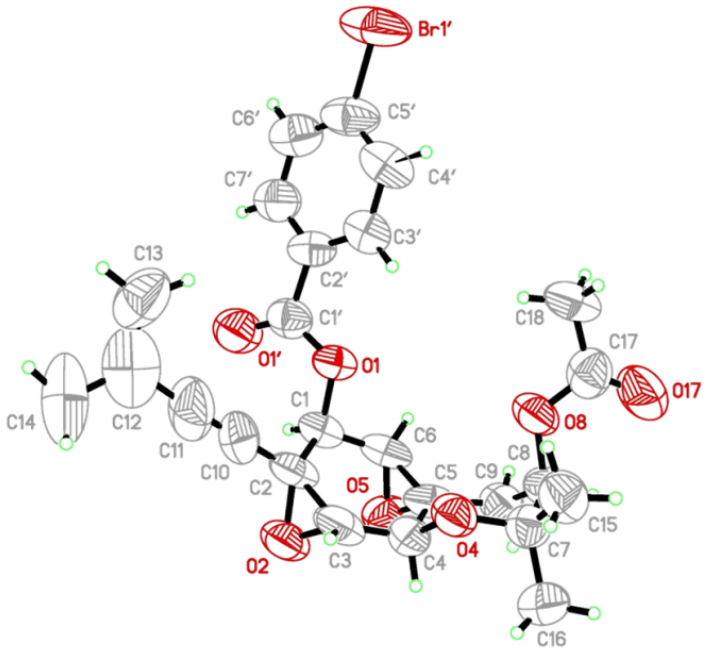

Figure 14. X-ray ORTEP Model of the *p*-Bromobenzoate Derivative of Dihydrooxirapentyne (**4.1**)

Dihydrooxirapentyne (**4.1**) and oxirapentyne (**4.3**) are closely related to a rare class of highly oxygenated, prenylated cyclohexanoid fungal natural products that

includes asperpentyn (**4.4**) and 7-desoxypanepoxydol (**4.5**). Compounds **4.1** and **4.3** are presumably constructed of a similar benzenoid aromatic precursor and incorporation of two modified isoprene units at positions C-2 and C-5 of the resulting modified cyclohexane ring.[125]

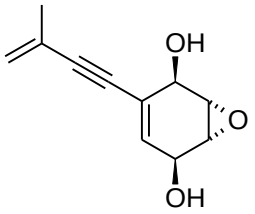

4.4

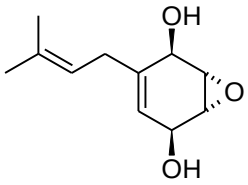

4.5

Dihydrooxirapentyne (**4.1**) is a dihydro analogue of the known compound oxirapentyne (**4.3**). Oxirapentyne was originally reported as a metabolite of the fungus *Beauveria feline.* Although *Beauveria* spp. are not closely-related phylogenetically to *P. curvatum*, destruxins have also been previously reported from marine-derived fungal isolates of *B. feline*.[126] Compound **4.3** was reportedly active against the Gram-positive bacteria *S. aureus* (FDA 209P JC-1), *B. subtilis* (PCI 219), and *Micrococcus luteus* (PCI1001) with MIC values of 25 μg/mL, and inactive against *E. coli* (NIHJ JC-2). However, dihydroxyoxirapentyne (**4.1**) did not show activity in standard disk diffusion assays when tested against against *F. verticillioides*, *C. albicans* (ATCC 14053), *S. aureus* (ATCC 29213), *B. subtilis* (ATCC 6633), or *E. coli* (ATCC 25922) at 200 μg/disk. As previously mentioned, the antiinsectan activity observed for the original crude extract was due to the known antifungal and phytotoxic compound destruxin A_4

(**4.2**) present in the extract, as a dietary concentration of 420 ppm resulted in 67% mortality of *S. frugiperda* at 2 days and 100% mortality after 5 days.

CHAPTER 5
CHEMICAL INVESTIGATION OF AN ISOLATE OF GLIOCLADIUM SPECIES

Gliocladium species are mitosporic fungi that are typically found in soil and decaying vegetation.[127] During a study of sclerotium survival in soil,[128] an unidentified fungal isolate of *Gliocladium* sp. (NRRL 22971) was obtained as a colonist of *A. flavus* sclerotium that had been buried for three years in sandy field soil near Kilbourne, IL. Some *Gliocladium* spp. were observed to colonize the sclerotia and sometimes render the sclerotia non-viable. A subculture of this particular isolate was sent to the Centraalbureau voor Schimmelcultures (CBS) Fungal Biodiversity Centre in the Netherlands for further taxonomic evaluation. It was determined that this isolate likely represents an undescribed *Gliocladium* species. The EtOAc extract of solid-substrate fermentation cultures of this isolate did not exhibit activity in antifungal assays against *F. verticillioides* or *A. flavus*, but its unusual taxonomic characteristics and its occurrence as a sclerotial colonist led to a chemical investigation in an effort to determine if there might be interesting chemistry and/or biological activity related to minor components present in the crude extract. The extract was subjected to silica gel and Sephadex LH-20 column chromatography, as well as reversed-phase HPLC to yield the commonly encountered known fungal metabolite ergosterol (**5.1**) and two new compounds; a β-carboline-containing metabolite (**5.2**), a regioisomer of the known compound dichotomide I (**5.3**), and a new cytochalasin analogue (**5.4**).

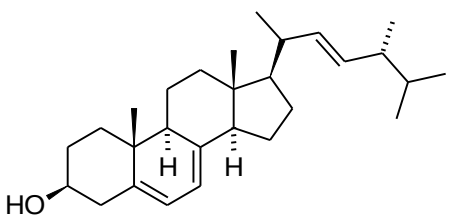

5.1

Structure Elucidation of 1-Acetyl-9*H*-pyrido[3,4-*b*]indole-3-[*S*-(3)-aminobutyric acid]amide (**5.2**)

Compound **5.2** was assigned the molecular formula $C_{18}H_{17}N_3O_4$ on the basis of HREIMS data. The ^{1}H NMR spectrum obtained using DMSO-d_6 as a solvent contained signals for a 1,2-disubstituted benzenoid ring, an additional aromatic proton, one CH_3-CH-CH_2 unit, and one acetyl methyl group (Table 10). The ^{13}C and DEPT NMR data showed signals for 18 carbons, including one ketone, two ester, amide, or carboxylic acid carbons, six non-protonated sp^2 carbons, five protonated sp^2 carbons, one sp^3 methine, one sp^3 methylene, one acetyl methyl group, and one other methyl group. Further analysis of the ^{1}H, ^{13}C, and DEPT-135 NMR data led to the identification of three exchangeable protons, signals for two of which were present in the ^{1}H NMR spectrum, including the signals for 9-NH at δ_H 12.2 (s) and 17-NH at δ_H 8.87 (d).

HMBC correlations from H-5 of the disubstituted benzenoid system to non-protonated sp^2 carbons C-13 and C-11, from H-6 to C-12, and from H-9 to C-13, C-10, and C-11 led to extension of the benzenoid ring to an indole unit (Figure 15). Correlations from a significantly downfield-shifted (δ_H 9.10), isolated aromatic/olefinic proton (H-4) to C-1 and C-12 extended the indole unit beyond C-11. Because amide NH-17 appears as a broad doublet, this NH must be attached to the only methine CH (CH-18). Correlations from H-18 of the NHCH(CH_3)CH_2 unit to carbonyls C-20 and C-16 and from H_2-19 to C-20 linked the NHCH(CH_3)CH_2 unit to the two carboxy-type carbonyl carbons C-16 and C-20. The side-chain (C16-C20) was placed alpha to H-4 on the basis of the HMBC correlation from H-4 to carbonyl C-16. The acetyl group and two non-protonated sp^2 carbons remained unassigned. There were no HMBC correlations to one of these sp^2 carbons (C-3), but there was a correlation from the somewhat downfield-shifted acetyl methyl (H_3-15) to ketone carbon C-14, leading to the identification of a methyl ketone. A weak, long-range correlation was also observed from H_3-15 to C-1.

Table 10. ^{1}H, ^{13}C, and HMBC NMR Data for β-Carboline **5.2** in DMSO-d_6

C#	δ_H (mult., J)[a]	δ_C[b]	HMBC (H→C)[c]
1	-	133.8	-
2	-	-	-
3	-	138.5	-
4	9.10 (s)	117.8	10, 12, 14, 16
5	8.44 (d, 7.8)	122.2	7, 8, 11, 12, 13
6	7.33 (t, 7.8)	120.8	5, 7, 8, 11, 12, 13
7	7.61 (t, 7.8)	129.3	5, 8, 13
8	7.82 (d, 7.8)	113.3	6, 12, 13
9-NH	12.2 (s)	-	10, 11, 12, 13
10	-	134.8	-
11	-	132.0	-
12	-	120.3	-
13	-	142.3	-
14	-	200.9	-
15	2.90 (s)	25.8	1, 14
16	-	163.1	-
17-NH	8.87 (br d, 7.8)	-	-
18	4.35 (m)	41.8	-
19	2.64 (dd, 16, 2.6) 2.60 (dd, 16, 6.0)	39.8	-
20	-	172.9	-
21	1.29 (d, 6.6)	20.2	-

[a]Recorded at 360 MHz.

[b]Recorded at 90 MHz. Assignments are consistent with multiplicities obtained by analysis of DEPT-135 data.

[c]Recorded at 600 MHz.

Because the indole NH-9 signal appears as a sharp singlet at δ12.2, this proton seemed likely to be intramolecularly hydrogen-bonded. Placement of the acetyl group nearby at C-1 (and linking C-1 to C-10) would rationalize this shift. One nitrogen atom and one

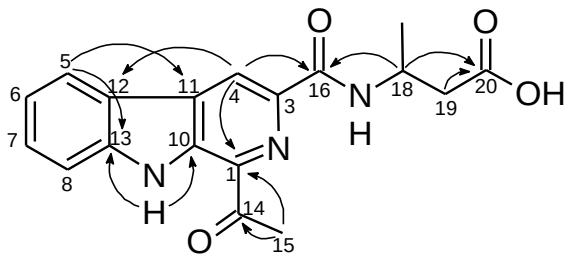

Figure 15. Key HMBC Correlations Employed in Assigning the Structure of compound **5.2**

exchangeable proton were not yet accounted for. However, at this point, the structure could only be linked as shown in **5.2**. Comparison with literature data showed that **5.2** is a structural isomer of the known plant metabolite dichotomide I (**5.3**), which has been reported from the roots of *Stellaria dichotoma*.[129] Both compounds contain the same acylated β-carboline unit, but differ with respect to the identity of their side-chains.

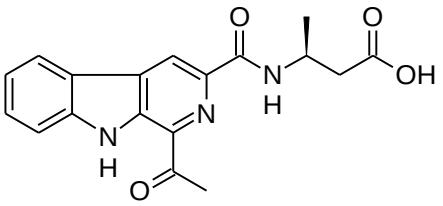

5.2

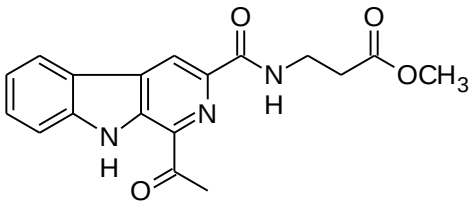

5.3

Because of sample-limitations (0.5 mg), acidic hydrolysis was not performed on **5.2** until a suitable method for assignment of the stereocenter in the amino acid unit was found. In an initial effort to develop such a method, a standard sample of (*S*)-3-aminobutyric acid was obtained (Aldrich Chemical Co.) in order to prepare *N*-TFA-(±)-2-

butyl ester derivatives for GCMS analysis (Figure 16) as described earlier in Chapter 3. However, efforts to separate the resulting diastereomers using GC-MS were not successful. When this approach failed, efforts were undertaken to employ Marfey's method, another approach commonly used for amino acid analysis.

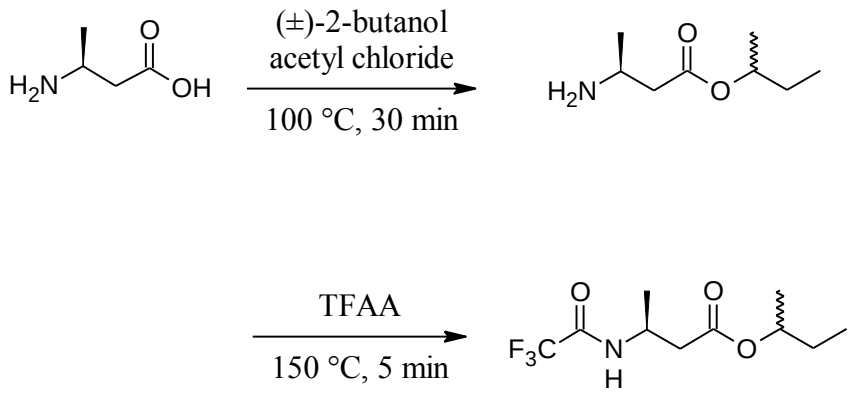

Figure 16. (*S*)-3-Aminobutyric Acid *N*-TFA-2-butyl ester Derivatization Scheme

Because we had previously prepared a modified Marfey's reagent 1-fluoro-2-4-dinitrophenyl-5-L-phenylalanine amide (FDPA), as discussed in Chapter 3, and used it successfully, this reagent was again employed to prepare FDPA derivatives of D- and L-3-aminobutyric acid standards instead of using the standard Marfey's reagent 1-fluoro-2-4-dinitrophenyl-5-L-alanine amide (FDAA). The resulting diastereomers were subjected to RP-HPLC with UV-detection at 340 nm. Upon initial analysis of the chromatogram of the resulting standard derivative matrices, four peaks were present at 9, 10, 14, and 29 min. The peak at 29 min corresponded to unreacted FDPA reagent. After comparison to a blank, it was found that the other peaks present were due to various components and/or impurities in the reaction mixture, and not to the amino acid derivatives. Ultimately, it was determined that the initial sample volume used for analysis (10% of the total

mixture) was too low to observe the amino acid derivatives. After injecting more appropriate quantities (1/3 of the mixture), the D- and L-3-aminobutyric acid FDPA derivatives were detected and found to resolve, and their retention times were determined (15.5, 14.5 min, respectively). A sample of compound **5.2** was then subjected to acidic hydrolysis conditions and the hydrolyzate was subjected to the FDPA derivatization conditions. Coinjection of the reaction product with the D- and L-standards showed an enhancement of the peak at 14.5 min corresponding to the L-3-aminobutyric acid derivative. Thus, compound **5.2** was assigned the 18*S* absolute configuration.

β-Carboline alkaloids are tricyclic pyrido[3,4-b]indole structures that are distributed widely in nature. The biogenetic precursor from which they are derived is tryptophan. The biosynthesis of β-carboline-type alkaloids typically occurs through the formation of a Schiff base from tryptamine and an aldehyde or keto acid followed by an intramolecular Mannich reaction to form a tetrahydro-β-carboline.[130] Subsequent oxidation results in the formation of dihydro-β-carboline or β-carboline moieties. This class of indole alkaloids reportedly exhibit a broad range of activities, including antimicrobial, antiviral, cytotoxic, and anticarcinogenic effects.[131] Compounds of this structural class have been isolated from numerous sources including plants, insects, mammals, marine organisms, and human tissues.[132] However, there are only a few reports of β-carboline derivatives from fungal isolates. β-Carboline itself has been reported as a metabolite from an unidentified marine fungal isolate obtained from a mangrove in the South China Sea.[133] Also, (3*R*,12a*S*)-3-methyl-2,3,6,7,12,12a-hexahydropyrazino[1,2-b]β-carboline-1,4-dione was isolated from another unidentified fungus obtained as an endophyte of *Cephalotaxus hainanensis*,[134] and brunneins A–C and 3-(7-hydroxy-9H-β-carboline-1-yl)propanoic acid have been isolated from the basidiomycete *Cortinarius brunneus*.[135] To our knowledge, there are no previous reports of β-carboline-containing metabolites from *Gliocladium* spp.

Structure Determination of Cytochalasin Analogue **5.4**

Cytochalasins are fungal polyketide- and amino acid-derived metabolites that display a wide range of biological activities including antimicrobial, phytotoxic, and cytotoxic effects against a variety of cancer cell lines.[136] These compounds are structurally similar to the chaetoglobosins, which are discussed in Chapter 7. Cytochalasins differ from chaetoglobosins primarily in the fact that they contain a phenylalanine-derived benzyl moiety in the structure instead of the tryptophan-derived (indol-3-yl)methyl group found in chaetoglobosins.

Cytochalasin analogue **5.4** was assigned the molecular formula $C_{28}H_{35}NO_6$ on the basis of HRESIMS data. The use of $CDCl_3$ or acetone-d_6 as solvents did not result in well-resolved signals in the ^{1}H NMR spectrum, but the data were suggestive of the cytochalasin family of compounds. A search of the literature revealed that the majority of data reported for cytochalasins lists pyridine-d_5 as a commonly utilized solvent. Indeed, a well-resolved ^{1}H NMR spectrum of the sample was obtained using pyridine-d_5 as the solvent. The ^{1}H NMR spectrum indicated the presence of an amide proton, a benzyl moiety, two vinyl methyl units, a *trans*-disubstituted olefin, and two other methyl groups (Table 11). The ^{13}C NMR data revealed the presence of one ester (or amide or acid), two ketone units, a phenyl group, four olefinic carbons, and three oxygenated sp^3 carbons. A partial substructure search of the literature based on MS data and structure fragments evident from these NMR data revealed a close match to a related compound, deacetyl-19,20-epoxy-cytochalasin C (**5.5**),[137] which enabled assignment of most of the NMR signals. Although a considerable portion of the structure could be assigned on the basis of this analysis, it was necessary to collect HMQC and HMBC data to determine the overall connectivity, particularly the portion corresponding to C-15 to C-21 in **5.4**. Analysis of the extensive set of HMBC correlations obtained (Table 11) was fully consistent with the proposed partial connectivity, and afforded additional information

Table 11. ^{1}H NMR, ^{13}C NMR, HMBC, and NOESY Data for Compound **5.4** in Pyridine-d_5

position	δ_H (mult., J_{HH})[a]	δC[b]	HMBC (H → C#)[c]	NOESY (H → H#)[c]
1		174.8		
2	9.22 (s)		3, 4, 9	3
3	3.69 (td, 7.3, 1.7)	59.0	1, 4, 5, 9	2, 10α, 10β, 11, 2', 3'
4	3.62 (br s)	49.3	1, 5, 6, 10	10α, 10β, 11, 2', 3'
5		125.7		
6		134.4		
7	4.70 (br d, 10)	69.3		12, 13
8	2.68 (t, 10)	53.8	1, 6, 13, 14	13, 14
9		64.2		
10α	2.68 (dd, 13, 7.3)	43.1	1', 2'	10β
10β	2.60 (dd, 13, 8.1)		3, 4, 1', 2'	10α
11	1.42 (s)	17.0	4, 5, 6	3, 4, 12, 2', 3'
12	1.86 (s)	14.8	5, 6, 7	11, 7
13	6.73 (dd, 15, 10)	133.0	7, 8, 15	7, 8, 14, 15α, 20α
14	5.42 (ddd, 15, 11, 4.4)	130.7	8, 15	8, 13, 15β, 16, 19
15α	2.76 (t, 11)	38.4	13, 14, 16, 17	13, 15β, 16, 22
15β	1.93 (m)		13, 14, 16, 17, 22	14, 15α, 16, 22
16	3.02 (m)	41.3	14, 15, 22	14, 15α, 15β, 22, 23
17		216.4		
18		84.6		
19	4.78 (d, 7.5)	68.6	18, 20, 21	14, 16, 20α, 23
20α	4.05 (d, 20)	46.3	18, 21	13, 19, 20β
20β	3.05 (dd, 20, 7.5)		19, 21	20α
21		209.2		
22	1.00 (d, 6.7)	20.2	15, 16, 17	15α, 15β, 16
23	1.78 (s)	21.2	17, 18, 19	13, 16, 19
1'		138.1		
2'	7.13	129.4	1', 3', 4'	3, 4, 11
3'	7.17	128.4	1', 2', 4'	3, 4
4'	7.17	126.6	1', 2', 3'	

[a]Recorded at 400 MHz.

[b]Recorded at 90 MHz; Relatively weak signals not clearly observed in the ^{13}C NMR spectrum were assigned on the basis of HMQC and HMBC crosspeaks.

[c]Recorded at 600 MHz.

enabling completion of the structure. Most importantly, key HMBC correlations from H_2-20 to C-21 and from H_3-23 to C-19 completed the gross structure as depicted for **5.4**.

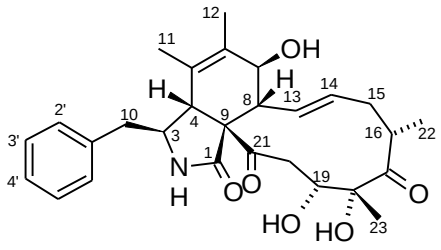

5.4

The relative configuration of compound **5.4** was established on the basis of NOESY experiments. NOESY data are listed in Table 11 and stereochemically relevant NOESY correlations are shown in Figure 17. The macrocycle contained in the known cytochalasin **5.6** is similar to that of **5.4** with the exception that **5.4** possesses a ketone at C-17, while **5.6** does not. On the basis of ^{1}H NMR data coupling constants, H-7 and H-8 must be in a pseudo *trans*-diaxial relative orientation (J = 10). Like most other cytochalasins, the γ-lactam ring is *cis*-fused, with the benzyl moiety positioned on the same face of the molecule as H-4. The stereochemistry of the perhydroisoindol-1-one unit is consistent with that assigned for other cytochalasins, including several that have been assigned on the basis of X-ray crystallographic analysis.[138-142] The macrocycle is *trans*-fused with the six-membered ring as shown in Figure 17 on the basis of NOESY data and comparison to literature values for similar cytochalasin-type compounds.[142] In the known compound **5.6**, the macrocycle is oriented such that the C-13/C-14 and C-19/C-20 bonds are roughly parallel to each other based on NOESY and NOE difference experiments.[142] Adoption of a similar relative orientation in **5.4** was supported by NOESY correlations from H-19 to H-16 and H_3-23 (Figure 17), and from H-20 to H-13, which were consistent with those reported in the literature for **5.6**. Although the absolute configuration of **5.4** was not directly determined, upon comparison to the known

cytochalasins **5.5** and **5.6**, and consideration of the fact that Phe generally occurs as the L-form, the absolute configuration of **5.4** was proposed as 3*S*,4*R*,7*S*,13*E*,16*S*,18*R*,19*R*.

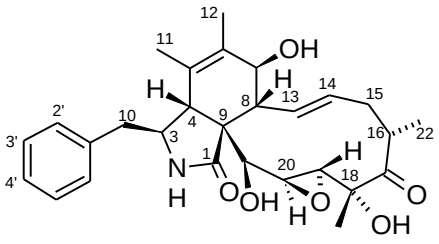

5.5

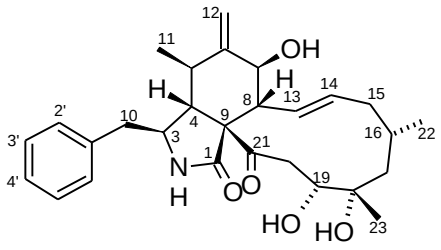

5.6

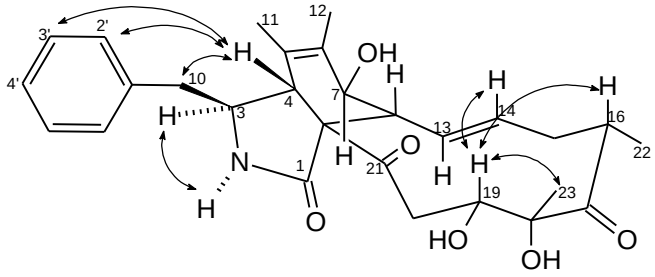

Figure 17. Key NOESY Correlations for Compound **5.4**

Compound **5.4** has not yet been tested in biological assays, but cytochalasins are well known to display a variety of biological activities, including antibacterial effects.[143] To our knowledge, this is the first report of a cytochalasin analogue from a *Gliocladium* sp. Compound **5.2** was not tested due to sample limitations. Although the crude extract did not exhibit antifungal activity in our assays, some β-carboline alkaloids are known to exhibit activity in assays against *Aspergillus niger* and *Candida albicans*.[144] Antibacterial activity has also been reported for such compounds against *E. coli*, *S. aureus*, and *B. subtilis*.[144]

CHAPTER 6

CHEMICAL INVESTIGATION OF AN ISOLATE OF *ACREMONIUM ZEAE* (NRRL 45893)

Acremonium zeae is a widely-occurring endophyte of maize and displays antifungal activity against *Aspergillus flavus* and *Fusarium verticillioides*.[41] During an earlier chemical investigation of fermentation extracts of an *A. zeae* isolate (NRRL 45893) in our laboratory, the unusual metabolites pyrrocidines A (**1.14**) and B (**1.15**) were encountered, identified, and shown to account for the antifungal activity observed in assays.[40,41] As discussed in Chapter 1, these metabolites were active in antifungal assays against *A. flavus* and *F. verticillioides*, as well as other major corn pathogens including *F. graminearum, N. oryzae, S. maydis, and R. zeae*. These compounds were also active in antibacterial assays against gram-positive bacteria, including bacterial endophytes and pathogens of maize such as *S. aureus, S. haemolyticus, E. faecalis, E. faecium, B. mojavensis, C. michiganense* subsp. *Nebraskense*, and *P. fluorescens*. Because of the potent biological effects exhibited by compounds **1.14** and **1.15** against maize pathogens, *A. zeae* has been described as a protective endophyte of maize.

As described in Chapter 1, the *A. zeae* isolates deposited with the ARS and CBS culture collections varied in the ability to produce pyrrocidines. This observation led to a

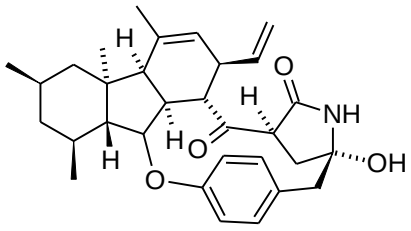

1.14

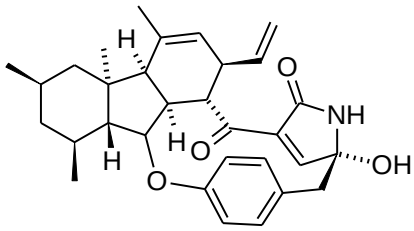

1.15

population survey of *A. zeae* isolates from nine states to determine their ability to produce these metabolites. During this survey, a structurally unrelated secondary metabolite produced in amounts comparable to the pyrrocidines was found in 105 of 154 isolates. Chemical studies of fermentation extracts from a representative isolate (NRRL 45893), originally obtained as "Az-115" from a sample of whole maize seeds received from Hopkinsville, KY, led to the identification of this new natural product as dihydroresorcylide (**6.1**), a reduced analogue of *cis*- and *trans*-resorcylide.[145] The absolute stereochemistry at C-3 was not directly determined, but is presumed to be the same as that of resorcylide, which was originally assigned the *S*-configuration. Along with dihydroresorcylide and the pyrrocidines, two known diastereomers were encountered that differ from **6.1** by the addition of a hydroxyl group at C-7 in both possible relative orientations. These compounds, which will be referred to as 7*R*-hydroxydihydroresorcylide (**6.3**) and 7*S*-hydroxydihydroresorcylide (**6.4**), were encountered as a mixture and identified as *A. zeae* metabolites. Details of all of these studies are presented in this chapter.

Structure Elucidation of Dihydroresorcylide (**6.1**)

The molecular formula of **6.1** was determined to be $C_{16}H_{20}O_5$ (7 units of unsaturation) on the basis of HRESIMS data. The ^{1}H NMR spectrum contained resonances characteristic of a benzenoid aromatic ring containing two *meta*-coupled protons, an OCH-CH_3 unit, an isolated diastereotopic methylene unit, and numerous aliphatic protons (Table 12). Many of the aliphatic ^{1}H NMR signals were complex and/or overlapping. The ^{13}C NMR spectrum contained resonances for one ester or acid unit, one ketone, six aromatic carbons, two of which are oxygenated, one oxygenated sp^3 methine, six sp^3 methylene units, and one methyl group (Table 12). Inspection of MS, ^{1}H NMR, and ^{13}C NMR data for the major metabolite initially suggested that this compound

was the known fungal metabolite curvularin (**6.2**), and the units described above would be consistent with such a conclusion. However, comparison of the NMR data with those reported for curvularin showed minor differences in some of the chemical shifts.[146] Thus, a full set of 2D NMR data was obtained in order to unambiguously establish the structure.

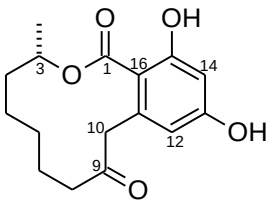

6.1

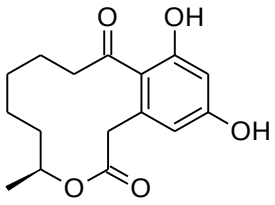

6.2

An extended spin-system including the OCH-CH_3 unit and five methylene units was constructed as shown in Figure 18 on the basis of ^{1}H NMR data and corresponding *J*-values, including the ddq observed in the ^{1}H NMR spectrum for oxygenated methine proton H-3. An HMBC correlation was observed from the oxygenated methine H-3 to an ester carbonyl signal at δ_C 170.9 (Table 12). However, the ester linkage could be formed by connection of O-3 to C-1 or C-9, rendering this correlation inadequate to determine the connectivity of the macrocycle to the aromatic ring unit as shown in Figure 18. HMBC correlations were observed from the isolated benzylic methylene unit protons (H_2-10) to aromatic carbons C-11, C-12, and C-16, as well as to the ketone carbon (δ_C 209.6), which indicated that the ketone was connected to the benzylic methylene group and the ester was therefore connected directly to the benzene ring. Further evidence to support this assignment included correlations from H_2-8 to the benzylic methylene unit at C-10 and the ketone carbon at C-9. Analysis of these data therefore led to identification of the structure as **6.1**, a regioisomer of **6.2**.

Table 12. ^{1}H and ^{13}C NMR Data for Dihydroresorcylide (**6.1**) in $CDCl_3$

Position #	δ_H (mult; *J* in Hz)[a]	δ_C[b]	HMBC Correlations (H→C#)
1		170.9	
3	5.13 (ddq, 2.7, 6.3, 6.3)	73.6	1, 3-Me, 4, 5
3-Me	1.29 (d, 6.3)	19.1	3, 4
4a	1.67 m	31.7	3, 5, 6, 3-Me
4b	1.57 m		3, 5, 6, 3-Me
5	1.49 m	21.1	overlapped
6	1.45 m	26.9	overlapped
7a	2.00 m	21.3	5, 6, 8, 9
7b	1.78 m		5, 6, 8, 9
8a	2.59 (ddd, 1.9, 9.7, 15)	41.8	6, 7, 9, 10
8b	2.37 (ddd, 1.9, 9.7, 15)		6, 7, 9, 10
9		209.6	
10a	4.64 (d, 18)	50.8	9, 11, 12, 16
10b	3.66 (d, 18)		9, 11, 12, 16
11		138.3	
12	6.02 (d, 2.6)	112.7	10, 13, 14, 16
13		160.7	
OH-13	6.47 (br s)[c]		
14	6.27 (d, 2.5)	103.0	12, 13, 15, 16
15		165.6	
OH-15	12.01 (s)		
16		106.3	

[a] Recorded at 600 MHz.

[b] Recorded at 150 MHz.

[c] Position variable.

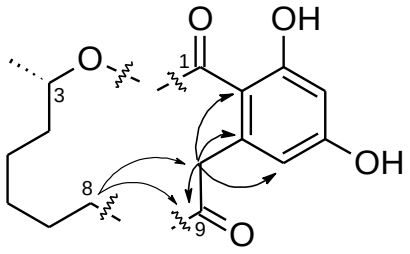

Figure 18. Key HMBC Correlations for Dihydroresorcylide (**6.1**)

Both curvularin (**6.2**) and the regioisomer of curvularin found in the *A. zeae* extracts (**6.1**) contain the same set of ^{1}H NMR spin systems, but differ in that the ketone carbonyl in curvularin is directly linked to the aromatic ring rather than to the isolated CH_2 corresponding to C-10 in **6.1**. Conversely, the isolated benzylic CH_2 in curvularin is linked to the ester carbonyl, rather than to the ketone carbonyl. A search of the literature revealed that compound **6.1** has not been previously reported, although a related compound called resorcylide that incorporates a double bond between carbons 7 and 8 is known.[147] The new analogue from *A. zeae* (**6.1**) was therefore assigned the name dihydroresorcylide.

The absolute configuration at C-3 of **6.1** was not directly determined, but is presumed to be the same as that of resorcylide. The sign of the specific rotation matches those of both *cis*- and *trans*-resorcylide (*cis*-resorcylide = $[\alpha]_D^{25}$ = +2.7, c = 0.26 g/100 mL in MeOH; *trans*-resorcylide = $[\alpha]_D$ = +47, c = 0.66 g/100 mL in MeOH; dihydroresorcylide (**6.1**) = $[\alpha]_D$ = +15, c = 0.33 g/100 mL in MeOH).[148] Resorcylide was originally assigned the 3*S*-configuration on the basis of chemical degradation studies, and this was later confirmed by total synthesis.[147,148]

A minor peak occurring in some of the LC-MS chromatograms was also collected and analyzed. The ^{1}H NMR spectrum resembled that of dihydroresorcylide (**6.1**), but showed doubling of signals, suggesting the presence of a mixture of analogues. On the basis of ESIMS data, the mass of these analogues was determined to be 16 mass units greater than that of **6.1**, suggesting these compounds possessed one additional oxygen unit ($C_{16}H_{20}O_6$). A search of the literature led to the identification of these compounds as a mixture of diastereomers that differ from dihydroresorcylide by the addition of a hydroxyl group at carbon 7 (in both possible relative stereochemical orientations). The methylene unit H_2-8 was located next to the ketone at C-9, and each of these two diastereotopic proton signals appeared as a dd in the ^{1}H NMR spectrum, which required that C-9 must be a methine, and the hydroxyl group must therefore be located at C-7.

Table 13. ^{1}H NMR Data for 7α-hydroxydihydroresorcylide (**6.3**) and 7β-hydroxydihydroresorcylide (**6.4**) in CD_3OD

position	7α-hydroxy dihydroresorcylide[a]	**6.3**[b]	7β-hydroxy dihydroresorcylide[a]	**6.4**[b]
3	4.95 (ddq, 9.8, 1.7, 6.1)	4.93 (m)	5.16 (m)	5.17 (m)
3-Me	1.30 (d, 6.1)	1.31 (d, 6.1)	1.28 (d, 6.4)	1.29 (d, 6.5)
4a	1.83 (m)	1.50 – 1.88 (m)	1.65 (m)	1.50 – 1.88 (m)
4b	1.73 (m)	1.50 – 1.88 (m)	1.65 (m)	1.50 – 1.88 (m)
5a	1.72 (m)	1.50 – 1.88 (m)	1.58 (m)	1.50 – 1.88 (m)
5b	1.41 (m)	1.50 – 1.88 (m)	1.58 (m)	1.50 – 1.88 (m)
6a	1.58 (m)	1.50 – 1.88 (m)	1.80 (m)	1.50 – 1.88 (m)
6b	1.58 (m)	1.50 – 1.88 (m)	1.52 (m)	1.50 – 1.88 (m)
7	4.35 (m)	4.30 – 4.40 (m)	4.34 (m)	4.30 – 4.40 (m)
8a	2.97 (dd, 13, 3.2)	3.00 (dd, 13, 3.2)	2.96 (dd, 15, 10)	2.98 (dd, 16, 10)
8b	2.48 (dd, 13, 10)	2.48 (dd, 13, 11)	2.59 (dd, 15, 1.9)	2.60 (dd, 16, 1.3)
10a	4.74 (d, 19)	4.77 (d, 19)	4.54 (d, 19)	4.57 (d, 19)
10b	3.72 (d, 19)	3.73 (d, 19)	3.83 (d, 19)	3.85 (d, 19)
12	6.11 (d, 2.5)	6.12 (d, 2.4)	6.11 (d, 2.5)	6.12 (d, 2.4)
14	6.24 (d, 2.5)	6.25 (d, 2.4)	6.24 (d, 2.5)	6.25 (d, 2.4)

[a] Literature values for Reference 149; Recorded at 360 MHz.

[b] Recorded at 300 MHz.

This assignment was further verified by analysis of the *J*-values for H_2-8 and comparison to literature values (Table 13).[149] These compounds, 7-hydroxydihydroresorcylides **6.3** and **6.4**, have been reported previously.[149] The structures of the samples from *A. zeae* were confirmed by comparison of MS and NMR data with literature values.[149] However, the relative configurations of the two individual compounds were not assigned in the literature report, and the absolute configurations of these compounds were also not determined. Thus, the ^{1}H NMR assignments reported for

compounds **6.3** and **6.4** are interchangeable, with the most notable differences being the *J*-values for H_2-8 (Table 13). As expected, these values were somewhat different from those of the corresponding hydroxy curvularin analogues, which are also known.[150] Unfortunately, the relative configuration at C-7 for the individual components could not be proposed on the basis of *J*-values. Because both compounds **6.3** and **6.4** were known compounds and because they were later found to be inactive in our assays, efforts were not made to separate the mixture of diastereomers, nor were attempts made to assign the absolute configuration of the individual constituents of the mixture.

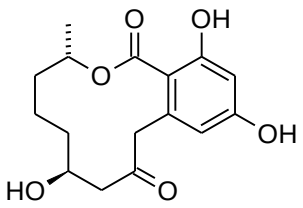

6.3

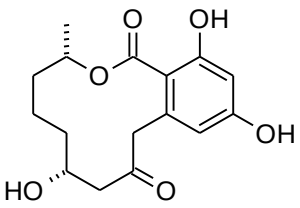

6.4

Although dihydroresorcylide has not been previously reported, the closely related *cis*- and *trans*-resorcylides have been isolated from *Penicillium* spp. *Pyrenophora teres*, the cause of net-type net blotch of barley, and *Drechslera phlei*, a pathogenic fungus on timothy grass.[147,149,151,152] *cis*-Resorcylide has also been isolated from *Penicillium roseopurpureum*.[153] The 7-hydroxydihydroresorcylides have been reported as metabolites of *D. phlei* and a *Penicillium* species.[149,152]

The resorcylides have been shown to have several different biological activities. *trans*-Resorcylide is a plant growth inhibitor and is >10 times more effective than *cis*-resorcylide at inhibiting rice seedling root elongation (IC_{50} = 50 ppm).[154] *trans*-Resorcylide is cytotoxic and is an inhibitor of 15-hydroxyprostaglandin dehydrogenase

(IC_{50} = 35 μM), whereas *cis*-resorcylide does not inhibit that enzyme.[154] On the other hand, *cis*-resorcylide is an inhibitor of activated factor XIII (FXIIIa), which is an enzyme that catalyzes a number of covalent cross-linking reactions of fibrin in blood clots.[153]

trans-Resorcylide also reportedly showed antifungal activity against *Pyricularia oryzae* using a paper disk assay.[154] However, when dihydroresorcylide was tested using our paper disk assay against *A. flavus* or *F. verticillioides* at 250 μg/disk, no fungistatic activity was detected. It has been previously shown that virulent fungal pathogens of maize were sensitive to pyrrocidine A (**1.14**; the other major metabolite from *A. zeae*), whereas other fungal endophytes and mycoparasites displayed little or no sensitivity at the concentrations tested (up to MIC = 50 μg/mL).[155] MIC tests were performed using dihydroresorcylide and the 7-hydroxydihydroresorcylide mixture to see if they showed a similar pattern of activity against endophytes and pathogens of maize. However, no significant growth inhibition (MIC > 50-μg/mL) was recorded for any of the test fungi.

trans-Resorcylide and 7*R*-hydroxydihydroresorcylide have been shown to be phytotoxic to several plant species, including maize, using leaf-wound puncture assays.[152] *trans*-Resorcylide was the more active compound, whereas *cis*-resorcylide and 7*S*-hydroxydihydroresorcylide showed little or no effect on these hosts.[152] Dihydroresorcylide and the 7-hydroxydihydroresorcylides were also phytotoxic in our own leaf-wound assays in maize, producing elongated lesions extending in both directions along the length of the leaf. Dihydroresorcylide, 7-hydroxydihydroresorcylides, and oxalic acid produced lesions averaging 1.4, 1.1, and 1.9 mm long, respectively when tested at 5 μg/wound. The untreated controls exhibited only the 0.25-mm needle puncture wounds. Thus, the dihydroresorcylides are phytotoxic, but appear to be less active than *trans*-resorcylide.

Dihydroresorcylide and pyrrocidines A and B were detected by LC-APCI-MS in intact, discolored maize kernels that were removed at harvest in the field from ears that were wound-inoculated in the milk stage with *A. zeae* NRRL 34559. Pyrrocidines A and

B (**1.14** and **1.15**) were readily detected in extracts of these *A. zeae*-infected maize kernels on the basis of LCMS selective ion chromatograms for the corresponding $(M + H)^+$ ions at *m*/*z* 488 and 490, respectively. There were no background metabolites in the control extract that interfered with this analysis. Although the $(M + H)^+$ ion at *m*/*z* 293 was the most intense ion in the spectrum of a standard sample of dihydroresorcylide when analyzed by LC-APCI-MS, the presence of dihydroresorcylide was more difficult to establish because there were other co-eluting compounds in the maize extracts that showed an ion at *m*/*z* 293. Thus, LC-APCI-MS/MS was found to be a better method for detecting dihydroresorcylide. Under the LC-APCI-MS/MS conditions used (Figure 19), the *m*/*z* 293 ion of dihydroresorcylide was fragmented to give two major ions at *m*/*z* 275 $(M+H-H_2O)^+$ and *m/z* 231 $(M+H-62)^+$. The interfering compound(s) in the corn extract also gave fragment(s) at *m*/*z* 275, so this mass was also not useful for distinguishing the other compounds from dihydroresorcylide. However, the fragment ion at *m*/*z* 231 was found to be characteristic of dihydroresorcylide on the basis of HRESIMS data, which established the molecular formula of the fragment ion as $C_{15}H_{19}O_2$, corresponding to $(M+H-H_2O-CO_2)^+$. Therefore, dihydroresorcylide was readily identified in these maize kernel extracts by LC-APCI-MS/MS analysis.

This result demonstrates the potential for pyrrocidines and dihydroresorcylide to occur in field corn. When cultured on potato dextrose agar, rice, or corn, some *A. zeae* strains obtained from the ARS and CBS Culture Collections produced greater quantities of pyrrocidines and dihydroresorcylide than *A. zeae* NRRL 34559, whereas other strains produced neither. *A. zeae* strains showing a greater ability to produce such compounds in laboratory culture presumably have the potential to produce higher levels in preharvest grain.

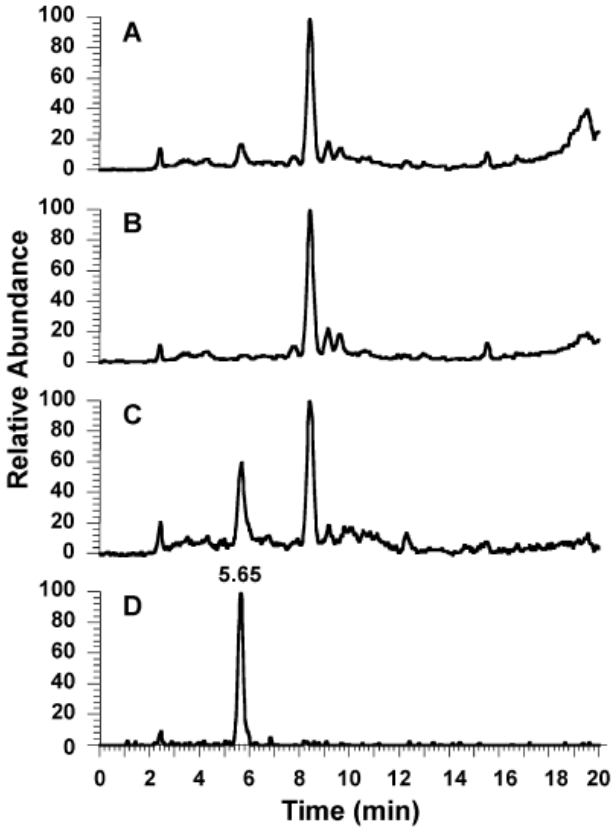

Figure 19. LC-APCI-MS/MS chromatograms of the EtOAc extract of *A. zeae*-infected maize kernels (with large, sample-unrelated background peak at 8.75 min): (**A**) TIC; (**B**) *m/z* 293; (**C**) *m/z* 275; (**D**) *m/z* 231 (retention time of **6.1** standard = 5.65

Potential Suppression of Maize Defense Responses by Resorcylide Analogues

Dihydroresorcylide (**6.1**) and the 7-hydroxydihydroresorcylides (**6.3** and **6.4**). are structurally related to the zearalenone, radicicol, and curvularin macrolides. These macrolides are known inhibitors of heat shock protein 90 (Hsp90). Hsp90 is one of the most abundant proteins in eukaryotic cells. Hsp90 plays an important role as an ATP-dependent chaperone that is critical for the regulation, stabilization, activation, and degradation of a number of key proteins involved in cell cycle regulation and signal

transduction.[156,157] Although some of these client proteins are essential for normal cell processes, others are known oncogenic proteins, such as C-RAF, B-RAF, ERBB2, AKT, telomerase, and p53.[158] Inhibition of Hsp90 may cause client proteins to adopt abnormally folded conformations, triggering proteosomal degradation of these proteins and disruption of a number of cancer causing pathways simultaneously.[159] The natural products geldanamycin (**6.5**), an actinomycete metabolite, and monorden (= radicicol, **6.6**), a fungal metabolite, are two of the most potent known inhibitors of Hsp90. Geldanamycin (**6.5**) inhibits yeast ATPase activity (IC_{50} = 2.86 μM), but radicicol (**6.6**) has a stronger ability to inhibit this activity (IC_{50} = 0.26 μM).[160] The values for the ATPase activities were slightly different than those reported in an earlier report,[161] but this is presumed to be due to differing Hsp90 protein concentrations used in the assays; larger concentrations were used in the earlier report (0.42 μM vs. 1.69 μM for **6.5**; 0.26 μM vs. 0.90 μM for **6.6**).

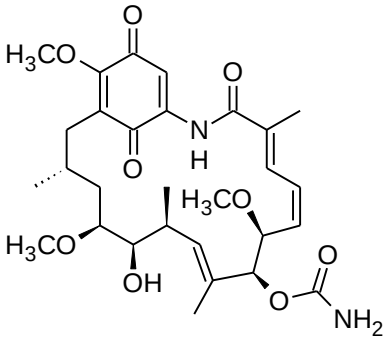

6.5

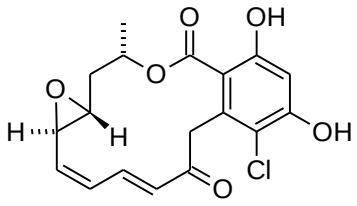

6.6

Thermodynamic and X-ray crystallographic analyses of geldanamycin and monorden have shown that both compounds cause inhibition of Hsp90 through disruption of the N-terminal ATP domain within the ATP binding pocket of Hsp90.[162]

Thermodynamically, the binding of both **6.5** and **6.6** is accompanied by enthalpy changes that are of opposite signs, determined using isothermal titration calorimetry, suggesting that the modes of binding for the two compounds at the N-terminal ATP-binding domain are different. No detectable binding occurred for either **6.5** or **6.6** at the C-terminus.[162] The crystal structures of yeast Hsp90 complexed with **6.5** and **6.6** were determined by molecular replacement with the free N-domain structure.[163] Electron density features were determined using difference Fourier maps, which were used to determine the orientation of compounds **6.5** and **6.6** at the N-terminal binding site within the Hsp90 binding pocket.[162]

A structure-activity relationship study of the 14-membered "natural" ring and conformational analogues of monorden was reported, and included 12-, 13-, 15-, and 16-membered synthetic analogues. Using X-ray data of the 13-, 14-, and 15-membered lactones co-crystallized with the N-terminal domain of Hsp90, it was found that they may bind to Hsp90 in a manner similar to that of monorden.[158] Monorden interacts through two H_2O molecules and the aspartate 79 residue via the phenolic hydroxyl groups and the carbonyl oxygen of the ester moiety (Figure 20).[2,164]

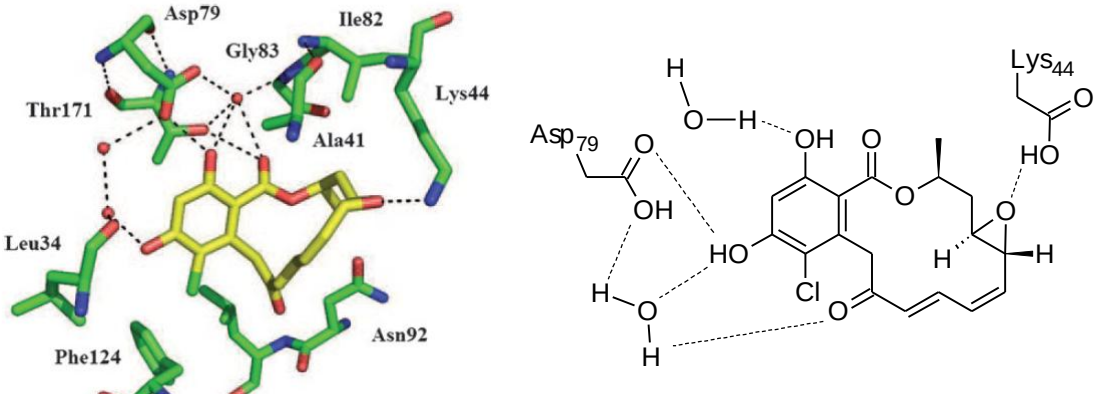

Figure 20. Binding Interactions of Monorden (**6.6**) within the Hsp90 Binding Pocket[2,3]

Although the 14-membered-ring analogues have been found to be the most active in these assays, it has been reported that 12-membered-ring-containing curvularin derivatives also inhibit Hsp90 at levels between 16-100 μM.[165] Based upon the ring size and structural similarity to Hsp90-inhibiting curvularin derivatives, it is proposed that dihydroresorcylide and related analogues would also likely bind at the N-terminal ATP binding site and inhibit Hsp90. Our colleagues at the USDA NCAUR in Peoria, IL are currently working to establish an Hsp90 assay in their laboratory to determine if this hypothesis is correct, and if so, determine the inhibitory effect of these compounds.

Colletotrichum graminicola, another fungal endophyte previously studied by our group, is a pathogen that causes anthracnose stalk rot and leaf blight of maize. The EtOAc extract of solid-substrate fermentations was active in assays against *A. flavus* and *F. verticillioides*. During our previous investigation of the potential presence and roles of *C. graminicola* in maize, the known compound monorden (= radicicol, **6.6**) was identified as a major metabolite of the EtOAc extract.[166] Compound **6.6** accounted for the antifungal activity in our assays, but, as noted above, **6.6** is also one of the most potent known Hsp 90 inhibitors. With the hypothesis that dihydroresorcylide and related analogues will inhibit Hsp90, and because curvularin analogues and monorden are known Hsp90 inhibitors, it is suggested that inhibition of Hsp90 in plants may assist with the colonization of fungal endophytes in host plants by suppressing the plant immune system or defense mechanisms.[166] As described in our previous work, it is possible that these compounds are released prior to fungal penetration of the plant to hinder the formation of lignified papillae and prevent other fungi from infecting the plant. Alternatively, these metabolites may be delivered through a penetration peg on maize leaves. The infection hypha will grow biotrophically, and during this period, the Hsp90-inhibiting metabolites may enter into individual plant cells, bind to the N-terminal ATP binding site of Hsp90, and suppress the hypersensitive response (HR), a form of apoptosis that limits the spread of invasive pathogens. Inhibition of Hsp90 may also reduce pathogen-associated

molecular patterns-triggered immunity, a second major component of the plant immune system. The suggested disease cycle of these fungal metabolites may be promoted by biotrophic "symptomless" infection to the plant by inhibiting Hsp90 R-protein chaperones and disrupting plant HR, suppressing basal plant defenses, and excluding other fungi from infected maize tissues.[166] If dihydroresorcylide and/or the 7-hydroxydihydroresorcylides are found to inhibit Hsp90, as might be expected based on their structural similarities to both monorden and curvularin, this would provide further support for the concept that Hsp90 inhibition is a common occurrence among successful endophytic fungi, and that such activity may be important in the colonization process.

CHAPTER 7

CHEMICAL INVESTIGATION OF *STENOCARPELLA MAYDIS*

As described in Chapter 1, *Stenocarpella macrospora* and *Stenocarpella maydis* are worldwide in their distribution and recognized as the most important ear rot pathogens in nearly all countries that produce maize. Chemical studies of EtOAc extracts from rice-fermented cultures of *S. maydis* NRRL 53565, NRRL 53566, and NRRL 53567, each of which displayed potent antifungal activity (*A. flavus* and *F. verticillioides*) and potent antiinsectan activity (*S. frugiperda*), afforded the four known *Stenocarpella* metabolites diplodiatoxin (**1.16**) and chaetoglobosins K (**1.18**), L (**7.1**), and M (**7.2**), along with chaetoglobosin O (**7.3**) and the bisdienediol, (all-*E)* trideca-4,6,10,12-tetraene-2,8-diol (**7.4**). The latter metabolites (**7.3** and **7.4**) have not been previously reported from *Stenocarpella,* but **7.3** was previously reported from *Phomopsis leptostromiformis*[167] and **7.4** was previously reported from *Xylaria obovata*.[168] The presence of diplodiatoxin as well as chaetoglobosins K, L, M, and O was also demonstrated for *S. maydis* NRRL 53562. Diplodiatoxin is the only compound previously reported from *S. maydis*,[48] but the authors of the corresponding study did not indicate that their culture of *S. maydis* was deposited in a culture collection. Diplosporin (**1.17**), and chaetoglobosins K[53] and L[169] (**1.18** and **7.1**) were also obtained from fermented-rice cultures inoculated with *Stenocarpella macrospora* NRRL 13611 (=MRC 143b) isolated from maize collected in Zambia.

The EtOAc extract of NRRL 43670 was partitioned between MeCN and hexanes, and the MeCN-soluble fraction subjected to Sephadex LH-20 column chromatography to yield the major component **1.16**. The molecular formula of **1.16** was determined to be $C_{18}H_{28}O_4$ (five units of unsaturation) on the basis of HRESIMS data. The ^{1}H NMR spectrum indicated the presence of one olefinic CH, two isolated methyl groups, four methylenes, three methines, and two -CH-CH_3 units. The ^{13}C NMR and DEPT-135 data

showed signals for 18 carbons including one ketone, one acid or ester (the signal at δ_C 177 could not be an amide since there are no nitrogens present in the molecule based upon HRESIMS data), two olefinic carbons, four methyls, four methylenes, and six methines. Analysis of the ^1H and ^{13}C NMR data also suggested the presence of two exchangeable protons. Evaluation of these NMR and MS data, a database search, and a survey of the literature led to the identification of the compound as diplodiatoxin (**1.16**), the only metabolite that had been previously reported from *S. maydis*.

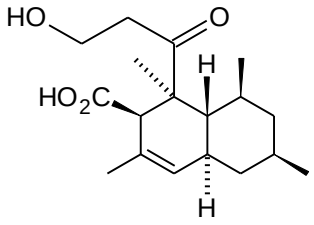

1.16

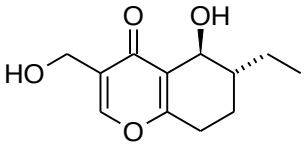

1.17

The EtOAc extract of NRRL 13611was partitioned between MeCN and hexanes, and the MeCN-soluble portion was subjected to reversed-phase column chromatography to yield compounds **1.17**, **1.18**, **7.1**, **7.2**, and **7.3.** The molecular formula of **1.17** was found to be $C_{12}H_{16}O_4$ (five units of unsaturation) on the basis of MS and NMR data. In the ^1H NMR spectrum, signals were observed for an isolated olefinic or aromatic proton, one isolated oxygenated sp^3 methylene unit, one oxygenated sp^2 methine unit, several methylene or methine units, and one CH_3CH_2 unit. COSY data revealed three spin-systems corresponding to substructures C-5 through C-8/C-11/C-12, and two isolated systems including C-13 and C-2. A search of the literature was performed using the mass range of 224-225 and one $CH_3CH_2CH(CH)CH_2CH_2$ unit. Comparison of the MS and NMR data to literature values led to the identification of diplosporin (**1.17**).[52]

The molecular formula of **1.18** was determined to be $C_{34}H_{40}N_2O_5$ (16 units of unsaturation) on the basis of HRESIMS data. The ^{1}H NMR spectrum contained a broad singlet at δ_H 8.05 and resonances for an olefinic proton at δ_H at 6.90, four aromatic protons between δ_H 7.00-7.50, characteristic of an indole moiety; five methyl groups including one CH_3-CH_2 unit, two CH_3-CH units, one vinyl methyl group, and one isolated methyl unit; two pairs of *trans*-coupled olefins at δ_H 7.75 and 6.45 (J = 18 Hz), and at δ_H 6.09 and 5.20 (J = 16 Hz); and eleven sp^3 methylene and/or methine units. The molecular formula required two additional protons not evident in the ^{1}H NMR spectrum, suggesting the presence of two exchangeable protons. These data were characteristic of a well-known class of compounds known as the chaetoglobosins. Using the MS and ^{1}H NMR data, a database search, and a survey of the literature, this compound was identified as chaetoglobosin K (**1.18**).[53]

The molecular formula of **7.1** was determined to be an isomer of chaetoglobosin K on the basis of HRESIMS data. There were a few differences between the ^{1}H NMR spectrum and that of **1.18**, including absence of the singlet for H_3-12, which was replaced by two broad terminal olefin singlets at δ_H 5.33 and 5.13, and a downfield shift of the H-7 signal from δ_H 2.75 to 3.93. The MS and ^{1}H NMR data were compared to literature values, and the compound was subsequently identified as chaetoglobosin L (**7.1**).[169]

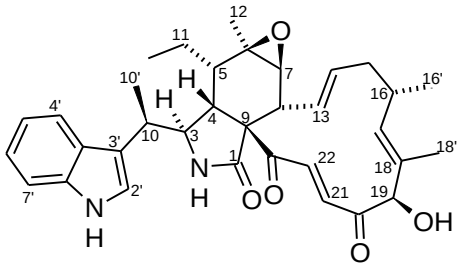

1.18

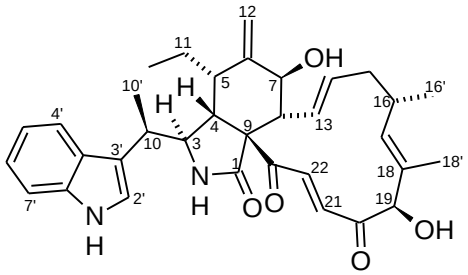

7.1

Compound **7.2** was again determined to be an isomer of chaetoglobosin K and L. There were slight differences in the ^{1}H NMR data relative to those of **1.18** and **7.1** including absence of signals for H-19, H-21, and H-22 protons in the spectrum of **7.2.** Also, two new signals appeared between δ_H 2.1 and 2.8, and H_3-18' was shifted downfield from δ_H 1.31 to 1.80. The MS data, a database search, and comparison to the literature led to the identification of this compound as chaetoglobosin M (**7.2**).[170]

The molecular formula of **7.3** was determined to be $C_{34}H_{42}N_2O_5$ (15 units of unsaturation) on the basis of ESIMS data. The ^{1}H NMR data closely resembled those of **7.2**, but with an additional oxygenated methine signal present in the spectrum at δ_H 4.69 and upfield shifted methylene protons from δ_H 1.85 to 1.75 suggesting that one of the ketone units in **7.2** had been reduced to an alcohol. MS data, a database search, and comparison to the literature led to identification of this compound as chaetoglobosin O (**7.3**).[167] The authors of the prior work attempted to assign the relative configuration of the new alcohol at C-20. Some NOE correlations were present between non-vicinal protons of the macrocycle ring, including H-20 and H-17, but these data did not enable conclusive assignment of the configuration. This stereocenter remains undefined.

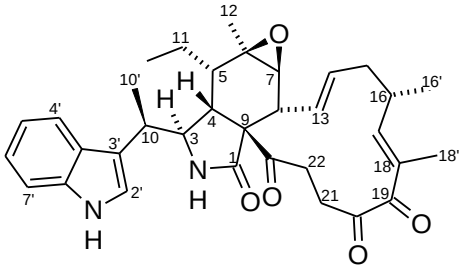

7.2

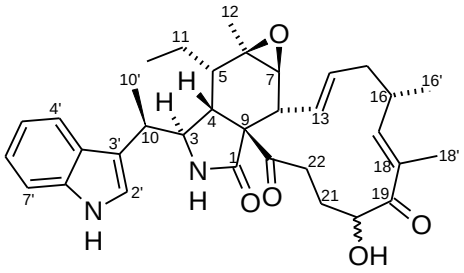

7.3

The EtOAc extract of NRRL 53566 was partitioned between MeCN and hexanes, and the MeCN-soluble portion was subjected to silica gel column chromatography and reversed-phase column chromatography to yield compound **7.4.** Despite its apparent abundance in the crude acetonitrile fraction of the extract, compound **7.4** was difficult to isolate in quantity using a silica gel gravity column and purification by preparative RP-HPLC (1.0 mg isolated from 365 mg of MeCN fraction), apparently due to a tendency toward decomposition. Various attempts to isolate more material following our original isolation procedure using a silica gel gravity column were not successful. Other approaches were explored, including a Sephadex LH-20 gravity column, and C_{18} and diol semi-prep RP-HPLC columns, but these attempts were also unsuccessful. The molecular formula of **7.4** could not be determined by EIMS, ESIMS, or APCIMS apparently due to decomposition in the mass spectrometer, but the structure was ultimately identified on the basis of NMR data and comparison to literature values.[168]

The ^{1}H NMR data for **7.4** collected using $CDCl_3$ solutions were difficult to fully interpret due to signal overlap, although units that could be identified included a monosubstituted terminal olefin, six other olefinic protons, two methylene units, and two oxygenated methines including one attached to a methyl group. After a substructure search, a close literature match was found, albeit with data reported in C_6D_6. Analysis of the sample using C_6D_6 as the solvent resolved the signals and matched the data reported for compound **7.4**. A useful aspect of the simplification observed in the spectrum of the C_6D_6 solution was the appearance of the two diastereotopic sp^3 methylene units as distinct triplets instead of dd's, which can be rationalized by the close similarity of the two corresponding vicinal *J*-values. Decoupling experiments were also performed and verified the connectivity of the structure as that shown in **7.4**. As previously mentioned, the molecular formula of **7.4** could not be directly determined using MS. It was recognized that this structure might easily undergo dehydration, resulting in the formation of a conjugated hexaene system. The MS data were further analyzed in hopes of

identifying the resulting hexaene ($C_{13}H_{16}$) product, but the corresponding ion was also not detected when the sample was analyzed by either EIMS or ESIMS.

The absolute configuration of **7.4** was not reported in the literature and it was felt that perhaps ozonolysis, preparation of a volatile derivative, and subsequent analysis by GCMS might enable an assignment, by analogy to the amino acid analysis discussed in Chapter 3 for bionectrin A (**3.1**). Standards were obtained for the expected ozonolysis products of **7.4** that contained a stereocenter, which included DL-malic acid and (±)-3-hydroxybutyric acid. The respective N-TFA-2-butyl ester derivatives were prepared and analyzed by GCMS. Unfortunately, the standards were not useful for GCMS analysis because the diastereomers of the desired products either coeluted or were not detected. Because **7.4** could not be obtained in pure form in greater quantities for further experiments, no further attempts were made to resolve these peaks and the absolute configuration was not determined.

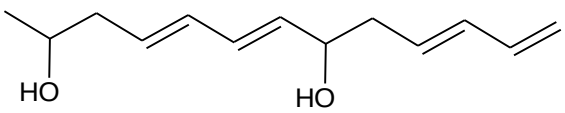

7.4

Analysis of ^{1}H NMR and MS data demonstrated that all isolates of *S. maydis* analyzed produce diplodiatoxin (**1.16**) as a major constituent. This constitutes the first report of chaetoglobosins (**1.18**, and **7.1**-**7.3**) and (all-*E*) trideca-4,6,10,12-tetraene-2,8-diol (**7.4**) being produced by *S. maydis*. Other minor constituents were present in the extract of NRRL 13611, but because these compounds were in low abundance when compared to the other compounds identified in the extract, no attempt was made to isolate these metabolites. However, some of these metabolites are presumed to be other

chaetoglobosin analogues on the basis of their close chromatographic proximity to the chaetoglobosins and their similar masses, which were determined using LCMS data.

Diplosporin (**1.17**) and chaetoglobosins K, L, M, and O (**1.18**, and **7.1-7.3**) were obtained from fermented-rice cultures inoculated with *S. macrospora* NRRL 13611 (=MRC 143b) isolated from maize grown in Zambia. This is the same culture that had previously been reported by other researchers to afford diplosporin (**1.17**), as monitored by bioassay in ducklings.[51] Neither diplodiatoxin nor (all-*E)* trideca-4,6,10,12-tetraene-2,8-diol were detected in extracts of *S. macrospora*. Cutler *et al.* isolated and characterized chaetoglobosin K and diplosporin (= diplodiol) from a culture of *S. macrospora* ATCC 36896 (NRRL 13610) isolated from maize in Costa Rica.[52,53] Both compounds were shown to be toxic to one-day-old chicks, and chaetoglobosin K was also shown to be a potent growth inhibitor of wheat coleoptiles (*Triticum aestivum*).[53] Chaetoglobosins L, M, and O have also been isolated and characterized from cultures of *S. macrospora*.[169,170] Chaetoglobosins M and O have since been reported from two strains of *Phomopsis leptostromiformis* cultured on sterile maize.[167]

Bioactivity of *Stenocarpella* metabolites

Diplodiatoxin (**1.16**), diplosporin (**1.17**), and chaetoglobosin K (**1.18**) were evaluated in disc assays against *A. flavus* and *F. verticillioides*. Chaetoglobosin K displayed potent activity at 300 μg/disc while diplodiatoxin and diplosporin were ineffective at 200 μg/disc. In more quantitative assays performed using 96-well plates, chaetoglobosin K displayed significant activity against *A. flavus* (MIC ≈ 50 μg/mL; GI_{50} ≤ 25-50 μg/mL) and *F. verticillioides* (GI_{50} >3-50 μg/mL), while diplodiatoxin, diplosporin, and the (all-*E*) trideca-4,6,10,12-tetraene-2,8-diol were ineffective (MIC and GI_{50} both > 50 μg/mL). There have been few reports on the antifungal activity of chaetoglobosins, although chaetoglobosin A reportedly exhibited potent *in vitro*

antifungal activity against the rice blast disease pathogen *Pyricularia oryzae*, while chaetoglobosin D and 19-O-acetylchaetoglobosins A and D were found to be strongly inhibitory to *A. flavus* at 250 µg/disc.[171,172]

Chaetoglobosin K and diplosporin displayed significant antiinsectan activity in dietary assays against the fall armyworm at 1000 ppm, causing 74% and 50% reduction in growth rate (RGR), respectively, relative to controls with no larval mortality, while diplodiatoxin was inactive when tested at 1000 ppm. The bisdienediol (all-*E)* trideca-4,6,10,12-tetraene-2,8-diol was inactive when tested at a dietary level of 100 ppm, but higher testing levels were precluded by difficulties in isolating pure material in quantity. Chaetoglobosin K also displayed significant activity (RGR = 69%) against corn earworm (*Helicoverpa zea;* Lepidoptera: Noctuidae) when tested at a dietary level of 1000-ppm. The antiinsectan activity of the EtOAc extracts from *S. maydis* NRRL 53562 was therefore at least partly attributed to chaetoglobosin K, while the antiinsectan activity of the EtOAc extracts from *S. macrospora* NRRL 13611 was ascribed to both chaetoglobosin K and diplosporin. However, other chaetoglobosin analogues present (see below) also seem likely to contribute. In dietary assays against corn earworms at 100 ppm, 19-O-acetylchaetoglobosins A and D, and chaetoglobosin D reportedly exhibited potent activity (RGR = 95%), while at dietary levels of 300 ppm, chaetoglobosin A also exhibited potent activity (RGR = 98%), chaetoglobosin B showed moderate activity (39% RGR), and chaetoglobosin C was found to have relatively low oral toxicity in this assay.[172,173] In spite of these results, Jarvis *et al.* observed that stalk rot infection by *S. maydis* had no effect on natural infestation by the European corn borer *Ostrinia nubilalis* (Lepidoptera: Noctuidae).[174] This observation is ultimately consistent with the present study, as selected isolates of *S. maydis* did not produce detectable levels of chaetoglobosins K and L or any other compounds with demonstrated antiinsectan activity in diseased/necrotic stalks inoculated with *S. maydis*.

Sap beetles (Coleoptera: Nitidulidae) have been implicated as vectors of *Fusarium* spp. and have been shown to act as vectors for *Gibberella zeae* and *A. flavus* specifically to preharvest maize ears.[175-177] It has also been demonstrated that volatiles produced by *F. verticillioides* attract sap beetles.[178] Sap beetles could therefore similarly serve as vectors of *S. maydis* to maize ears and our colleagues at the USDA, NCAUR wanted to determine if severely rotted kernels supporting *S. maydis* pycnidia would attract or deter adult beetles. A four-day assay choice test was conducted with paired vials in each feeding chamber containing 50 mg of milled powder from seeds rotted by *S. maydis* NRRL 53565 with controls representing 50 mg of milled powder from seeds removed from symptomless ears of the same corn hybrid. Throughout the experimental period, higher numbers of beetles were consistently observed in vials containing powder from *S. maydis*-rotted seeds. At the conclusion of the experiment, the weight of powder remaining in each of the vials was recorded. The mean weight of powder removed (presumably consumed) by 20 adult beetles in each feeding chamber was 17.9 mg for the *S. maydis* rotted seeds and 5.8 mg of powder from symptomless control seeds ($F=26.21$; $P<0.0001$). The sap beetles were thus attracted to the *S. maydis* rotted seeds, but were not consuming the powder. It is possible that the presence of chaetoglobosin K might be at least partially responsible for this result due to the antiinsectan activity displayed in our assays.

A leaf-puncture wound assay revealed that, among the *Stenocarpella* metabolites tested at 10 µg/wound and recorded as an average of six wounds, diplodiatoxin exhibited significant phytotoxicity to maize leaves, producing elongated lesions (avg. 2.6 mm), extending in both directions along the leaves of Burrus 794 and B73 corn (avg. 2.8 mm), that were equivalent to lesions produced by the oxalic acid positive control at 5 µg/wound (avg. 2.40 mm). The presence of diplodiatoxin as a major metabolite could explain the somewhat greater lesion lengths produced by solvent extracts of *S. maydis* than those of

S. macrospora, which does not produce this compound. This is the first report of phytotoxicity of diplodiatoxin to maize.

At the same time, chaetoglobosin K was tested at 10 μg/wound and produced only minor lesions (avg. 1.10 mm), while needle wounds treated with diplosporin at the same level did not exceed those of a solvent blank and would therefore not explain the blighting of entire leaves of plants attributed to *S. macrospora*.[45] On the other hand, chaetoglobosin K and other cytochalasin-type compounds are known to block actin filament elongation and may function in disrupting alterations in the actin cytoskeleton associated with a plant cellular defense response to fungal infection.[179-181] Cutler *et al.* reported that chaetoglobosin K inhibited the growth of wheat coleoptiles at even lower concentrations (10^7 M) than the standard plant growth inhibitor abscisic acid.[53] This suggests that very small amounts of chaetoglobosin K could bring about profound effects on effector targets. Therefore, while chaetoglobosin K was not detected in diseased maize tissues in this work, it may be present at levels that are sufficient to support biotrophy.

Detection of *Stenocarpella* metabolites in maize

Diplodiatoxin (**1.16**) was detected in severely rotted grain from maize ears inoculated in the late milk stage of kernel maturation with *S. maydis* NRRL 53565, NRRL 53566, or NRRL 53567. This grain was distinguished by the presence of numerous black pycnidia on kernel surfaces. Initially, we were unable to detect other *Stenocarpella* metabolites (**1.18**, **7.1**, and **7.2**) by ^{1}H NMR or MS techniques in any of these extracts. However, upon further investigation, we were able to detect these metabolites at a higher concentration (2 μg extract/injection) than initially analyzed (200 ng extract/injection) using LC-MS techniques (Figure 21). Diplodiatoxin and chaetoglobosin K could be detected at 200 ng extract/injection of the MeCN-soluble

portion of naturally-infected *S. maydis* corn fermentation extracts as could minor chaetoglobosin analogues. The limit of detection of these compounds has not yet been determined, but on the basis of the LCMS results, these values are expected to be <200 ng for diplodiatoxin and chaetoglobosin K, and between 200 ng and 2 μg for chaetoglobosins L, M, and O.

Diplodiatoxin (**1.16**) was also detected upon LC-ESITOFMS analysis of MeCN partition fractions from extracts of green stalks and stalk residues that had been steam-sterilized and inoculated with either of two isolates of *S. maydis* (NRRL 53562 or NRRL 53565). Diplodiatoxin was detected in wound-inoculated necrotic discolored stalk lesions at 59 days post inoculation (dpi) for plants inoculated with *S. maydis* strains NRRL 53562 or NRRL 53565, but was not detected in necrotic discolored lesions harvested at either 17 or 31 dpi. The production of diplodiatoxin by *S. maydis* may coincide with the switch from biotrophic growth to a necrotrophic growth phase. Explaining the mode of action of diplodiatoxin in pathogen virulence awaits further study. The presence of this compound could also be detected simply by ^{1}H NMR analysis of the crude extract. Using ^{1}H NMR or MS techniques, no other *Stenocarpella* metabolites were detected in any of the extracts from living maize plants or steam-sterilized stalk residues (200 ng/injection) that had been inoculated with isolates of *S. maydis* strains (NRRL 53562 or NRRL 53565) that had been found to produce these metabolites in fermented rice culture. The LC-MS method employed enabled us to determine the presence of **1.16** in an organic extract, or its absence above the limit of detection, but did not afford detailed quantitative information about its concentrations. This constitutes the first reported detection of diplodiatoxin or any other fungal metabolite in *S. maydis*-rotted seeds and diseased stalk tissues.

In fermented rice cultures, each of these fungi produced compounds **1.16**, **1.18**, **7.1**, and **7.2** as major components, and numerous unidentified minor metabolites. These unidentified analogues are likely related to the chaetoglobosins identified in this work

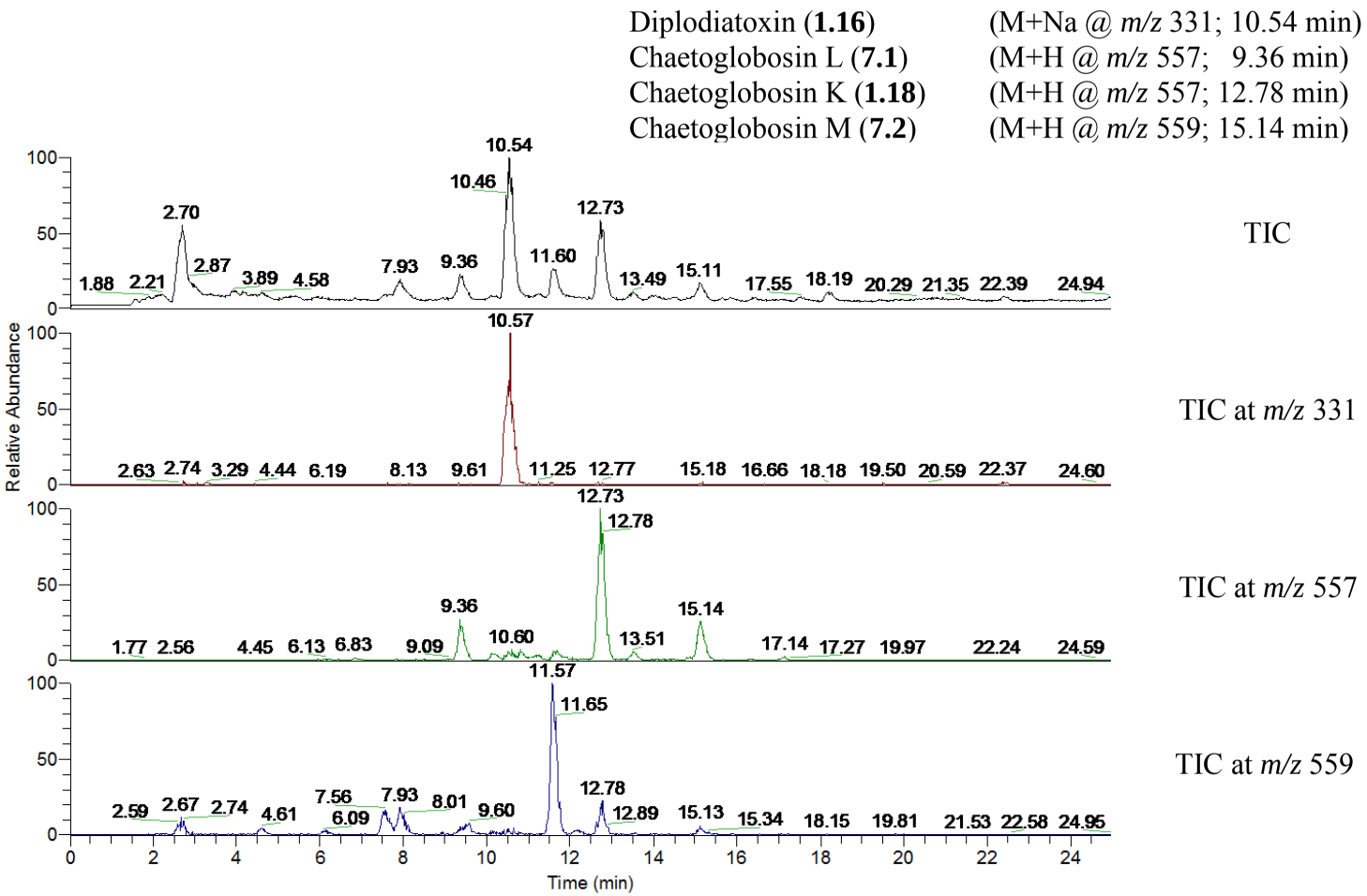

Figure 21. LC-ESIMS Data for EtOAc Extract of *S. maydis* Fermented Rice (NRRL 53562)

based upon the close chromatographic proximity of these compounds to the chaetoglobosins, as well as the LCMS data, in which some of these analogues had the same mass as chaetoglobosins K, L, and M, while others had the same mass as chaetoglobosin O.

None of these *Stenocarpella* metabolites were detected in extracts of grain from naturally infected ears in 2007 that were the source of *S. maydis* isolates NRRL 53565, NRRL 53566, or NRRL 53567. While these ears showed visible symptoms of *Stenocarpella* ear rot, as evidenced by the appearance of white cottony mycelium between the seeds, no pycnidia were observed and the yellow seed endosperm was only moderately discolored. Chambers demonstrated that the opportunity to produce substantial *S. maydis* ear-rotting decreases sharply with a later inoculation date after mid-silk and is associated with a corresponding decrease in seed moisture.[182] Furthermore, as maize seeds mature they accumulate abundant amounts of two class IV chitinases, Chit A and Chit B, which have been shown to inhibit the growth of fungi on agar plates and may contribute to resistance to ear rot caused by *S. maydis*.[183,184] Late-infected ears may appear sound until the ears are shelled and evidence of "hidden diplodia" is found with symptoms of seed infection, "darkened germs" associated with a loss in seed viability being restricted to the tip-end.[44]

Interpreting diplodiosis

As described in Chapter 1, diplodiatoxin has been dismissed as the toxin responsible for outbreaks of diplodiosis in cattle. Based upon our work, we proposed that the "unknown toxin" was likely to be a mixture of chaetoglobosins including chaetoglobosins K and L as major components, with other chaetoglobosin analogues occurring as minor metabolites. First, reported evaluation of the oral toxicity of chaetoglobosin K to one-day-old chicks gave an LD_{50} between 25 and 62.5 mg/kg.[53] The

presence of chaetoglobosins in *S. maydis*-fermented maize seed culture material could explain its acute toxicity to poultry.[60,185] No other studies of vertebrate toxicology using purified chaetoglobosins K or L have been reported. Chaetoglobosins are metabolites belonging to the family of cytochalasins which includes chaetoglobosin K and other compounds that have been shown to disrupt actin polymerization and therefore can interfere with the myelination process.[179,186,187] Disrupting actin polymerization with cytochalasin D blocked the differentiation and myelination of Schwann cells co-cultured with dorsal root ganglion neurons.[188] An "unknown toxin" was reportedly responsible for causing diplodiosis in sheep and interfering with the myelination process, the fetus being particularly vulnerable in the later part of pregnancy.[46,189] *Stenocarpella maydis*-fermented maize culture material also caused mycotoxic peripheral myelinopathy in vervet monkeys.[190] Odriozola *et al.* have since reported histopathological evidence of moderate to severe degeneration of myelin shafts in white matter of the cerebellum of heifers that died from an outbreak of diplodiosis after consuming harvested maize from fields parasitized with *S. maydis* in Argentina.[47] Further evidence for chaetoglobosins comprising the "unknown toxin" comes from studies showing that the toxin(s) in *S. maydis*-fermented maize seed culture material are heat labile.[48,60,61,190,191] Chaetoglobosin A in dried solvent extracts decomposes when heated to 75°C for 24h or 100°C for 90 min.[192] We have found that chaetoglobosins produced by *S. maydis* in fermented rice culture material are decomposed to a significant extent by autoclaving at 121°C for 45 min., and this was accompanied by losses in antifungal and antiinsectan activity of the solvent extracts.

Our results suggest that the biosynthesis of chaetoglobosins K and L is not supported during the necrotrophic phase of infection yielding dry-ear rot, so association of these metabolites with symptoms of diplodiosis is uncertain. On the other hand, it is possible that chaetoglobosins may form in maize crop residues following harvest. Marasas noted that in southern Africa all outbreaks of diplodiosis are recorded in late

winter (July-Sept.) when farm-stored roughage becomes depleted and livestock are turned out to graze harvested maize fields.[191] In this subtropical climate, *S. maydis* has the potential for continued saprotrophic growth and/or metabolic activity during this period, which could lead to the biosynthesis of both diplodiatoxin and chaetoglobosins. No analytical methods have been developed for determining accurate levels of *Stenocarpella* metabolites in rotted seeds or maize stalks, information that could be used to better predict the occurrence of diplodiosis in ruminants consuming *Stenocarpella*-rotted ears.

A report by a South African research group has very recently appeared in the literature and identifies a neurotoxin from *Stenocarpella maydis* responsible for the induction of diplodiosis in guinea pigs.[193] This metabolite, which they named diplonine (**7.5**), was obtained from a methanolic extract of a corn fermentation inoculated with isolates of two *S. maydis* cultures (in separate jars) that had previously induced diplodiosis in sheep (MRC 2829 and ARC-GCI 6). The absolute configuration of this compound was not determined, but the relative configurations of the two diastereomers were proposed based on crosspeaks observed in the NOE data from H_3-6 to H-2 and H_a-3; from H_b-3 to H_a-3 and H-4; and from H-4 to H-2 and H_b-3, resulting in the two possible structures shown (**7.5a** and **7.5b**). In our work, we had used a medium-polarity solvent (EtOAc) for extraction of the fermented material. Therefore, if diplonine had been present, the polarity of our solvent was likely insufficient to extract significant quantities of this metabolite. The authors described in the report that diplodiatoxin has not been linked to neurotoxicity in ruminants, and the chaetoglobosins have not been tested in such assays. As a result, it is unknown if these compounds induce diplodiosis in ruminants, but the authors reported that diplonine resulted in neurological symptoms in guinea pigs at 158 mg diplonine per 100 g guinea pig that were consistent with those reported for ruminants and may therefore be the toxic metabolite responsible for these effects, or may at least contribute significantly.

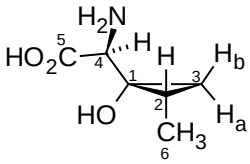

7.5a

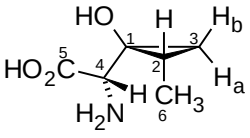

7.5b

In light of this recent report, extracts of *Stenocarpella maydis*-rotted kernels from wound-inoculated ears of Burrus ZD51 (2009) were extracted twice with EtOAc as before, then air-dried, extracted twice with MeOH, air-dried, and extracted twice with H_2O. The H_2O extract was frozen and freeze-dried. The resulting extracts will be tested in our standard antifungal and antiinsectan assays, and analyzed by NMR and/or MS to determine if diplonine, or other as-yet unidentified, more polar toxic metabolites are present in wound-inoculated maize ears. During our preliminary investigation of these extracts using ^1H NMR, we were unable to detect compound **7.5** in MeOH or H_2O extracts, thus requiring further detailed investigations in future. If diplonine is identified, a survey will be conducted to determine if this toxin is also present in corn naturally-infested with *S. maydis.*

CHAPTER 8

CONCLUSIONS

The work in our group focuses on the isolation and structure determination of chemically and biologically interesting secondary metabolites from fungi targeted on the basis of ecological and/or taxonomic consideration. Fungicolous and mycoparasitic fungal isolates were obtained from host fungi in Hawaii, and endophytic fungal isolates were obtained as colonists of maize in a number of U.S. regions. As described in Chapter 2, fungal isolates were generally selected for investigation because their fermentation extracts displayed antifungal activity against two pathogens of corn, *Aspergillus flavus* and *Fusarium verticillioides*, and/or antiinsectan activity in an assay against an economically important crop insect (*Spodoptera frugiperda*). Chapters 3-5 describe studies of 11 fungicolous fungal isolates, which led to the identification of six new and 18 known metabolites. Chapter 6 describes our studies of the corn endophyte *Acremonium zeae*, which led to the identification of one new and four known metabolites, and Chapter 7 describes seven metabolites that had not been previously reported from U.S. isolates of endophytic *Stenocarpella* spp.

In the studies involving fungicolous fungi, several well-known fungal metabolites, such as cyclosporin A, mevalonolactone, sterigmatocystin, nicotinic acid, and mycophenolic acid, were encountered. Some of the new metabolites contained unusual amino acid residues, such as isovaline and aminoisobutyric acid (Aib) units, both of which appeared in bionectrin A, a peptaibol-type metabolite. Aib units were also encountered in the cyclic chlamydocin analogues, which is interesting because nearly all known naturally-occurring Aib-containing peptides are linear. A new dihydro analogue of the known metabolite oxirapentyne was also encountered. This metabolite belongs to a rare class of highly oxygenated, prenylated cyclohexanoid fungal natural products. Finally, from extracts of a mycoparasitic fungal isolate, a new cytochalasin analogue and

a β-carboline-containing metabolite were obtained during the course of this work. Cytochalasins are well-known fungal metabolites, whereas β-carbolines are rarely obtained from fungal sources.

In other studies, fermentation extracts of widely-occurring endophytes of maize, including isolates of *Acremonium* zeae, *Stenocapella maydis*, and *S. macrospora,* were found to display antifungal activity against *A. flavus* and *F. verticillioides*. Initial work with *A. zeae* had led to the identification of pyrrocidines A and B, which were responsible for the antifungal effects observed in our assays. The work presented in this thesis focus on three resorcylic-acid lactone (RAL)-type metabolites that occurred in amounts comparable to the pyrrocidines and with even greater frequency among *A. zeae* isolates. These RALs are structurally related to the known heat shock protein 90 (Hsp90) inhibitors curvularin and monorden. Considering other work in our research group involving isolates of another fungal endophyte, *Colletotrichum graminicola*, which produces monorden, it is suggested that such compounds may assist endophyte colonization of host plants through the suppression of plant defense mechanisms by inhibition of Hsp90 in plants. *S. maydis* and *S. macrospora* are worldwide in their distribution in maize. Some chemistry is known from these metabolites; however, no metabolites had been reported from U.S. isolates. *S. maydis* has been associated with diplodiosis, which is a common nervous disorder, or neuromycotoxicosis, of cattle and sheep that graze on infected grain. However, the only metabolite reported from *S. maydis*, diplodiatoxin, is apparently not responsible for these effects. Chemical investigation of extracts of isolates of *S. maydis* and *S. macrospora* led to the identification of diplodiatoxin, chaetoglobosins K, L, M, O, and (all-*E*)-trideca-4,6,10,12-tetraene-2,8-diol. Because of the bioactivities of some of these metabolites, production of such compounds may contribute to the host plant defense. Through efforts described in this thesis, some of these metabolites were found to form in the field, and may be at least partly responsible for diseases of livestock.

The structures of the metabolites encountered in this workwere determined by analysis of MS and NMR data, and the relative and absolute configurations were proposed on the basis of NOESY data, coupling constants, chemical derivatizations, and X-ray crystallographic analysis. Some of the structures were difficult to characterize, such as dihydrooxirapentyne, which possessed a near-planar six-membered ring, which in turn reduced the number of useful coupling constants and NOESY correlations. In the case of the linear peptide bionectrin A, many of the signals in the ^{1}H NMR spectrum were broad and/or overlapping, and required application of other methods beyond standard 2D NMR approaches, including HRESITOFMSMS, LC-ESIMS, ^{1}H-^{15}N HMBC, and Marfey's method, to determine the identity and connectivity of the amino acid residues. The chaetoglobosins were difficult to isolate in quantity due to the presence of multiple, closely-related analogues.

The metabolites described in this thesis represent a number of structural classes, including terpenoid, polyketide, peptide, and mixed biogenetic origins, and have various bioactivities. The studies of corn endophytes described here have provided further knowledge that may ultimately be useful in determining the roles that these fungi and their metabolites, may play in maize.

CHAPTER 9

EXPERIMENTAL

General Experimental Procedures

Solvents and Reagents

Reagent grade solvents used for partitioning and HPLC grade solvents used for chromatography were purchased from Fisher Scientific. Distilled H_2O for HPLC applications was purified using a SYBRON/Barnstead NANOpure system with a pre-treatment cartridge (catalog number D0835), two ultrapure cartridges (D0809), and a 0.2-μm hollow fiber filter (D3750). Reagents and deuterated solvents were purchased from Sigma-Aldrich Chemical Company, Fisher Chemical Company, or Cambridge Isotope Laboratories.

Weight Measurements

Weights of reagents, crude extracts, partitions, column fractions, and pure compounds were measured using a Mettler AR 160 balance.

Evaporation

Removal of solvents was accomplished by evaporation under streams of air.

Chromatography

Silica gel TLC separations were carried out using pre-coated plastic sheets (Alltech, 0.25-mm thickness silica gel with fluorescent indicator, 40 x 80 mm). TLC spots were visualized by exposure to UV light at 254 nm, by exposure to iodine vapor, or by staining with phosphomolybdic acid followed by drying with a heat gun. Column

chromatography and vacuum liquid chromatography (VLC) separations were performed with J. T. Baker silica gel 40-µm flash chromatography packing. VLC separations were conducted using a column with a ground glass fitting, side arm, and frit that was secured onto a 500-mL Erlenmeyer flask. Gel filtration column chromatography was accomplished using Sephadex LH-20 (Sigma). Fractions from column chromatography were collected manually using beakers.

Semi-preparative reversed-phase HPLC separations were peformed using one of three Beckman Instrument systems: (**1**) System Gold solvent delivery module with model 168 photodiode array detector, both controlled by System Gold 32 Karat software using an IBM 300PL PC; (**2**) System Gold solvent delivery module with a model 168 variable wavelength UV detector, both controlled with system Gold software (version 5.1); or (**3**) System Gold solvent delivery module with a model 166 variable wavelength UV detector. The three HPLC systems employed Rheodyne model 7725 injectors. Separations were conducted using Alltech Altima C_{18} (5-µm particle size, 10.0 mm x 250 mm), and Alltech Apollo C_{18} (5-µm particle size, 10.0 mm x 250 mm) at a flow rate of 2.0 mL/min, or a Rainin Dynamax C_{18} (8-µm particle size, 21.4 x 250 mm) column at a flow rate of 5.0 mL/min. The column used for LCMS studies was a Supelco Discovery reversed-phase C_{18} column (5-µm particle size, 2.1 x 150 mm) at a flow rate of 0.20 mL/min. Semi-preparative and preparative HPLC chromatograms were recorded using a model 1200 Linear chart recorder, and were monitored at selected wavelengths between 210-260 nm.

Spectroscopic Instrumentation

Optical rotations were measured using a Rudolph Research Autopol III automatic polarimeter. Melting points were obtained on a Fisher-Johns micro melting point apparatus, and are uncorrected. UV spectra were recorded using a Varian Cary 100 Bio

UV-visible spectrophotometer. Low-resolution EI mass spectra, including those obtained by GC-MS, were acquired at 70 eV on a Finnigan Voyager quadrupole mass spectrometer. Low-resolution ESIMS data, including LC-MSMS data, were obtained using a ThermoFinnigan LCQ ion trap instrument unless otherwise indicated. High-resolution EI and ESI mass spectra were recorded using a Micromass Autospec or Q-TOF Premier mass spectrometer. Tandem mass spectrometry (MS^n) data were obtained using the Q-TOF premier mass spectrometer.

^1H NMR data were recorded on Bruker AVANCE-600, DRX-400, or AVANCE-300 spectrometers (5-mm probes) at room temperature. ^1H NMR data were also recorded on a second Bruker AVANCE-600 spectrometer using a 1.7-mm probe. ^{13}C NMR, DEPT, NOE difference, and homonuclear decoupling experiments were performed on the DRX-400 instrument. All spectrometers used XWINNMR 3.1 or Topspin 1.3 software. The AVANCE-600 operates at ^1H and ^{13}C frequencies of 600.1422 and 150.9203 MHz, respectively. ^1H NMR and inverse detection experiments (COSY, HMQC, HMBC, ^1H-^{15}N HMBC, TOCSY, NOESY, and ROESY) were recorded on the AVANCE-600 instrument using a 5-mm inverse probe (BBI). A second AVANCE-600 spectrometer was also available to record data using a 1.7-mm microprobe. The Bruker DRX-400 spectrometer operates at a ^1H frequency of 400.1355 MHz and a ^{13}C frequency of 100.6230 MHz, and used a 5-mm proton-carbon-fluorine-phosphorous (HCFP) probe. The Avance-300 spectrometer was operated at a ^1H frequency of 300.1675 MHz and a ^{13}C frequency of 75.4768 MHz, and used a 5-mm Quadra Nuclei probe (QNP) that detects proton, carbon, fluorine, and phosphorus nuclei.

All NMR spectra were recorded in the deuterated equivalents of benzene, chloroform, acetone, methanol, dimethylsulfoxide, acetonitrile, or pyridine, and the chemical shifts are reported in ppm downfield from tetramethylsilane (TMS), with the appropriate residual solvent peaks used as internal reference standards (δ_H/δ_C, 7.16/128.1, 7.24/77.0, 2.05/29.8, 3.31/49.0, 2.50/39.5, 1.94/118.3, and 8.74, 7.58, 7.22/150.4, 135.9,

123.9, respectively). NOESY experiments were conducted on the DRX-400 or AVANCE-600 spectrometers (5-mm and 1.7-mm probes). HMQC, HMBC, TOCSY, and ROESY experiments were conducted on the AVANCE-600 spectrometers (5-mm and 1.7-mm probes). COSY, and ^{1}H-^{15}N HMBC experiments were conducted on the AVANCE-600 spectrometer (5-mm probe). 1D NMR data were processed using the NUTS program (Acorn NMR Inc., version 5.02). 2D-data were processed using XWINNMR 3.1 on a Silicon Graphics workstation (SGI O2), TopSpin 1.3, or TopSpin 3.0. Five-mm 535-pp and 5-mm 528-J4-7 NMR sample tubes were purchased from Wilmad Glass Company, and 1.7-mm sample tubes were purchased from Bruker.

General Procedures for NMR Experiments

DEPT Experiment

DEPT experiments were used to establish carbon multiplicities. Data were recorded on the DRX-400 spectrometer using a file size of 16 K and a suitable receiver gain (RG) for a carbon spectrum. The experiment gives CH and CH_3 carbons as positive signals, CH_2 signals as negative signals in the spectrum, and non-protonated carbons do not appear. The experimental parameters were set for the DRX-400 instrument (Bruker software, version 3.1) in the program DEPT135. Once the program was loaded, a suitable number of scans were entered and the experiment was started by typing zg.

Homonuclear Decoupling Experiment

Homonuclear decoupling is used to determine which protons in a compound are mutually coupled and/or to help obtain ^{1}H-^{1}H coupling constants for individual signals. These experiments were carried out on the DRX-400 spectrometer. A ^{1}H NMR spectrum was first obtained with a suitable number of scans, and saved as a file, entering “1” in the

cell labeled as EXPO. The frequencies (O2 values in Hz) of all proton signals to be irradiated were recorded. Different files were created equivalent to the number of protons to be irradiated, and saved with the numbers "2", "3", etc. in the cell labeled EXPO. The decoupling power P24 was set between 50 and 70, usually at 55, and the frequency to be irradiated (O2 value) was then entered for each EXPO experiment. The number of scans for each experiment was equivalent to the number of scans in EXPO 1. The EXPO 2 file was recalled by typing re 2. The acquisition was started by typing multizg and entering the number of experiments into the dialog box. The resulting data were processed using NUTS software.

Homonuclear COSY Experiment

This two-dimensional NMR technique was used to identify proton spin-systems. COSY experiments were conducted using the AVANCE-600 spectrometer. The procedure began with a well-shimmed proton spectrum that was obtained after carefully tuning the probe. Suitable SW and O2 values were calculated from the proton spectrum. A proton pulse calibration was carried out using the pulse program "zg", from which the parameters P0 (90º pulse), P1 (90º pulse), and P2 (180º pulse) were determined.

For the 5-mm inverse detection probe, the following parameters were set with the COSYPH pulse program: D1 = 4, TC = 2K, NS = 16 (multiples of 16), DS = 16. DW was automatically set, IN0 = 2 x DW, ND0 = 1, parameter mode was set to 2D, SFO1 = SFO2, SW = SW2 = the desired spectrum window of the proton spectrum, SW 1 = ½ (SW), TD1 = 256W, NE = 256, PW = 0, RD – 0, O1 =)2 = O11 = center of the desired spectrum window in Hz, SR = SR1 = SR2 = reference for the proton spectrum (δ 0 in Hz). Acquisition was started by typing zg.

For the 1.7-mm microprobe, the following parameters were set with the COSY pulse program. D1 = 20, NS = multiples of 8, DS = 0, DW was automatically set, IN0 =

2 x DW, ND0 = 1, parameter mode was set to 2D, SFO1 = SFO2, SW = SW2 = the desired spectrum window of the proton spectrum, SW 1 = ½ (SW), TD1 = 256W, NE = 256, PW = 0, RD – 0, O1 =)2 = O11 = center of the desired spectrum window in Hz, SR = SR1 = SR2 = reference for the proton spectrum (δ 0 in Hz). Acquisition was started by typing zg.

TOCSY Experiment

This two-dimensional NMR technique is similar to COSY, except that the second 90º pulse is replaced by a spin-lock stage, and correlations can be observed for all protons within a spin system, and not just those directly coupled to one another. TOCSY experiments were conducted using the AVANCE-600 spectrometer. The procedure began with a well-shimmed proton spectrum that was obtained after carefully tuning the probe. Suitable SW and O2 values were calculated from the proton spectrum.

For the 5-mm inverse detection probe, a proton pulse calibration was carried out using the pulse program "zg", from which the parameters P0 (90º pulse), P1 (90º pulse), and P2 (180º pulse) were determined. The following parameters were set with the "clmlevphpr" pulse program: D1 = 4, TC = 2K, NS = 16 (multiples of 16), DS = 16. DW was automatically set, IN0 = 2 x DW, ND0 = 1, parameter mode was set to 2D, SFO1 = SFO2, SW = SW2 = the desired spectrum window of the proton spectrum, SW 1 = ½ (SW), TD1 = 256W, NE = 256, PW = 0, RD – 0, O1 =)2 = O11 = center of the desired spectrum window in Hz, SR = SR1 = SR2 = reference for the proton spectrum (δ 0 in Hz). Acquisition was started by typing zg.

For the 1.7-mm microprobe, a proton pulse calibration was carried out using the pulse program "zg," from which the parameters P0 (90° pulse), P1 (90° pulse), and P2 (180° pulse) were determined at the power level -8.30 dB (PLW1). A second proton pulse calibration was also carried out using the pulse program "zg," from which the P6

value was determined (P1/4) at the power level 6.02 dB (PLW10). The following parameters were set with the "clmlevphpr" pulse program. D1 = 4, TC = 2K, NS = 16 (multiples of 16), DS = 16. DW was automatically set, IN0 = 2 x DW, ND0 = 1, parameter mode was set to 2D, SFO1 = SFO2, SW = SW2 = the desired spectrum window of the proton spectrum, SW 1 = ½ (SW), TD1 = 256W, NE = 256, PW = 0, RD – 0, O1 =)2 = O11 = center of the desired spectrum window in Hz, SR = SR1 = SR2 = reference for the proton spectrum (δ 0 in Hz). Acquisition was started by typing zg.

NOESY Experiment

The relative configuration of certain compounds could sometimes be determined based on the results of NOESY experiments. This experiment provides through-space ^{1}H-^{1}H correlations based on the nuclear Overhauser effect. The AVANCE-600 spectrometer was used to carry out NOESY experiments. The procedure began by tuning the probe followed by obtaining a well-shimmed proton spectrum. Suitable SW and O2 values were calculated from the proton spectrum. A proton pulse calibration was carried out using the pulse program "zg", from which the parameters P0 (90º pulse), P1 (90º pulse), and P2 (180º pulse) were determined. A second pulse calibration was created by using the pulse program "t1ir1d" to determine the mixing time by varying the parameter D7 until all peaks in the sample were positive or null. Then d8, the mixing time, was set (D7/0.7).

For both the 1.7- and 5-mm inverse detection probes, the following parameters were set with the "noesygpph" pulse program: D1 (relaxation delay) = 4, D8 = (value determined by pulse calibration), TD = 2k or 4k, NS = 8 (multiples of 8), DS = 16. The DW parameter was automatically set and the IN0 parameter was entered as double the value of DW. The parameter mode was set to 2D, ND0 = 1, and FnMODE = TPPI.

After verifying that SWH in F1 was the same as SWH in F2 and TD = 256 or 512 in F1, acquisition was started by typing zg.

ROESY Experiment

ROESY is similar to NOESY since both experiments provide through-space ^{1}H-^{1}H correlations based on the nuclear Overhauser effect. ROESY is used primarily for intermediate and high molecular weight compounds that have a small or zero NOE for all distances and mixing times.

For the 1.7-mm microprobe, the procedure began with a well-shimmed proton spectrum that was obtained after carefully tuning the probe. Suitable SW and O2 values were calculated from the proton spectrum. A proton pulse calibration was carried out using the pulse program "zg," from which the parameters P0 (90° pulse), P1 (90° pulse), and P2 (180° pulse) were determined at the power level -8.30 dB (PLW1). A second proton pulse calibration was also carried out using the pulse program "zg," from which the P25 value was determined at the power level 10.19 dB (PLW27). The following parameters were set with the "roesyph.2" pulse program: D1 (relaxation delay) = 4, D12 (value determined by pulse calibration), TD = 2K or 4K, NS = 8, 16, or 32, DS = 128. The DW parameter was automatically set and the IN0 parameter entered as double the value of DW. The parameter mode was set to 2D, ND0 = 1, and FnMODE = TPPI. After verifying SWH in F1 is the same as SWH in F2, and TD = 512 in F1, acquisition was started by typing zg.

HMQC Experiment

The HMQC experiment was used to provide one-bond proton-carbon correlations. This method relies on indirect detection of ^{13}C nuclei by observing their effect on the more sensitive proton nuclei to which they are coupled (inverse detection). HMQC

experiments were conducted on the AVANCE-600 spectrometer. The procedure began by tuning the probe followed by obtaining a well-shimmed proton spectrum. Suitable SW and O2 values were calculated from the proton spectrum. The proton pulse calibration was carried out using the pulse program "zg," from which the parameters P0 (90° pulse), P1 (90° pulse), and P2 (180° pulse) were determined. The following parameters were set with the pulse program "hmqcgpnd1d": D1 = 4 sec, D2[1/(2xJ_{XH})] = 3.3 msec (if the experiment is optimized for J = 150 Hz), D13 = 3 μsec, DS = 4, NS = 16, TD = 8k. After the acquisition, the commands FT and MC were entered in order to observe signals for protons bound to ^{13}C atoms and to determine signal intensity to predict the number of scans required for the HMQC experiment.

The HMQC experiment was then conducted using the pulse program "hmqcgpqf" with the following parameters: DS = 96, TD = 2k, NS = multiple of 8, RG = 16k, TD (F1 dimension) = 256 or 512, SI = 1k, SFO1 (F1 dimension) = 150.92 MHz, ND0 = 2, IN0 = 15 μsec, O2P = 80. The parameter mode was set to 2D and the acquisition was initiated by typing zg.

HMBC Experiment

Long-range two- and three-bond ^{1}H-^{13}C correlations were obtained from this type of experiment. The experiment was conducted on the AVANCE-600 spectrometer using a 5-mm inverse detection probe, and used the pulse program "hmbcgplpndqf". The parameters and procedures were nearly identical to those of HMQC, with the exception that IN0 = 13 μsec, and O2P = 100. The D6 parameter was used to optimize the experiment for the desired J-value. In most cases, a typical value of 8 Hz was used, which corresponds to a D6 value of 60 msec.

^{1}H-^{15}N HMBC Experiment

Long-range two- and three-bond ^{1}H-^{15}N correlations were obtained from this type of experiment. The AVANCE-600 spectrometer was used to carry out this experiment. The procedure began by tuning the probe followed by obtaining a well-shimmed proton spectrum. Suitable SW and O2 values were calculated from the proton spectrum. A proton pulse calibration was carried out using the pulse program "zg" from which the parameters P0 (90º pulse), P1 (90º pulse), and P2 (180º pulse) were determined. The following parameters were set with the pulse program "hmbcgplpndqf": DS = 64; TD = 2K; NS = multiple of 8; RG = 8K; TD (F1 dimension) = 256 or 512K; SI = 1K; SFO1 (F1 dimension) = 60.82889 MHz; ND0 = 2; IN0 = 82.4 μsec; O2P = 100 ppm; D1 = 4 sec, 90° pulse (^{1}H); D2 [1/(2 x JXH)] = 5.56 msec (if the experiment is optimized for $^{1}J_{N\text{-}H}$ = 90 Hz); D16 = 0.2 msec, 180° pulse (^{1}H);. The D6 parameter was used to optimize the experiment for the desired $^{2/3}J_{N\text{-}H}$-value for 90 ° pulse (^{15}N). In this case, 4 Hz was used, which corresponds to a D6 value of 125 msec, where D6 = [1/(2 x cnst 13)]. The parameter mode was set to 2D and the acquisition was initiated by typing zg.

General Procedures for Collection and Refinement of X-Ray Data

Procedures for collection and refinement of X-ray data for the *p*-bromobenzoate derivative of dihydrooxirapentyne are included in Appendix A. Crystallographic data have been deposited with the Cambridge Crystallographic Data Centre (CCDC). Copies of the data can be obtained, free of charge, on application to the Director, CCDC, 12 Union Road, Cambridge CB2 1EZ, UK (fax: +44-(0) 1223-336033 or email: deposit@ccdc.cam.ak.uk).

General Procedures for Isolation of Fungal Species from Wood-Decay Fungi

Collection of wood-decay fungi was carried out by Dr. Donald T. Wicklow of the Bacterial Foodborne Pathogens and Mycology Research Unit, Agricultural Research Service, National Center for Agricultural Utilization Research (NCAUR), United States Department of Agriculture in Peoria, Illinois. Samples of wood-decay fungi were returned to the laboratory in Peoria in plastic bags and placed in a freezer (-7 ºC). In order to isolate microfungal colonies, direct plating of resulting filings from the surface of the samples was accomplished by sprinkling a small portion (100-200 mg) of the powders over the surface of each of two plates of dextrose-peptone-yeast extract agar (DPYA) containing streptomycin (25 mg/L) and tetracycline (1.25 mg/L). Plates were incubated in the dark at 25 ºC for five days, and representative cultures were isolated from each colony type showing distinctive morphology on DPYA. After 7-12 days of incubation, tube cultures isolated were segregated into groups of presumptive species and maintained for solid-substrate fermentation and potential identification.

General Procedures for Solid-Substrate Fermentations

Fermentation of mycoparasitic/fungicolous fungi was conducted in the laboratory of Dr. Donald T. Wicklow of the NCAUR. Fungal strains were cultured on slants of potato dextrose agar (PDA) at 25 ºC for 14 days. Spore inoculum was suspended in sterile distilled H_2O to give a final spore/cell suspension of 1 x 10^6/mL. Fermentation was carried out in 500-mL Erlenmeyer flasks each containing 50 g of rice (Botan Brand; J.F.C. International). Distilled H_2O (50 mL) was added to each flask and the contents were soaked overnight before autoclaving at 15 lb/in^2 for 30 min. After cooling to room temperature, each was inoculated with 1.0 mL of a selected fungal spore inoculum and incubated at 25 ºC for 15-30 days. After incubation, the fermented substrate was

mechanically fragmented and extracted with EtOAc (3 x 50 mL). The combined EtOAc extracts were filtered and concentrated under vacuum to give a crude extract. In cases where additional material was needed, this process was scaled up using the number of flasks expected to give the desired amount of crude extract for a given species.

General Procedures for *A. zeae* Solid-Substrate Fermentations

A hyphal fragment-spore suspension (propagule density) 10^6/mL of sterile distilled H_2O) prepared from the PDA slants served as the inoculum. Fermentations were carried out in 10 Fernbach flasks, each containing 200 g of rice. Distilled H_2O (200 mL) was added to each flask, and the contents were soaked overnight before autoclaving at 15 lb/in^2 for 30 min. The flasks were cooled to room temperature, inoculated with 3.0 mL of spore inoculum, and incubated for 21 days at 25 °C. The fermented substrate in each flask was first fragmented with a spatula and then extracted three times with EtOAc (200 mL each time). The extract from each flask was separately filtered and evaporated.

General Procedures for *S. maydis* Solid-Substrate Fermentations

Strains of *S. maydis and S. macrospora* were maintained as PDA slant cultures (6 days, 25°C). A suspension of conidia and hyphal cells was prepared from these cultures giving a propagule density of approximately 4 x 10^4/mL and served as inoculum. Initial fermentations were carried out in two 500-mL Erlenmeyer flasks each containing 50 g of rice that was soaked overnight in distilled H_2O (50 mL) before being autoclaved at 1.055 kilogram-force (kgf)/cm^2 for 30 min. After the flasks had cooled to room temperature, they were inoculated with 1.0 mL of the hyphal fragment-spore inoculum, and incubated

for 30 days at 25°C. A second fermentation of *S. maydis* NRRL 53562 was carried out as above in eighteen 500-mL Erlenmeyer flasks each containing 50 g of rice.

General Procedures for Antifungal Assays

Antifungal assays against *Aspergillus flavus* (NRRL 6541) and *Fusarium verticillioides* (NRRL 25457) were conducted in the laboratory of Dr. Donald T. Wicklow of the NCAUR. A portion of the EtOAc extract of the solid-substrate fermentation cultures (approximately 6 mg) was redissolved in EtOAc. One-mg and 0.5-mg equivalents of extractable residue were pipetted onto individual analytical grade filter paper disks (12.5 mm diameter), which were then placed in individual Petri dish lids and dried for 30 min in a laminar flow hood. After each disk was allowed to dry, up to four disks were placed equidistant from one another on the surface of freshly poured and solidified PDA that was seeded with a spore suspension of *A. flavus* conidia to give a final spore suspension of 1 x 10^2 cells per mL. These bioassay plates were incubated at 25 ºC for four days and examined for inhibition of *A. flavus* at two and four days as indicated by the presence of a clear or mottled zone around the disk, which is evidence of the inhibition of germination and a measure of fungistatic activity. An analogous procedure was employed for the assay against *F. verticillioides*. Solvent used for extract transfer was used as a negative control. Positive control disks were not used for testing of crude extracts, but were used for later testing of pure compounds.

Antifungal assays against *Candida albicans* (ATCC 14053) were conducted in our own laboratory. *C. albicans* test plates were prepared as needed. In assays using *C. albicans* (ATCC 14053) bactrol disks (Difco), the disk was dissolved in 50 mL of sterile Difco yeast maintenance broth. The culture was allowed to aerate on an orbital shaker at 150 rpm at room temperature for 36-48 hr. One hundred mL of Tryptic soy agar (Difco) was prepared, sterilized by autoclaving, and cooled to 45 ºC. One mL of the *C. albicans*

inoculum suspension was transferred to the warm fluid and mixed thoroughly by gentle swirling to avoid bubbles. In assays using *C. albicans* pellets (BioMerieux), one pellet was dissolved in 1 mL of sterile H_2O, and 250 µL of the inoculum suspension was transferred to warm agar and mixed thoroughly by gentle swirling. In both cases, the agar was poured into Petri plates (100 x 15 mm; 5 mL each) which were stored in the refrigerator at 4 ºC. In conducting the disk diffusion assay, each filter paper disk (6.25 mm in diameter) was impregnated with the sample to be tested (100 or 200 µg/disk). After evaporation of the solvent, the disk was placed on the agar surface and incubated at room temperature for 24-72 h. Activity was reported by measuring the diameter (in mm) of the inhibition zone around each disk. A stock solution of the control antifungal agents filipin or nystatin (Sigma Chemical Co.) at 25 µg/disk was used as a positive control.

General Procedures for MIC Determinations

Minimum inhibitory concentration (MIC) determinations were carried out in the laboratory of Dr. Donald T. Wicklow of the NCAUR. *Aspergillus flavus* (NRRL 6541) was grown in Roux bottles containing PDA for 14 days (25 ºC). A conidial spore suspension (propagule density 10^6/mL in sterile distilled H_2O) prepared from the Roux bottle cultures served as the inoculum. Hyphal fragments and conidium-bearing structures were removed by filtering through a double layer of sterile cheese cloth. Compounds were evaluated in 96-well plates with a growth area of 0.32 cm^2 and volume of 370 µL (BD Primaria Clear 96-well Microtest Plate No. 353872, Becton-Dickinson) at concentrations of 1, 3, 5, 10, and 25 µg/mL. Appropriate amounts of test compound in 10 µL of MeOH were added to each of eight replicate wells and evaporated to dryness. Eight replicate wells received only 10 µL MeOH and served as controls. Potato dextrose broth (PDB) was seeded with *A. flavus* conidia, giving a final conidial suspension of approximately 4 x 10^4/mL PDB. A small quantity of MeOH (10 µL) was added to each

well to solubilize the test compound, and the 200 µL of PDB containing ca. 8,000 *A. flavus* conidia were added to each test well. The plates were incubated for 48 hr at 25 ºC and examined at 8-16 hr intervals using a plate reader (Dynatech MR 5000 with BioLynx Version 2.0 Assay Management Software; Dynatech Laboratories, Inc.) for evidence of inhibition of fungal growth in the wells. A minimum inhibitory concentration (MIC) was assigned to the lowest treatment concentration for which no fungal growth was observed. Nystatin was used as a positive control, and gave an MIC value of approximately 10 µg/mL using this protocol. An analogous process was used for the assay against *Fusarium verticillioides* (NRRL 25457).

General Procedures for Antiinsectan Assays

Antiinsectan assays were developed and conducted by Dr. Patrick F. Dowd, also of the NCAUR. Selection of crude extracts for chemical investigation in search of antiinsectan metabolites was based on bioactivity against the fall armyworm (*Spodoptera frugiperda*).

Spodoptera frugiperda

S. frugiperda larvae were maintained on a standard pinto bean diet, consisting of the following ingredients: 120 g dried pinto beans, 43 g wheat germ, 28 g brewer's yeast, 8 g Vanderzant's vitamin mix, 2.8 g ascorbic acid, 1.75 g methylparaben, 0.9 g sorbic acid, 12 g sugar, 2 mL formaldehyde (39%), 1.5 mL propionic-phosphoric acid solution (4.2% phosphoric acid), and 550 mL of H_2O. For screening purposes, crude extracts were incorporated into the diet at levels of 200 ppm. Column fractions and pure compounds were tested at levels of 100 ppm (wet weight). The samples were added in 125 µL of acetone to test tubes (100 x 16 mm) containing 5-mL aliquots of molten diet (60 ºC). The mixture was then blended with a vortex mixer for 20 seconds. The diets

were dispensed into Petri plates, allowed to cool to room temperature, and placed in a fume hood for *ca.* 20 min to remove residual solvent. The diet was cut into equal blocks (*ca.* 250 mg). Each block was placed into a single well of a 24-well immunoassay plate, and then a single neonate *S. frugiperda* larva was added to each well. To prevent dessication of the diet, the plate was covered by a sheet of Parafilm, a sheet of cardboard, and a plastic cover. The cover was secured by two rubber bands. Bioassays were conducted at 27 ºC for seven days at 40% humidity with a 14:10 (light:dark) photoperiod. The insects were inspected at two, four, and seven days for mortality, and seven-day survivors were weighed. A solvent blank was used as a control. Each sample was tested on a total of 40 neonate larvae. Antiinsectan activity was measured by comparison of the test larval weights relative to those of controls. Data were reported as percent reduction in weight gain relative to controls. Percent mortality was recorded in cases where mortality was also observed.

Sap Beetle Choice Analysis

A choice analysis was performed with sap beetle *Carpophilus freemanii* (Coleoptera, Nitidulidae) adults using the following approach: Healthy seeds from symptomless ears and rotted seeds from *S. maydis* NRRL 53565 wound-inoculated ears were sampled at harvest from commercial maize grown at Kilbourne, IL in 2009. Each of the grain samples (100 g) was first ground using a Stein mill (Steinlite, Atchison, KS). Fifty milligrams (air dried) of *S. maydis*-rotted and control corn powder were added to separate, pre-weighed, uncapped 2-mL vials. A separate H_2O reservoir was made by cutting a 35-mm film canister in half and using the bottom half and the cap. A 4-mm diameter hole was drilled in the film canister cap and cotton was placed in the vial to pick up H_2O on the top. The canister was filled with sterile, distilled H_2O, which was sufficient to supply H_2O for the beetles for the duration of the assay. The two vials

containing the corn powder were secured in an upright position to the canister with a rubber band. The vial-canister setup was placed inside a 6-cm diameter × 6.5 cm high glass jar. A 4-mm diameter hole was drilled in the jar lid and the hole covered with organdy secured with hot glue to provide ventilation. A total of 20 adult beetles were added to each of 10 jars used in the assays. The feeding chambers containing beetles were incubated for 5 d at 27+/- 1 °C., 40+/- 10% relative humidity, and a 14:10 h (light:dark) photoperiod. Following incubation, beetles were removed from the vials which were then reweighed.

General Procedures for Antibacterial Assays

Bacillus subtilis

Bacillus subtilis (ATCC 6633) assay plates were prepared as needed. One ampule (1 mL of *B. subtilis*) was added to 100 mL of sterile Penassay seed agar. In assays using *B. subtilis* (ATCC 6051) pellets (BioMerieux), one pellet was dissolved in 1 mL of sterile H_2O, and 250 µL of the inoculum suspension was transferred to warm Penassay seed agar and mixed thoroughly by gentle swirling. In both cases, the agar was poured into Petri plates (100 x 15 mm; 5 mL each) which were stored in the refrigerator at 4 ºC. The control antibiotic agent gentamycin (Sigma Chemical Co.) was used as a control at a level of 25 µg/disk.

Staphylococcus aureus

Staphylococcus aureus (ATCC 29213) plates were prepared as needed. In assays using *S. aureus* bactrol disks (Difco), the disk was dissolved in 50 mL of sterile Difco nutrient broth in a 250-mL Erlenmeyer flask. The culture was allowed to aerate on an orbital shaker at 150 rpm at room temperature for 36-48 hr. One hundred mL of Tryptic

soy agar (Difco) was prepared, sterilized by autoclaving, and cooled to 45 ºC. One mL of the *S. aureus* inoculum suspension was transferred to the warm fluid and mixed thoroughly by gentle swirling to avoid bubbles. In assays using *S. aureus* (ATCC 29213) pellets (BioMerieux), one pellet was dissolved in 1 mL of sterile H_2O, and 250 µL of the inoculum suspension was transferred to warm agar and mixed thoroughly by gentle swirling. In both cases, the agar was poured into Petri plates (100 x 15 mm; 5 mL each) which were stored in the refrigerator at 4 ºC. The antibiotic gentamycin (Sigma Chemical Co.) was used as the positive control at 25 µg/disk.

Escherichia coli

Escherichia coli (ATTC 25922) plates were prepared as needed. In assays using *E. coli* bactrol disks (Difco), the disk was dissolved in 50 mL of sterile Difco nutrient broth in a 250-mL Erlenmeyer flask. The culture was allowed to aerate on an orbital shaker at 150 rpm at room temperature for 36-48 hr. One hundred mL of Tryptic soy agar (Difco) was prepared, sterilized by autoclaving, and cooled to 45 ºC. One mL of the *E. coli* inoculum suspension was transferred to the warm fluid and mixed thoroughly by gentle swirling to avoid bubbles. In assays using *E. coli* (ATCC 25922) pellets (BioMerieux), one pellet was dissolved in 1 mL of sterile H_2O, and 250 µL of the inoculum suspension was transferred to warm agar and mixed thoroughly by gentle swirling. In both cases, the agar was poured into Petri plates (100 x 15 mm; 5 mL each) which were stored in the refrigerator at 4 ºC. The antibiotic gentamycin (Sigma Chemical Co.) was used as the positive control at 25 µg/disk.

In conducting all of the above disk diffusion assays, the filter paper disks (6.25 mm in diameter) were impregnated with the sample to be tested (200 µg/disk). After evaporation of the solvent, the disk was placed on the agar surface of a *B. subtilis*, *S. aureus*, or *E. coli* Petri plate, and the plate was then incubated at room temperature for

24-48 hr. The antimicrobial activity of the sample was reported by measuring the diameter (in mm) of the inhibition zone around the disk in which no growth of the test organism was observed.

General Procedure for Needle-Puncture Wound Assays

A droplet (5 μL) of a MeOH/H_2O solution (1:1, v/v) containing 5 μg of test compound was placed over each of six needle puncture wounds (~0.25 mm) on the upper surface of a maize leaf blade cut from 4-week-old maize seedlings of Mandan Bride, Gaspe, and FS 6873RR or Burrus 794sRR varieties, grown in a greenhouse. Oxalic acid (5 μg) served as a positive control. The leaf blades were incubated (72 h; 21–23 °C) on moistened filter paper in a sealed Petri dish. The lengths of the necrotic lesions spreading from needle puncture wounds were measured under a stereomicroscope.

Procedure for the Isolation and Characterization of Metabolites from an Isolate of the Family *Bionectriaceae* (MYC-2186)

Fungal Material

A fungicolous fungal isolate (MYC-2186) was obtained by Dr. Donald T. Wicklow from a basidioma of *Phellinus gilvus* found on a decaying hardwood branch collected on the island of Hawaii. This isolate was later identified as a mitosporic fungus of the family Bionectriaceae having 98% homology with the chemically unexplored species *Stilbocrea macrostoma* on the basis of partial sequence analysis of the internal transcribed spacer region (ITS) and domains D1 and D2 of the nuclear large subunit (28S) rDNA gene using ITS5 and NL4 as polymerase chain reaction and sequencing primers via a nucleotide-to-nucleotide BLAST query of the GenBank database.

Sequence information was deposited in the GenBank database with the accession number FJ821507. A subculture of this isolate was deposited at the USDA NRRL culture collection at the NCAUR, Peoria, IL, under accession number NRRL 54009.

Extraction and Isolation Procedure

MYC-2186 was grown on 100 g (2 x 50 g) of rice for 30 days at 25 °C and the resulting fermentations were combined and extracted 3 x 100 mL with EtOAc. The extract (1.1 g) was partitioned between MeCN and hexanes (10 mL of each). The entire MeCN fraction (303 mg) was chromatographed on a silica gel column using a hexanes–CH_2Cl_2–MeOH gradient to afford 10 fractions. Fraction 7 (33 mg) eluted with 5% MeOH–CH_2Cl_2, and a portion (9 mg) was further separated by reversed-phase HPLC (40% MeCN–H_2O for 10 min, 40–45% over 10 min, 45–60% over 2 min, 60% for 5 min, 60–100% over 2 min, 100% for 15 min) to afford pseurotin A (**3.3**; 0.5 mg),[89] *cyclo*[-Aib-*S*-Phe-*R*-Pro-*S*-Aoh-] (**3.4**; 0.4 mg),[90] *cyclo*[-D-Pro-Phe-Iva-(9R)-Aoh-] (**3.5**, 1.0 mg),[91] and *cyclo*[-L-Asu-Aib-L-Phe-D-Pro-] (**3.6**, 0.6 mg).[92] These compounds were identified by comparison of MS and ^{1}H NMR data to literature values. Fraction 9 eluted with 25% MeOH–CH_2Cl_2 and contained a pure sample of guaiane mannoside (**3.2**; 25 mg).[88] Fraction 10 (214 mg) eluted with a 100% MeOH wash. The major component of this fraction was bionectrin A (**3.1**), which was accompanied only by minor, inseparable homologues

.

Bionectrin A (**3.1**)

White amorphous solid; ^{1}H, ^{13}C, HMBC, and ^{1}H-^{15}N HMBC NMR data, see Table 7; HRESIMS obsd $(M+Na)^+$ 1085.6613, calcd for $C_{52}H_{90}N_{10}O_{13}Na$, 1085.6587, *m/z* $(M–H)^-$ 1061.6611, calcd for $C_{52}H_{90}N_{10}O_{13}$ – H, 1061.6611.

Preparation of Methyl Ester of Bionectrin A

A sample of **3.1** (10 mg) was dissolved in 1 mL MeOH. While stirring, a 2 M solution of $TMSCHN_2$ in hexanes was added dropwise until the yellow color of the $TMSCHN_2$ solution persisted. The solution was stirred for 3 hours, the solvent was removed under air, and the reaction product was analyzed by ^1H NMR. The ^1H NMR data matched that of bionectrin A, with one additional methyl singlet appearing at δ_H 3.70. *m/z* $(M+Na)^+$ 1099.6739, calcd for $C_{53}H_{92}N_{10}O_{13}Na$, 1099.6743. *m/z* $(M-H)^-$ 1075.6784, calcd for $C_{53}H_{92}N_{10}O_{13} - H$, 1075.6767.

Preparation of TFA-*n*-butyl, TFA-(*S*)-(+)-2-butyl, or TFA-(±)-2-butyl ester derivatives

A sample of **3.1** (1 mg) was hydrolyzed in 1.0 mL of 6 N HCl in a sealed hydrolysis tube *in vacuo* at 110 ºC for 24 h, then cooled in an ice bath and evaporated under air. The residue was combined with 1 mL *n*-butanol, (*S*)-(+)-2-butanol, or -(±)-2-butanol and 36 μL acetyl chloride in the hydrolysis tube, which was then sealed *in vacuo*, maintained at 110 ºC for 40 min, cooled in ice bath, and evaporated under air. The resulting residue was then combined with 0.5 mL TFAA and 1 mL CH_2Cl_2, in the hydrolysis tube, sealed *in vacuo*, heated at 150 ºC for 5 min, and cooled in an ice bath. The solution was transferred to a vial, evaporated under air until nearly all solvent had evaporated (stopping before completion in order to minimize loss of volatile derivatives), and mixed with 1 mL of CH_2Cl_2. The resulting solution was submitted for analysis by GC-MS using an Agilent JW1701 column (30 m, 0.25-mm ID) with a He flow of 1 mL/min and a temperature program of 70–280 ºC at 8 ºC/min. Standard amino acid derivatives were prepared using 1-mg samples of D-Iva, L-Ile, L-*allo*-Ile, L-Leu, L-Pro, *trans*-4-L-Hyp, *cis*-4-L-Hyp, and Aib following the procedure above (without the hydrolysis step) using *n*-butanol, (*S*)-(+)-2-butanol, or -(±)-2-butanol (Figure 6).

Preparation of 1-Fluoro-2,4-dinitrophenylalanineamide (FDPA) Derivatives of the Amino Acids in the Hydrolyzate of Bionectrin A (**3.1**)

A sample of **3.1** (1.5 mg) was hydrolyzed in 1.5 mL of 6N HCl in a hydrolysis tube sealed under vacuum at 110 °C for 24 h, then cooled in an ice bath and evaporated under air. A portion of the hydrolyzate (0.5 mg) was dissolved in 330 μL of H_2O, and mixed with 1 M $NaHCO_3$ (40 μL) and a solution of 1% 1-fluoro-2,4-dinitrophenyl-5-L-phenylalanineamide (FDPA) in acetone (40 μL). This modified Marfey's reagent (FDPA) was prepared following the protocol described previously for the standard Marfey's reagent,[109] using L-Phe-NH_2 in place of L-Ala-NH_2. The reaction mixture was maintained at 40 °C for 1 h in a H_2O bath. After cooling, 2 M HCl (40 μL) was added, and the resulting mixture was subjected to HPLC on a Grace 5-μm C_{18} column (10 x 250 mm) at a flow rate of 2 mL/min with UV detection at 340 nm (solvent A = 10 mM NaOAc, solvent B = CH_3CN, 20-100% over 40 min). This process was repeated for L- and D-Iva standards (Biofine International Inc.). The retention times of the FDPA derivatives of L-Iva, D-Iva, and the Iva in the hydrolyzate of **3.1** were 26, 13, and 13 min, respectively.

Guaiane Mannoside (**3.2**)

Yellow glass; ^1H, ^{13}C, and HMBC NMR data, see Table 8; HRESIMS obsd *m/z* $(M+Na)^+$ 407.2395, calcd for $C_{21}H_{36}O_6Na$, 407.2410. These data match those reported in the literature.[88]

Procedure for the Isolation and Characterization of Metabolites from *Phialemonium curvatum* (MYC-2005)

Fungal Material

A fungicolous isolate (MYC-2005) was obtained by Dr. Donald T. Wicklow from the black stromata of a pyrenomycete found on a dead hardwood branch on the island of Hawaii and was later identified as *Phialemonium curvatum*. This evaluation was based upon partial sequence analysis of the internal transcribed spacer region (ITS) and D1 and D2 domains of the nuclear large subunit (28X) rDNA gene using ITS5 and NL4 as polymerase chain reaction and sequencing primers via a nucleotide-to-nucleotide BLAST query of the GenBank database. Sequence information was deposited in the GenBank database with the accession number GU205097. A subculture of this isolate was deposited at the USDA NRRL culture collection at the NCAUR under accession number NRRL 46124.

Extraction and Isolation Procedure

P. curvatum (MYC-2005) was grown on 100 g (2 x 50 g) of rice for 30 days at 25 °C and the resulting fermentation was extracted with EtOAc. The crude extract (1.4 g) was partitioned between hexanes and MeCN. The MeCN fraction (787 mg) was fractionated on a silica gel column using a hexanes/CH_2Cl_2/MeOH solvent system. The column was eluted with 50-mL portions of hexanes-CH_2Cl_2 (100:0, 50:50, 0:100) and CH_2Cl_2-MeOH (2 x 99:1, 6 x 97:3, 2 x 95:5, 90:10, 75:25 v/v) to afford 15 fractions. Fractions 2-10 eluted with 50% hexanes-CH_2Cl_2 through 3% MeOH-CH_2Cl_2 and afforded dihydrooxirapentyne (**4.1**; 130 mg). Fraction 11 eluted with 3% MeOH-CH_2Cl_2 and was further separated using a silica column using a hexanes/EtOAc solvent system. The column was eluted with 100-mL portions of hexanes-EtOAc (100:0, 90:10, 80:20, 70:30, 60:40, 50:50, 40:60, 30:70, 20:80, 10:90, 0:100) and 100 mL MeOH to afford 12

fractions. Fractions 5-6 contained dihydrooxirapentyne (**4.1**; 115 mg**)** and fractions 8-11 contained the known compound destruxin A (**4.2**; 65 mg).[16]

Dihydrooxirapentyne (**4.1**)

White solid; ^{1}H, ^{13}C, and HMBC NMR data, see Table 9. HRESIMS obsd *m/z* $(M+Na)^{+}$ 357.1331, calcd for $C_{18}H_{22}O_6Na$, 357.1314.

Preparation of *p*-Bromobenzoate Derivative of Dihydrooxirapentyne (**4.1**)

p-Bromobenzoyl chloride (6.1 mg; 0.028 mmol) and 4-N,N-dimethylaminopyridine (DMAP; 6.2 mg; 0.051 mmol) in anhydrous CH_2Cl_2 (4 mL) in a 20-mL scintillation vial. The resulting solution was stirred at room temperature for 19 hours. Saturated aqueous $NaHCO_3$ (1 mL) and H_2O (2 mL) was then added, and the resulting mixture was extracted three times with CH_2Cl_2 (total 6 mL). The combined organic phase was evaporated under airflow to obtain a crude product mixture (14.6 mg). This mixture was purified by reversed-phase HPLC (50-100% CH_3CN/H_2O over 20 min and 100% CH_3CN over 10 min) with UV detection at 254 nm to afford the *p*-bromobenzoate derivative of dihydrooxirapentyne (2.2 mg). ^{1}H NMR (400 MHz, $CDCl_3$) δ_H 1.27 (s, H_3-16), 1.43 (s, H_3-15), 1.43 (dd, J = 3.0, 15.0, H_2-9) 1.63 (s, H_3-14), 1.76 (s, H_3-18), 2.50 (dd, J = 3.0, 15.0, H_2-9), 3.00 (s, H-6), 3.45 (s, H-3), 4.50 (s, H-4), 4.90 (t, J = 3.0, H-8), 5.09 (dq, J = 1.5, 1.5, H-13), 5.13 (dq, J = 1.5, 1.0, H-13), 5.93 (s, H-1), 7.61 (d, J = 8.5, H-4'and H-6'), 8.02 (d, J = 8.5, H-3' and H-7'). HRESIMS obsd *m/z* $(M+H)^{+}$ 733.0295, calcd for $C_{32}H_{31}O_{10}Br_2$, 733.0284. A colorless thin plate (0.20 x 0.11 x 0.11 mm) was obtained from 2:2:1 $CH_3CN/CHCl_3/H_2O$ and selected for analysis. X-ray crystallographic data for the *p*-bromobenzoate derivative are presented in Appendix B.

Oxidation Product of Dihydrooxirapentyne (**4.1**)

In an acetone/dry ice bath (-78 °C), CH_2Cl_2 (75 µL) and oxalyl chloride (6 µL) were added to a 0.5 dram vial. DMSO (5.1 µL) and CH_2Cl_2 (15 µL) were added to the oxalyl chloride solution. The resulting solution was stirred for two minutes. Dihydrooxirapentyne (5 mg) in CH_2Cl_2 (15 µL) was added within five minutes of the previous step. The solution was then stirred for an additional 30 minutes. Freshly distilled triethylamine (TEA, 15 µL) was added and the mixture was stirred for five minutes. The solution was then warmed to room temperature. Water (150 µL) was added dropwise, and the aqueous layer was extracted with an additional 150 µL CH_2Cl_2. The organic layers were combined and the mixture was purified by reversed-phase HPLC (20% CH_3CN/H_2O isocratic for 10 min and 20-100% CH_3CN over 2 min) with UV detection at 240 nm to afford the oxidation product of dihydrooxirapentyne (3.6 mg). The NMR data matched those reported for the known compound oxirapentyne (**4.3**).[122]

Procedure for the Isolation and Characterization of Metabolites from *Gliocladium* spp. (NRRL 22971)

Fungal Material

An isolate of *Gliocladium* sp. was obtained by Dr. D. T. Wicklow from a single sclerotium of *A. flavus* that was buried for two years in a sandy crop field soil near Kilbourne, IL. A subculture of this isolate was deposited with the ARS Culture Collection at the NCAUR with the accession number NRRL 22971.

Extraction and Isolation Procedure

NRRL 22971 was grown on 400 g (2 x 200 g) of rice for 45 days at 25 °C and the resulting rice fermentations were combined and extracted with EtOAc. The crude extract

(2.34 g) was subjected to silica gel column chromatography using a hexanes-CH_2Cl_2-MeOH gradient to afford eight fractions. Fraction three eluted with 80% CH_2Cl_2/hexanes to yield the known fungal metabolite ergosterol (**5.1**; 16 mg). Fractions six and seven were combined (83 mg) and subjected to Sephadex LH-20 column chromatography using a hexanes-CH_2Cl_2-acetone gradient to yield eight subfractions. Subfraction three was further separated by reversed-phase HPLC (10-70% CH_3CN/H_2O + 0.1% TFA) to afford a new cytochalasin analogue (**5.4**; 3.1 mg). Subfraction seven was further separated by reversed-phase HPLC (15-75% CH_3CN/H_2O + 0.1% TFA) to afford 1-acetyl-9*H*-pyrido[3,4-*b*]indole-3-[*S*-(3)-aminobutyric acid]amide (**5.2**; 3.0 mg).

1-Acetyl-9*H*-pyrido[3,4-*b*]indole-3-[*S*-(3)-aminobutyric acid]amide (**5.2**)

White solid; ^1H, ^{13}C, and HMBC NMR data, see Table 10. HREIMS *m*/*z* 339.1202 M^+ (rel int 77), 280.0988 (38), 237.0604 (78), 210.0754 (100), calcd for $C_{18}H_{17}N_3O_4$, 339.1209.

Preparation of TFA-(±)-2-butyl Ester Derivatives of 1-Acetyl-9*H*-pyrido[3,4-*b*]indole-3-[*S*-(3)-aminobutyric acid]amide **5.2**

A sample of **5.2** (1.2 mg) was hydrolyzed in 0.5 mL of 6 N HCl in a sealed hydrolysis tube *in vacuo* at 110 ºC for 24 h, then cooled in an ice bath and evaporated under air. The residue was combined with 0.5 mL (±)-2-butanol and 20 μL acetyl chloride in the hydrolysis tube, which was then sealed *in vacuo*, maintained at 110 ºC for 40 min, cooled in an ice bath, and evaporated under air. The resulting residue was then combined with 0.25 mL TFAA and 0.5 mL CH_2Cl_2, in the hydrolysis tube, sealed *in vacuo*, heated at 150 ºC for 5 min, and cooled in an ice bath. The solution was

transferred to a vial, evaporated under air until nearly all solvent had evaporated (stopping before completion in order to minimize loss of volatile derivatives), and mixed with 0.5 mL of CH_2Cl_2. The resulting solution was submitted for analysis by GC-MS using an Agilent JW1701 column (30 m, 0.25-mm ID) with a He flow of 1 mL/min and a temperature program of 70–280 ºC at 8 ºC/min. The resulting mixture of diastereomers was found to be inseparable by GC-MS, so another method of analysis was explored, as described below.

Preparation of 1-Fluoro-2,4-dinitrophenylalanineamide (FDPA) Derivatives of the Amino Acids in the Hydrolyzate of **5.2**

A sample of **5.2** (50 μg) was hydrolyzed in 0.5 mL of 6N HCl in a hydrolysis tube sealed under vacuum at 110 °C for 24 h, then cooled in an ice bath and evaporated under air. A portion of the hydrolyzate (10 μg) was mixed with 1 M $NaHCO_3$ (10 μL) and a solution of 1% 1-fluoro-2,4-dinitrophenyl-5-L-phenylalanineamide (FDPA) in acetone (63 μL). This modified Marfey's reagent (FDPA) was prepared following the protocol described previously for the standard Marfey's reagent,[109] using L-Phe-NH_2 in place of L-Ala-NH_2. The reaction mixture was maintained at 40 °C for 1 h in a H_2O bath. After cooling, 2 M HCl (10 μL) was added, and the resulting mixture was subjected to HPLC on a Grace 5-μm C_{18} column (10 x 250 mm) at a flow rate of 2 mL/min with UV detection at 340 nm (solvent A = 10 mM NaOAc, solvent B = CH_3CN, 20-100% over 40 min). The retention times of the D- and L-FDPA derivatives were determined to be 15.5 and 14.5 min. Coinjection of the reaction products with D- and L-amino acid standards showed an enhancement of the peak at 14.5 min, corresponding to the L-3-aminobutyric acid derivative.

Cytochalasin analogue (**5.4**)

Yellow solid; ^{1}H, ^{13}C, and HMBC NMR data, see Table 11. HRESIMS obsd $(M+Na)^{+}$ 504.2369, calcd for $C_{28}H_{35}NO_6Na$, 504.2362.

Procedure for the Isolation and Characterization of Metabolites from *Acremonium zeae* (NRRL 45893)

Fungal Material

A culture of *Acremonium zeae,* initially isolated as "Az-115" from a sample of whole maize seeds received from Hopkinsville, KY, was obtained by Dr. D. T. Wicklow and maintained on PDA. A subculture of this isolate was been deposited with the ARS Culture Collection at the NCAUR and assigned the accession number NRRL 45893.

Extraction and Isolation Procedure

Two groups of five extracts were combined to give two samples weighing 1115 and 877 mg, and each combination was separated as follows. A 2-g silica Sep-Pak cartridge (Waters Corp., Milford, MA) was conditioned with 20 mL of hexane and the extract in 50 mL of EtOAc/hexane (10:90, v/v) was loaded onto the column. The column was eluted with 20-mL portions of EtOAc-hexane (10:90, 15:85, 25:75, 30:70, 60:40, v/v) and 20 mL of EtOAc. Each fraction was analyzed by LC-MS. The 60:40 and EtOAc fractions were combined and separated as described below. The 25:75 EtOAc/hexane fraction was dried under N_2, dissolved in 20 mL of EtOAc/hexane (10:90, v/v), and loaded onto a 2-g silica cartridge that had been conditioned with 20 mL of hexane. The column was eluted with 20 mL-portions of EtOAc/hexane (10:90, 2 × 20:80, 30:70, 60:40, v/v) and 20 mL of EtOAc. After the second sample was separated the same way, the four 20:80 fractions were combined, dried under N_2, and further

purified using a 10 g C18 Sep-Pak cartridge (Waters Corp.). The cartridge was conditioned with 100 mL of MeOH followed by 100 mL of MeCN-H_2O (30:70, v/v). The combined 20:80 fraction was dissolved in 3 mL of EtOAc plus 27 mL of MeCN. Just before loading onto the conditioned cartridge, the fraction was diluted with 70 mL of H_2O. The cartridge was eluted with 100-mL portions of MeCN-H_2O (30:70, 40:60, 50:50, 60:40, 80:20, v/v) and MeCN. The 40:60 and 50:50 fractions were combined, diluted with 250 mL of H_2O, and loaded onto a new 10 g C18 cartridge that had been conditioned with 100 mL of MeOH followed by 100 mL of MeCN-H_2O (20:80, v/v). The cartridge was washed with 100 mL of MeCN-H_2O (20:80, v/v). Air was pulled briefly through the cartridge to remove the solvent, and it was then eluted with 50 mL of MeCN. The MeCN solution was dried under N_2 to give 35 mg of dihydroresorcylide (**6.1**)

The 60:40 EtOAc/hexane and EtOAc fractions from the first silica cartridges were combined and dried under N_2. A 2-g silica cartridge was conditioned with 20 mL of hexane and the extract in 20 mL of EtOAc/hexane (35:65, v/v) loaded onto the column. The column was eluted with 20-mL portions of EtOAc/hexane (2 × 30:70, 40:60, 50: 50, 60:40, 70:30, v/v) and 20 mL of EtOAc. The 50:50 and 60:40 fractions were combined and concentrated to 10 mL under air, at which point a precipitate formed. The solution was transferred to a syringe equipped with a 25-mm, 0.45-μm, nylon filter, and the vial was rinsed twice with 3-mL portions of EtOAc. After filtration, an additional 3 mL of EtOAc was used to rinse the vial and filter. The sample was dried under air and dissolved in 3 mL of MeCN. A 2-g C18 Sep-Pak cartridge was conditioned with 20 mL of MeOH, followed by 20 mL of MeCN-H_2O (15:85, v/v). The sample was diluted with 17 mL of H_2O just before it was loaded on the cartridge. The cartridge was eluted with 20-mL portions of MeCN-H_2O (15:85, 20:80, 30:70, 40:60, 50:50, v/v) and MeCN. A new 2 g C18 cartridge was conditioned as above. The 30:70 fraction was diluted with 20 mL of H_2O and loaded onto the cartridge. The cartridge was washed with 20 mL of

MeCN-H_2O (15:85, v/v). Air was pulled briefly through the cartridge to remove the solvent, and it was then eluted with 10 mL of MeCN. The MeCN solution was dried under N_2 to give 23 mg of a mixture consisting of approximately equal amounts of the diastereomeric 7-hydroxydihydroresorcylides **6.3** and **6.4**.[149]

Dihydroresorcylide (**6.1**)

Colorless oil; $[\alpha]_D$ = +15 (*c* 0.33, MeOH, 25 °C); ^1H,^{13}C, and HMBC NMR data, see Table 12. HREIMS *m*/*z* 292.1316 M^+ (rel int 100), 274.1196 (1), 256.1101 (12), 205.0509 (28), 204.0431 (16), 195.0296 (17), 192.0412 (50), 168.0416 (44), 167.0337 (45), 166.0265 (24), 125.0801 (82), 122.0109 (26), calcd for $C_{16}H_{20}O_5$, 292.1310.

Mixture of 7*R*- and 7*S*-hydroxydihydroresorcylides

(**6.3** and **6.4**)

Yellow solid; ^1H NMR data, see Table 13. EIMS *m*/*z* 308 $(M+H)^+$.

Inoculation of Maize Ears for Detection of

Dihydroresorcylide (**6.1**) by LC-APCI-MS

Inoculation of Maize Ears

Maize ears were wounded by a single inoculation with *A. zeae* (NRRL 34559) in the late milk to early dough stage of kernel maturity (21 days after mid silk; July 22, 2006) for a commercial maize hybrid (FS 6873RR) grown at Kilbourne, IL. Following natural dry-down in the field, ears were hand-harvested (September 21, 2006), and the seeds nearest each wound-site were sampled. Seeds with visible discoloration of 50% or more of the kernel surface, but none of the wounded seeds, were selected for analyses of dihydroresorcylide content.

Analysis of Inoculated Maize by LC-MS

The 50-100% discolored kernels were ground in a Stein mill (Steinlite, Atchison, KS). A 10-g sample was extracted with 50 mL of EtOAc for 1 h on an orbital shaker, then gravity-filtered through Whatman 2V filter paper, and 25 mL of the filtrate was transferred to a glass vial and dried under a filtered air stream at room temperature. The residue in the vial was dissolved in 10 mL of hexane and transferred to a 30-mL separatory funnel. It was then partitioned with three 5-mL portions of MeCN, each portion used to rinse the vial before being added to the separatory funnel. The MeCN was collected in a vial and dried under an air stream. The residue was dissolved in 2 mL of EtOAc and 1 mL of the solution was filtered through a 0.45-μm, 13-mm, nylon syringe filter (Gelman) and analyzed by LC-MS and LC-MS/MS.

A SpectraSYSTEM P4000 pump and an AS3000 autosampler were coupled to an LCQ Classic mass spectrometer via an atmospheric pressure chemical ionization (APCI) interface (Finnigan-MAT, San Jose, CA). A 150 x 2.0 mm i.d., 4-μm, Synergi Polar-RP column (Phenomenex, Torrance, CA) with a Polar-RP guard column and a 0.5-μm prefilter was used, and the entire HPLC eluent was introduced into the detector. A 10-min linear gradient from 30:50:20 (v/v/v) to 20:50:30 H_2O - 2% acetic acid in MeOH/100% MeOH, followed by a 10-min linear gradient from 20:50:30 to 0:50:50 was used, and the final composition was held for 10 min before the initial conditions were restored. The total run time was 45 min. The flow rate was 0.4 mL/min. Mass spectra were obtained by scanning from *m*/*z* 250 to 950 in the positive ion mode. The source voltage was 6 kV, the APCI vaporizer temperature was 350 °C, and the capillary temperature was 170 °C. The sheath gas flow was 70 arb.

Procedure for the Isolation and Characterization of Metabolites from *Stenocarpella maydis*

Fungal Material

Maize isolates of *Stenocarpella maydis* and *Stenocarpella macrospora* were obtained from the USDA Agricultural Research Service Culture Collection, Peoria, IL (NRRL) and included *S. maydis* NRRL 43670, NRRL 52415, and NRRL 53563, from white maize seeds, Cerro Gordo, IL; NRRL 53565, NRRL 53566, and NRRL 53567 from maize seeds, Kilbourne, IL; NRRL 31249, from maize seed, Indianapolis, IN; NRRL 53560 from white maize seed, Rochester, IN; NRRL 13608 (= ATCC 10235), from maize, KY; NRRL 53564, from white maize seed, Hopkinsville, KY; NRRL 53561, and NRRL 53562 from white maize seeds, Crete, NE; NRRL 13609 (= ATCC 16438), from maize, location unreported, R.B. Stevens; NRRL 13615, from maize seed, location unreported, USA; *S. macrospora* NRRL 13610 (= ATCC 36896) from maize, Costa Rica; NRRL 13611 (= ATCC 42808; MRC 143b) from maize, Zambia, and NRRL 13612 (= ATCC 18606) from maize, GA, USA. Each of the isolates from maize was cultured to produce pycnidia and the spores were examined microscopically and measured by Dr. D. T. Wicklow to confirm that these isolates were *S. maydis*. The cultures were also sequenced and the sequences deposited in GenBank[184] and are listed in Table 6. Test strains were all isolated from maize seeds and included: *Acremonium zeae* NRRL 13540, *Alternaria alternata* NRRL 6410, *Aspergillus flavus* NRRL 6541, *Bipolaris zeicola* NRRL 47238, *Colletotrichum graminicola* NRRL 47511, *Curvularia lunata* NRRL 6409, *Fusarium graminearum* NRRL 31250, *Fusarium verticillioides* NRRL 25457, *Nigrospora oryzae* NRRL 6414, *Rhizoctonia zeae* NRRL 40186, *S. maydis* NRRL 31249, and *Trichoderma viride* NRRL 6418.

Bioactivity of Fermented-Rice Cultures

Fermented-rice cultures produced using different strains of *Stenocarpella maydis* or *Stenocarpella macrospora* commonly displayed significant antifungal activity against *Aspergillus flavus* and *Fusarium verticillioides* in conventional paper disc agar diffusion assays on agar plates seeded with conidia of *A. flavus* (NRRL 6541) or *F. verticillioides* (NRRL 25457). We also evaluated 1-mg equivalents of the organic extract of *S. maydis* NRRL 31249 using paper discs placed on the surface of agar plates seeded with conidia and/or hyphal cells of the following test fungi (=zone of inhibition measured from the disc edge): *Acremonium zeae* (7 mm), *Alternaria alternata* (15 mm), *A. flavus* (12 mm), *Bipolaris zeicola* (11 mm), *Colletotrichum graminicola* (13 mm), *Curvularia lunata* (13 mm), *Fusarium graminearum* (15 mm), *F. verticillioides* (20 mm), *Nigrospora oryzae* (20 mm), *Rhizoctonia zeae* (20 mm), *S. maydis* NRRL 31249 (15 mm), *Trichoderma viride* (0 mm). These results suggest that, with the exception of *T. viride*, the antifungal metabolites produced by *S. maydis* are broadly active against common fungal endophytes and pathogens of maize. Ten of 17 *Stenocarpella* culture extracts exhibited potent antiinsectan activity in a dietary assay using neonate larvae of the fall armyworm (*Spodoptera frugiperda*) causing a reduction in weight gain of >75 % relative to the control, with three of the extracts also causing some larval mortality. Extracts showing potent antiinsectan activity also showed potent antifungal activity, while extracts showing limited antiinsectan activity were typically inactive in antifungal assays. Culture extracts from two strains of *S. maydis* (NRRL 13608; NRRL 13609) and two strains of *S. macrospora* (NRRL 13610; NRRL 13612) exhibited no antifungal activity and weak antiinsectan activity. Extracts from a replicated experiment produced the same bioassay results. These strains were previously maintained by periodic culture transfer for multiple years and may have lost their ability to produce such metabolites. Previously, 13 of 16 isolates of *S. maydis* tested were acutely toxic to ducklings, one of the exceptions being ATCC 10235 (=MRC 684; NRRL 13608) where deaths did not occur.

Several of the extracts produced significant necrotic lesions when applied to needle puncture wounds of maize leaves although none exceeded those produced by the oxalic acid controls. There was no consistent relationship between lesion length and measures of antifungal or antiinsectan activity, suggesting that different compounds may account for these activities.

Extraction and Isolation Procedure

The EtOAc extracts from two flasks, each containing 50 g of rice inoculated with *S. maydis* NRRL 43670, were combined, filtered, and evaporated to give 741 mg of crude extract. The crude extract was partitioned between MeCN and hexanes to afford 500 mg of an MeCN-soluble fraction. A portion of this fraction (248 mg) was subjected to Sephadex LH-20 column chromatography using the following solvents: 1:4 hexanes CH_2Cl_2 (solvent A); 3:2 CH_2Cl_2-acetone (solvent B); 1:4 CH_2Cl_2-acetone (solvent C); and MeOH (solvent D).[194] Twenty-four fractions were collected: fractions 1-7, 20 mL solvent A; frs 8-14, 20 mL solvent B; frs 15-23, 20 mL solvent C; 24, 150 mL solvent D. Fraction 13 consisted of 58 mg of the major component diplodiatoxin (**1.16**).

The EtOAc extract from two flasks, each containing 50 g of rice inoculated with *S. macrospora* NRRL 13611, were filtered and evaporated to give 256 mg of crude extract. A portion (210 mg) of the crude extract was partitioned between MeCN and hexanes to afford 189 mg of an MeCN-soluble fraction. A portion of this fraction (16 mg) was chromatographed over an Alltech Altima C18 column (10 mm x 250 mm) at a flow rate of 2.0 mL/min with UV detection at 220 nm using the following method: isocratic at 30% MeCN-H_2O over 5 min; ramp from 30-50% MeCN-H_2O over 10 min; ramp from 50 to 65% MeCN-H_2O over 5 minutes; ramp from 65 to 100% MeCN-H_2O over 15 minutes; isocratic at 100% MeCN over 5 minutes. This protocol afforded chaetoglobosin K[53] (**1.18**; t_R = 31 min; 1.4 mg), chaetoglobosin L[169] (**7.1**; t_R = 27 min; 0.7

mg), chaetoglobosin M[170] (**7.2**; t_R = 34 min; 1.4 mg) and diplosporin[51] (**1.17**; t_R = 12 min; 5.9 mg). These metabolites were identified by comparison of MS and NMR data to literature values.

The combined EtOAc extract from ten flasks, each containing 50 g rice inoculated with *S. maydis* NRRL 53566, was filtered and evaporated to give 1 g of crude extract. A portion of the crude extract (834 mg) was partitioned between MeCN and hexanes to afford 680 mg of a MeCN-soluble fraction. A portion of this fraction (365 mg) was subjected to silica gel column chromatography using the following solvents: hexanes (solvent A); hexanes/EtOAc (solvent B, % composition noted below); acetone (solvent C); and MeOH (solvent D). TLC on silica gel was used to analyze each fraction and those with similar components were combined to afford 14 fractions: fraction 1, 200 mL 5% solvent A, 200 mL 5% solvent B, 200 mL 10% solvent B, 200 mL 20% solvent B; fr 2, 100 mL 30% solvent B; fr 3, 100 mL 40% solvent B; fr 4 100 mL 50% solvent B, 100 mL 60% solvent B; fr 5, 50 mL 70% solvent B; fr 6, 50 mL 70% solvent B; fr 7, 100 mL 80% solvent B, 50 mL 90% solvent B; fr 8, 50 mL 90% solvent B, 100 mL 100% solvent B; fr 9, 50 mL solvent C; fr 10, 50 mL solvent C; fr 11, 50 mL solvent C; fr 12, 50 mL solvent C; fr 13, 50 mL solvent D; fr 14, 50 mL solvent D. Fraction 4 (11 mg) was chromatographed over a Rainin Dynamax-60/A C_{18} column (21.4 mm × 250 mm, 8-µm particle size) at a flow rate of 5.0 mL/min with detection at 256 nm using the following method: isocratic at 20% MeCN-H_2O over 5 min; ramp from 20 to 100% MeCN-H_2O over 40 minutes; isocratic at 100% MeCN over 5 minutes. This protocol afforded (all-*E*)-trideca-4,6,10,12-tetraene-2,8-diol (**7.4**; t_R = 22 min; 1.0 mg).[168]

Detection of *Stenocarpella* metabolites

Thirty naturally infected maize ears severely rotted by *S. maydis* were individually hand-harvested in September 2007 from a commercial production field near

Kilbourne, IL that was planted to Burrus 794sRR. Immediately following harvest, ears were individually shelled and a single rotted seed from each ear was selected for isolation of *S. maydis*. The remaining seeds from each ear were stored separately in the freezer (-20°C). Individual seeds were treated with 2% NaOCl plus 0.01% Triton X-100 for 2 min, rinsed twice in H_2O, and then transferred to individual Petri dishes containing 3% malt extract agar. After 4-5 days of incubation at 25°C, hyphal tips of *S. maydis* colonies growing from seeds were transferred to slants of PDA and incubated at 25°C. Five-gram subsamples of the rotted kernels from each of the 30 ears were pooled and extracted three times with EtOAc to afford a dried extract weighing 1497 mg. The remaining rotted seeds (84-130 g) from *S. maydis* rotted ears, from which NRRL 53565, NRRL 53566, and NRRL 53567 were isolated, were separately extracted with EtOAc. Seeds removed from symptomless ears were also extracted with EtOAc to serve as a control. The extracted residues were then examined for *Stenocarpella* metabolites.

Maize ears of the commercial corn hybrid Burrus ZD51 grown in Kilbourne, IL (crop year 2009) were wounded by a single inoculation with *S. maydis* (NRRL 53565, NRRL 53566, or NRRL 53567) in the late milk to early dough stage of kernel maturity (21 days after mid-silk). Briefly, twenty ears on plants within a single 7-m length of row were inoculated in the mid-ear region by inserting a single wooden toothpick penetrated by *S. maydis* through the husks and developing seeds as far as the rachis (cob). Following natural dry-down in the field (to 16% moisture content), ears were hand-harvested and the visibly diseased seeds from each ear were pooled and stored in a freezer at -7° prior to the preparation of solvent extracts.

Maize F-2 seeds from Burrus 794sRR were planted in eighteen 5-in pots containing a pasteurized potting mix and grown in an environmental chamber. The photoperiod was 16 hr, with temperatures at 26°C ± 1°C (day) and 21±1°C (night). After 41 days, plants were toothpick wound-inoculated with *S. maydis* NRRL 53562 or NRRL 53565 in each of the first three internodes above the root crown. Living plants displaying

symptoms of stalk rotting accompanied by wilting were harvested after 58 days (= 17 dpi), 72 days (= 31 dpi) and 100 days (= 59 dpi). Internodal sections were split longitudinally to reveal discolored regions of the pith. A small sample of discolored pith tissue near each site of wound-inoculation was cultured on PDA containing streptomycin to reveal colonization by *S. maydis*. Freeze-dried stalk segments showing symptoms of pith tissue necrosis with brown discoloration were individually extracted three times with EtOAc. In each case, the combined EtOAc extracts were filtered and evaporated to yield a crude extract.

The green stalk of a maize plant in the dent stage of kernel maturity was harvested and cut into segments (7 cm each), distributed among six humidity chambers, and autoclaved for 30 min. Maize stalk residues displaying no symptoms of stalk rot were collected following harvest, rinsed under running tap H_2O, cut into 7-cm segments, and distributed among six humidity chambers. Prior to autoclaving, H_2O was added to each humidity chamber to elevate the stalk residue moisture content to approximately 300% moisture content on a dry basis (Md). The steam-sterilized stem segments were individually inoculated by insertion of wooden toothpicks colonized by S. *maydis* NRRL 53562 or NRRL 53565 and incubated for 14 days (green stalks) or 21 days (stalk residues) at 25°C. Following incubation, the heavily molded stem segments were freeze-dried, cut into 1-2 cm pieces, and extracted three times with EtOAc.

The crude extracts of kernels from naturally infected ears (2007), wound-inoculated ears (2009), infected-necrotic stalk lesions, and steam-sterilized maize stalks inoculated with *S. maydis* were partitioned between hexanes and MeCN. A portion (1 mg) of the CH_3CN-soluble fraction was transferred to a vial for analysis by LC-ESIMS. MeCN (1.0 mL) was added to the vial, and a portion (10 µL) of the resulting stock solution was transferred to a 1.5 mL HPLC vial. An additional aliquot of MeCN (990 µL) was added to the vial and a portion of the resulting solution (20 µL) was used for LC-ESIMS analysis, which facilitated the employment of 200 ng/injection. In a later

screening of extracts of naturally-rotted maize (unpublished results), these metabolites were not detected at 200 ng/injection, however, a more concentrated sample (leading to the use of 2 μg extract/injection in the same solvent volume), enabled the detection of diplodiatoxin (**1.16**) and chaetoglobosin M (**7.2**) as metabolites occurring in naturally-infected corn found in the field. This solution was prepared by transferring a portion (100 μL) of the stock solution to an HPLC vial and adding MeCN (900 μL). Samples were analyzed using LC-ESIMS. Data were obtained over the mass range 100-1000 Da with parallel UV detection at 260 nm. The eluting solvents used were 5% MeCN in H_2O with 0.1% formic acid (solvent B). Solvents used for LC-ESIMS were H_2O with 0.1% formic acid (solvent A) and MeCN with 0.1% formic acid (solvent B). All solvents used for LC-ESIMS were Optima LC-MS grade (Fisher Scientific, Pittsburgh, PA). Samples were chromatographed over a Supelco Discovery reversed-phase C_{18} column (2.1 × 150 mm: 5-μm particle size) at a flow rate of 0.20 mL/min with a sample injection volume of 10 μL using the following method: isocratic at 40% solvent B over 2 min; ramp from 40% to 95% solvent B over 23 min. A fraction containing diplodiatoxin (**1.16**),[48] chaetoglobosin K (**1.18**),[53] chaetoglobosin L (**7.1**)[169] and chaetoglobosin M (**7.2**)[170] was used as a standard for determination of LC-ESIMS retention times (**1.16** t_R = 10.54 min; **1.18** t_R = 12.78 min; **7.1**: t_R = 9.36 min; **7.2**: t_R = 15.14 min). The MS and ^{1}H NMR data for these compounds were consistent with those reported in the literature.

APPENDIX A

SELECTED NMR SPECTRA

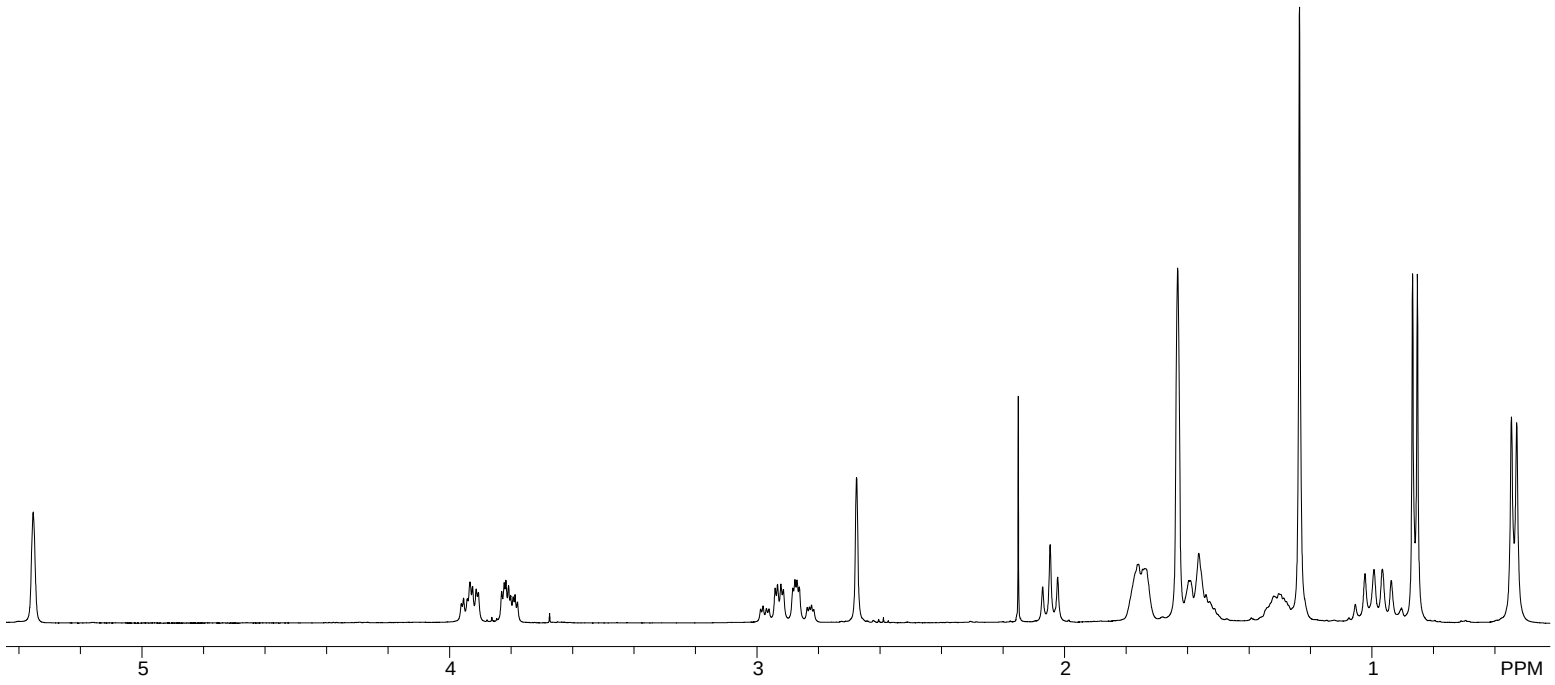

Figure A1. ^{1}H NMR Spectrum (400 MHz) of Diplodiatoxin (**1.13**) in $CDCl_3$

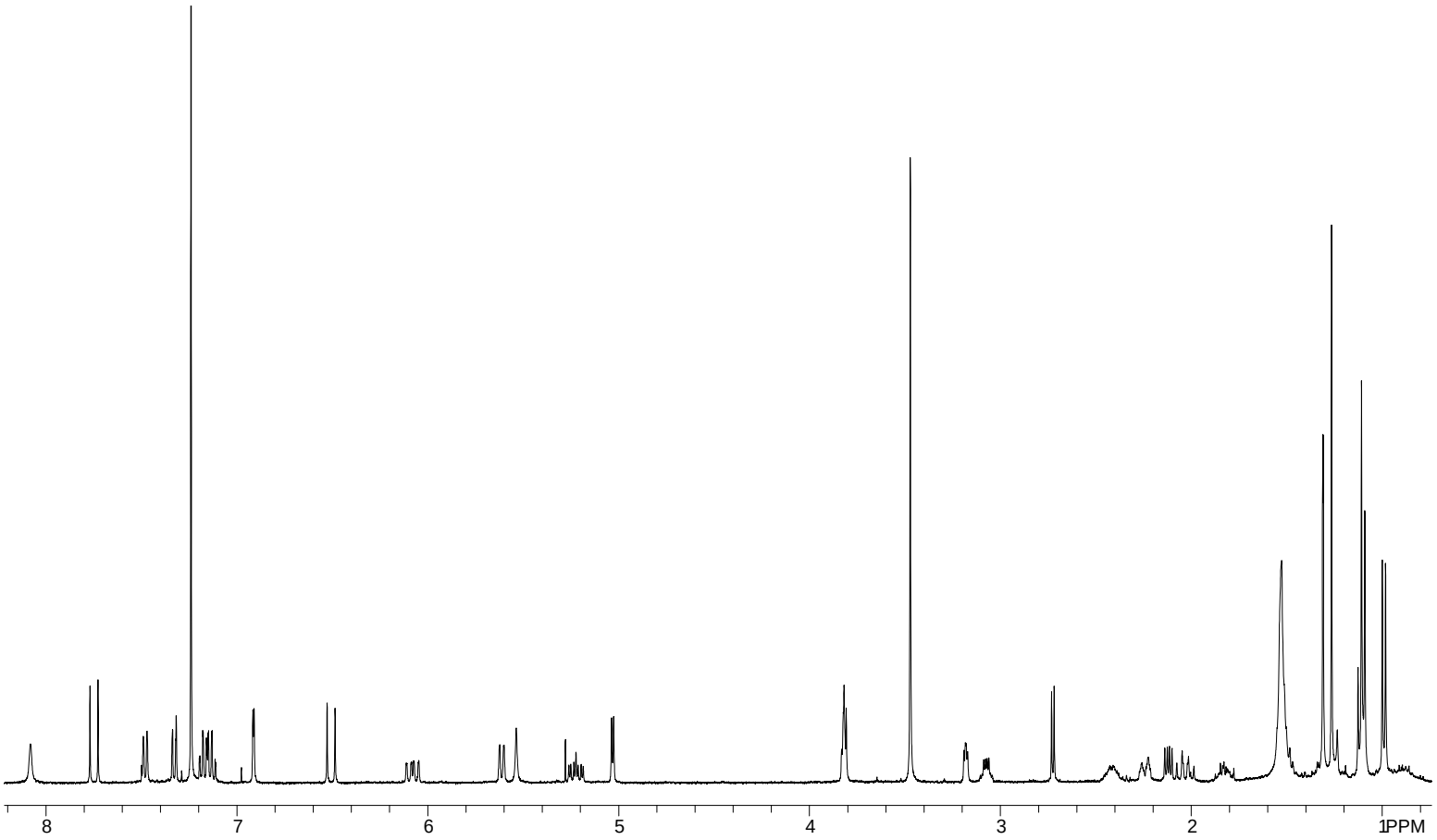

Figure A2. ^{1}H NMR Spectrum (400 MHz) of Chaetoglobosin K (**1.18**) in $CDCl_3$

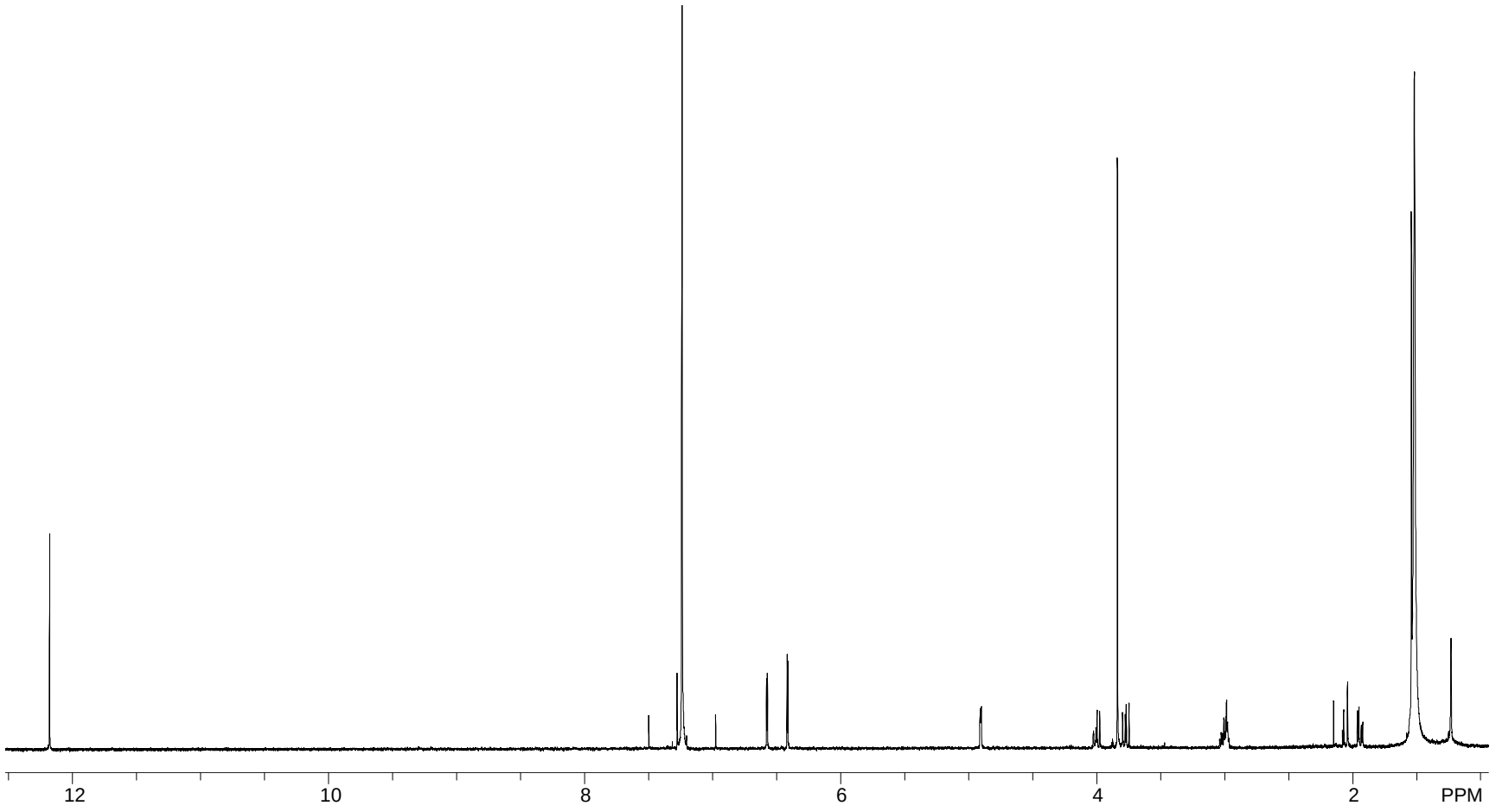

Figure A3. ^{1}H NMR Spectrum (400 MHz) of Scytalol A (**2.3**) in $CDCl_3$

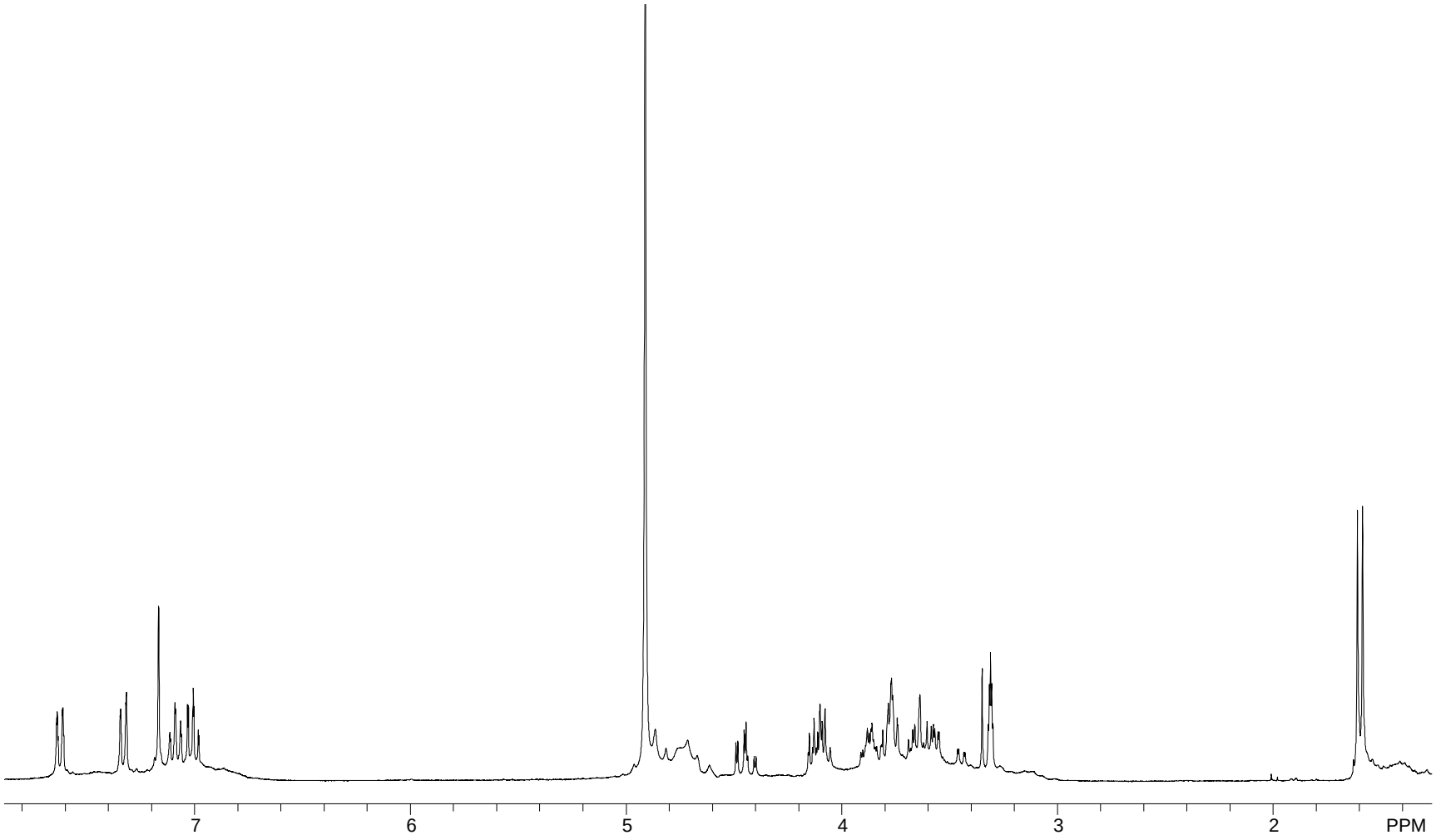

Figure A4. ^{1}H NMR Spectrum (400 MHz) of Acremoauxins A (major; **2.4**) and B (minor; **2.5**) in CD_3OD

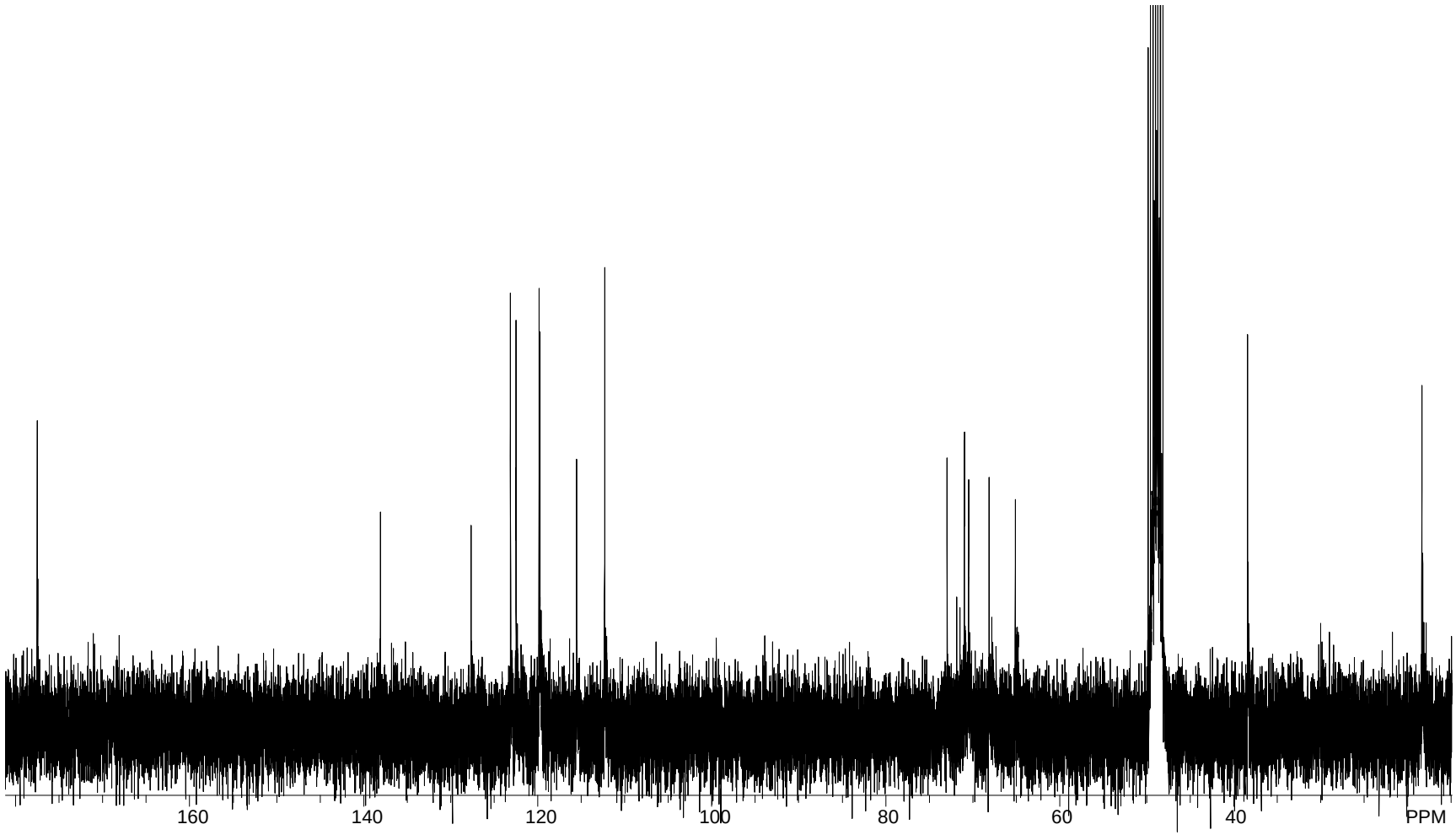

Figure A5. ^{13}C NMR Spectrum (100 MHz) of Acremoauxin A (major; **2.4**) and B (minor; **2.5**) in CD_3OD

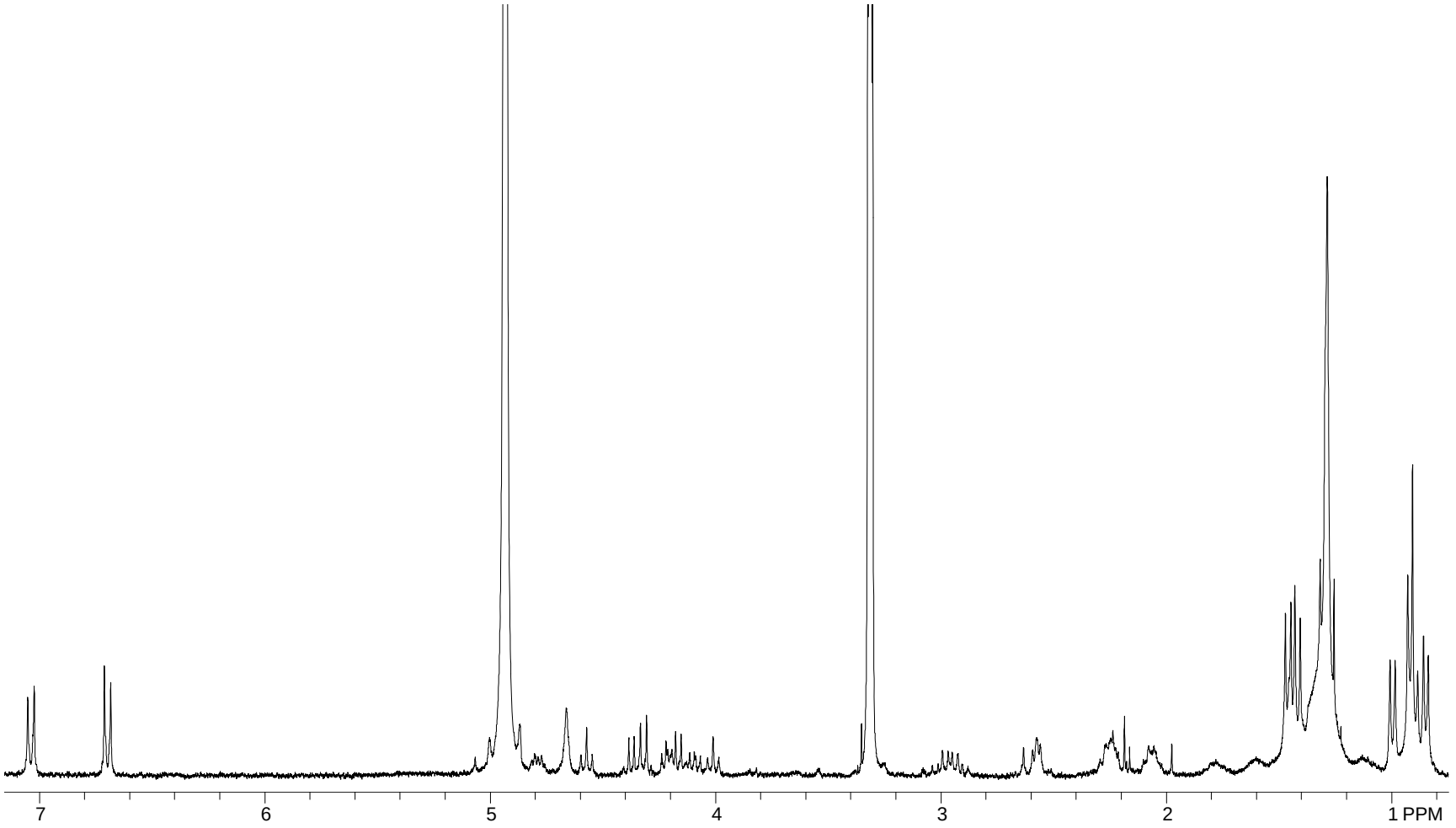

Figure A6. ^{1}H NMR Spectrum (400 MHz) of Acuminatum A (**2.6**) in CD_3OD

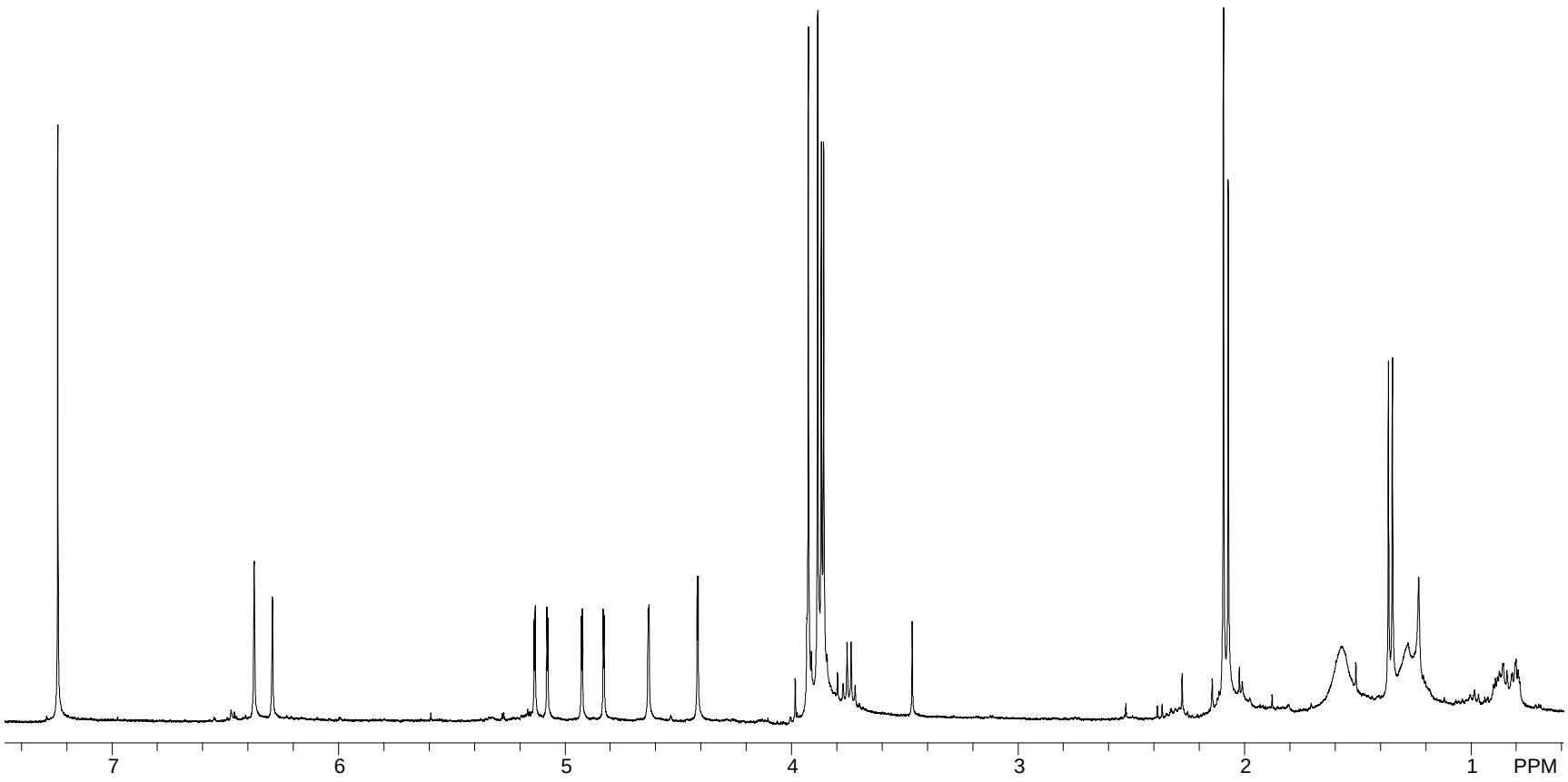

Figure A7. ^{1}H NMR Spectrum (400 MHz) of 6,8-Dimethoxy-4,5-dimethyl-3-methyleneisochroman-1-one (**2.9**) in $CDCl_3$

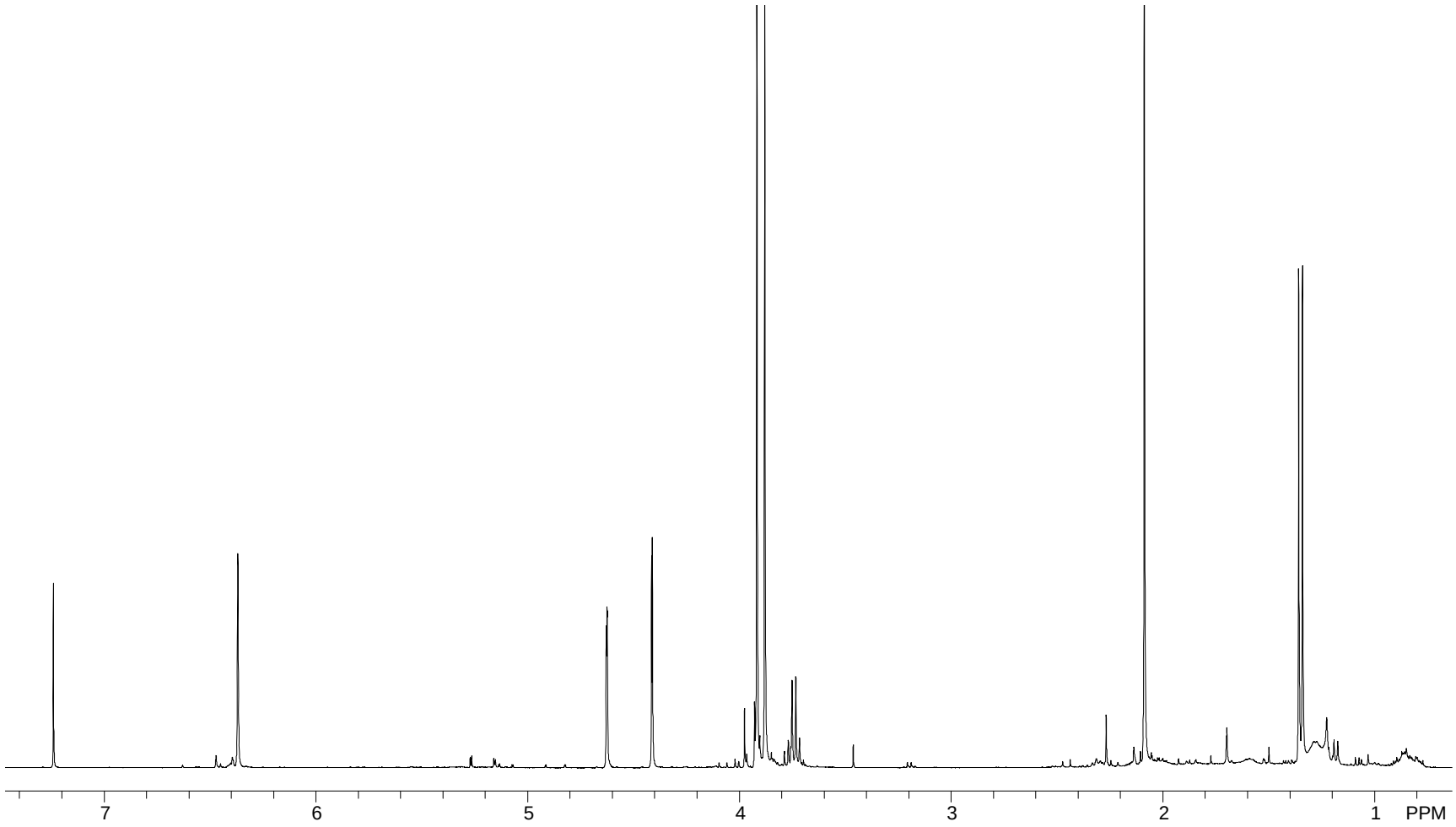

Figure A8. ^{1}H NMR Spectrum (400 MHz) of Compound **2.10** in $CDCl_3$

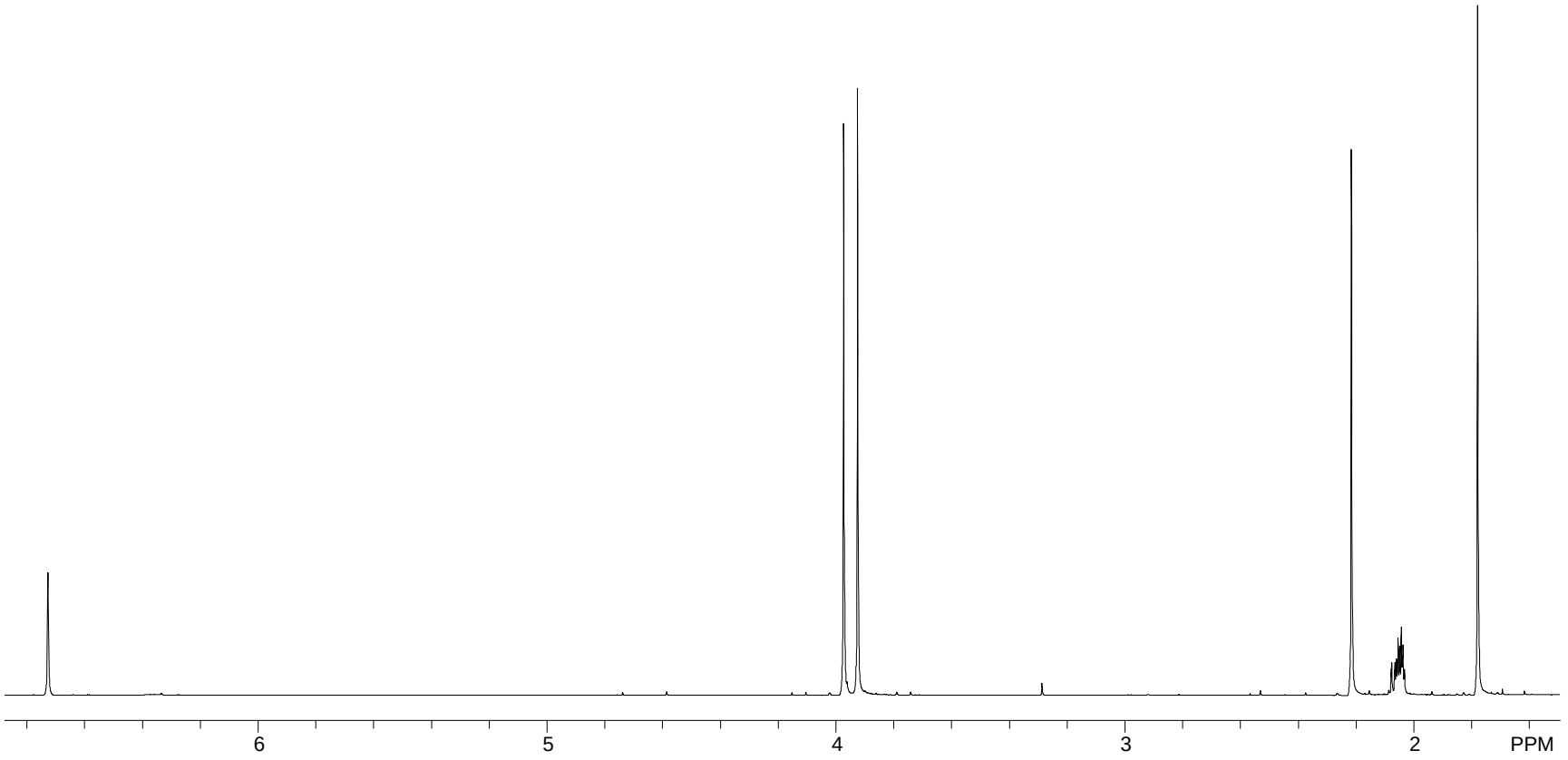

Figure A9. ^{1}H NMR Spectrum (400 MHz) of 5,7-Dimethoxy-3,4-dimethyl-3-hydroxyisobenzofuranone (**2.11**) in Acetone-d_6

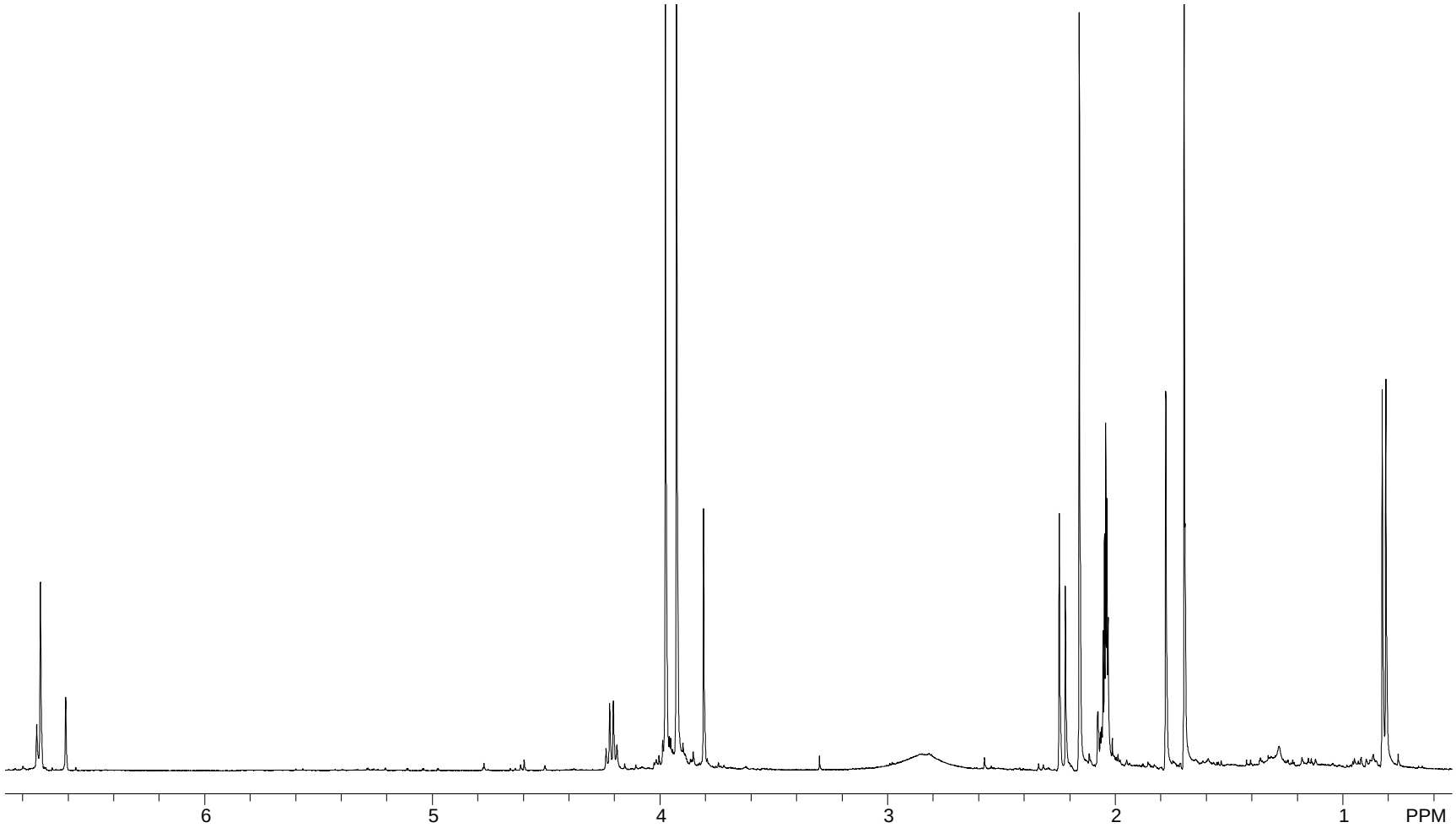

Figure A10. ^{1}H NMR Spectrum (400 MHz) of Compound **2.12** in Acetone-d_6

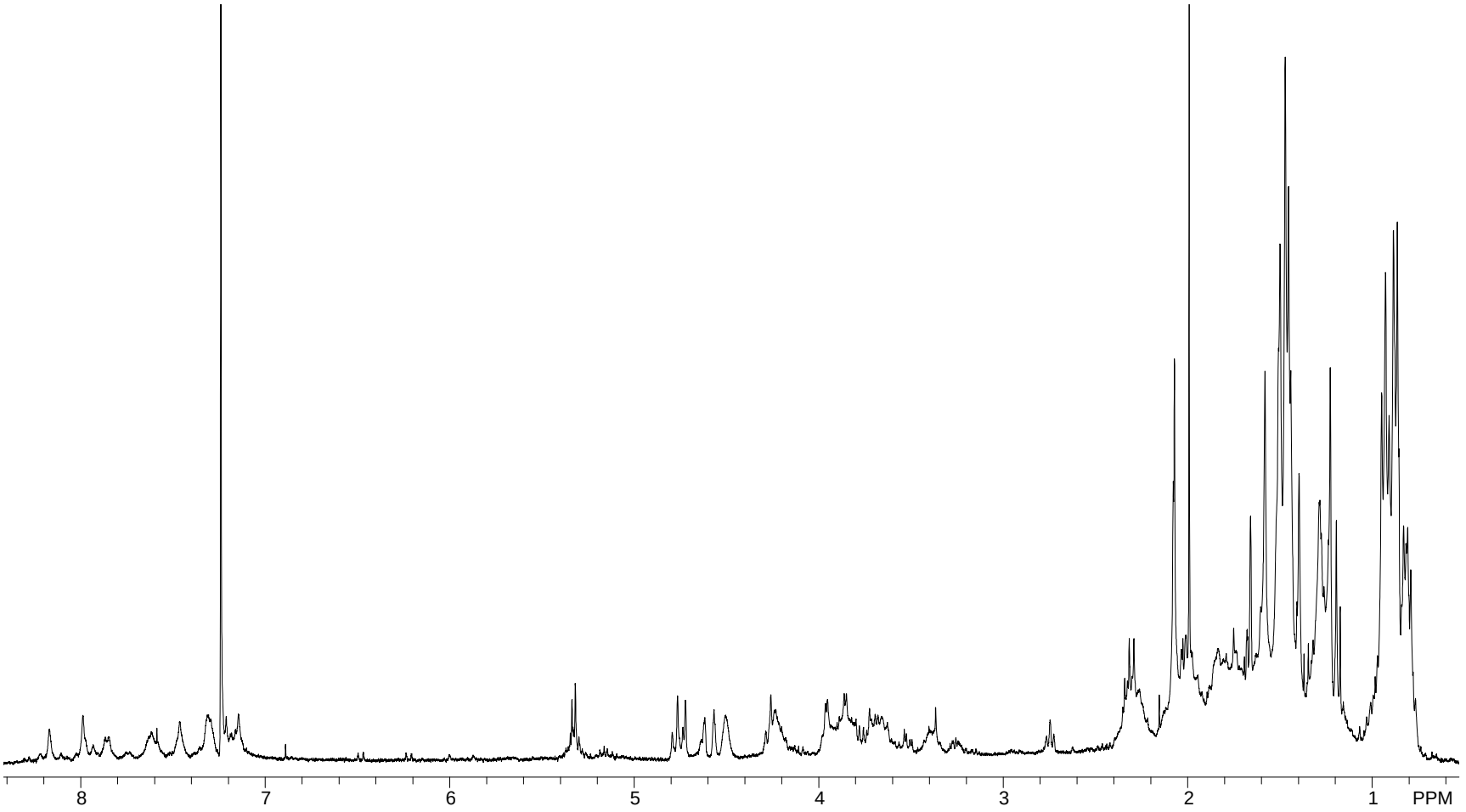

Figure A11. ^{1}H NMR Spectrum (400 MHz) of Bionectrin A (**3.1**) in $CDCl_3$

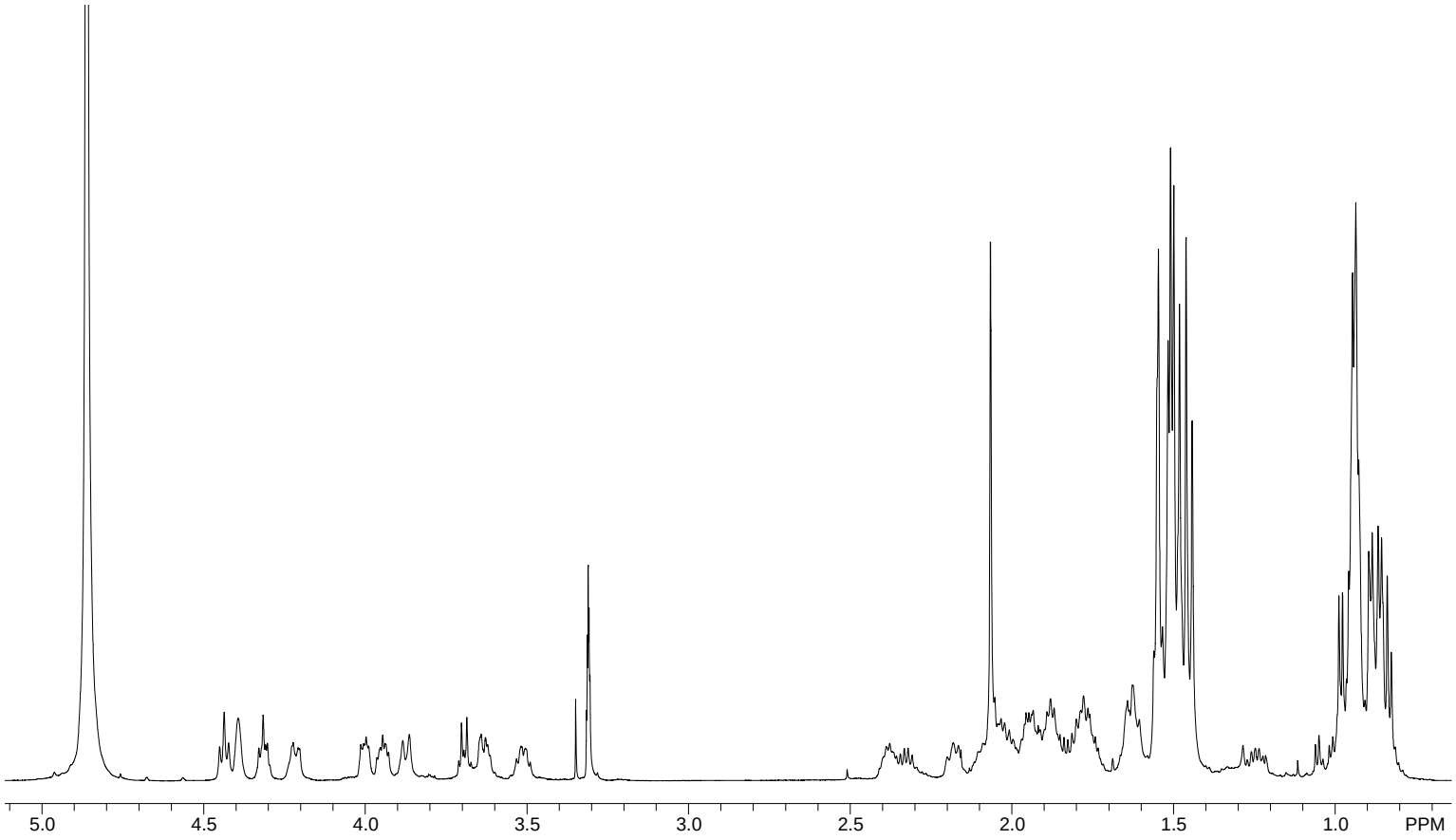

Figure A12. ^{1}H NMR Spectrum (400 MHz) of Bionectrin A (**3.1**) in CD_3OD

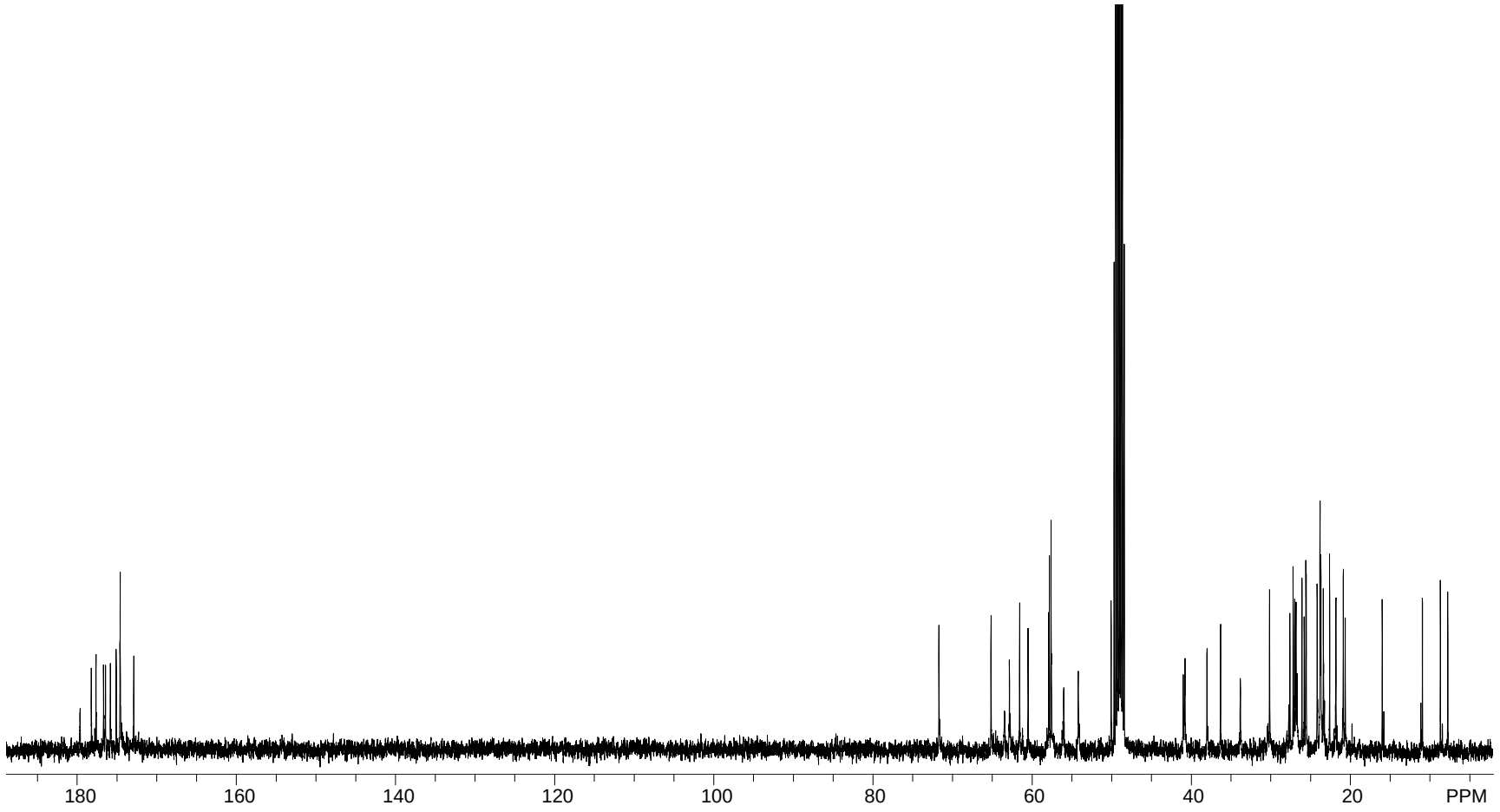

Figure A13. ^{13}C NMR Spectrum (100 MHz) of Bionectrin A (**3.1**) in CD_3OD

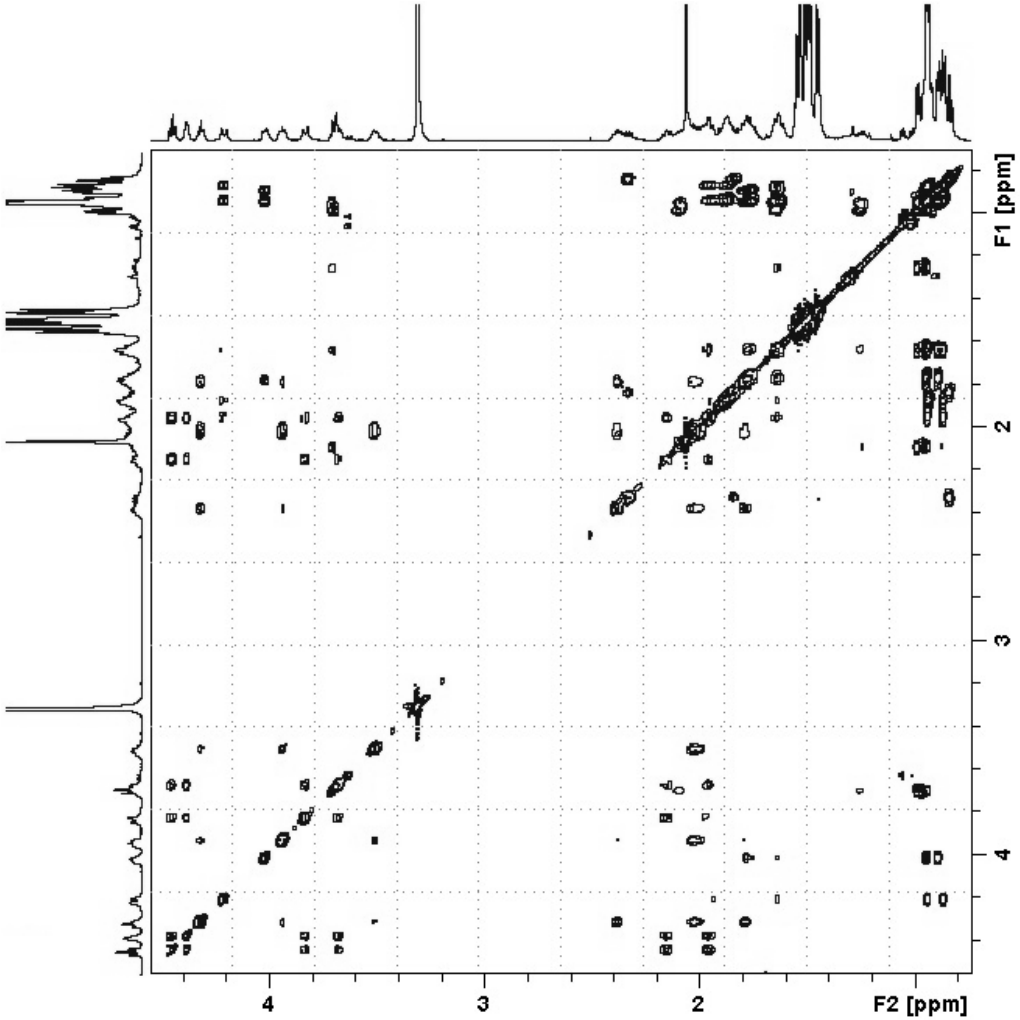

Figure A14. TOCSY Spectrum (600 MHz) of Bionectrin A (**3.1**) in CD_3OD

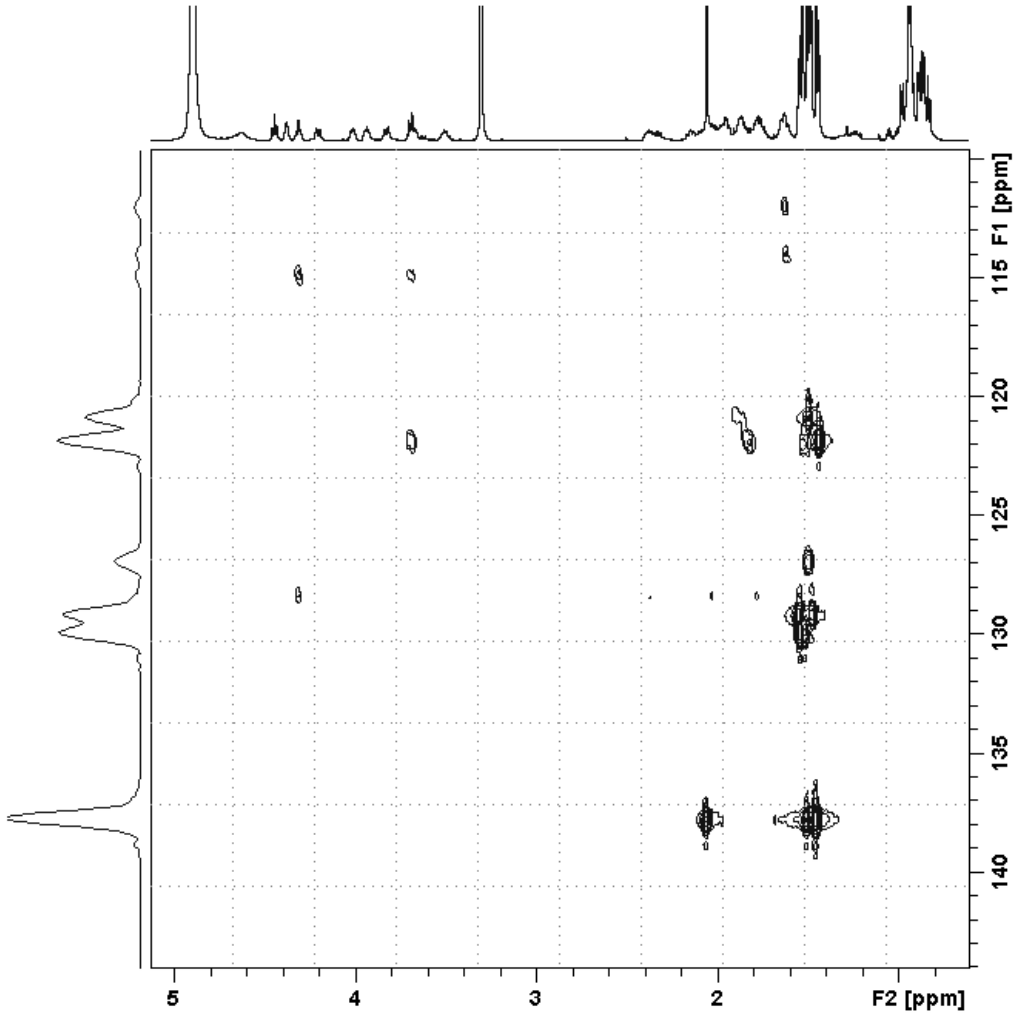

Figure A15. ^{1}H-^{15}N HMBC Spectrum (600 MHz ^{1}H dimension) of Bionectrin A (**3.1**) in CD_3OD

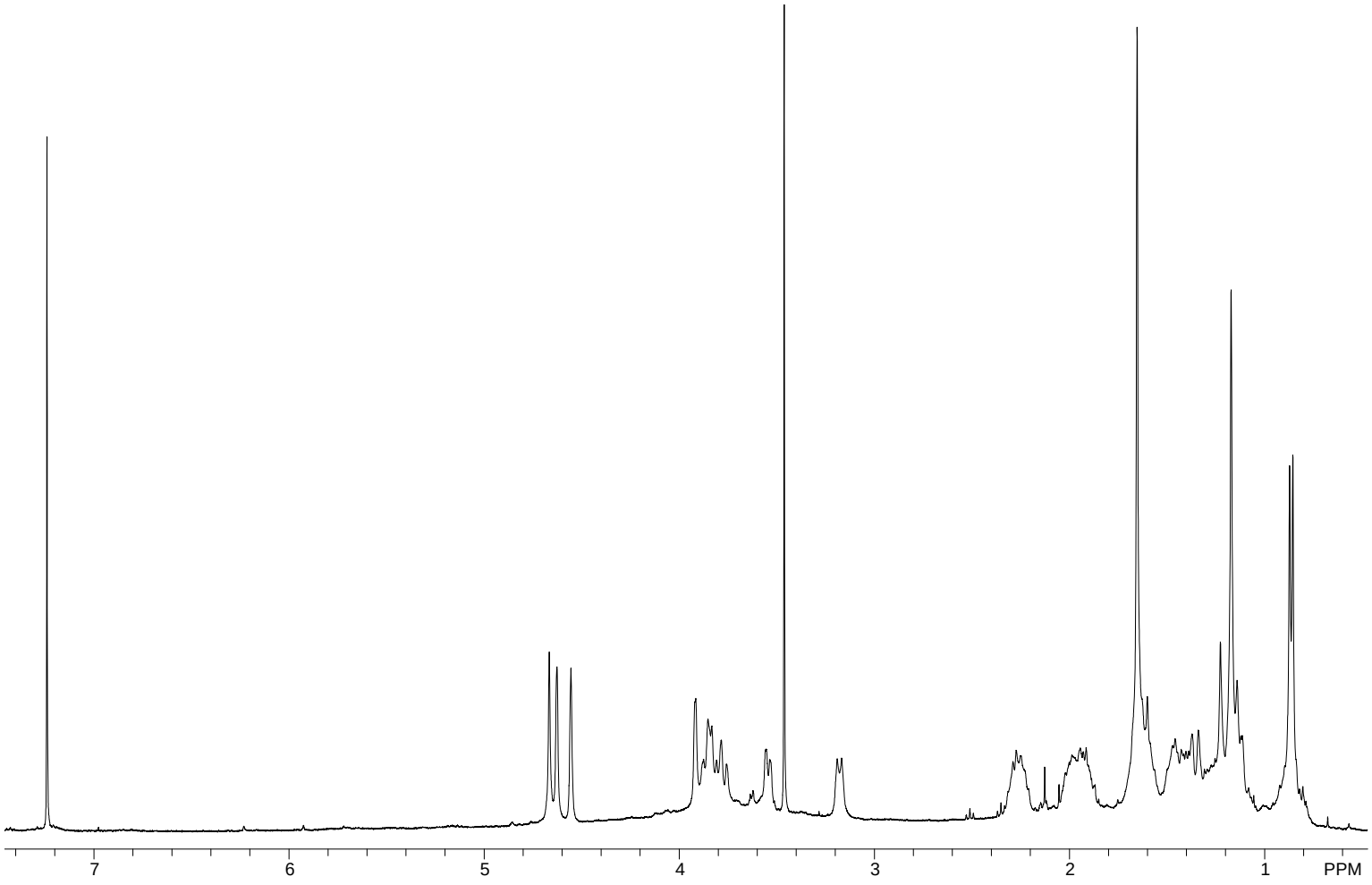

Figure A16. ^{1}H NMR Spectrum (400 MHz) of Guaiane Mannoside (**3.2**) in $CDCl_3$

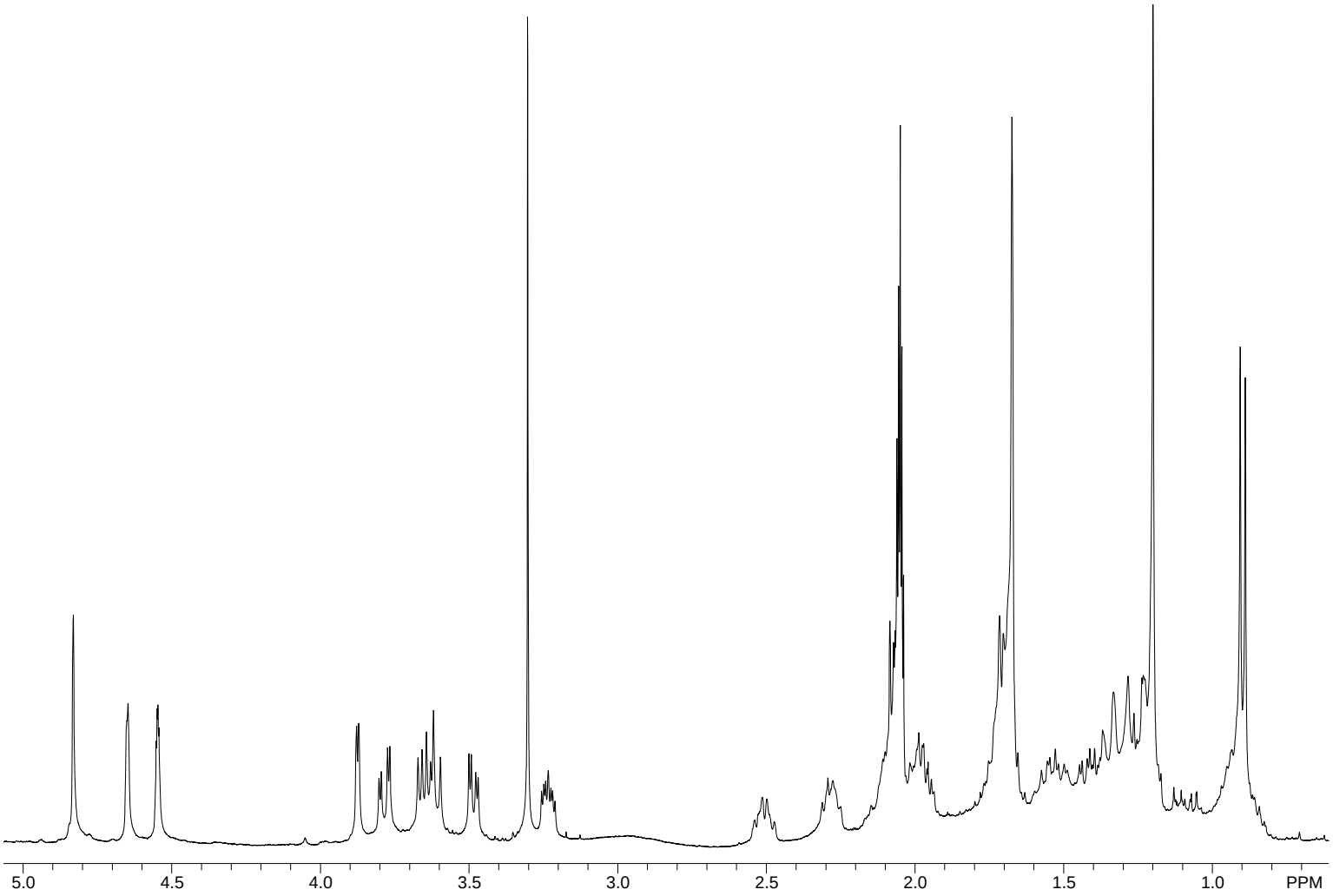

Figure A17. ^{1}H NMR Spectrum (400 MHz) of Guaiane Mannoside (**3.2**) in Acetone-d_6

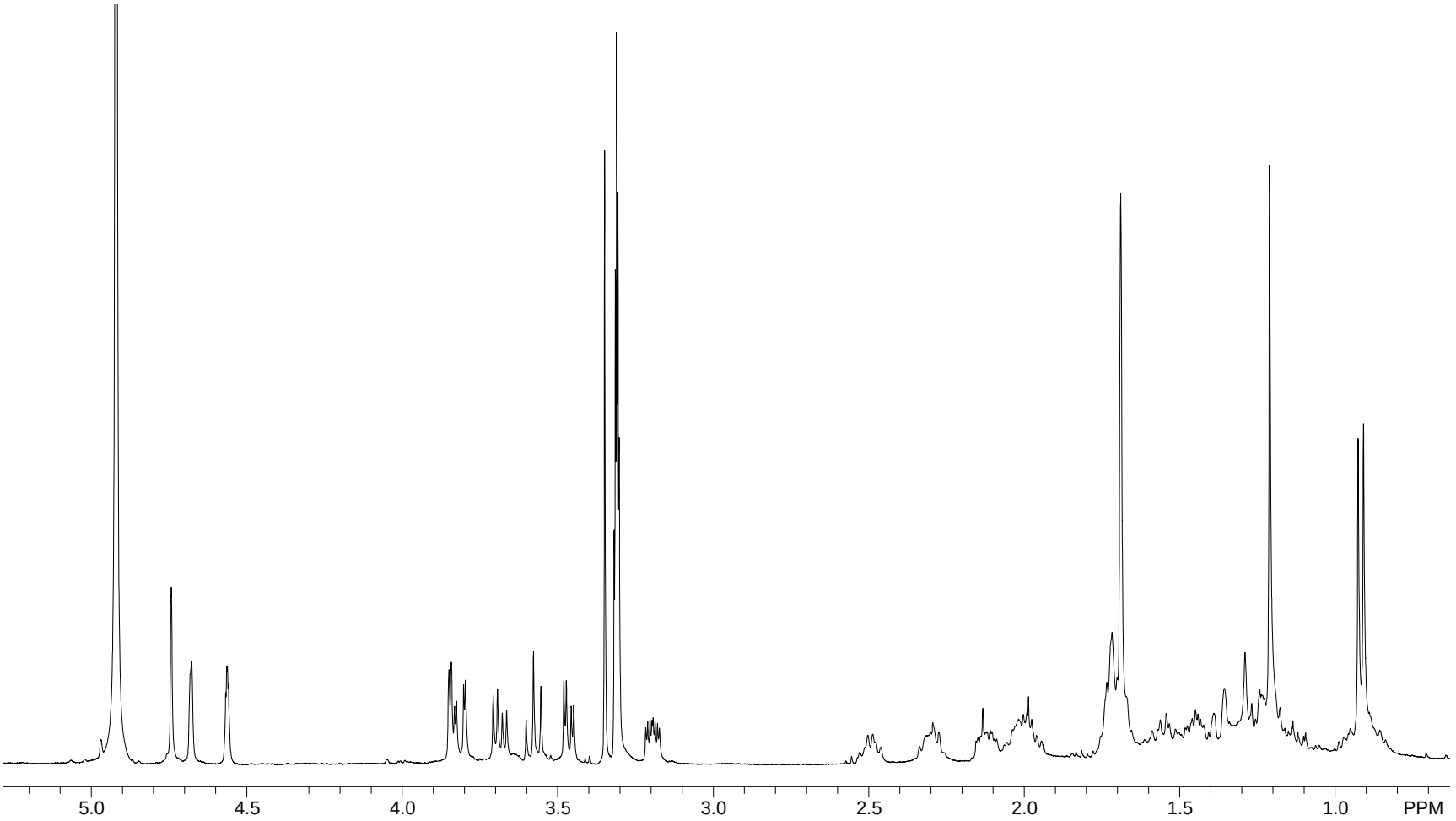

Figure A18. ^{1}H NMR Spectrum (400 MHz) of Guaiane Mannoside (**3.2**) in CD_3OD

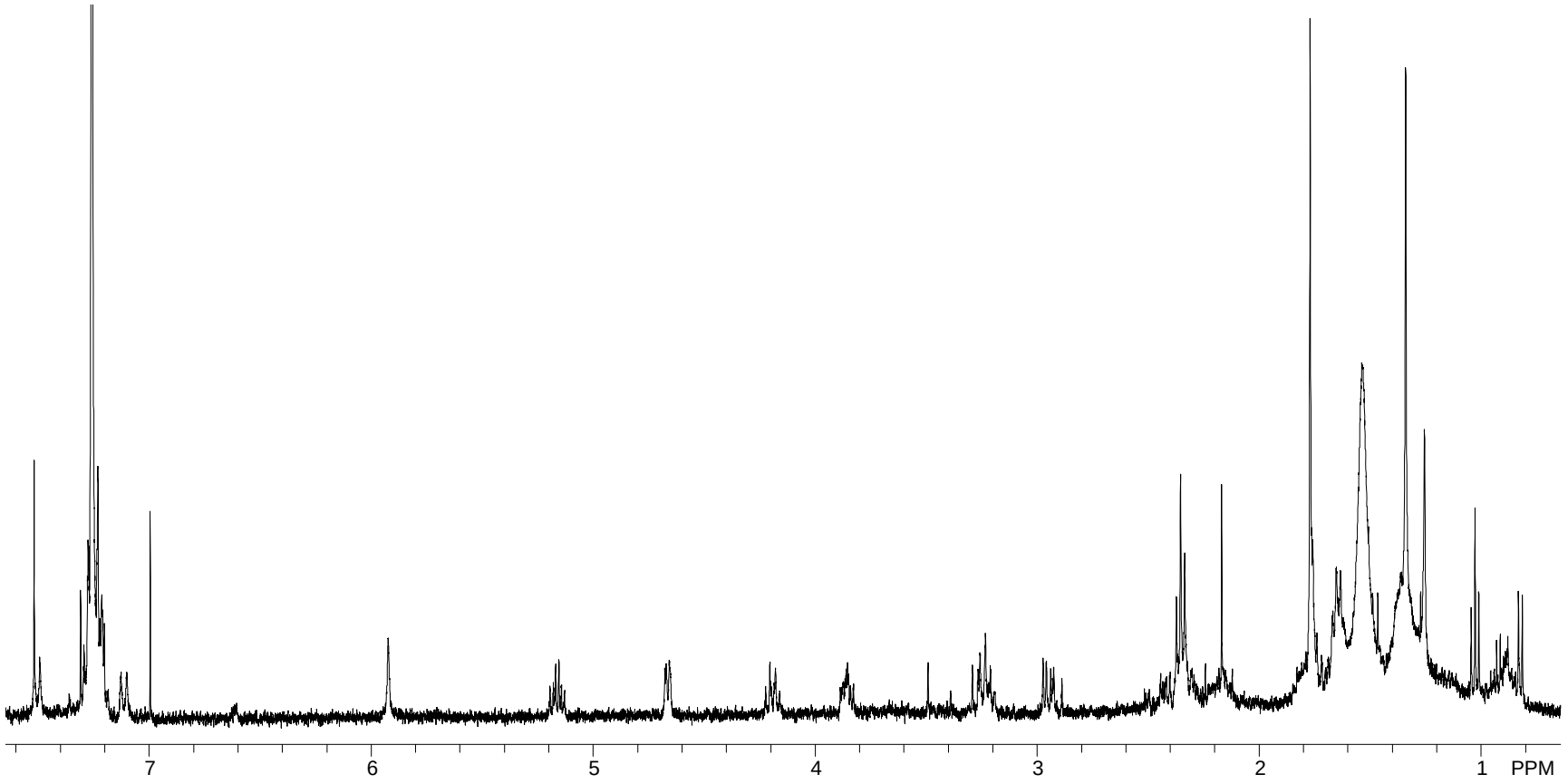

Figure A19. ^{1}H NMR Spectrum (400 MHz) of *cyclo*[-Aib-*S*-Phe-*R*-Pro-*S*-Aoh-] (**3.4**) in $CDCl_3$

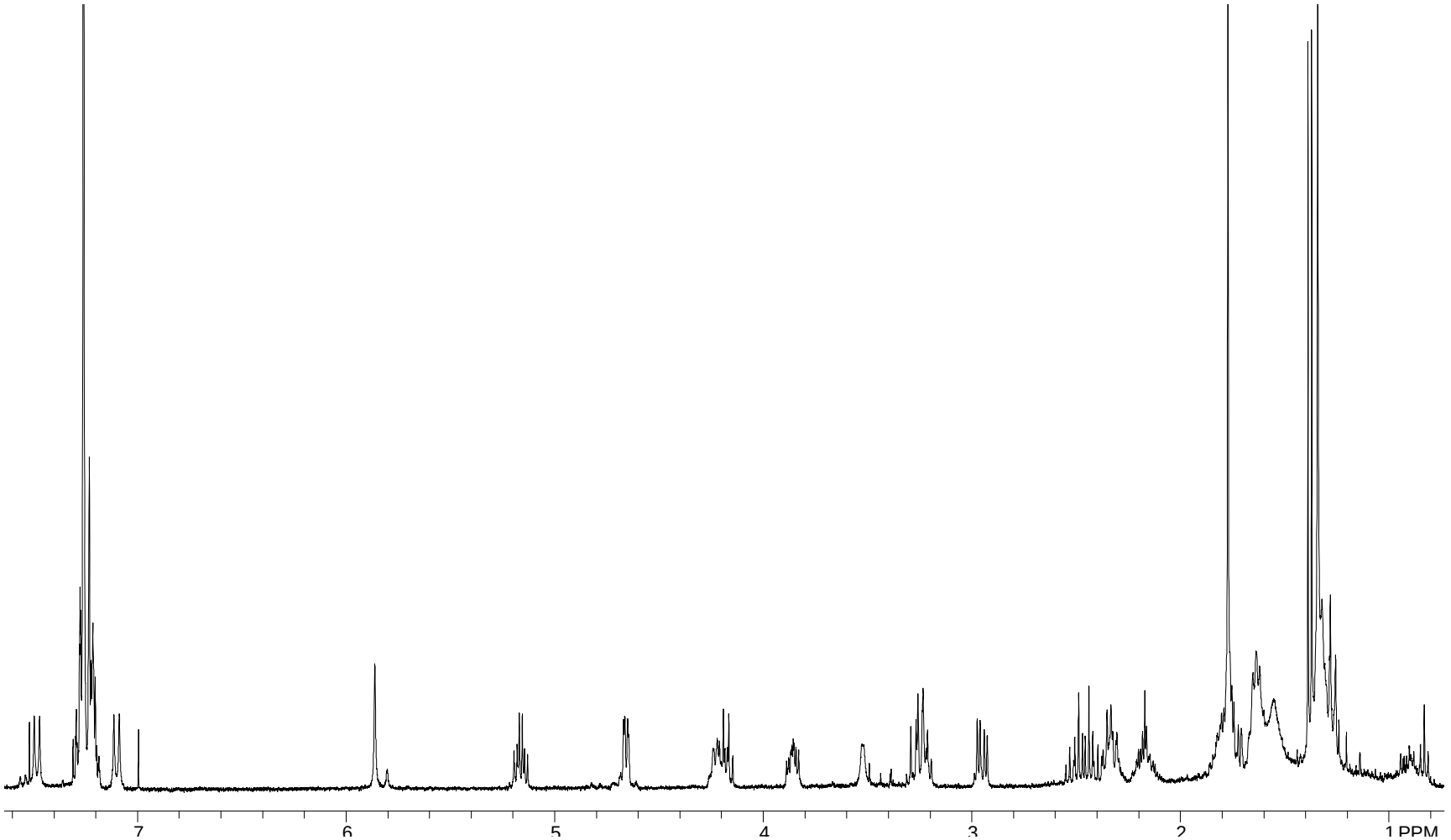

Figure A20. ^{1}H NMR Spectrum (400 MHz) of *cyclo*[-D-Pro-Phe-Iva-(9R)-Aoh-] (**3.5**) in $CDCl_3$

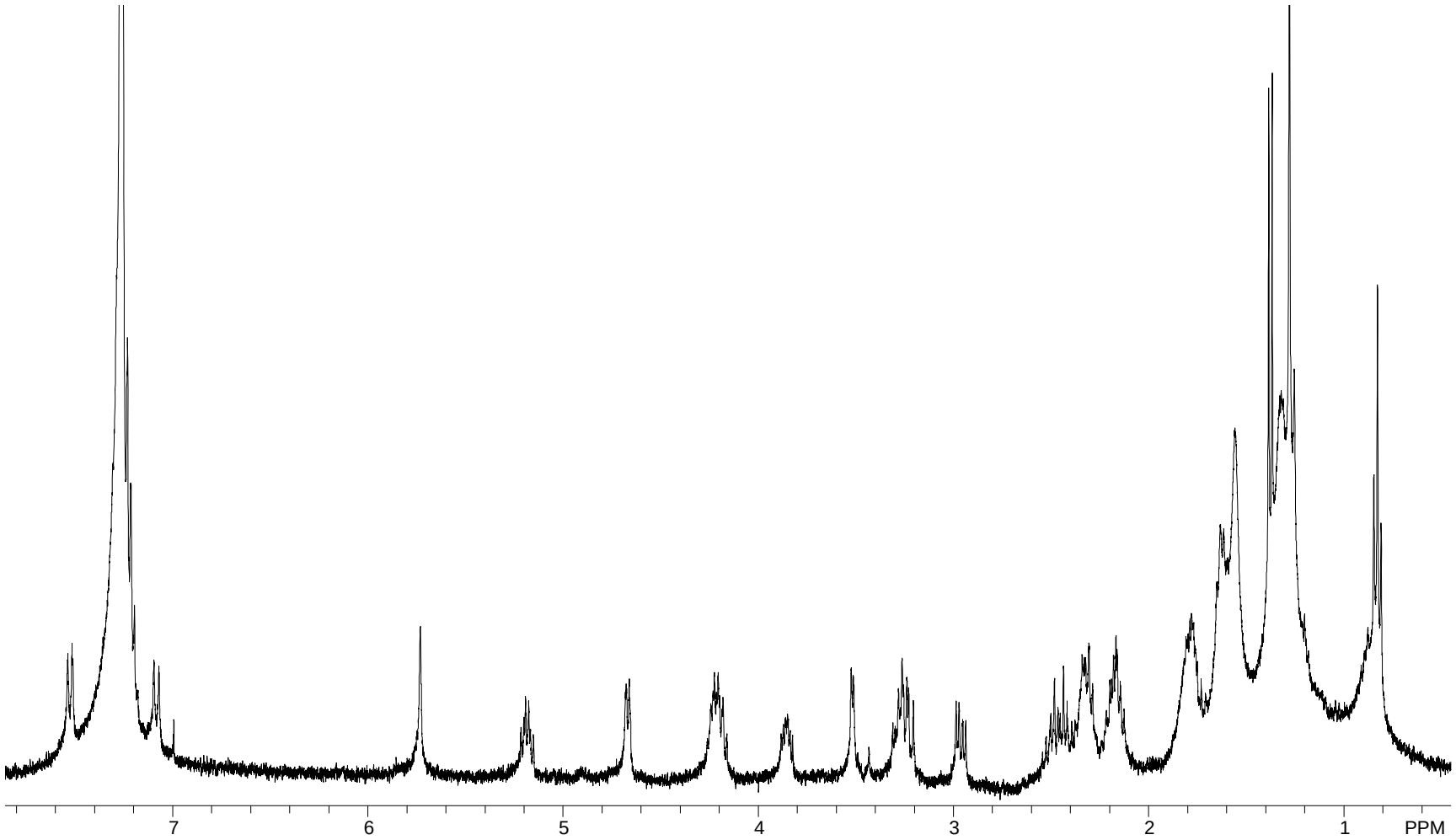

Figure A21. ^{1}H NMR Spectrum (400 MHz) of *cyclo*[-L-Asu-Aib-L-Phe-D-Pro-] (**3.6**) in $CDCl_3$

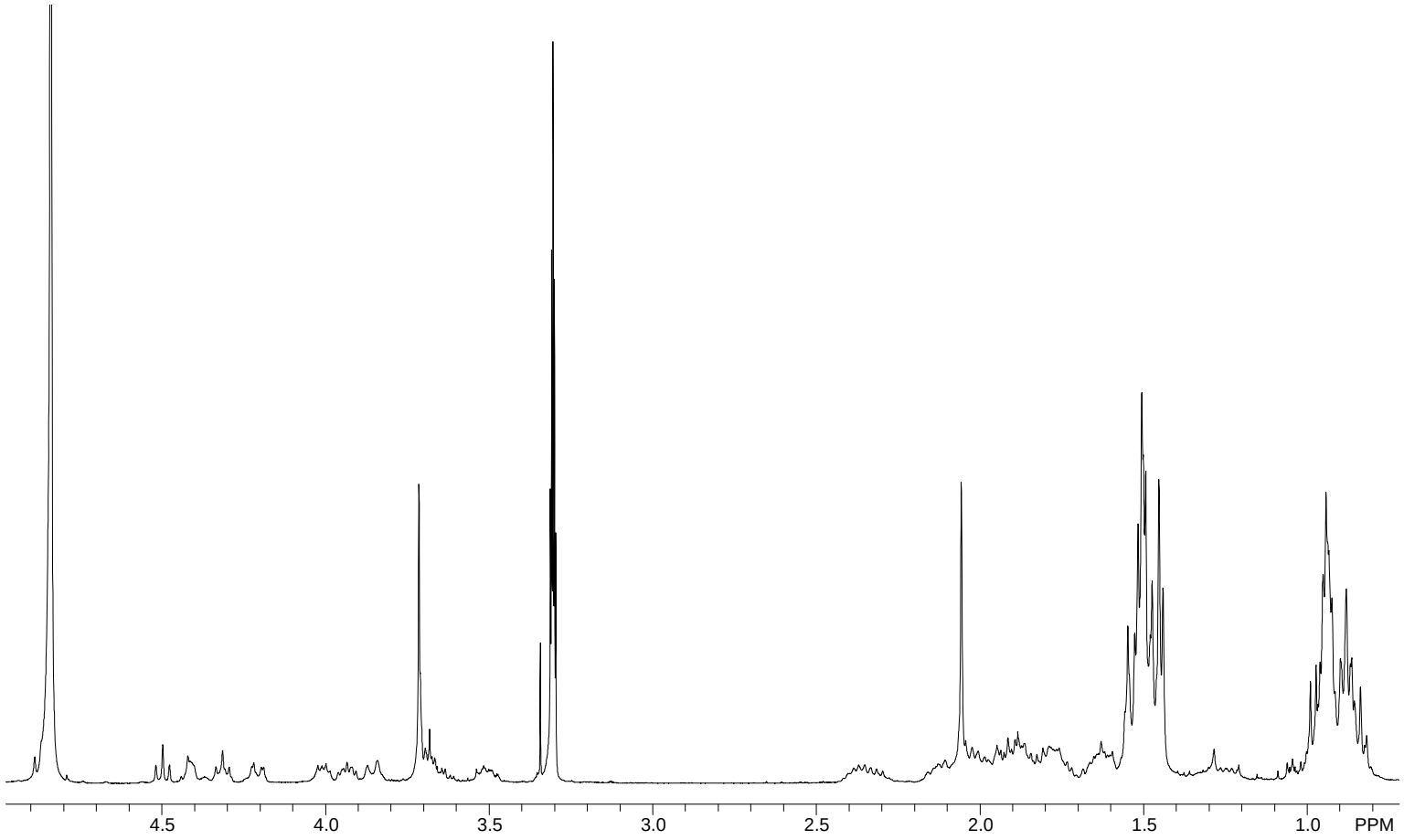

Figure A22. ^{1}H NMR Spectrum (400 MHz) of Bionectrin A Methylation Product (**3.7**) in CD_3OD

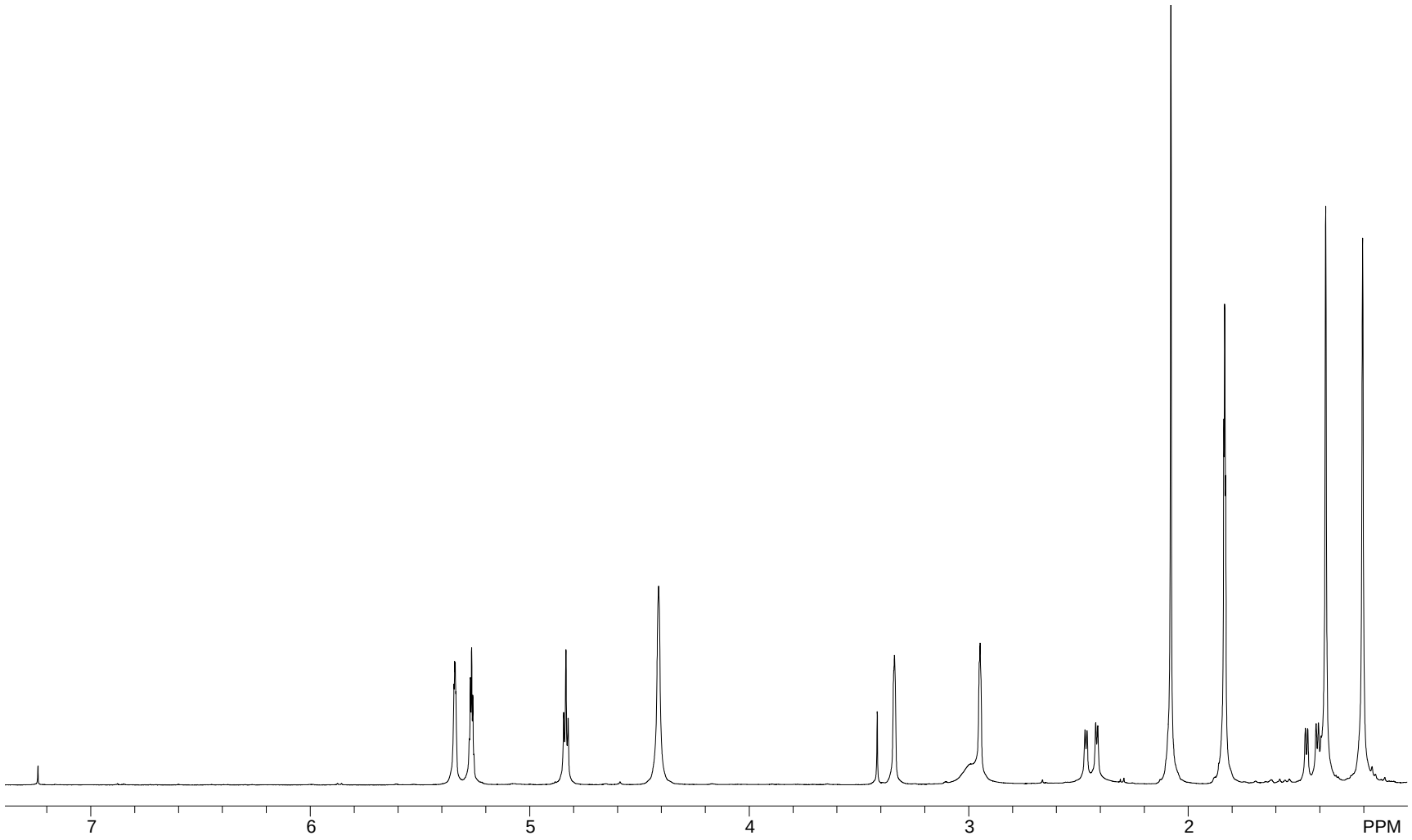

Figure A23. ^{1}H NMR Spectrum (400 MHz) of Dihydrooxirapentyne (**4.1**) in $CDCl_3$

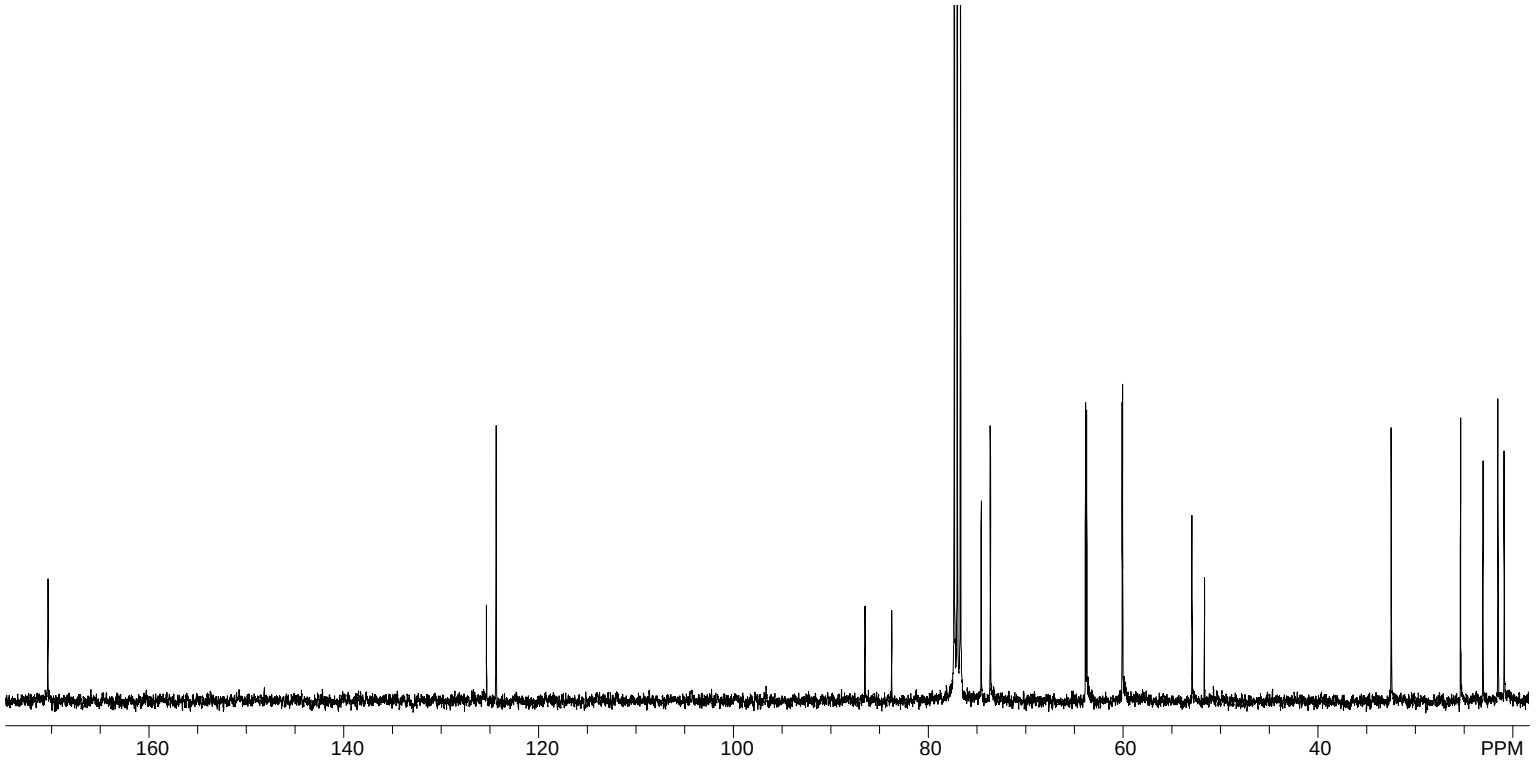

Figure A24. ^{13}C NMR Spectrum (100 MHz) of Dihydrooxirapentyne (**4.1**) in $CDCl_3$

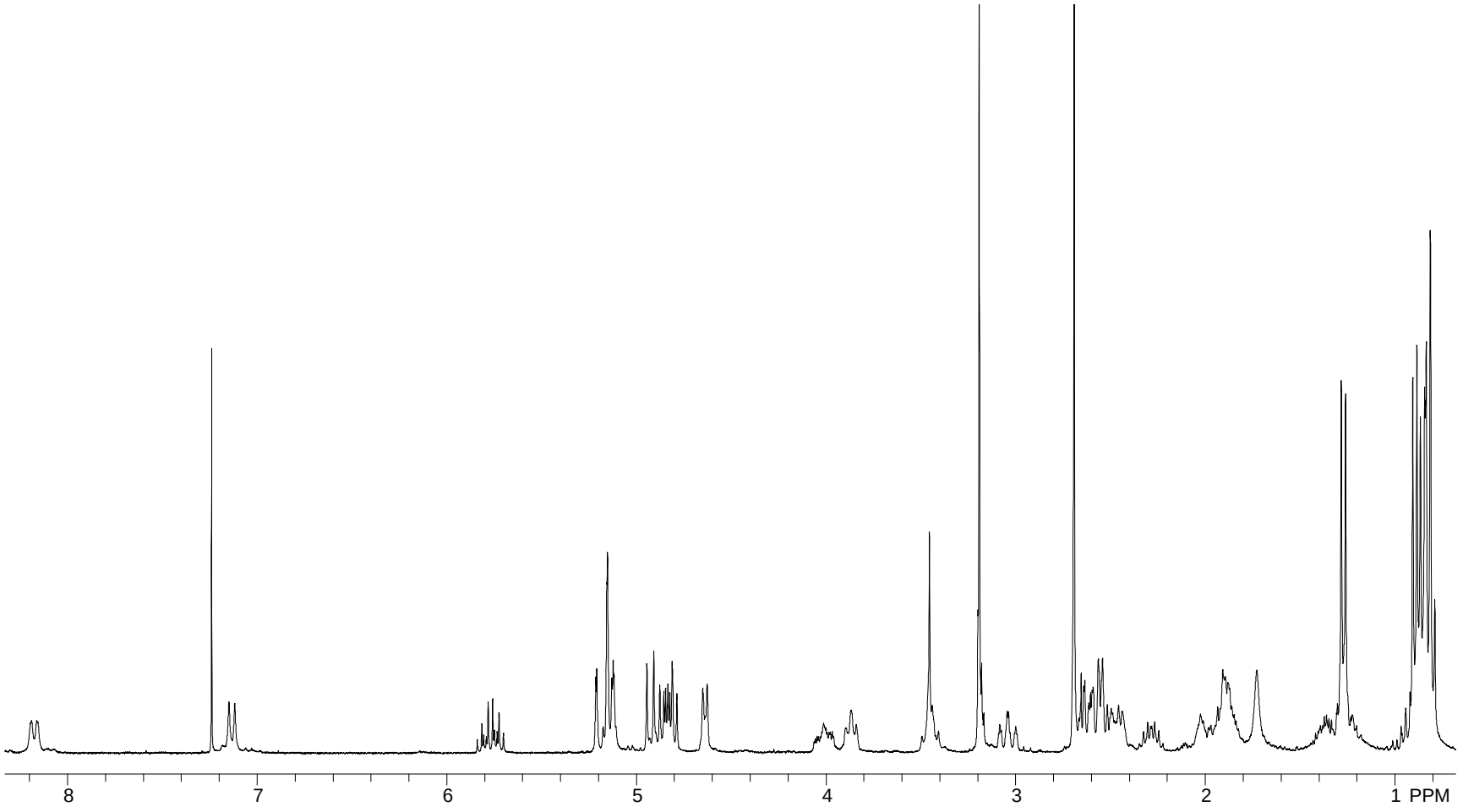

Figure A25. ^{1}H NMR Spectrum (400 MHz) of Destruxin A_4 (**4.2**) in $CDCl_3$

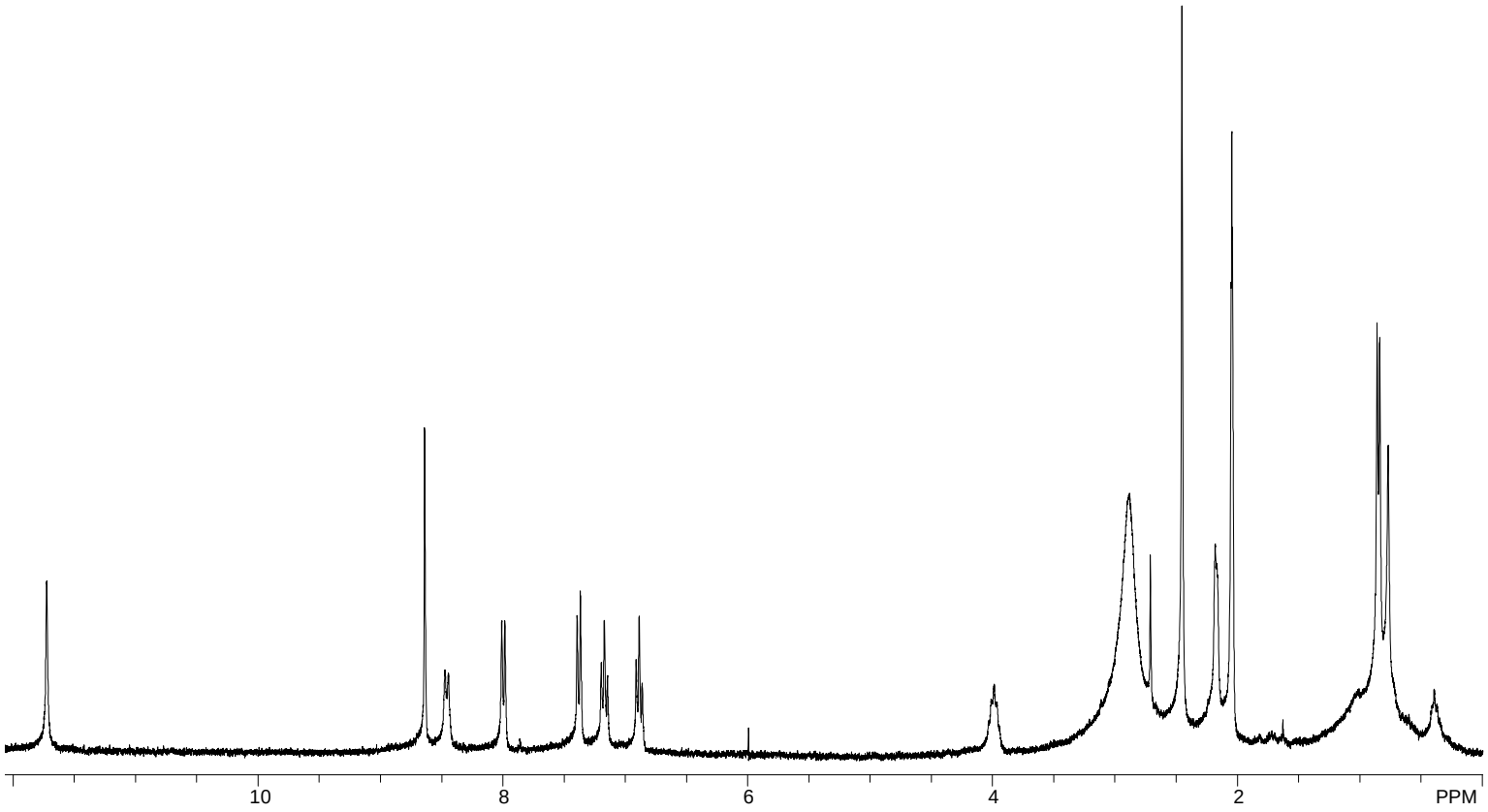

Figure A26. ^{1}H NMR Spectrum (400 MHz) of 1-Acetyl-9*H*-pyrido[3,4-*b*]indole-3-[*S*-(3)-aminobutyric acid]amide (**5.2**) in Acetone-d_6

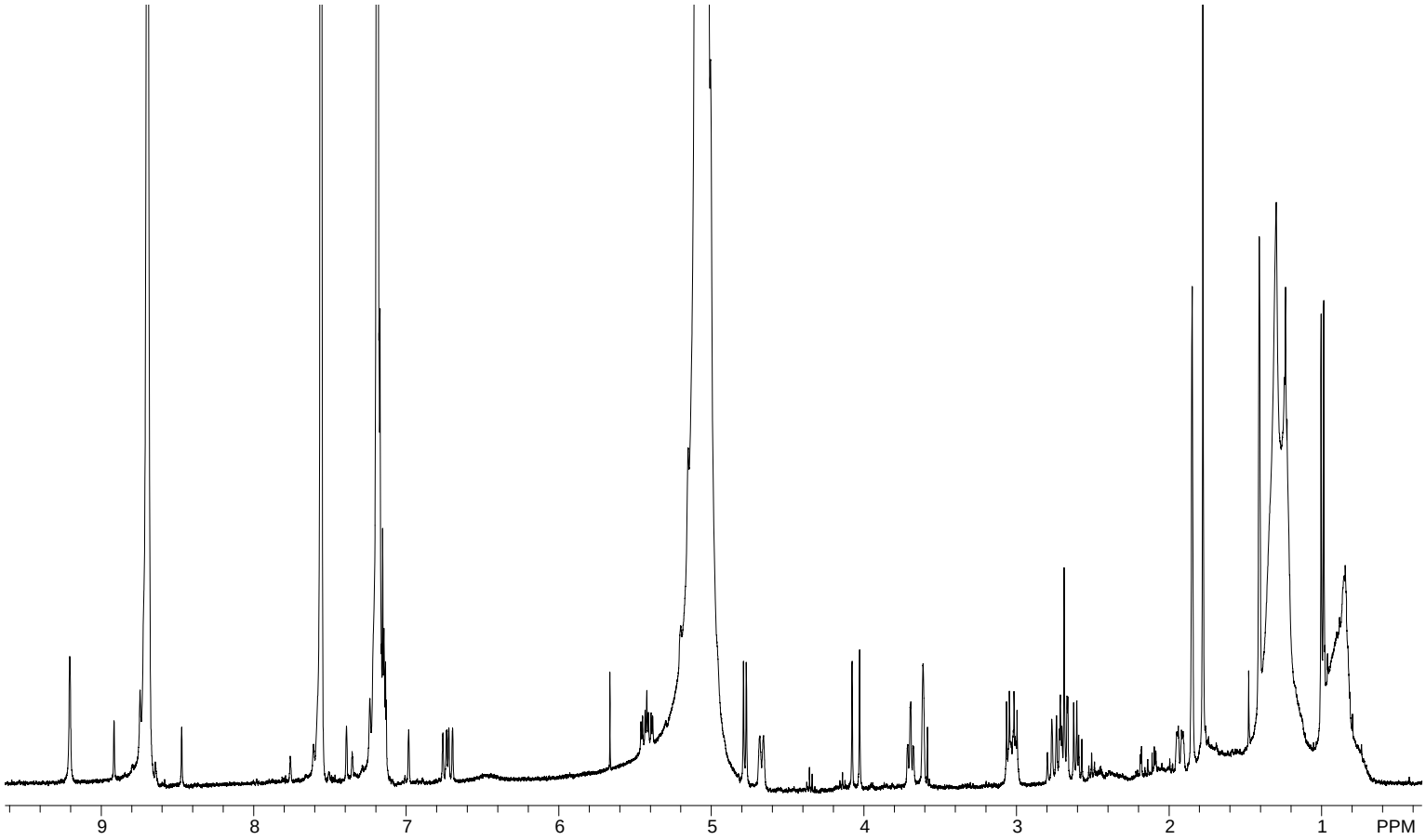

Figure A27. ^{1}H NMR Spectrum (400 MHz) of Cytochalasin Analogue (**5.4**) in Pyridine-d_5

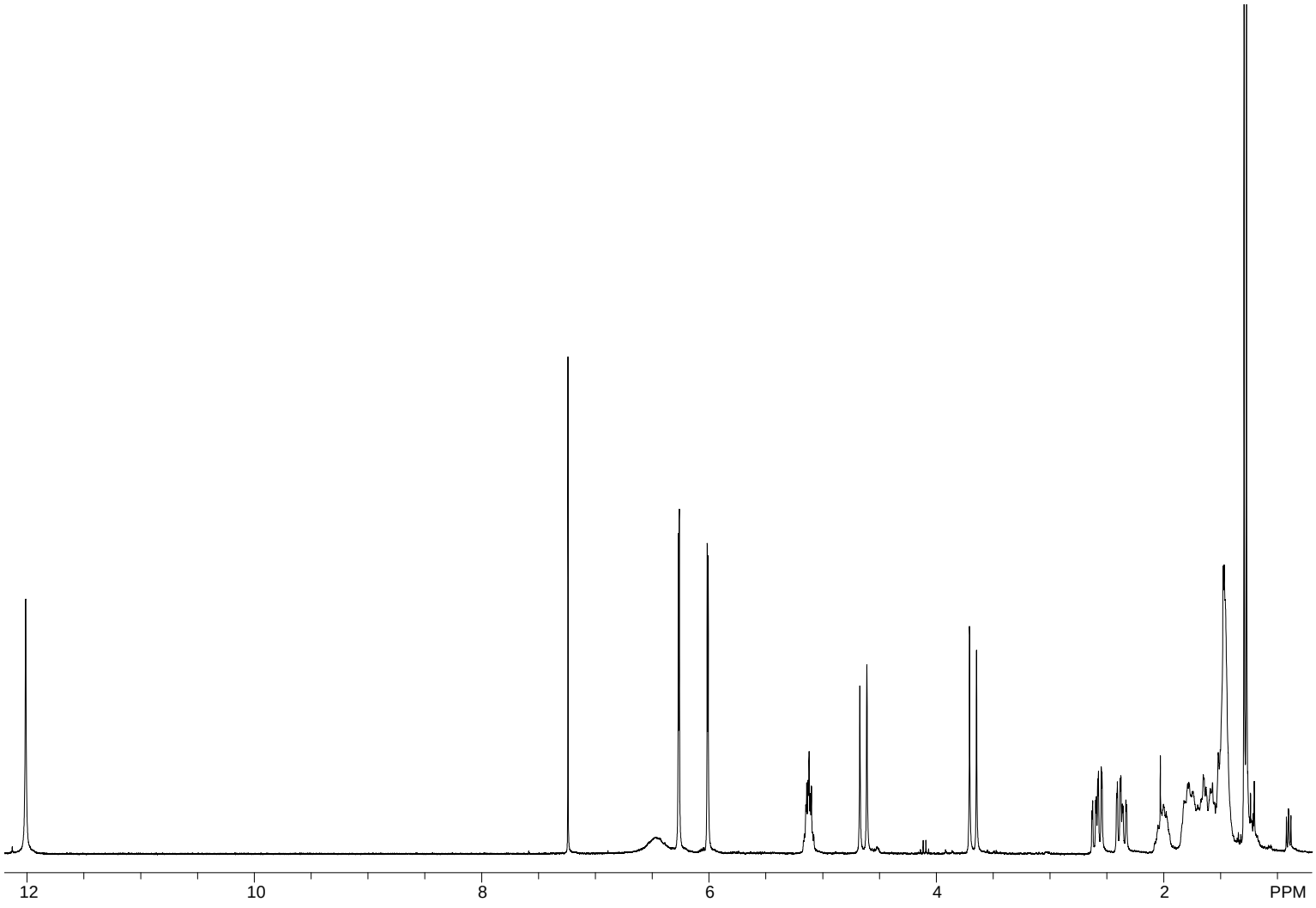

Figure A28. ^{1}H NMR Spectrum (300 MHz) of Dihydroresorcylide (**6.1**) in $CDCl_3$

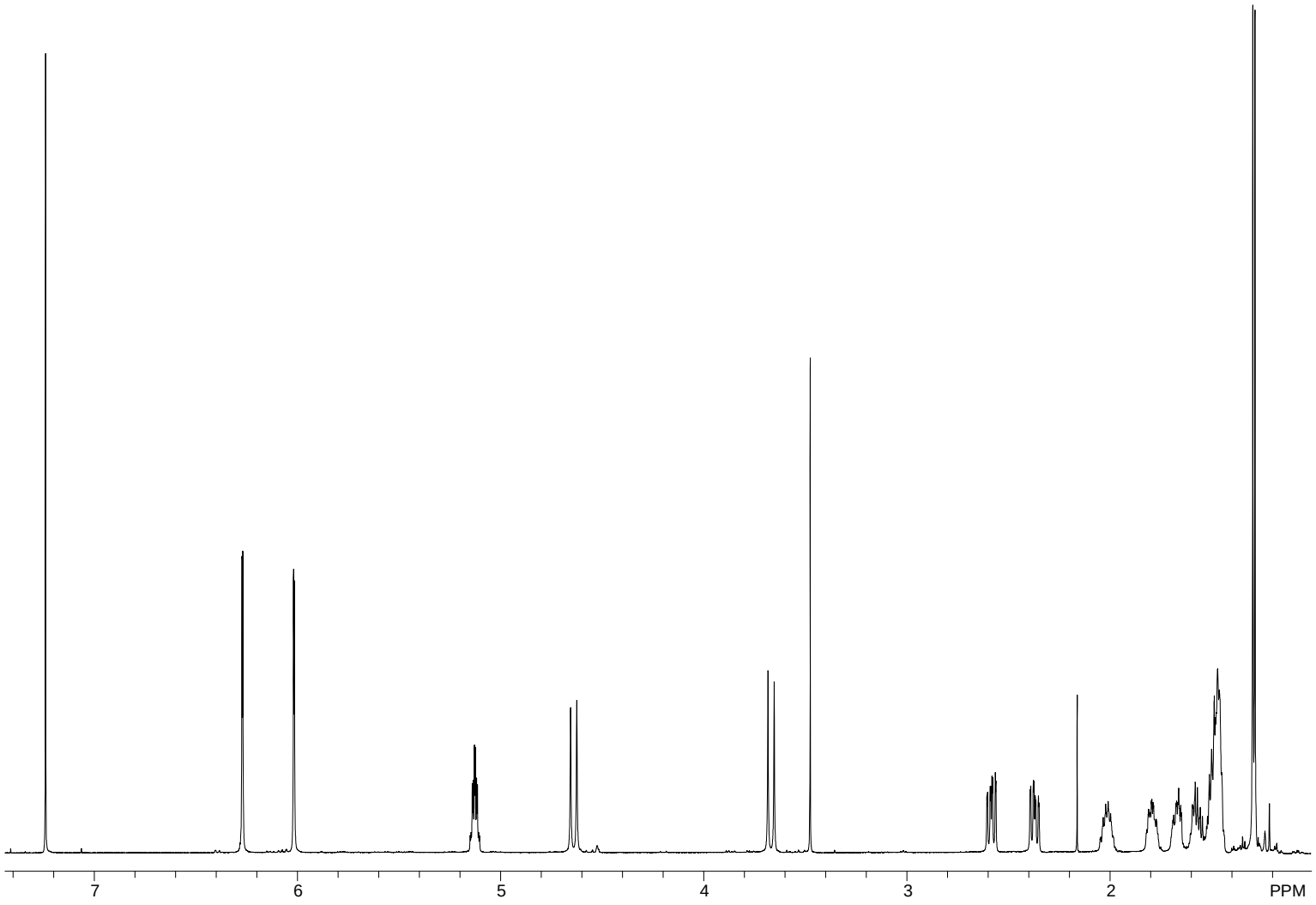

Figure A29. ^{1}H NMR Spectrum (600 MHz) of Dihydroresorcylide (**6.1**) in $CDCl_3$ (Singlet at δ 12.0 not shown)

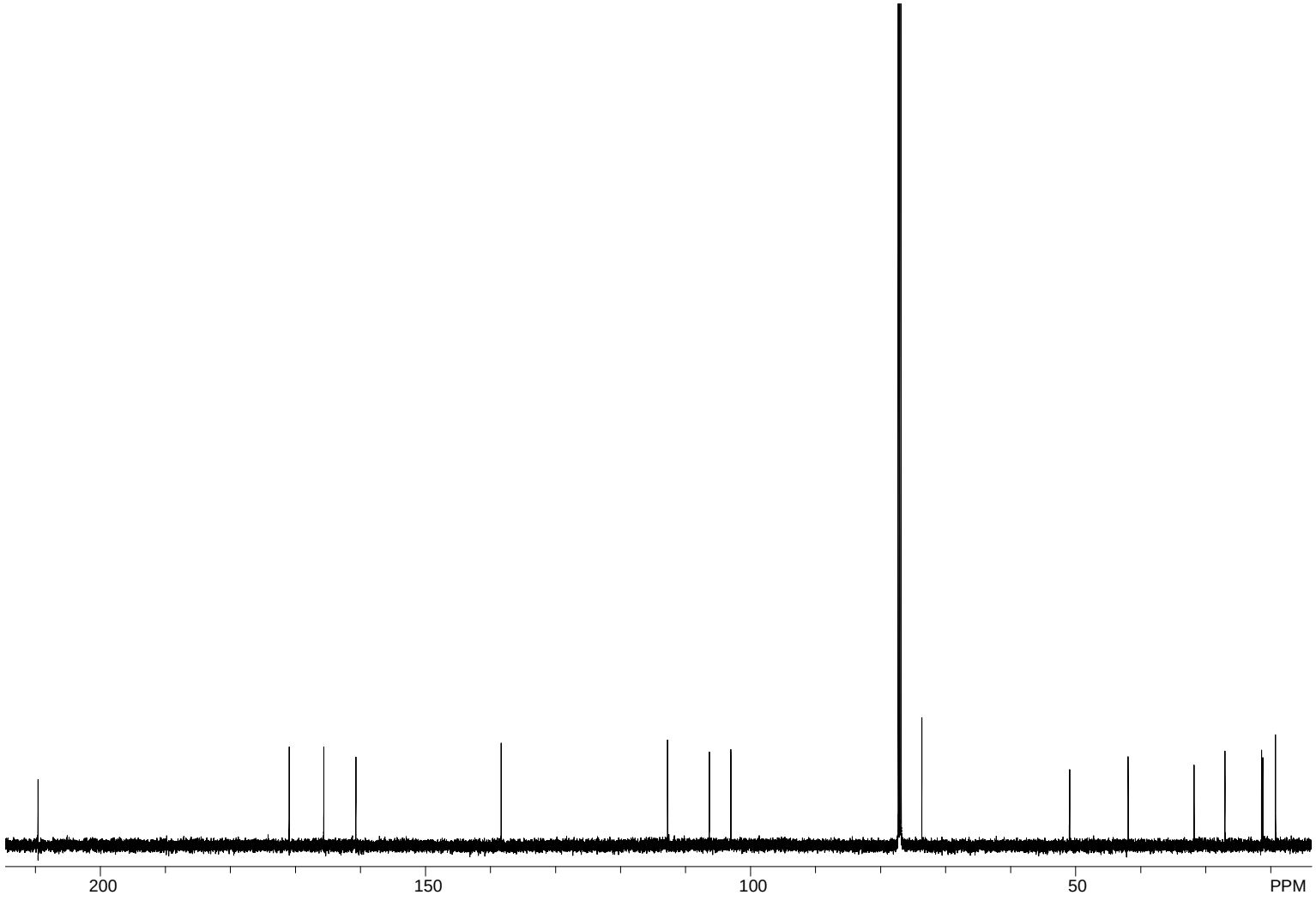

Figure A30. ^{13}C NMR Spectrum (75 MHz) of Dihydroresorcylide (**6.1**) in $CDCl_3$

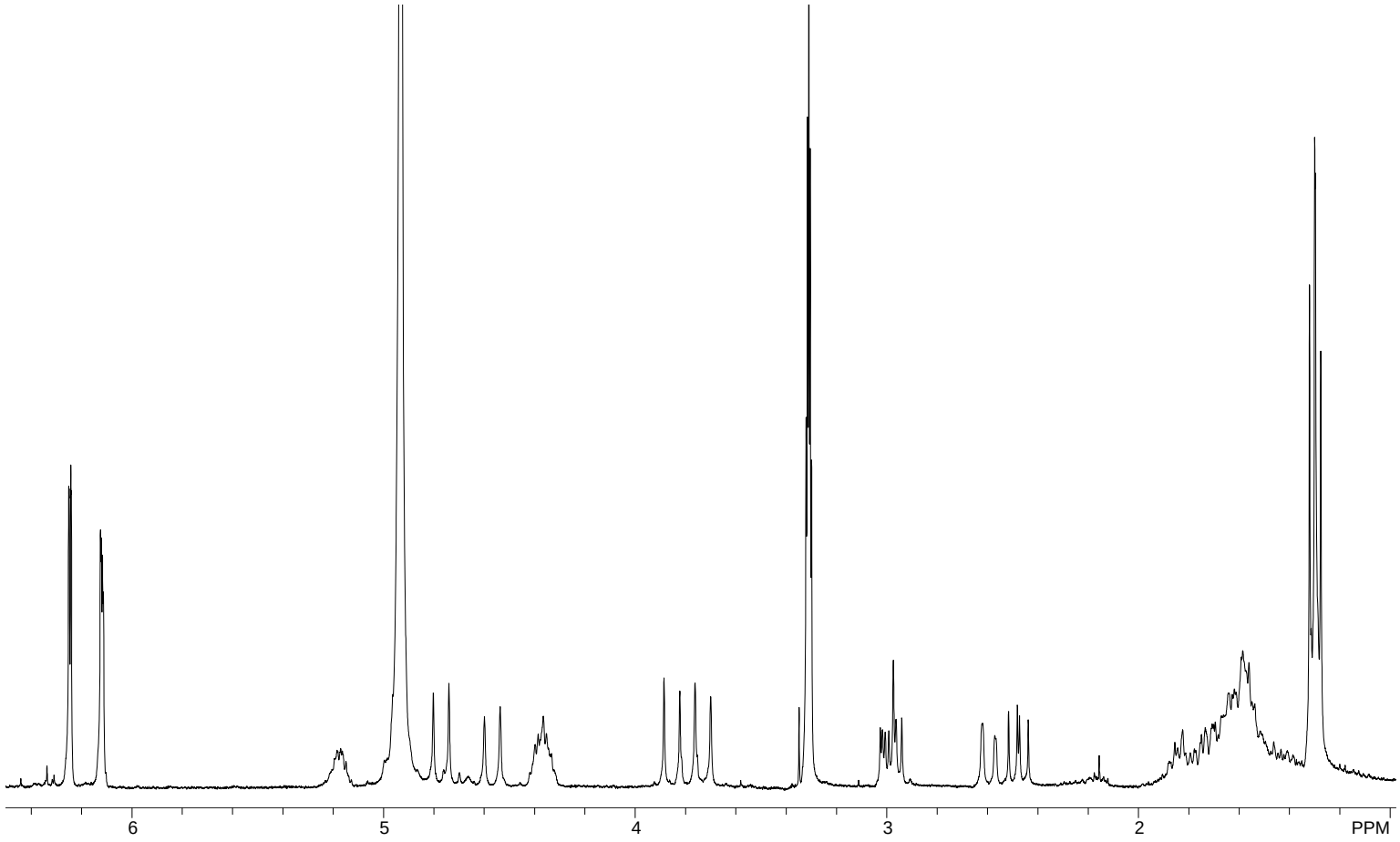

Figure A31. ^{1}H NMR Spectrum (400 MHz) of 7-(*R*)- and 7-(*S*)-Hydroxydihydroresorcylides Mixture (**6.3** and **6.4**) in CD_3OD

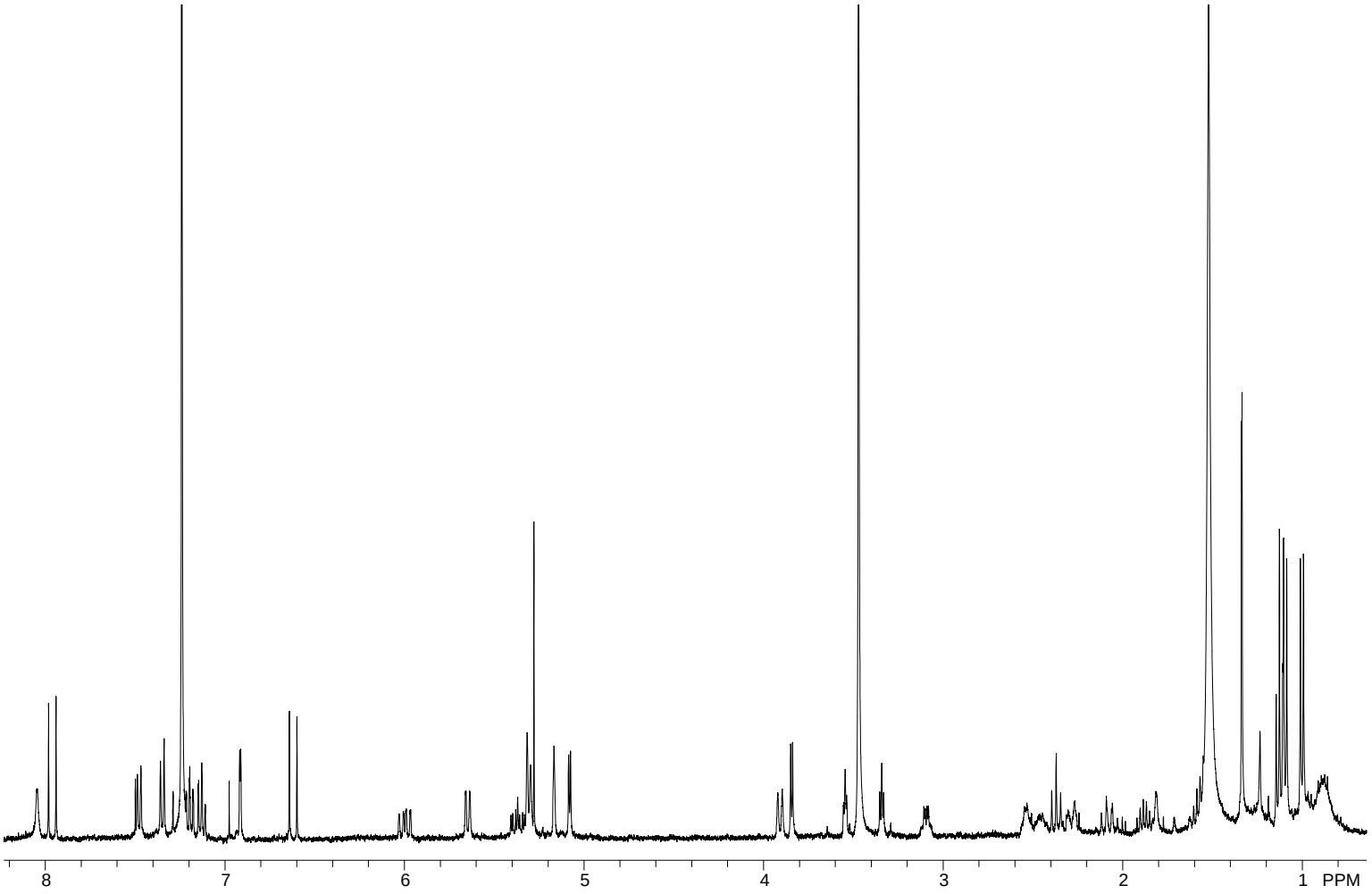

Figure A32. ^{1}H NMR Spectrum (400 MHz) of Chaetoglobosin L (**7.1**) in $CDCl_3$

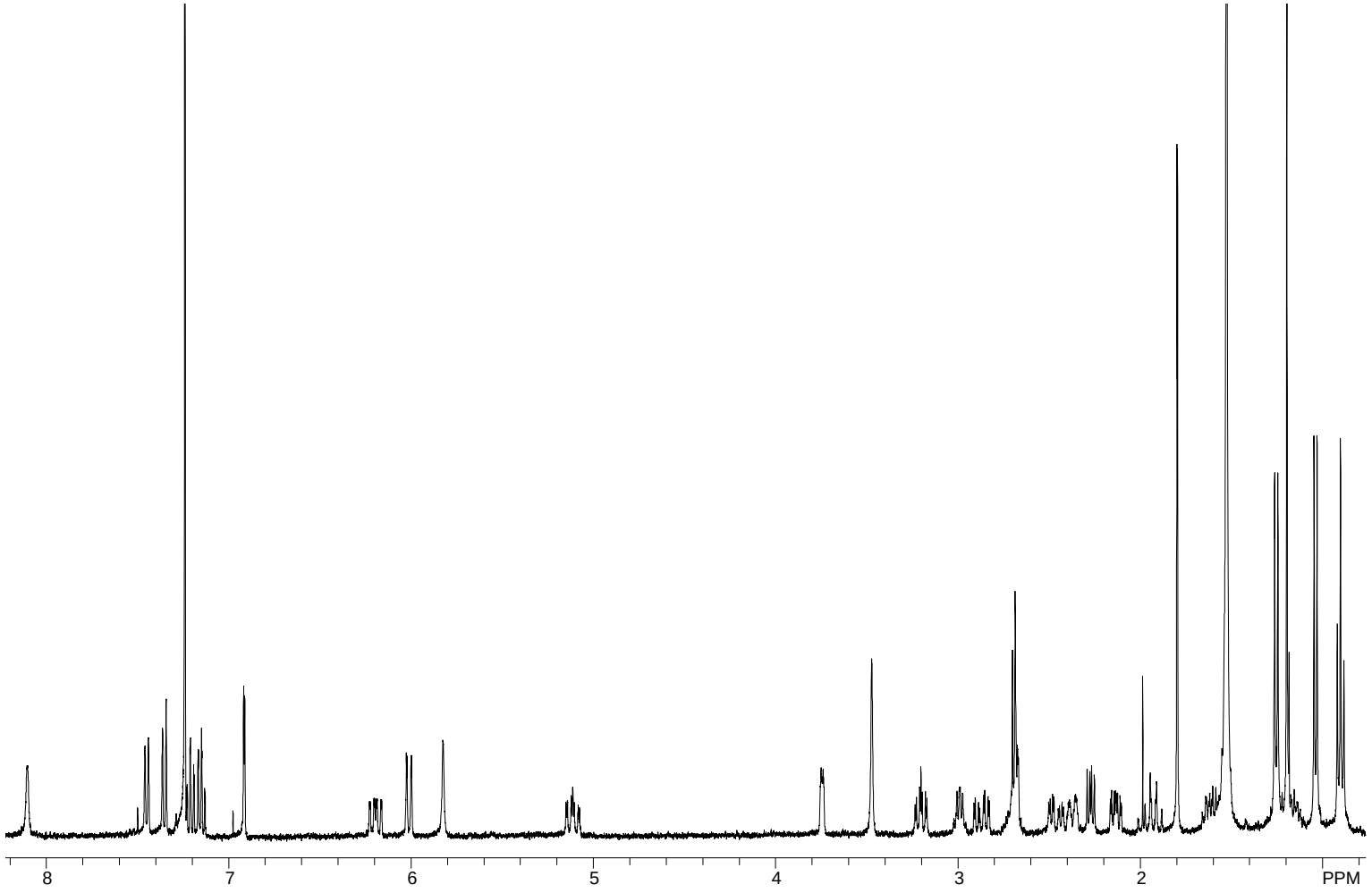

Figure A33. ^{1}H NMR Spectrum (400 MHz) of Chaetoglobosin M (**7.2**) in $CDCl_3$

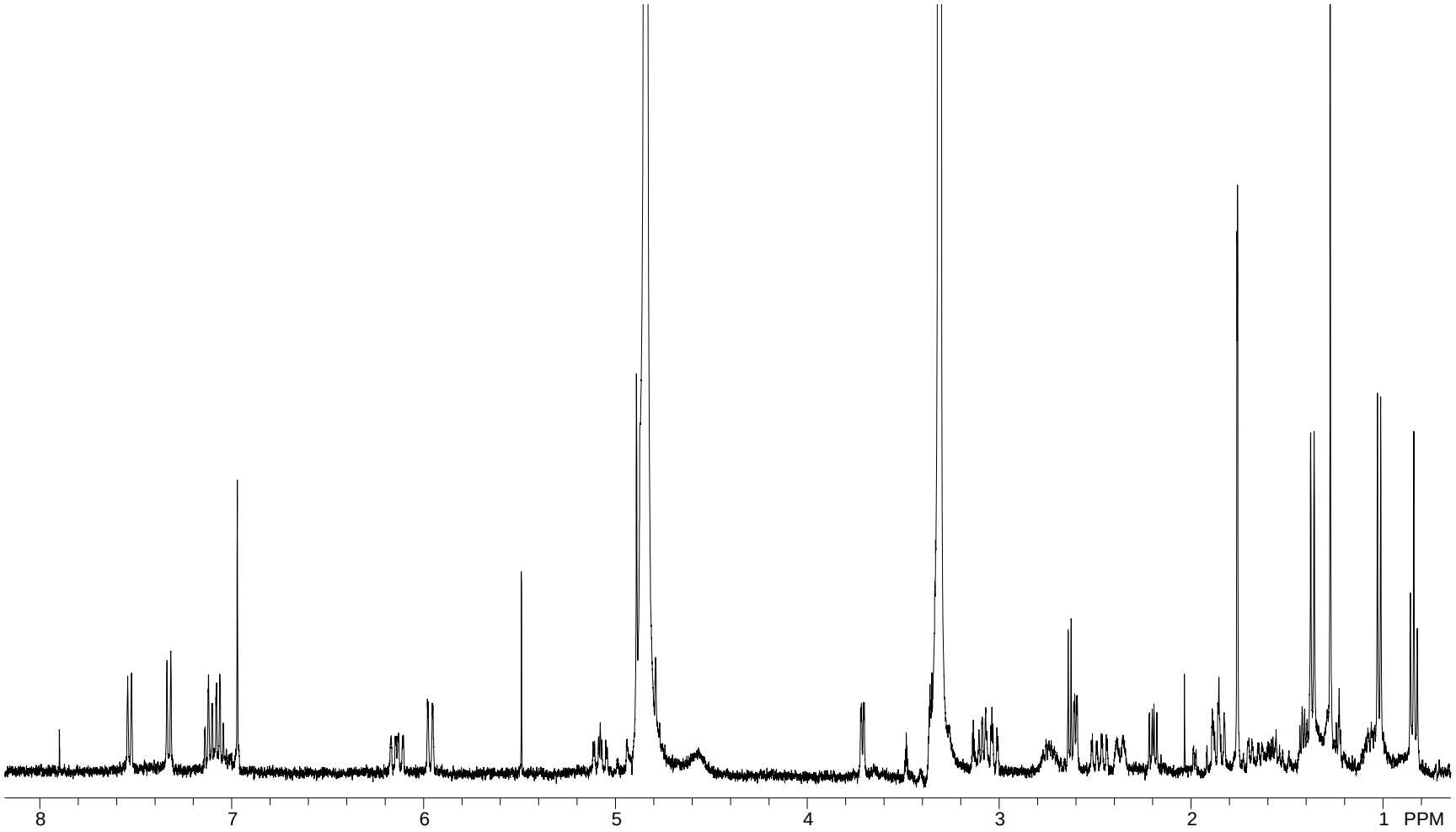

Figure A34. ^{1}H NMR Spectrum (400 MHz) of Chaetoglobosin M (**7.2**) in CD_3OD

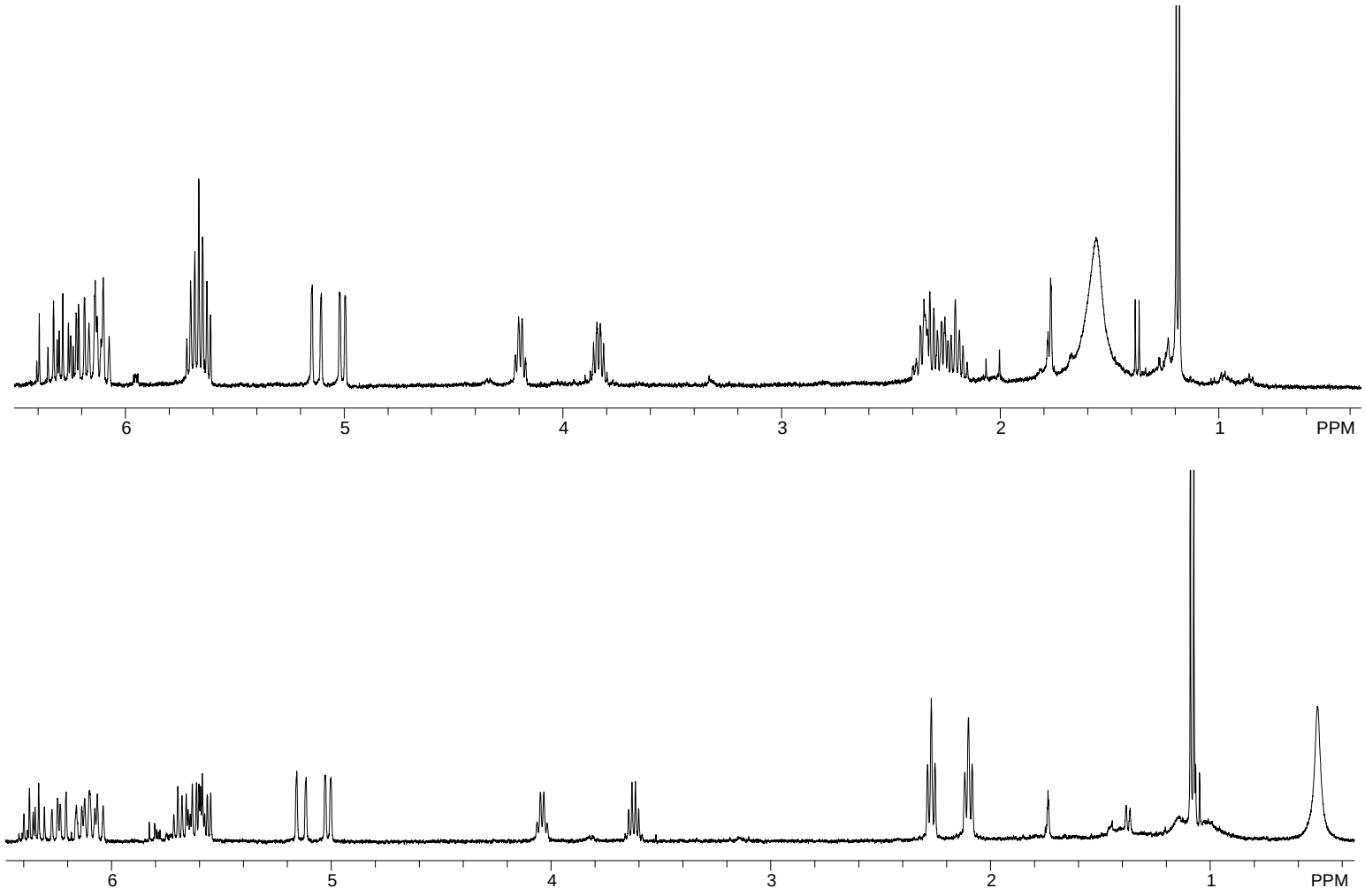

Figure A35. ^{1}H NMR Spectrum (400 MHz) of **7.4** in $CDCl_3$ (top) and C_6D_6 (bottom)

APPENDIX B

SELECTED SUPPLEMENTARY X-RAY DATA FOR THE *p*-BROMOBENZOATE DERIVATIVE OF DIHYDROOXIRAPENTYNE (**4.1**)

A colorless thin plate (0.20 x 0.11 x 0.01 mm) was isolated from the sample and mounted with paratone oil on the tip of a Mitegen polymeric mount and placed on the diffractometer with the long crystal dimension (unit cell body diagonal) approximately parallel to the diffractometer phi axis. Data were collected with a Nonius KappaCCD diffractometer (Mo K-alpha radiation, graphite monochromator) at 210(2) K (cold N_2 gas stream) using standard CCD techniques yielding 15872 data. Lorentz and polarization corrections were applied. A correction for absorption using the multi-scan technique was also applied (Tmax = 0.983, Tmin = 0.714). Equivalent data were averaged, yielding 2536 unique data (R-int = 0.078, 1507 F > 4*Sig(F), Friedel pairs not averaged). Based on a preliminary examination of the crystal, the space group P2(1) was assigned (no exceptions to the systematic absence: 0k0, k=odd were noted). The computer programs from the HKL package were used for data reduction. The preliminary model of the structure was obtained using XS, a direct methods program. Least-squares refining of the model vs. the data was performed with the XL computer program. Illustrations were made with the XP program and tables were made with the XCIF program. All of these programs are included in the SHELXTL v6.1 package. Thermal ellipsoids shown in the illustration are at the 50% level. All non-hydrogen atoms were refined with anisotropic thermal parameters. All hydrogen atoms were included with the riding model using the XL program default values. Several low angle reflections were omitted from refinement due to beam-stop shadowing effects. Data above 21 degrees theta were excluded from the final cycles of refinement as <5% of reflections were above background levels. The bromobenzoyl moiety showed high thermal motion and was modeled with two sites of half occupancy having the benzene rings as rigid groups. Half-atoms (C2', C2"; C3', C3"; etc) were constrained to have the same anisotropic displacement parameters, the groups with C1' were restrained to be flat, C-Br bonds were restrained to be the same, and C1'-C2(',") bonds were restrained to be the same. No further restraints or constraints were imposed on the refinement model.

Table B1. Crystal data and structure refinement for *p*-bromobenzoate derivative of dihydrooxirapentyne (**4.1**)

Identification code	dihydrooxirapentyne
Empirical formula	C25 H25 Br O7
Formula weight	517.36
Temperature	210(2) K
Wavelength	0.71073 A
Crystal system, space group	Monoclinic, P 21
Unit cell dimensions	a = 11.752(3) A alpha = 90 deg.
	b = 6.7809(18) A beta = 104.484(11) deg.
	c = 15.477(3) A gamma = 90 deg.
Volume	1194.1(5) A^3
Z, Calculated density	2, 1.439 Mg/m^3
Absorption coefficient	1.764 mm^-1
F(000)	532
Crystal size	0.20 x 0.11 x 0.01 mm
Theta range for data collection	2.50 to 21.00 deg.
Limiting indices	-11<=h<=11, -6<=k<=6, -15<=l<=15
Reflections collected / unique	15872 / 2536 [R(int) = 0.0782]
Completeness to theta = 21.00	99.8 %
Absorption correction	Semi-empirical from equivalents
Max. and min. transmission	0.9826 and 0.7138
Refinement method	Full-matrix least-squares on F^2
Data / restraints / parameters	2536 / 21 / 300
Goodness-of-fit on F^2	1.068
Final R indices [I>2sigma(I)]	R1 = 0.0594, wR2 = 0.1168
R indices (all data)	R1 = 0.1169, wR2 = 0.1416
Absolute structure parameter	0.05(2)
Largest diff. peak and hole	0.300 and -0.265 e.A^-3

Table B2. Atomic coordinates (x 10^4) and equivalent isotropic displacement parameters (A^2 x 10^3) for *p*-bromobenzoate derivative of dihydrooxirapentyne (**4.1**). U(eq) is defined as one third of the trace of the orthogonalized Uij tensor.

	x	y	z	U(eq)
C(2')	4620(16)	3870(20)	1454(5)	78(3)
C(3')	5200(30)	4410(30)	811(8)	66(5)
C(4')	4620(40)	4330(40)	-88(6)	83(7)
C(5')	3460(40)	3710(60)	-345(9)	98(5)
C(6')	2870(30)	3170(70)	299(16)	92(7)
C(7')	3456(18)	3250(50)	1198(14)	92(6)
Br(1')	2670(60)	3590(90)	-1547(12)	146(5)
C(2")	4659(16)	3800(20)	1449(5)	78(3)
C(3")	5330(30)	3760(30)	824(8)	66(5)
C(4")	4780(40)	3650(40)	-80(6)	83(7)
C(5")	3560(40)	3580(60)	-360(8)	98(5)
C(6")	2890(30)	3620(80)	265(16)	92(7)
C(7")	3439(17)	3730(60)	1170(14)	92(6)
Br(1")	2810(60)	3340(90)	-1567(12)	146(5)
C(1')	5205(12)	3916(13)	2431(7)	77(3)
O(1')	4647(7)	3749(17)	2995(5)	105(3)
O(1)	6364(6)	4025(11)	2595(4)	77(2)
C(1)	7018(9)	3792(19)	3520(5)	75(3)
C(2)	7360(12)	5809(19)	3922(6)	80(4)
O(2)	8107(7)	5706(13)	4815(4)	98(3)
C(3)	8631(12)	6350(20)	4122(7)	92(4)
C(4)	9543(11)	5149(19)	3890(7)	79(3)
O(4)	9869(7)	6213(11)	3174(4)	80(2)
C(5)	9262(11)	3086(19)	3606(6)	81(4)
O(5)	8825(7)	1908(13)	4270(5)	98(3)
C(6)	8016(12	2434(18)	3443(6)	85(4)
C(7)	10839(11)	5382(18)	2867(8)	78(3)
C(8)	10482(8)	3340(20)	2534(5)	82(3)
O(8)	9478(5)	3430(14)	1766(4)	88(2)
C(9)	10120(11)	1989(18)	3218(7)	89(4)
C(10)	6419(13)	7260(20)	3756(8)	87(4)
C(11)	5594(17)	8240(30)	3648(10)	124(5)
C(12)	4500(20)	9300(20)	3478(15)	145(7)
C(13)	3830(12)	9280(20)	2650(12)	132(6)
C(14)	4185(16)	10180(30)	4192(12)	185(9)
C(15)	10921(10)	6771(18)	2130(7)	104(4)
C(16)	11950(9)	5350(20)	3618(7)	110(5)
C(17)	9595(12)	2847(18)	968(9)	93(4)
O(17)	10448(10)	2096(17)	878(6)	146(4)
C(18)	8524(9)	3190(20)	250(6)	102(4)

Table B3. Bond lengths [Å] and angles [deg] for *p*-bromobenzoate derivative of dihydrooxirapentyne (**4.1**)

C(2')-C(3')	1.39	C(3)-H(3)	0.99
C(2')-C(7')	1.39	C(4)-O(4)	1.453(13)
C(2')-C(1')	1.497(11)	C(4)-C(5)	1.479(16)
C(3')-C(4')	1.39	C(4)-H(4)	0.99
C(3')-H(3')	0.94	O(4)-C(7)	1.453(13)
C(4')-C(5')	1.39	C(5)-O(5)	1.490(13)
C(4')-H(4')	0.94	C(5)-C(6)	1.490(15)
C(5')-C(6')	1.39	C(5)-C(9)	1.495(16)
C(5')-Br(1')	1.863(6)	O(5)-C(6)	1.435(11)
C(6')-C(7')	1.39	C(6)-H(6)	0.99
C(6')-H(6')	0.94	C(7)-C(8)	1.502(16)
C(7')-H(7')	0.94	C(7)-C(15)	1.501(15)
C(2")-C(3")	1.39	C(7)-C(16)	1.517(13)
C(2")-C(7")	1.39	C(8)-O(8)	1.452(8)
C(2")-C(1')	1.497(11)	C(8)-C(9)	1.537(15)
C(3")-C(4")	1.39	C(8)-H(8)	0.99
C(3")-H(3")	0.94	O(8)-C(17)	1.336(14)
C(4")-C(5")	1.39	C(9)-H(9A)	0.98
C(4")-H(4")	0.94	C(9)-H(9B)	0.98
C(5")-C(6")	1.39	C(10)-C(11)	1.151(18)
C(5")-Br(1")	1.863(6)	C(11)-C(12)	1.44(2)
C(6")-C(7")	1.39	C(12)-C(13)	1.33(2)
C(6")-H(6")	0.94	C(12)-C(14)	1.39(2)
C(7")-H(7")	0.94	C(13)-H(13A)	0.94
C(1')-O(1')	1.221(12)	C(13)-H(13B)	0.94
C(1')-O(1)	1.323(12)	C(14)-H(14A)	0.97
O(1)-C(1)	1.453(9)	C(14)-H(14B)	0.97
C(1)-C(2)	1.515(16)	C(14)-H(14C)	0.97
C(1)-C(6)	1.519(14)	C(15)-H(15A)	0.97
C(1)-H(1)	0.99	C(15)-H(15B)	0.97
C(2)-O(2)	1.442(11)	C(15)-H(15C)	0.97
C(2)-C(10)	1.456(17)	C(16)-H(16A)	0.97
C(2)-C(3)	1.493(15)	C(16)-H(16B)	0.97
O(2)-C(3)	1.430(13)	C(16)-H(16C)	0.97
C(3)-C(4)	1.459(16)	C(17)-O(17)	1.164(13)

Table B3 – Continued

C(17)-C(18)	1.475(14)	C(6")-C(7")-C(2")	120
C(18)-H(18A)	0.97	C(6")-C(7")-H(7")	120
C(18)-H(18B)	0.97	C(2")-C(7")-H(7")	120
C(18)-H(18C)	0.97	O(1')-C(1')-O(1)	125.4(9)
C(3')-C(2')-C(7')	120	O(1')-C(1')-C(2')	121.8(13)
C(3')-C(2')-C(1')	122.3(8)	O(1)-C(1')-C(2')	112.7(12)
C(7')-C(2')-C(1')	117.7(8)	O(1')-C(1')-C(2")	123.4(13)
C(4')-C(3')-C(2')	120	O(1)-C(1')-C(2")	110.9(12)
C(4')-C(3')-H(3')	120	C(1')-O(1)-C(1)	116.6(8)
C(2')-C(3')-H(3')	120	O(1)-C(1)-C(2)	109.1(9)
C(5')-C(4')-C(3')	120	O(1)-C(1)-C(6)	102.6(8)
C(5')-C(4')-H(4')	120	C(2)-C(1)-C(6)	116.6(10)
C(3')-C(4')-H(4')	120	O(1)-C(1)-H(1)	109.4
C(4')-C(5')-C(6')	120	C(2)-C(1)-H(1)	109.4
C(4')-C(5')-Br(1')	120.5(4)	C(6)-C(1)-H(1)	109.4
C(6')-C(5')-Br(1')	119.5(4)	O(2)-C(2)-C(10)	117.1(10)
C(7')-C(6')-C(5')	120	O(2)-C(2)-C(3)	58.3(6)
C(7')-C(6')-H(6')	120	C(10)-C(2)-C(3)	123.3(11)
C(5')-C(6')-H(6')	120	O(2)-C(2)-C(1)	112.7(10)
C(6')-C(7')-C(2')	120	C(10)-C(2)-C(1)	115.2(10)
C(6')-C(7')-H(7')	120	C(3)-C(2)-C(1)	117.0(12)
C(2')-C(7')-H(7')	120	C(3)-O(2)-C(2)	62.6(7)
C(3")-C(2")-C(7")	120	O(2)-C(3)-C(4)	119.8(11)
C(3")-C(2")-C(1')	122.3(8)	O(2)-C(3)-C(2)	59.1(7)
C(7")-C(2")-C(1')	117.7(8)	C(4)-C(3)-C(2)	124.9(11)
C(2")-C(3")-C(4")	120	O(2)-C(3)-H(3)	114
C(2")-C(3")-H(3")	120	C(4)-C(3)-H(3)	114
C(4")-C(3")-H(3")	120	C(2)-C(3)-H(3)	114
C(5")-C(4")-C(3")	120	O(4)-C(4)-C(3)	105.2(10)
C(5")-C(4")-H(4")	120	O(4)-C(4)-C(5)	108.9(10)
C(3")-C(4")-H(4")	120	C(3)-C(4)-C(5)	118.4(12)
C(4")-C(5")-C(6")	120	O(4)-C(4)-H(4)	108
C(4")-C(5")-Br(1")	120.5(4)	C(3)-C(4)-H(4)	108
C(6")-C(5")-Br(1")	119.4(4)	C(5)-C(4)-H(4)	108
C(5")-C(6")-C(7")	120	C(4)-O(4)-C(7)	115.8(8)
C(5")-C(6")-H(6")	120	C(4)-C(5)-O(5)	113.1(11)
C(7")-C(6")-H(6")	120	C(4)-C(5)-C(6)	117.9(12)

Table B3 – Continued

O(5)-C(5)-C(6)	57.6(7)	H(13A)-C(13)-H(13B)	120
C(4)-C(5)-C(9)	117.9(12)	C(12)-C(14)-H(14A)	109.5
O(5)-C(5)-C(9)	113.2(10)	C(12)-C(14)-H(14B)	109.5
C(6)-C(5)-C(9)	121.2(11)	H(14A)-C(14)-H(14B)	109.5
C(6)-O(5)-C(5)	61.2(6)	C(12)-C(14)-H(14C)	109.5
O(5)-C(6)-C(5)	61.2(6)	H(14A)-C(14)-H(14C)	109.5
O(5)-C(6)-C(1)	115.7(9)	H(14B)-C(14)-H(14C)	109.5
C(5)-C(6)-C(1)	123.6(11)	C(7)-C(15)-H(15A)	109.5
O(5)-C(6)-H(6)	115.1	C(7)-C(15)-H(15B)	109.5
C(5)-C(6)-H(6)	115.1	H(15A)-C(15)-H(15B)	109.5
C(1)-C(6)-H(6)	115.1	C(7)-C(15)-H(15C)	109.5
O(4)-C(7)-C(8)	107.2(9)	H(15A)-C(15)-H(15C)	109.5
O(4)-C(7)-C(15)	102.1(9)	H(15B)-C(15)-H(15C)	109.5
C(8)-C(7)-C(15)	112.6(10)	C(7)-C(16)-H(16A)	109.5
O(4)-C(7)-C(16)	110.5(9)	C(7)-C(16)-H(16B)	109.5
C(8)-C(7)-C(16)	111.4(10)	H(16A)-C(16)-H(16B)	109.5
C(15)-C(7)-C(16)	112.6(10)	C(7)-C(16)-H(16C)	109.5
O(8)-C(8)-C(7)	109.9(10)	H(16A)-C(16)-H(16C)	109.5
O(8)-C(8)-C(9)	106.3(9)	H(16B)-C(16)-H(16C)	109.5
C(7)-C(8)-C(9)	114.5(9)	O(17)-C(17)-O(8)	122.1(12)
O(8)-C(8)-H(8)	108.6	O(17)-C(17)-C(18)	125.3(14)
C(7)-C(8)-H(8)	108.6	O(8)-C(17)-C(18)	112.6(11)
C(9)-C(8)-H(8)	108.6	C(17)-C(18)-H(18A)	109.5
C(17)-O(8)-C(8)	119.6(8)	C(17)-C(18)-H(18B)	109.5
C(5)-C(9)-C(8)	108.1(10)	H(18A)-C(18)-H(18B)	109.5
C(5)-C(9)-H(9A)	110.1	C(17)-C(18)-H(18C)	109.5
C(8)-C(9)-H(9A)	110.1	H(18A)-C(18)-H(18C)	109.5
C(5)-C(9)-H(9B)	110.1	H(18B)-C(18)-H(18C)	109.5
C(8)-C(9)-H(9B)	110.1		
H(9A)-C(9)-H(9B)	108.4		
C(11)-C(10)-C(2)	172.0(15)		
C(10)-C(11)-C(12)	174.8(17)		
C(13)-C(12)-C(14)	124(2)		
C(13)-C(12)-C(11)	117.3(18)		
C(14)-C(12)-C(11)	118.5(19)		
C(12)-C(13)-H(13A)	120		
C(12)-C(13)-H(13B)	120		

Table B4. Anisotropic displacement parameters (A^2 x 10^3) for the *p*-bromobenzoate derivative of dihydrooxirapentyne (**4.1**). The anisotropic displacement factor exponent takes the form: $-2\pi^2$ [$h^2 a^{*2}$ U11 + ... + 2 h k a* b* U12]

	U11	U22	U33	U23	U13	U12
C(2')	78(8)	76(9)	67(6)	-2(7)	-4(6)	-9(7)
C(3')	109(10)	14(16)	71(7)	0(7)	12(7)	15(10)
C(4')	163(16)	20(20)	63(7)	16(7)	16(7)	33(17)
C(5')	124(12)	66(9)	82(7)	-8(9)	-20(7)	5(10)
C(6')	102(8)	59(19)	100(8)	-9(12)	-3(7)	-6(10)
C(7')	106(9)	70(16)	89(7)	-15(11)	4(7)	22(11)
Br(1')	206(11)	115(11)	77(1)	-4(2)	-38(3)	47(8)
C(2")	78(8)	76(9)	67(6)	-2(7)	-4(6)	-9(7)
C(3")	109(10)	14(16)	71(7)	0(7)	12(7)	15(10)
C(4")	163(16)	20(20)	63(7)	16(7)	16(7)	33(17)
C(5")	124(12)	66(9)	82(7)	-8(9)	-20(7)	5(10)
C(6")	102(8)	59(19)	100(8)	-9(12)	-3(7)	-6(10)
C(7")	106(9)	70(16)	89(7)	-15(11)	4(7)	22(11)
Br(1")	206(11)	115(11)	77(1)	-4(2)	-38(3)	47(8)
C(1')	88(9)	63(8)	74(8)	-12(7)	9(7)	-6(8)
O(1')	96(6)	135(8)	84(5)	-6(7)	24(4)	-24(7)
O(1)	78(5)	93(7)	52(3)	-5(4)	1(3)	2(5)
C(1)	90(8)	79(9)	49(5)	-5(7)	6(5)	-10(8)
C(2)	98(11)	98(10)	41(6)	-9(6)	9(6)	-28(9)
O(2)	100(6)	139(7)	56(4)	-20(5)	20(4)	-30(5)
C(3)	111(12)	107(10)	54(7)	-20(7)	13(8)	-27(9)
C(4)	75(9)	105(11)	58(7)	3(8)	16(6)	1(8)
O(4)	89(6)	88(5)	60(4)	0(4)	14(4)	8(5)
C(5)	95(10)	82(10)	54(6)	9(7)	-7(6)	-27(9)
O(5)	95(6)	120(7)	69(5)	19(5)	1(5)	2(5)
C(6)	115(11)	83(8)	44(6)	-3(5)	-4(7)	-10(9)
C(7)	78(9)	81(9)	75(8)	-3(7)	18(7)	-4(7)
C(8)	77(7)	112(10)	52(5)	11(9)	7(5)	21(9)
O(8)	108(5)	99(5)	54(3)	-4(6)	14(4)	17(6)
C(9)	90(9)	99(10)	70(8)	-6(8)	5(7)	34(8)
C(10)	97(11)	88(10)	88(8)	-3(8)	48(8)	-3(9)
C(11)	132(15)	93(12)	157(12)	-35(12)	58(12)	16(12)
C(12)	180(20)	72(11)	220(20)	12(13)	113(19)	-24(13)

Table B4. – Continued

C(13)	97(11)	103(12)	187(15)	-13(11)	18(10)	17(9)
C(14)	230(20)	143(16)	240(20)	25(15)	165(18)	53(14)
C(15)	109(10)	121(11)	85(8)	5(8)	31(7)	6(9)
C(16)	81(9)	160(13)	82(8)	-4(8)	4(7)	-4(8)
C(17)	93(10)	80(12)	107(10)	-7(7)	30(9)	11(7)
O(17)	155(10)	186(11)	99(6)	-45(6)	34(7)	43(8)
C(18)	122(9)	111(10)	60(5)	-7(8)	2(6)	-26(10)

Table B5. Hydrogen coordinates (x 10^4) and isotropic displacement parameters (A^2 x 10^3) for *p*-bromobenzoate derivative of dihydrooxirapentyne (**4.1**).

	x	y	z	U(eq)
H(3')	5990	4823	984	80
H(4')	5014	4690	-523	99
H(6')	2087	2756	125	111
H(7')	3063	2889	1633	110
H(3")	6151	3812	1013	80
H(4")	5227	3626	-503	99
H(6")	2064	3566	76	111
H(7")	2988	3752	1592	110
H(1)	6518	3117	3857	90
H(3)	8780	7782	4122	110
H(4)	10233	5133	4411	95
H(6)	7789	1342	3010	102
H(8)	11146	2717	2349	99
H(9A)	9759	780	2926	107
H(9B)	10813	1623	3690	107
H(13A)	3088	9888	2518	158
H(13B)	4096	8653	2195	158
H(14A)	3498	11006	3972	278
H(14B)	4830	10992	4522	278
H(14C)	4006	9175	4582	278
H(15A)	10165	6844	1698	155
H(15B)	11509	6294	1838	155
H(15C)	11142	8071	2376	155
H(16A)	11932	4232	4003	166
H(16B)	12002	6562	3962	166
H(16C)	12629	5251	3371	166
H(18A)	8266	1963	-56	152
H(18B)	8693	4141	-172	152
H(18C)	7909	3708	504	152

Table B6. Torsion Angles [deg] for *p*-bromobenzoate derivative of dihydrooxirapentyne

C(7')-C(2')-C(3')-C(4')	0
C(1')-C(2')-C(3')-C(4')	179.7(7)
C(2')-C(3')-C(4')-C(5')	0
C(3')-C(4')-C(5')-C(6')	0
C(3')-C(4')-C(5')-Br(1')	-180(2)
C(4')-C(5')-C(6')-C(7')	0
Br(1')-C(5')-C(6')-C(7')	179.8(19)
C(5')-C(6')-C(7')-C(2')	0
C(3')-C(2')-C(7')-C(6')	0
C(1')-C(2')-C(7')-C(6')	-179.7(7)
C(7")-C(2")-C(3")-C(4")	0
C(1')-C(2")-C(3")-C(4")	179.9(7)
C(2")-C(3")-C(4")-C(5")	0
C(3")-C(4")-C(5")-C(6")	0
C(3")-C(4")-C(5")-Br(1")	-178(2)
C(4")-C(5")-C(6")-C(7")	0
Br(1")-C(5")-C(6")-C(7")	177.8(19)
C(5")-C(6")-C(7")-C(2")	0
C(3")-C(2")-C(7")-C(6")	0
C(1')-C(2")-C(7")-C(6")	-179.9(7)
C(3')-C(2')-C(1')-O(1')	168.2(13)
C(7')-C(2')-C(1')-O(1')	-12.1(15)
C(3')-C(2')-C(1')-O(1)	-16.0(15)
C(7')-C(2')-C(1')-O(1)	163.8(14)
C(3')-C(2')-C(1')-C(2")	-63(32)
C(7')-C(2')-C(1')-C(2")	116(32)
C(3")-C(2")-C(1')-O(1')	-172.2(13)
C(7")-C(2")-C(1')-O(1')	7.7(15)
C(3")-C(2")-C(1')-O(1)	1.6(14)
C(7")-C(2")-C(1')-O(1)	-178.5(13)
C(3")-C(2")-C(1')-C(2')	135(32)
C(7")-C(2")-C(1')-C(2')	-45(32)
O(1')-C(1')-O(1)-C(1)	4.3(16)
C(2')-C(1')-O(1)-C(1)	-171.4(10)
C(2")-C(1')-O(1)-C(1)	-169.4(9)
C(1')-O(1)-C(1)-C(2)	-99.3(11)

Table B6. – Continued

C(1')-O(1)-C(1)-C(6)	136.4(9)
O(1)-C(1)-C(2)-O(2)	-174.5(9)
C(6)-C(1)-C(2)-O(2)	-59.0(13)
O(1)-C(1)-C(2)-C(10)	47.4(12)
C(6)-C(1)-C(2)-C(10)	163.0(9)
O(1)-C(1)-C(2)-C(3)	-109.8(10)
C(6)-C(1)-C(2)-C(3)	5.8(14)
C(10)-C(2)-O(2)-C(3)	-114.1(12)
C(1)-C(2)-O(2)-C(3)	108.7(13)
C(2)-O(2)-C(3)-C(4)	-115.2(12)
C(10)-C(2)-C(3)-O(2)	103.6(12)
C(1)-C(2)-C(3)-O(2)	-101.2(10)
O(2)-C(2)-C(3)-C(4)	106.7(13)
C(10)-C(2)-C(3)-C(4)	-149.7(12)
C(1)-C(2)-C(3)-C(4)	5.5(16)
O(2)-C(3)-C(4)-O(4)	179.8(9)
C(2)-C(3)-C(4)-O(4)	108.7(12)
O(2)-C(3)-C(4)-C(5)	57.9(13)
C(2)-C(3)-C(4)-C(5)	-13.3(16)
C(3)-C(4)-O(4)-C(7)	175.6(9)
C(5)-C(4)-O(4)-C(7)	-56.5(12)
O(4)-C(4)-C(5)-O(5)	-175.5(8)
C(3)-C(4)-C(5)-O(5)	-55.4(12)
O(4)-C(4)-C(5)-C(6)	-111.2(11)
C(3)-C(4)-C(5)-C(6)	8.9(14)
O(4)-C(4)-C(5)-C(9)	49.3(13)
C(3)-C(4)-C(5)-C(9)	169.4(10)
C(4)-C(5)-O(5)-C(6)	109.4(12)
C(9)-C(5)-O(5)-C(6)	-113.3(11)
C(5)-O(5)-C(6)-C(1)	-115.8(12)
C(4)-C(5)-C(6)-O(5)	-100.9(11)
C(9)-C(5)-C(6)-O(5)	99.3(11)
C(4)-C(5)-C(6)-C(1)	2.4(14)
O(5)-C(5)-C(6)-C(1)	103.3(10)
C(9)-C(5)-C(6)-C(1)	-157.5(10)
O(1)-C(1)-C(6)-O(5)	-179.4(9)
C(2)-C(1)-C(6)-O(5)	61.4(14)

Table B6. – Continued

O(1)-C(1)-C(6)-C(5)	109.4(10)
C(2)-C(1)-C(6)-C(5)	-9.8(14)
C(4)-O(4)-C(7)-C(8)	60.1(10)
C(4)-O(4)-C(7)-C(15)	178.6(8)
C(4)-O(4)-C(7)-C(16)	-61.5(12)
O(4)-C(7)-C(8)-O(8)	64.0(10)
C(15)-C(7)-C(8)-O(8)	-47.5(13)
C(16)-C(7)-C(8)-O(8)	-175.0(9)
O(4)-C(7)-C(8)-C(9)	-55.6(11)
C(15)-C(7)-C(8)-C(9)	-167.1(10)
C(16)-C(7)-C(8)-C(9)	65.4(13)
C(7)-C(8)-O(8)-C(17)	114.4(12)
C(9)-C(8)-O(8)-C(17)	-121.2(11)
C(4)-C(5)-C(9)-C(8)	-46.0(12)
O(5)-C(5)-C(9)-C(8)	178.8(8)
C(6)-C(5)-C(9)-C(8)	113.8(11)
O(8)-C(8)-C(9)-C(5)	-72.7(12)
C(7)-C(8)-C(9)-C(5)	48.9(11)
C(8)-O(8)-C(17)-O(17)	7(2)
C(8)-O(8)-C(17)-C(18)	-175.1(11)

REFERENCES

1. Hawksworth, D. L. *Mycol. Res.* **2001**, *105*, 1422-1432.

2. Janin, Y. L. *J. Med. Chem.* **2005**, *48*, 7503-7512.

3. Day, J. E. H.; Sharp, S. Y.; Rowlands, M. G.; Aherne, W.; Workman, P.; Moody, C. J. *Chem. Eur. J.* **2010**, *16*, 2758-2763.

4. Cohen, R.; Persky, L.; Hadar, Y. *Appl. Microbiol. Biotechnol.* **2002**, *58*, 582-594.

5. Berger, A.; Rein, D.; Kratky, E.; Monnard, I.; Hajjaj, H.; Meirim, I.; Piguet-Welsch, C.; Hauser, J.; Mace; Niederberger, P. *Lipids Health Dis.* **2004**, *18*, 2.

6. Kim, H. S.; Kacew, S.; Lee, B. M. *Carcinogenesis* **1999**, *20*, 1637-1640.

7. Guterrez, Z. R.; Mantovani, M. S.; Eira, A. F.; Ribeiro, L. R.; Jordao, B. Q. *Toxicol. In Vitro* **2004**, *18*, 301-309.

8. Wasser, S. P. *Appl. Microbiol. Biotechnol.* **2011**, *89*, 1323-1332.

9. Biasucci, L. M.; Italo, P. *Eur. Heart J.* **2010**, *31*, 2567-2568.

10. Wenger, R. *Pharm. Rev.* **1989**, *41*, 243-247.

11. Wicklow, D. T.; Rogers, K. D.; Dowd, P. F.; Gloer, J. B. *Fungal Biol.* **2011**, *115*, 133-142.

12. Jiao, P.; Mudur, S. V.; Gloer, J. B.; Wicklow, D. T. *J. Nat. Prod.* **2007**, *70*, 1308-1311.

13. Shim, S. H.; Sy, A. A.; Gloer, J. B.; Wicklow, D. T. *Bull. Korean Chem. Soc.* **2008**, *29*, 863-865.

14. Jiao, P.; Swenson, D. C.; Gloer, J. B.; Campbell, J.; Shearer, C. A. *J. Nat. Prod.* **2006**, *69*, 1667-1671.

15. Deyrup, S. T.; Swenson, D. C.; Gloer, J. B.; Wicklow, D. T. *J. Nat. Prod.* **2006**, *69*, 608-611.

16. Krasnoff, S. B.; Reategui, R. F.; Wagenaar, M. M.; Gloer, J. B.; Gibson, D. M. *J. Nat. Prod.* **2005**, *68*, 50-55.

17. Schmidt, L. E.; Deyrup, S. T.; Baltrusaitis, J.; Swenson, D. C.; Wicklow, D. T.; Gloer, J. B. *J. Nat. Prod.* **2010**, *73*, 404-408.

18. Manocha, M. S. *J. Plant Dis. Prot.* **1990**, *97*, 655-669.

19. Cortes, C.; Gutierrez, A.; Olmedo, V.; Inbar, J.; Chet, I.; Herrera-Estrella, A. *Mol. Gen. Genet.* **1998**, *260*, 218-225.

20. Viterbo, A.; Inbar, J.; Hadar, Y.; Chet, I., In *The Mycota: Environmental and Microbial Relationships*, 2nd ed.; Kubicek, C. P.; Druzhinina, I. S., Eds.; Springer-Verlag: Berlin, 2007; Vol. IV, pp 127-146.

21. Harman, G. E.; Howell, C. R.; Viterbo, A.; Chet, I.; Lorito, M. *Nat. Rev. Microbiol.* **2004**, *2*, 43-56.

22. Lumsden, R. D., In *The Fungal Community: Its Organization and Role in the Ecosystem*, 2nd ed.; Carroll, G. C.; Wicklow, D. T., Eds.; Marcel Dekker, Inc.: New York, 1992; Vol. 9, pp 275-293.

23. Shim, S. H.; Baltrusaitis, J.; Gloer, J. B.; Wicklow, D. T. *J. Nat. Prod.* **2011**, *74*, 395-401.

24. Joshi, B. K.; Gloer, J. B.; Wicklow, D. T. *J. Nat. Prod.* **2002**, *65*, 1734-1737.

25. Faeth, S. H. *Oikos* **2002**, *98*, 25-36.

26. Bayman, P., In *The Mycota: Environmental and Microbial Relationships*, 2nd ed.; Kubicek, C. P.; Druzhinina, I. S., Eds.; Springer-Verlag: Berlin, 2007; Vol. IV, pp 213-227.

27. Gunatilaka, A. A. L. *J. Nat. Prod.* **2006**, *69*, 509-526.

28. Schardl, C. L.; Phillips, T. D. *Plant Dis.* **1997**, *81*, 430-438.

29. Christensen, M. J.; Leuchtmann, A.; Rowan, D. D. *Mycol. Res.* **1993**, *97*, 1083-1092.

30. Francis, S. M.; Baird, D. B. *New Zealand J. Agric. Res.* **1989**, *32*, 437-440.

31. Bacon, C. W.; Porter, J. K.; Robbins, J. D. *Appl. Eniron. Microbiol.* **1975**, *29*, 553-556.

32. Lyons, P. C.; Plattner, R. D.; Bacon, C. W. *Science* **1986**, *232*, 487-489.

33. Bacon, C. W.; Porter, J. K.; Robbins, J. D.; Luttrell, E. S. *Appl. Eniron. Microbiol.* **1977**, *34*, 576-581.

34. Siegel, M. R.; Latch, G. C. M.; Johnson, M. C. *Ann. Rev. Phytopathol.* **1987**, *25*, 293-315.

35. Robbins, J. D.; Sweeney, J. G.; Wilkinson, S. R.; Burdick, D. *J. Agric. Food Chem.* **1972**, *20*, 1040-1043.

36. Gallagher, R. T.; White, E. P.; Mortimer, P. H. *N. Z. Vet. J.* **1981**, *29*, 189-190.

37. Gallagher, R. T.; Hawkes, A. D.; Steyn, P. S.; Vleggar, R. *J. Chem. Soc., Chem. Commun.* **1984**, 614-616.

38. Bush, L. P.; Burrus, P. B. I. *J. Prod. Agric.* **1987**, *1*, 55-60.

39. White, J. F. J.; Cole, G. T. *Mycologia* **1986**, *79*, 148-152.

40. He, H.; Yang, H. Y.; Bigelis, R.; Solum, E. H.; Greenstein, M.; Carter, G. T. *Tetrahedron Lett.* **2002**, *43*, 1633-1636.

41. Wicklow, D. T.; Roth, S.; Deyrup, S. T.; Gloer, J. B. *Mycol. Res.* **2005**, *109*, 610-618.

42. Wicklow, D. T.; Poling, S. M. *Phytopathology* **2009**, *99*, 109-115.

43. Crous, P. W.; Slippers, B.; Wingfield, M. J.; Rheeder, J.; Marasas, W. F. O.; Philips, A. J. L.; Alves, A.; Burgess, T.; Barber, P.; Groenewald, J. Z. *Stud. Mycol.* **2006**, *55*, 235-253.

44. Rossouw, J. D.; Pretorius, Z. A.; Silva, H. D.; Lamkey, K. R., *Breeding for resistance to Stenocarpella ear rot in maize*. John Wiley & Sons: 2009; Vol. 31.

45. Latterell, F. M.; Rossi, A. E. *Plant Dis.* **1983**, *67*, 725-729.

46. Kellerman, T. S.; Prozesky, L.; Schultz, R. A.; Rabie, C. J.; Van Ark, H.; Maartens, B. P.; Lubben, A. *Onderstepoort J. Vet. Res.* **1991**, *58*, 297-308.

47. Oridiozola, E.; Odeon, A.; Canton, G.; Clemente, G.; Escande, A. *New Zeal. Vet. J.* **2005**, *53*, 160-161.

48. Steyn, P. S.; Wessels, P. L.; Holzapfel, C. W.; Potgieter, D. J. J.; Louw, W. K. A. *Tetrahedron* **1972**, *28*, 4775-4785.

49. Rabie, C. J.; Kellerman, T. S.; Kriek, N. P.; van der Westhuizen, G. C.; De Wet, P. J. *Food Chem. Toxicol.* **1985**, *23*, 349-353.

50. Kriek, N. P. J.; Marasas, W. F. O. *Food Cosmet. Toxicol.* **1979**, *17*, 233-236.

51. Chalmers, A. A.; Gorst-Allman, C. P.; Kriek, N. P. J.; Marasas, W. F. O.; Steyn, P. S.; Vleggar, R. *S. Afr. J. Chem.* **1978**, *31*, 111-114.

52. Cutler, H. G.; Crumley, F. G.; Cox, R. H.; Cole, R. J.; Dorner, J. W.; Latterell, F. M.; Rossi, A. E. *J. Agric. Food Chem.* **1980**, *28*, 135-138.

53. Cutler, H. G.; Crumley, F. G.; Cox, R. H.; Cole, R. J.; Dorner, J. W.; Springer, F. M.; Thaen, J. E.; Rossi, A. E. *J. Agric. Food Chem.* **1980**, *28*, 139-142.

54. Pfender, W. F., Microbial interactions preventing fungal growth in senescent and necrotic aerial plant surfaces. In *Aerial Plant Surface Microbiology*, Morris, C. E.; Nicot, P. C.; Nguyen, C., Eds. Springer: 1996; pp 125-138.

55. Flett, B. C.; McLaren, N. W.; Wehner, F. C. *Plant Dis.* **2001**, *85*, 92-94.

56. Bensch, M. J.; van Staden, J.; Rijkenberg, F. H. J. *J. Phytopathol.* **1992**, *136*, 265-269.

57. Wysong, D. S.; Hooker, A. L. *Phytopathology* **1966**, *56*, 26-35.

58. Rahman, M. F.; Rao, S. K.; Achar, P. N. *Ecotoxicol. Environ. Saf.* **2002**, *52*, 267-272.

59. Rao, S. K.; Achar, P. N. *Indian J. Exp. Biol.* **2001**, *39*, 1243-1248.

60. Rabie, C. J.; van Rensburg, S. J.; Kreik, N. P. J.; Lubben, A. *Appl. Environ. Microbiol.* **1977**, *34*, 111-114.

61. Kellerman, T. S.; Rabie, C. J.; van der Westhuizen, G. C.; Kreik, N. P.; Prozesky, L. *Onderstepoort J. Vet. Res.* **1985**, *52*, 35-42.

62. Nucci, M.; Anaissie, E. *Clin. Microbiol. Rev.* **2007**, *20*, 695-704.

63. Dickinson, C. H. *Mycol. Pap.* **1968**, *115*, 1-27.

64. Traber, R.; Kuhn, M.; Ruegger, A.; Lichti, H.; Loosli, H.-R.; von Wartburg, A. *Helv. Chim. Acta* **1977**, *60*, 1247-1255.

65. Podsiadlowski, L.; Matha, V.; Vilcinskas, A. *Comp. Biochem. Phys. B* **1998**, *121*, 443-450.

66. Moussaif, M. J., P.; Schaarwachter, P.; Budzikiewica, H.; Thonart, P. *Appl. Environ. Microbiol.* **1997**, *63*, 1739-1743.

67. Mori, K.; Okada, K. *Tetrahedron* **1985**, *41*, 557-559.

68. Niku-Paavola, M.-L.; Laitila, A.; Mattila-Sandholm, T.; Haikara, A. *J. Appl. Microbiol.* **1999**, *86*, 29-35.

69. Thines, E.; Anke, H.; Sterner, O. *J. Antibiot.* **1998**, *51*, 387-393.

70. Hamilton, A. J.; Gomez, B. L. *J. Med. Microbiol.* **2002**, *53*, 189-191.

71. Langfelder, K.; Streibel, M.; Jahn, B.; Haase, G.; Brakhage, A. A. *Fungal Genet. Biol.* **2003**, *38*, 143-158.

72. Sy, A. A. Ph.D. Dissertation, Iowa City, IA, **2007**, pp. 107-110.

73. Sassa, T.; Yoshida, N.; Haruki, E. *Agric. Biol. Chem.* **1989**, *53*, 3105-3107.

74. Zou, W. X.; Meng, J. C.; Lu, H.; Chen, G. X.; Shi, X.; Zhang, T. Y.; Tan, R. X. *J. Nat. Prod.* **2000**, *63*, 1529-1530.

75. Carr, S. A.; Block, E.; Costello, C. E.; Vesonder, R. F.; Burmeister, H. R. *J. Org. Chem.* **1985**, *50*, 2854-2858.

76. Burmeister, H. R.; Vesonder, R. F.; Peterson, R. E.; Costello, C. E. *Mycopathologia* **1985**, *91*, 53-56.

77. Soman, A. G.; Gloer, J. B.; Wicklow, D. T. *J. Nat. Prod.* **1999**, *62*, 386-388.

78. Davies, J. E.; Kirkaldy, D.; Roberts, J. C. *J. Chem. Soc.* **1960**, 2169-2178.

79. Bullock, E.; Roberts, J. C.; Underwood, J. G. *J. Chem. Soc.* **1962**, 4179-4183.

80. Sy, A. A. Ph.D. Dissertation, Iowa City, IA, **2007**, pp. 86-87.

81. Schmidt, L. E.; Gloer, J. B.; Wicklow, D. T. *J. Nat. Prod.* **2007**, *70*, 1317-1320.

82. Shim, S. H.; Gloer, J. B.; Wicklow, D. T. *J. Nat. Prod.* **2006**, *69*, 1601-1605.

83. Deyrup, S. T.; Gloer, J. B.; O'Donnell, K.; Wicklow, D. T. *J. Nat. Prod.* **2007**, *70*, 378-382.

84. O'Donnell, K. *Sydowia* **1996**, *48*, 57-70.

85. White, T. J.; Bruns, T.; Lee, S.; Taylor, J. W., In *PCR Protocols: A Guide to Methods and Applications*, Innis, M. A.; Gelfand, D. H.; Sninsky, J. J.; White, T. J., Eds.; Academic Press: New York, 1990; pp 315-322.

86. *Dictionary of Natural Products* database, web version 2011; CRC Press: Boca Raton, FL (accessed October 29, 2011)

87. *SciFinder Scholar*, web version; Chemical Abstracts Service: Columbus, OH, 2011 (accessed October 29, 2011)

88. Souza, A. D.; Rodrigues-Filho, E.; Souza, A. Q. L.; Henrique-Silva, F.; Pereira, J. O. *J. Braz. Chem. Soc.* **2006**, *19*, 1321-1325.

89. Bloch, P.; Tamm, C.; Bollinger, P.; Petcher, T. J.; Weber, H. P. *Helv. Chim. Acta.* **1976**, *59*, 133-137.

90. Gupta, S.; Peiser, G.; Nakajima, T.; Hwang, Y.-S. *Tetrahedron Lett.* **1994**, *35*, 6009-6012.

91. Di Micco, D.; Terracciano, S.; Bruno, I.; Rodriquez, M.; Riccio, R. *Bioorg. Med. Chem.* **2008**, *16*, 8635-8642.

92. Shute, R. E.; Dunlap, B.; Rich, D. H. *J. Med. Chem.* **1987**, *30*, 71-78.

93. Nishino, N.; Jose, B.; Shinta, R.; Kato, T.; Komatsu, Y.; Yoshida, M. *Bioorg. Med. Chem.* **2004**, *12*, 5777-5784.

94. Marahiel, M. A.; Stachelhaus, T.; Mootz, H. D. *Chem. Rev.* **1997**, *97*, 2651-2673.

95. Wiest, A.; Grzegorski, D.; Xu, B. w.; Goulard, C.; Rebuffat, S.; Ebbole, D. J.; Bodo, B.; Kenerley, C. *J. Biol. Chem.* **2002**, *277*, 20862-20868.

96. Ruiz, N.; Wielgosz-Collin, G.; Poirier, L.; Grovel, O.; Petit, K. E.; Mohamed-Benkada, M.; du Pont, T. R.; Bisset, J.; Verite, P.; Barnathan, G.; Pouchus, Y. F. *Peptides* **2007**, *28*, 1351-1358.

97. Whitmore, L.; Wallace, B. A. *Nucl. Acids Res.* **2004**, *32*, D593-D594.

98. Whitmore, L.; Wallace, B. A. *Eur. Biophys. J.* **2004**, *33*, 233-237.

99. Brogden, K. A. *Nature Rev. Microbiol.* **2005**, *3*, 238-250.

100. Liepke, C.; Baxmann, S.; Heine, C.; Breithaupt, N.; Standker, L.; Forssmann, W.-G. *J. Chromatogr. B Analyt. Technol. Biomed. Life Sci.* **2003**, *791*, 345-356.

101. Kroemer, G.; Galluzzi, L.; Brenner, C. *Physiol. Rev.* **2007**, *87*, 99-163.

102. Yamaguchi, S.; Huster, D.; Waring, A.; Lehrer, R. I.; Kearney, W.; Tack, B. F.; Mei, H. *Biophys. J.* **2001**, *81*, 2203-2214.

103. Bechinger, B. *Biochim. Biophys. Acta* **1999**, *1462*, 157-183.

104. Martin, D. R.; Williams, R. J. *J. Am. Chem. Soc.* **1976**, *153*, 181-190.

105. Gostimskaya, I. S.; Grivennikova, V. G.; Zharova, T. V.; Bakeeva, L. E.; Vinogradov, A. D. *Anal. Biochem.* **2003**, *313*, 46-52.

106. Khalfa, A.; Tarek, M. *J. Phys. Chem. B* **2011**, *114*, 2676-2684.

107. Pretsch, E.; Buhlmann, P.; Affolter, C., *Structure Determination of Organic Compounds*. Springer-Verlag: Berlin, Heidelberg, New York, 2000.

108. Bhushan, R.; Bruckner, H., Chiral Separations Using Marfey's Reagent. In *Thin Layer Chromatography in Chiral Separations and Analysis*, Kowalska, T.; Sherma, J., Eds.; CRC Press: Boca Raton, 2007; Vol. 98, pp 383-407.

109. Marfey, P. *Carlsberg Res. Commun.* **1984**, *49*, 591-596.

110. Hoffmann, H. M. R.; Rabe, J. *Angew. Chem. Int. Ed. Engl.* **2003**, *24*, 94-110.

111. de Kraker, J.-W.; Franssen, M. C. R.; Joerink, M.; de Groot, A.; Bouwmeester, H. J. *Plant Physiol.* **2002**, *129*, 257.

112. Ali, M. S.; Ibrahim, S. A.; Ahmed, S.; Lobkovsky, E. *Chem. Biodiv.* **2007**, *4*, 98-104.

113. Yae, E.; Yahara, S.; El-Aasr, M.; Ikeda, T.; Yoshimitsu, H.; Masuoka, C.; Ono, M.; Hide, I.; Nakata, Y.; Nohara, T. *Chem. Pharm. Bull.* **2009**, *57*, 719-723.

114. Takaya, Y.; Kurumada, K.; Takeuji, Y.; Kim, H.-S.; Shibata, Y.; Ikemoto, N.; Wataya, Y.; Oshima, Y. *Tetrahedron Lett.* **1998**, *39*, 1361-1364.

115. Wang, L.-Y.; Unehara, T.; Kitanaka, S. *Chem. Pharm. Bull.* **2005**, *53*, 137-139.

116. Freeman, S.; Maymon, M.; Pinkas, Y. *Phytopathology* **1999**, *89*, 456-461.

117. Spatafora, J. W.; Blackwell, M. *Mycologia* **1993**, *85*, 912-922.

118. Neuveglise, C.; Brygoo, Y.; Vercambre, B.; Riba, G. *Mycol. Res.* **1994**, *98*, 322-328.

119. Berbee, M. L.; Taylor, J. W. *Mol. Phylogenet. Evol.* **1992**, *1*, 59-71.

120. Gams, W.; McGinnis, M. R. *Mycologia* **1983**, *75*, 977-987.

121. Pedras, M. S. C.; Zaharia, L. I.; Ward, D. E. *Phytochemistry* **2002**, *59*, 579-596.

122. Takahashi, S.; Itoh, Y.; Takeuchi, M.; Furuya, K.; Kodama, K.; Naito, A.; Haneishi, T.; Sato, S.; Tamura, C. *J. Antibiot.* **1983**, *36*, 1418-1420.

123. Seto, H.; Furihata, K.; Otake, N.; Itoh, Y.; Takahashi, S.; Haneishi, T.; Ohuchi, M. *Tetrahedron Lett.* **1984**, *25*, 337-340.

124. Dale, J. A.; Mosher, H. S. *J. Am. Chem. Soc.* **1973**, *95*, 512-519.

125. Muhlenfeld, A.; Achenbach, H. *Phytochemistry* **1988**, *27*, 3853-3855.

126. Lira, S. P.; Vita-marques, A. M.; Seleghim, M. H. R.; Bugni, T. S.; Labarbera, D. V.; Sette, L. D.; Sponchiado, S. R. P.; Ireland, C. M.; Berlinck, R. G. S. *J. Antibiot.* **2006**, *59*, 553-563.

127. Pandey, A.; Agrawal, G. P.; Singh, S. M. *Mycoses* **1990**, *33*, 116-125.

128. Wicklow, D. T.; Joshi, B. K.; Gamble, W. R.; Gloer, J. B.; Dowd, P. F. *Appl. Environ. Microbiol.* **1998**, *64*, 4482-4484.

129. Sun, B.; Morikawa, T.; Matsuda, H.; Tewtrakul, S.; Wu, L. J.; Harima, S.; Yoshikawa, M. *J. Nat. Prod.* **2004**, *67*, 1464-1469.

130. Dewick, P. M., *Medicinal Natural Products: A Biosynthetic Approach*. 2nd ed.; John Wiley & Sons, Ltd.: 2002; p 349-350.

131. Herraiz, T., β-Carboline Alkaloids. In *Bioactive Compounds in Foods*, Blackwell Publishing Ltd.: 2009; pp 199-223.

132. Cao, R.; Peng, W.; Wang, Z.; Xu, A. *Curr. Med. Chem.* **2007**, *14*, 479-500.

133. Song, X.-h.; Liu, X.-h.; Lin, Y.-c. *Redai Haiyang Xuebao* **2004**, *23*, 66-71.

134. Chen, P.; Dai, H.; Wu, J.; Dai, W.; Mei, W. *Zhongguo Yaoxue Zazhi (Beijing, China)* **2009**, *44*, 825-827.

135. Teichert, A.; Schmidt, J.; Porzel, A.; Arnold, N.; Wessjohann, L. *J. Nat. Prod.* **2007**, *70*, 1529-1531.

136. Scherlach, K.; Boettger, D.; Remme, N.; Hertweck, C. *Nat. Prod. Rep.* **2010**, *27*, 869-886.

137. Abate, D.; Abraham, W.-R.; Meyer, H. *Phytochemistry* **1997**, *44*, 1443-1448.

138. Beno, M. A.; Cox, R. H.; Wells, J. M.; Cole, R. J.; Kirksey, J. W.; Christoph, G. C. *J. Am. Chem. Soc.* **1977**, *99*, 4123.

139. Cameron, A. F.; Freer, A. A.; Hesp, B.; Strawson, J. *J. Chem. Soc., Perkin Trans.* **1974**, *2*, 1741.

140. Buchi, G.; Kitaura, Y.; Yuan, S.-S.; Wright, H. E.; Clardy, J.; Demain, A. L.; Glinsukon, T.; Hunt, N.; Wogan, G. N. *J. Am. Chem. Soc.* **1973**, *95*, 5423.

141. Neupert-Laves, K.; Dobler, M. *Helv. Chim. Acta.* **1982**, *65*, 1426.

142. Buchanan, M.; Hashimoto, T.; Asakawa, Y. *Phytochemistry* **1995**, *40*, 135-140.

143. Betina, V.; Micekova, D.; Nemec, P. *J. Gen. Microbiol.* **1972**, *71*, 343-349.

144. Nennah, G. *Filoterapia* **2010**, *81*, 779-782.

145. Poling, S. M.; Wicklow, D. T.; Rogers, K. D.; Gloer, J. B. *J. Agric. Food Chem.* **2008**, *56*, 3006-3009.

146. Ghisalberti, E. L.; Hockless, D. C. R.; Rowland, C. Y.; White, A. H. *Aust. J. Chem.* **1993**, *46*, 571-575.

147. Oyama, H.; Sassa, T.; Ikeda, M. *Agric. Biol. Chem.* **1978**, *42*, 2407-2409.

148. Couladouros, E. A.; Mihou, A. P.; Bouzas, E. A. *Org. Lett.* **2004**, *6*, 977-980.

149. Barrow, C. J. *J. Nat. Prod.* **1997**, *60*, 1023-1025.

150. Lai, S.; Shizuri, Y.; Yamamura, S.; Kawai, K.; Terada, Y.; Furukawa, H. *Tetrahedron Lett.* **1989**, *30*, 2241-2244.

151. Nukina, M.; Sassa, T.; Oyama, H.; Ikeda, M. *Tennen Yuki Kagobutsu Toronkai Koen Yoshishu, 22nd* **1979**, *36*, 2-9.

152. Fu, Y. Ph.D. Dissertation, Cornell University, Ithaca, NY, **1989**, pp.

153. West, R. R.; Martinez, T.; Franklin, H. R.; Bishop, P. D.; Rassing, B. R. Factor XIIIA inhibitor. U.S. Patent 5,710,174, 1998.

154. Sassa, T.; Nukina, M.; Ikeda, M. *Nippon Kagaku Kaishi* **1981**, 883-885.

155. Wicklow, D. T.; Poling, S. M. *Phytopathology* **2006**, *96*, S122.

156. Whitesell, L.; Lindquist, S. *Nat. Rev. Cancer* **2005**, *5*, 761-772.

157. Pearl, L. H.; Prodromou, C. *Annu. Rev. Biochem.* **2006**, *75*, 271-294.

158. Proisy, N.; Sharp, S. Y.; Boxall, K.; Connelly, S.; Roe, S. M.; Prodromou, C.; Slawin, A. M. Z.; Pearl, L. H.; Workman, P.; Moody, C. J. *Chem. Biol.* **2006**, *13*, 1203-1215.

159. Day, J. E. H.; Sharp, S. Y.; Rowlands, M. G.; Aherne, W.; Lewis, W.; Roe, S. M.; Prodromou, C.; Pearl, L. H.; Workman, P.; Moody, C. J. *Chem. Eur. J.* **2010**, *16*, 10366-10372.

160. Howes, R.; Barril, X.; Dymock, B. W.; Grant, K.; Northfield, C. J.; Robertson, A. G. S.; Surgenor, A.; Wayne, J.; Wright, L.; James, K.; Matthews, T.; Cheung, K.-M.; McDonald, E.; Workman, P.; Drysdale, M. J. *Anal. Biochem.* **2006**, *350*, 202-213.

161. Rowlands, M. G.; Newbatt, Y. M.; Prodromou, C.; Pearl, L. H.; Workman, P.; Aherne, W. *Anal. Biochem.* **2004**, *327*, 176-183.

162. Roe, S. M.; Prodromou, C.; O'Brien, R.; Ladbury, J. E.; Piper, P. W.; Pearl, L. H. *J. Med. Chem.* **1999**, *42*, 260-266.

163. Prodromou, C.; Roe, S. M.; Piper, P. W.; Pearl, L. H. *Nature Struct. Biol.* **1997**, *4*, 477-482.

164. Day, J. E. H.; Sharp, S. Y.; Rowlands, M. G.; Aherne, W.; Lewis, W.; Roe, S. M.; Prodromou, C.; Pearl, L. H.; Workman, P.; Moody, C. J. *Chem. Eur. J.* **2010**, *16*, 10366-10372.

165. Agatsuma, T.; Kanda, Y.; Onodera, H.; Matsushita, N.; Ogawa, T.; Akinaga, S.; Soga, S. Hsp90 Family Protein Inhibitors. WO 2004 24,141, 2004.

166. Wicklow, D. T.; Jordan, A. M.; Gloer, J. B. *Mycol. Res.* **2009**, *113*, 1433-1442.

167. Burlot, J.-C.; Cherton, O.; Convert, L.; Correia, L.; Dennetiere, B. *Spectroscopy* **2003**, *17*, 725-734.

168. Abate, D.; Abraham, W.-R.; Meyer, H. *Phytochemistry* **1997**, *44*, 1443-1448.

169. Probst, A.; Tamm, C. *Helv. Chim. Acta* **1982**, *65*, 1543-1546.

170. Spoendlin, C.; Tamm, C. *Helv. Chim. Acta* **1988**, *71*, 1881-1884.

171. Kobayashi, H.; Namikoshi, M.; Yoshimoto, T.; Yokochi, T. *J. Antibiot.* **1996**, *49*, 873-879.

172. Wicklow, D. T.; Dowd, P. F.; Gloer, J. B., *Chaetomium* mycotoxins with antiinsectan or antifungal activity. In *Preceedings of International Symposium of Mycotoxicology '99*, Chiba, Japan, 2000; pp 267-271.

173. Dowd, P. F.; Cole, R. J.; Vesonder, R. F. Control of insects by fungal tremorgenic mycotoxins. U.S. Patent No. 4,973,601, 1990.

174. Jarvis, J. L.; Clark, R. L.; Guthrie, W. D. *Phytopathology* **1982**, *72*, 1149-1152.

175. Windels, C. E.; Windels, M. B.; Komedahl, T. *Phytopathology* **1976**, *66*, 328-331.

176. Attwater, W. A.; Busch, L. V. *Can. J. Plant Pathol.* **1983**, *5*, 158-163.

177. Lussenhop, J. L.; Wicklow, D. T. *Trans. Mycol. Soc. Jpn.* **1990**, *31*, 63-74.

178. Bartelt, R. J.; Wicklow, D. T. *J. Agric. Food Chem.* **1999**, *47*, 2447-2454.

179. Yahara, I.; Harada, F.; Sekita, S.; Yoshihira, K.; Natori, S. *J. Cell. Biol.* **1982**, *92*, 69-78.

180. Kobayashi, I.; Kobayashi, Y.; Yamada, M.; Kunoh, H., The involvement of the cytoskeleton in the expression of nonhost resistance in plants. In *Molecular Aspects of Pathogenicity and Resistance: Requirement for Signal Transduction*, 1996; pp 185-195.

181. Staiger, C. J. *Ann. Rev. Plant Physiol. Plant Mol. Biol.* **2000**, *51*, 257-288.

182. Chambers, K. R. *Plant Dis.* **1988**, *72*, 529-531.

183. Huynh, Q.; Hironaka, C.; Levine, E.; Smith, C.; Borgmeyer, J.; Shah, D. *J. Biol. Chem.* **1992**, *267*, 6635-6640.

184. Naumann, T. A.; Wicklow, D. T. *Phytopathology* **2010**, *100*, 645-654.

185. Rabie, C. J.; Du Preez, J. J.; Hayes, J. P. *Poult. Sci.* **1987**, *66*, 1123-1128.

186. Kumagai, H.; Imazawa, M.; Miyamoto, K. *Dev. Brain Res.* **1988**, *27*, 270-274.

187. Tikoo, A.; Cutler, H.; Lo, S. H.; Chen, L. B.; Maruta, H. *Cancer J. Sci. Am.* **1999**, *5*, 293-300.

188. Fernandez-Valle, C.; Gorman, D.; Gomez, A. M.; Bunge, M. B. *J. Neurosci.* **1997**, *17*, 241-250.

189. Prozesky, L.; Kellerman, T. S.; Swart, D. P.; Maartens, B. P.; Schultz, R. A. *Onderstepoort J. Vet. Res.* **1994**, *61*, 247-253.

190. Fincham, J. E.; Hewlett, R.; DeGraaf, A. S.; Taljaard, J. J. F.; Steytler, J. G.; Rabie, C. J.; Seier, J. V.; Venter, F. S.; Woodruff, C. W.; Wynchank, S. *J. Med. Primatol.* **1991**, *20*, 240-250.

191. Marasas, W. F. O., Diplodiosis in Cattle. In *Mycotoxic Fungi, Mycotoxins, and Mycotoxicoses: an Encyclopedic Handbook*, Wyllie, D.; Morehouse, G. L., Eds.; 1977; Vol. 2, pp 163-165.

192. Fogle, M. R.; Douglas, D. R.; Jumper, C. A.; Straus, D. C. *Can. J. Microbiol.* **2008**, *54*, 423-425.

193. Snyman, L. D.; Kellerman, T. S.; Vleggaar, R.; Flett, B. C.; Basson, K. M.; Schultz, R. A. *J. Agric. Food Chem.* **2011**, *59*, 9039-9044.

194. Cardellina II, J. H. *J. Nat. Prod.* **1983**, *46*, 196-199.